# UNIVERSITY OF SOUTHAMPTON

**FACULTY OF SOCIAL AND HUMAN SCIENCES**

**GEOGRAPHY AND ENVIRONMENT**


# Cascading Natural Hazards: Probability and Loss Modelling for Earthquakes and Earthquake-Triggered Landslides

by


**Mirianna Elizabeth Alessandra Budimir**


Thesis for the degree of Doctor of Philosophy

July 2014

**UNIVERSITY OF SOUTHAMPTON**

# ABSTRACT

Multi-hazard risk assessments rarely account for the effects of natural hazards interacting, such as amplification of losses and increased probability of secondary hazards. This could underestimate the risk caused by cascading events interacting; an example of this is earthquakes and triggered landslides. This thesis aims to improve the accuracy of multi-hazard risk assessment by accounting for the interaction between hazards: specifically earthquakes and landslides.

The amplification effect on fatalities of earthquake-and-landslide events are compared to earthquake-only events. Data limitations made it unviable to quantify whether aggregating single hazard risk underestimates the total risk from multi-hazard events, because loss data are typically attributed to the primary hazard. However, there was a significant increase in fatalities caused by earthquake-and-landslide events compared to earthquake-only events, irrespective of other factors such as earthquake magnitude, population exposed, and building strength.

Landslides are often treated as a single hazard type in multi-hazard risk assessment. This could underestimate the risk from earthquake-triggered landslides. A systematic literature search found the trigger type affects the significant covariates associated with landsliding in logistic regression analysis. Therefore, earthquake-triggered landslides should be assessed separately to rainfall-triggered landslides.

The landslide inventory map and the peak ground acceleration data from the 1994 $M_w$6.7 Northridge, California earthquake were used with environmental covariates to fit a logistic regression landslide hazard model. The model can be used with any earthquake scenario in the Northridge region to predict landslide probability, given a peak ground acceleration variable.

The OpenSHA application was used to simulate seven different earthquake magnitude scenarios for the Northridge study site. Coupled with the landslide hazard model, the potential impact on assets of high earthquake shaking and high landslide hazard probability was estimated. Results show that if the Northridge earthquake occurred today as in 1994, there would be an expected increase in losses and damage. As the earthquake scenario magnitude increases, the potential impact from earthquake shaking levels out and becomes saturated, but potential losses from landslides increase at a rapid rate. The scenario maps can also be used by land use and emergency planners as a reference for areas at risk of landsliding and high levels of earthquake shaking during a similar event to the Northridge 1994 earthquake.

FACULTY OF SOCIAL AND HUMAN SCIENCES

Geography and Environment

Thesis for the degree of Doctor of Philosophy

**CASCADING NATURAL HAZARDS:**

**PROBABILITY AND LOSS MODELLING FOR**

**EARTHQUAKES AND EARTHQUAKE-TRIGGERED LANDSLIDES**

Mirianna Elizabeth Alessandra Budimir

# DECLARATION OF AUTHORSHIP

I, Mirianna Budimir, declare that this thesis and the work presented in it are my own and have been generated by me as the result of my own original research.

Cascading Natural Hazards: Probability and Loss Modelling for Earthquakes and Earthquake-Triggered Landslides.

I confirm that:

This work was done wholly or mainly while in candidature for a research degree at this University; where any part of this thesis has previously been submitted for a degree or any other qualification at this University or any other institution, this has been clearly stated; where I have consulted the published work of others, this is always clearly attributed; where I have quoted from the work of others, the source is always given. With the exception of such quotations, this thesis is entirely my own work; I have acknowledged all main sources of help; where the thesis is based on work done by myself jointly with others, I have made clear exactly what was done by others and what I have contributed myself; parts of this work have been published as:

Budimir, M., Atkinson, P., and Lewis, H., (2014), 'Earthquake-and-Landslide Events are Associated with More Fatalities than Earthquakes Alone', *Natural Hazards*, Volume 72, Issue 2, Page 895-914.

Budimir, M.E.A., Atkinson, P.M., and Lewis, H.G., (2015), 'A Systematic Review of Landslide Probability Mapping Using Logistic Regression', *Landslides Journal*.

Budimir, M.E.A., Atkinson, P.M., and Lewis, H.G., (2015), 'Seismically-Induced Landslide Hazard and Exposure Modelling in Southern California Based on the 1994 Northridge, California Earthquake Event', *Landslides Journal*.

Signed:

Date:

# ACKNOWLEDGEMENTS

I would like to thank my supervisors Professor Pete Atkinson and Dr Hugh Lewis for their support and supervision throughout my PhD. I am indebted to you both for the time and effort you have spent guiding me through my PhD, and providing feedback for my research and work. I am grateful to the University of Southampton Geography and Environment Department and the Engineering and the Environment Department for the funding which made this PhD possible.

To Charlotte Norlund, Melanie Kappes, Joel Gill and Melanie Duncan, thank you for your support, sharing of data and time spent discussing multi-hazards, it was invaluable to realise I was not alone in my research topic. To the Geography Department support staff (in particular Julie Drewitt), thank you for keeping me on track and backing me up. To Emma Tompkins, thank you for the coffee and lunch breaks you spent encouraging me; my enthusiasm always increases after talking to you. To Kevin Milner at OpenSHA, thank you for your help and dogged determination to fix any problem I came up with. To all those I met at conferences over the past few years, thank you for your advice, anecdotes and encouragement in my research and the PhD, it was greatly appreciated.

A huge thank you to my wonderful fiancé Olly Catford for supporting me for so long and always being there to cheer me on and help me reach my goals. You always know the right thing to say or do to keep me sane and positive; whether it's a hug, a chat, or a kick in the right direction. I don't think I would be where I am without you. A massive thank you to my fantastic family for supporting, encouraging and believing in me for so long; your love always keeps me going. And also a huge thank you to my friends, particularly Poppy Wood, Becky Wilson and Francesca Haarer, for being there with a cup of tea (or a glass of wine) and a willing ear; your support means the world to me. To all my friends, you have always

been there to brighten my day by making me laugh, or sweat it out with exercise; it has been invaluable and kept me sane. Thank you.

To my Geography PhD colleagues-in-arms, particularly Helen MacKay, Kim Davies, Ellie Tighe, John Duncan, and Joanna Kuleszo, thank you for all the chats and encouragement over the years, whether PhD-related or not. You made it bearable to come into University when the PhD was at its toughest, and made it fun to come in when times were good. I will always have fond memories of my time with you all. And to my fellow-PhD friends Niamh O'Meara, Teresa Binks, Katherine Penny, Suzanne Peacock, Emma Johnston, Sassiwimol Nawawiphisit, and Sam Engwell, thank you for your encouragement, belief and advice throughout the PhD; you made me believe it was possible.

To all those who helped make this PhD possible, thank you.

Mirianna Budimir

*University of Southampton*

July 2014

# TABLE OF CONTENTS

# LIST OF FIGURES

# LIST OF TABLES

# 1. INTRODUCTION

## Overview

Multi-hazard risk assessment has previously been neglected in favour of single-hazard risk analysis. Where multi-hazard risk assessment has been carried out, the risk posed by multiple hazards occurring in the same spatial location has been calculated by aggregating the single hazard risk assessments for each hazard. This method does not take into consideration the symbiosis, interaction and cascading effects of natural hazards.

Little research has been conducted to date on cascading hazards. To more accurately represent reality and to reduce the error and uncertainty inherent in multi-hazard risk models, including the interaction of natural hazards is vital in multi-hazard risk assessment. It is presumed in the literature that cascading events result in an amplified risk or loss that is greater than the sum of the independent hazards. Current multi-hazard risk assessment could be under-assessing the risk to communities or assets exposed to more than one hazard.

If such interactions and amplifications can be accounted for, this can help in disaster risk reduction, saving lives and can aid the insurance industry. This thesis examines the potential amplification effects of a cascading event compared to a single event, uses primary hazard data to predict the location of the secondary hazard, and estimate the exposure as a result of high levels of hazard, using earthquakes and triggered landslides as an example of cascading hazards.

## Aim

To explore probability of landsliding given the earthquake hazard, and the potential impacts of coseismic landslides, within the context of the field of cascading hazards.

## Thesis Outline

The research is presented as a literature review, four chapters (papers) which were submitted for publication, and a discussion section. An introduction before each paper outlines the paper's contribution to the overall thesis, identifies research questions, and links the papers together.

Paper 1 is titled 'Earthquake-and-landslide events are associated with more fatalities than earthquakes alone'. This paper was published in *Natural Hazards.* This first paper analyses fatality data from earthquake events where landslides have been recorded, and when no landslides have been recorded to explore relationships between the number of fatalities during earthquake-only (single hazard event) and earthquake-and-landslide events (cascading event).

Paper 2 is titled 'A systematic review of landslide probability mapping using logistic regression'. This paper has been submitted to *Landslides*. This second paper reviews all available publications which use logistic regression analysis to predict landslide probability, separating them by landslide type, and by landslide trigger.

Paper 3 is titled 'Coseismic landslide hazard probability modelled as a function of the earthquake trigger for the 1994 Northridge, California event'. This paper has been submitted to *Engineering Geology.* This third paper compares a landslide susceptibility model with a landslide hazard model for the Northridge, California 1994 earthquake. The landslide hazard model uses inputs from the primary hazard (earthquake peak ground acceleration) to predict the secondary hazard (landslide probability).

Paper 4 is titled 'Seismically-induced landslide hazard and exposure modelling in Southern California based on the 1994 Northridge, California earthquake event'. This paper has been submitted to *Landslides.* The fourth and final paper uses the landslide hazard model method

from Paper 3 to estimate the impact of earthquake shaking and potential triggered landslides on assets for seven earthquake scenarios at Northridge, California.

# 2. LITERATURE REVIEW

## 1.0 Natural Hazards

The UN defines natural hazards as ‘natural processes or phenomena occurring in the biosphere that may constitute a damaging event’, and a natural disaster as ‘a serious disruption triggered by a natural hazard causing human, material, economic or environmental losses, which exceed the ability of those affected to cope’ (UNDP, 2004).

The UNDP report (2004) estimated that 75% of the world's population live in areas affected by earthquakes, cyclones, floods or drought between 1980 and 2000. Rising losses from natural hazards sparked the International Decade for Natural Disaster Reduction 1990-2000; however, there has still been an increase in losses since then (Kappes *et al*, 2010a). Research is needed to analyse hazards, vulnerability to disasters and risk in order to inform management strategies to decrease losses from natural hazards (Kappes *et al*, 2010a).

## 2.0 Risk

In this review, the term ‘risk’ will be used in relation to natural hazards. As such, the UN’s definition will be used. The UN defines risk as ‘the probability of harmful consequences or expected loss of lives, people injured, property, livelihoods, economic activity disrupted (or environment damaged) resulting from interactions between natural or human induced hazards and vulnerable conditions’ (UNDP, 2004).

Risk is conventionally expressed by the equation:

$$Risk = f(Hazard, Exposure, Vulnerability) \qquad \text{Equation 1}$$

## 3.0 Vulnerability

The UN defines human vulnerability as ‘a human condition or process resulting from physical, social, economic and environmental factors, which determine the likelihood and

scale of damage from the impact of a given hazard' (UNDP, 2004). Vulnerability is the degree of loss given that a hazard of a particular magnitude occurs (Peduzzi *et al*, 2009). It is the concept that explains why, with a given level of physical exposure, people are more or less at risk. A measurement of vulnerability is modified by coping capacity and adaptive capacity (UNDP, 2004).

Vulnerability is needed in risk assessment because without the 'human' element (e.g. people, buildings, land, utilities, assets that are valued), there is no considered loss. Vulnerability is spatially variable and dependent on multiple factors. Some people, buildings, regions and countries are more vulnerable to some hazards than others. Developing countries are vulnerable to high mortality during droughts, but less vulnerable to economic losses. However, more developed countries are more vulnerable to economic losses and less susceptible to mortality loss during droughts. Therefore vulnerability factors must be taken into account when analysing hazard risk.

The vulnerability of an asset is dependent on the magnitude of the hazard and the characteristics of the asset (RiskScape, 2011). Vulnerability is often expressed through a fragility or damage function (Figure 1) which relates hazard exposure to mean damage ratio for different assets (RiskScape, 2011).

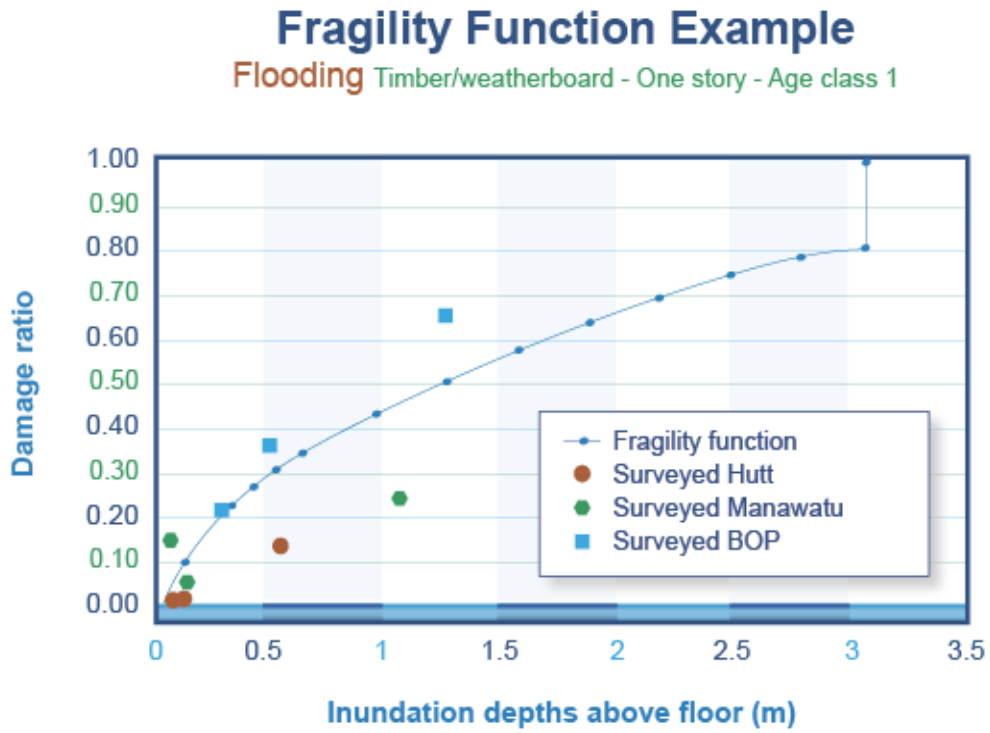


Figure 1. Flood fragility function for a one storey timber weatherboard building. Acquired from RiskScape (2011), accessed 3/5/11.

In the natural risk engineering literature, vulnerability is defined on a scale from 0 (no loss/damage) to 1 (total loss/damage) (Zschau, 2010). Physical vulnerability is time-dependent and changes when it comes into contact with natural hazards. This can be seen in Figure 2, where an element's fragility function changes when subjected to an earthquake. Before an earthquake event, the element has a defined fragility curve, after the earthquake, the element's vulnerability is increased, making it more susceptible to damage than previously to a potential future earthquake. If a secondary hazard occurred at this stage, the potential losses would be greater as there would be an increase in the risk and vulnerability of the population following the primary hazard. Following reconstruction, the vulnerability of the element is reduced, as its coping capacity is improved.

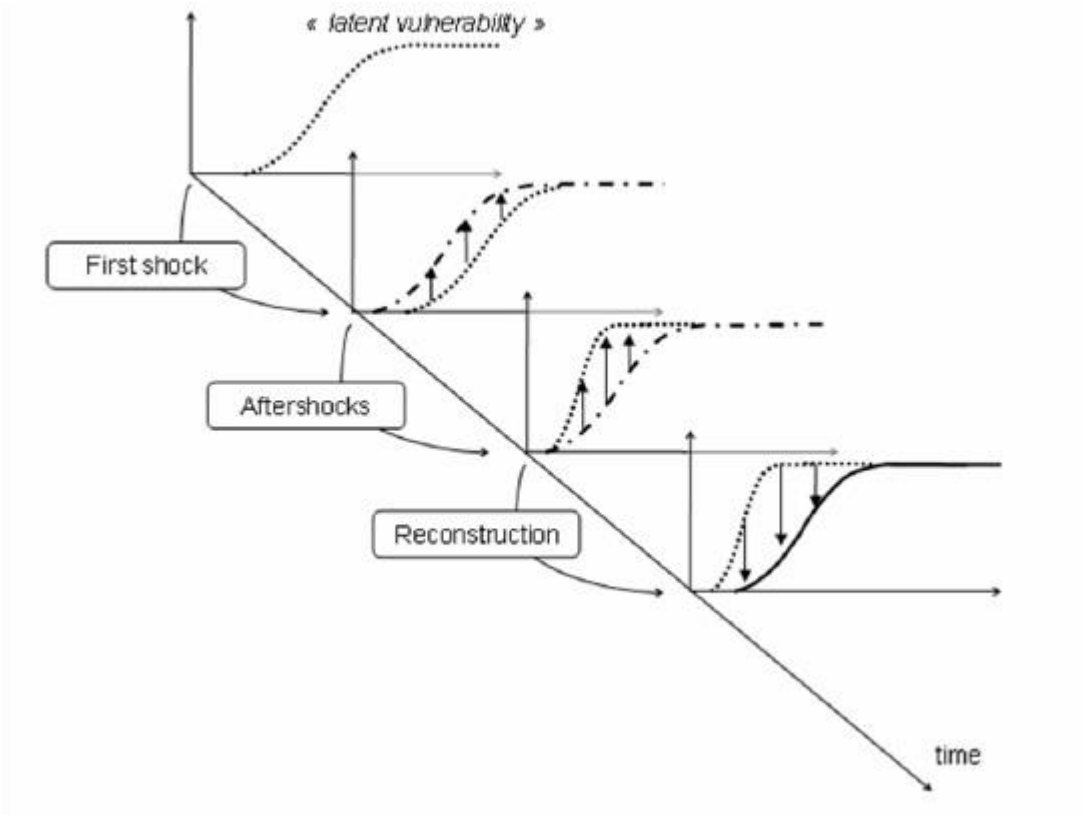


Figure 2. Possible evolution of an element's fragility function subjected to an earthquake. Acquired from Zschau (2010), fig 2, p12.

Carpignano *et al* (2009) suggest multi-vulnerability is required when examining the effect of hazards. Rather than examining the potential effect of an event on a single entity (for example population or economy), the effect on a variety of exposed sensitive targets should be examined, such as population, infrastructure, buildings, cultural heritage etc. (Carpignano *et al*, 2009).

## 4.0 Catastrophe Risk Modelling

Catastrophe, also referred to as 'cat', risk modelling developed out of spatial modelling in the late 1970s (Dlugolecki et al., 2009). Commercially available catastrophe risk modelling has been available for the past 25 years (Maynard et al., 2014). The three biggest cat risk modelling companies are AIR (1987), RMS (1988), and EQECAT (1994) (Maynard et al., 2014; Dlugolecki et al., 2009; Atkinson et al., 2011). Catastrophe modelling is now used by insurers, reinsurers, governments, and other financial markets (Maynard et al., 2014).

Although variations between catastrophe models exist, they are generally composed of four main parts: (1) a hazard component, (2) a vulnerability component, (3) a financial component, and (4) an exposure component (Figure 3).

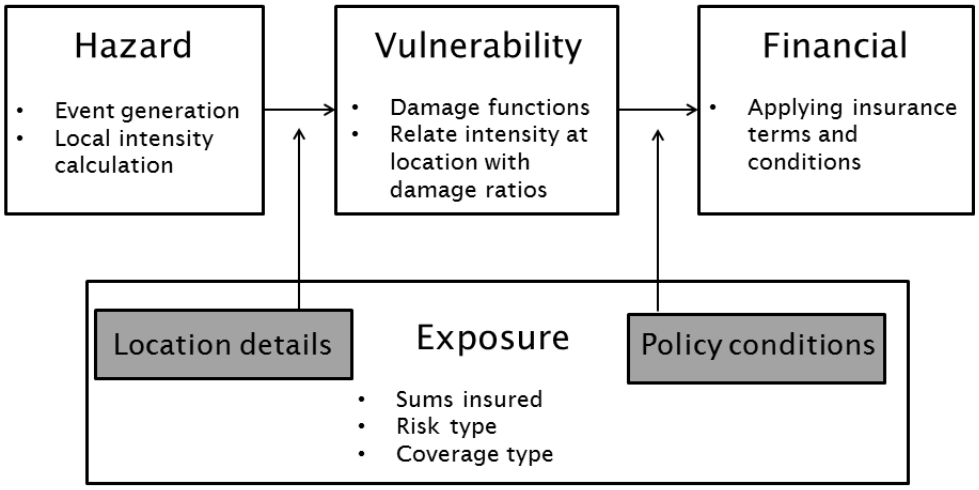


Figure 3. Key elements of a catastrophe model (adapted from Dlogolecki et al., 2009).

The hazard module simulates the relevant features of a hazard, such as the frequency, severity (intensity) and geographic location (Dlogolecki et al., 2009; Murnane et al., 2005). For probabilistic methods, this requires an extensive library catalogue of events; in most catastrophe models, these events are synthetic catalogues, comprised of imaginary but realistic events, representing the expected range of events expected at the location (Dlogolecki et al., 2009; Murnane et al., 2005).

The vulnerability component of the model calculates how structures respond to the hazard, describing the expected damage or insured losses (Dlogolecki et al., 2009; Murnane et al., 2005). They are typically based on observed relationships between hazard intensity (e.g. wind speed or flood depth) and the level of expected insured loss (as a ratio to total insured value) (Dlogolecki et al., 2009). This module also describes how losses vary with respect to type of asset.

The exposure component describes the geographical and physical properties of the asset, such as location, type and construction, and its value (Dlugololecki et al., 2009). The

physical properties can include aspects such as year built, construction type, and secondary characteristics such as roof material (Lloyds, 2013).

The financial, or loss, component estimates the value of claims the insurance company will be liable to pay by using the estimated damage to the property and applying the policy conditions (Dlugolecki et al., 2009). Maynard et al. (2014) highlight the cat modelling process is inherently complex, depending on multiple assumptions, which naturally result in a degree of uncertainty around the loss estimates.

If secondary hazards are included in the risk assessment, they are typically included in the vulnerability component of the model (Murnane et al., 2005). These are sometimes termed "follow-on" hazards or "perils" (Murnane et al., 2005; Atkinson et al., 2011). Examples of these "follow-on" hazards are fires following an earthquake and interior water damage from broken windows leading to rain entering buildings (Murnane et al., 2005).

### 4.1 AIR

AIR is a global provider of risk modelling software and consultancy service set up in 1987. It currently models risk from natural catastrophes and terrorism in more than 90 countries. The natural catastrophe models currently include earthquakes, extratropical cyclones, floods, severe thunderstorms, tropical cyclones, and wildfires.

The AIR United States Earthquake Model was first developed in 1990, with an earthquake-induced fire loss (fire-following model) added in 1991 (AIR, 2014). Today, the earthquake model includes most of the Americas, the Mediterranean region, and at-risk countries in the Asia-Pacific region (AIR, 2014). In 2009, AIR introduced nonlinear dynamic analysis (NDA), a detailed virtual representation of the effects to a building when shaken with dozens of actual ground motion records (AIR, 2014). In 2002, the first workers' compensation loss model for earthquake risk was added. In 2013, AIR was employed by the Insurance Bureau of Canada (IBC) to conduct a study of the impact and the insurance and economic costs of

earthquakes in two regions of Canada (AIR, 2013). Several new perils were added to the Earthquake Model for Canada; the final model contained shaking, fire following, tsunami, liquefaction, and landslides components (AIR, 2013).

AIR's extratropical cyclone model was first developed for Europe, pioneering the use of physical modelling in the insurance industry's first probabilistic catastrophe model to use numerical weather predication (NWP) (AIR, 2014). It was later expanded to the United States, using NWP technology to simulate distinct footprints, and separate damage functions, for damaging winds, precipitation, and freeze (AIR, 2014).

The AIR inland flood models have been developed for the United States, Germany, and Great Britain (AIR, 2014). A physical approach is used to develop fully probabilistic inland flood models (AIR, 2014). The severe thunderstorm model developed by AIR capture the effect of three perils: tornadoes, hail, and straight-line winds (AIR, 2014). Each peril has separate damage functions developed individually, and the severe thunderstorm model covers the United States and Canada (AIR, 2014).

AIR's U.S. Hurricane Model was developed 25 years ago, and today has been expanded to include tropical cyclone risk in 44 countries and territories across several ocean basins, as well as oil and gas platforms in the Gulf of Mexico (AIR, 2014). The tropical cyclone model incorporates high-resolution data on elevation, topography, land cover, and distance to coast, and a country-specific detailed industry exposure database is used to estimate industry loss (AIR, 2014). The model's damage functions capture building response to wind, and in some regions, precipitation-induced flooding and storm surge (AIR, 2014). The effect of climate change on tropical cyclones globally is an active area of research for AIR (AIR, 2014).

The wildfire model developed by AIR are fully probabilistic, using comprehensive data on vegetation (types, locations, densities and volatilities), and fire-spread algorithms which take into account topography, local wind-speeds and fire suppression activities (AIR, 2014). The

AIR California model incorporates an Urban Conflagration Effects (UCE), and the AIR Australia captures bushfire tendencies to cluster in space and time (AIR, 2014).

### 4.2 RMS

Risk Management Solutions (RMS) models risk in nearly 100 countries (Figure 4), covering North America, South America, Europe, Asia, Australia and Oceania, and the Middle East (RMS, 2014). The hazard models include earthquakes, hurricanes, windstorms, severe convective storms, winter storms, floods, terrorism, pandemics, and longevity (Figure 4) (RMS, 2014). The earthquake model includes ground shaking and tsunami components (Tabucchi and Grossi, 2012).

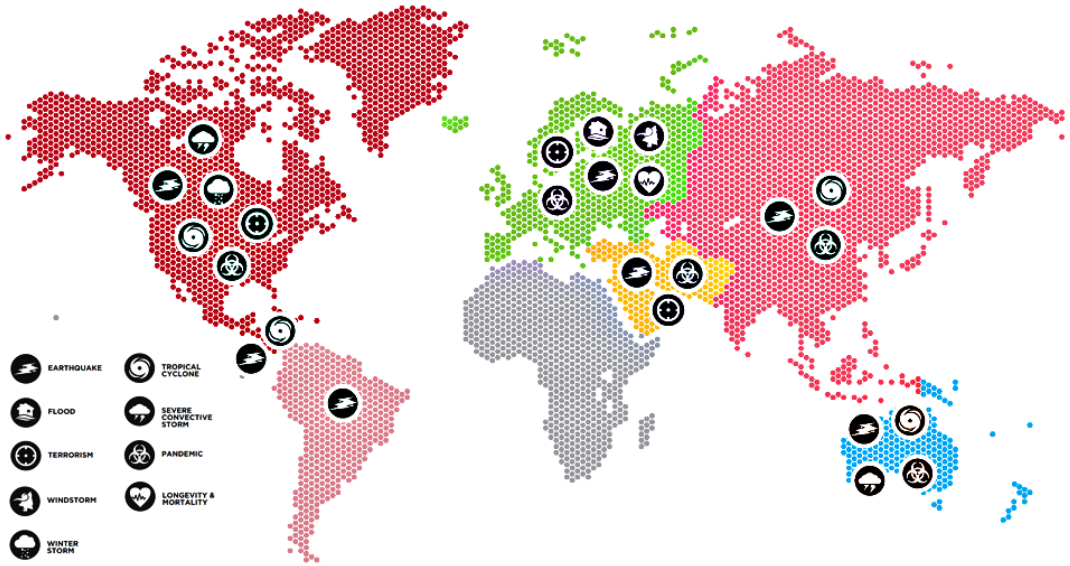


Figure 4. Location and type of hazards covered by the RMS catastrophe model suite globally. Acquired from RMS (2014).

The US hurricane model integrates into its suite a hydrodynamic, time-stepping storm surge model, simulating the complex interactions between wind and waves throughout the hurricane life-cycle (RMS, 2014). The model accounts for the changes of a storm's intensity of size whilst at sea, and the build-up of surge prior to landfall, and the dynamic flow of water around complex coastlines (RMS, 2014). The storm surge model combines with a

coastal flood model from Texas to Maine in the US, and in the Bahamas, Cayman Islands, and the Turks and Caicos Islands in the Caribbean (RMS, 2014).

### 4.3 EQECAT

EQECAT's 180 natural hazard software models for 96 countries spanning six continents include earthquakes, floods, hurricanes, severe convective storms (tornado/hail), typhoons, tropical cyclones, wildfires, windstorms, winter storms, and offshore energy (EQECAT, 2014). It hosts a RQE (Risk Quantification and Engineering) catastrophe risk modelling software platform, providing clients the ability to quantify and manage the potential impact of natural hazards financially (EQECAT, 2014).

EQECAT's 88 earthquake models have incorporated time dependence since 1998, soil based attenuation since 2005, and pioneered 3D vulnerability function to represent seismic performance of residential exposure in 2005 (EQECAT, 2014). The models have regional vulnerability components and include coverage of Latin America, Japan, Europe, Canada, and Australia. Both the Canada and Japan models include modelling sub-perils of fire-following earthquake and sprinkler leakage. The fire-following component incorporates a ground-up methodology, covering the physical mechanism of conflagration, ignition, spread, and suppression (EQECAT, 2014). The Japan earthquake model also includes a personal accident component, and ground failure hazards can be modelled using secondary modifiers when their potential is known (EQECAT, 2014).

The flood models developed by EQECAT cover both the United States and European regions. The Euroflood model covers both riverine and off-plain flooding, precipitation-induced events, and flood defence failure propagation (EQECAT, 2014). Flash flooding as a result of flowing water, coastal storm surge, mudslides, and drainage system backup is not modelled (EQECAT, 2014).

The North Atlantic Hurricane Model for the US, Caribbean, and Bermuda developed by EQECAT contains a storm surge hazard component (EQECAT, 2014). The storm surge model is a numerical finite-element model, which takes into account bathymetry and wind stress (EQECAT, 2014). The European windstorm model also contains a model for storm surges in the UK, France, and Sweden (EQECAT, 2014). EQECAT's Asia typhoon model assesses damage caused by sub-perils such as extreme wind damage to structures, damage due to storm surge, and rainfall-induced flooding (EQECAT, 2014). The U.S. severe convective storm model for tornado and hail risk has separate damage functions for structures and automobiles to hail vulnerability, and models for damage from tornadoes, and straight-line wind events spanning multiple states (EQECAT, 2014).

EQECAT's U.S. offshore energy model is a fully probabilistic risk model quantifying prospective risk from hurricanes in the Gulf of Mexico (EQECAT, 2014). It has hazard components for wind, waves, landslides, and sub-sea currents (EQECAT, 2014).

## 5.0 Multi-Hazards

Natural processes such as hazards are connected and affect each other, however are often studied discretely in science (Kappes *et al*, 2010b). The approach of multi-hazard research previously has been to treat hazards as occurring independently of each other. Multi-hazard risk assessments typically aggregate risk from single hazards. This does not account for the interaction between natural hazards. Research into interacting hazards has become of interest recently. However very few studies have been undertaken to quantify and explore these relationships (Kappes *et al*., 2012; Duncan *et al*., 2013, Gill and Malamud, 2013). Neither a uniform conceptual approach nor generally used terminology is applied to the concept of interacting hazards (Kappes *et al*., 2012).

## 5.1 Cascading Hazards: Definitions

A diverse range of terms are used in reference to the interaction between natural hazards. The term ‘cascading hazards’ is typically used to describe the phenomenon whereby one hazard triggers another, which triggers another and so on, so that the situation worsens (Helbing and Kuhnert, 2003). Delmonaco *et al* (2007) define the domino effect or cascading failures as ‘a failure in a system of interconnected parts, where the service provided depends on the operation of a preceding part and the failure of a preceding part can trigger the failure of successive parts’. This phenomenon is also referred to as the ‘avalanche’ or ‘domino’ effect or a catastrophe ‘chain’ by Helbing and Kuhnert (2003). Helbing *et al* (2005) demonstrate the interconnected network of natural hazards, linking the effects and causation of each hazard (Figure 5).

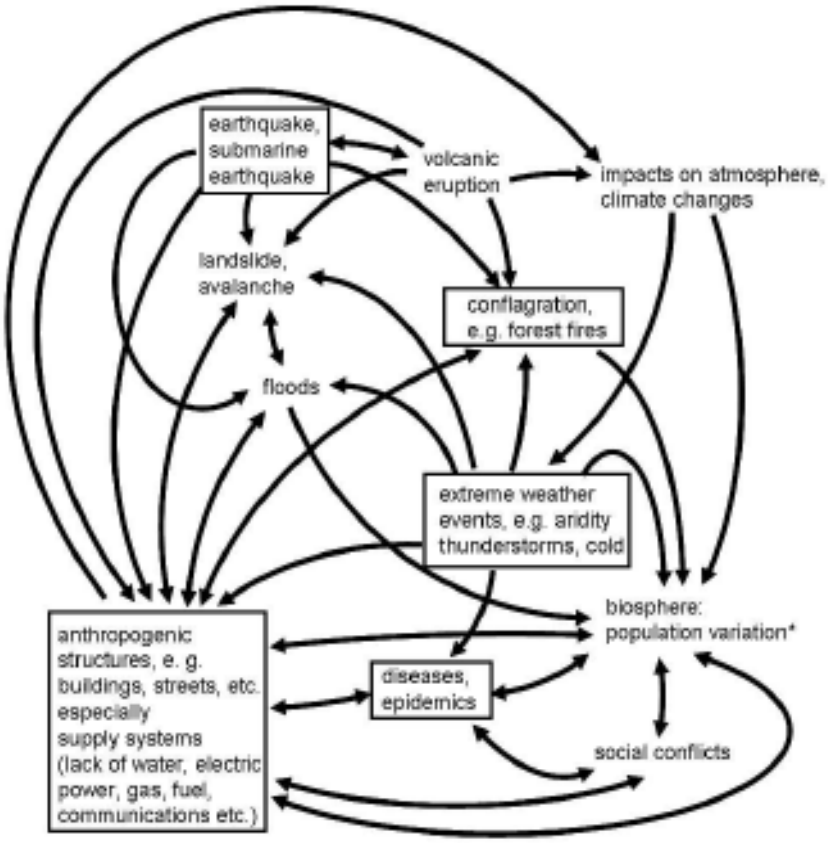


Figure 5. Taken from Helbing *et al*, 2005, p14. The figure illustrates the interconnected network of one hazard affecting another.

A multitude of terms are used in the literature to describe various types of relationships between hazards (Table 1) (Kappes *et al*., 2012). Precise definitions of the terms are rare, and often implicit understanding is assumed without further exploration or description (Kappes *et al*., 2012).

Table 1. Terms used in the literature to describe several types of relationships between processes. Taken from Kappes *et al* (*2012*), p11.

| **Terms** | **References** |
|---|---|
| Cascades, cascading effects, cascading failures, or cascade events | Delmonaco *et al*. (2006b), Carpignano *et al*. (2009), Zuccaro and Leone (2011), European Commission (2011) |
| Chains | Shi (2002), Erlingsson (2005) |
| Coincidence of hazards in space and time | Tarvainen *et al*. (2006) |
| Coinciding hazards | European Commission (2011) |
| Compound hazards | Hewitt and Burton (1971), Alexander (2001) |
| Coupled events | Marzocchi *et al*. (2009) |
| Cross-hazards effects | Greiving (2006) |
| Domino effects | Luino (2005), Delmonaco *et al*. (2006b), Perles Rosello´ and Cantarero Prados (2010), European Commission (2011) |
| Follow-on events | European Commission (2011) |
| Interactions | Tarvainen *et al*. (2006), dePippo *et al*. (2008), Marzocchi *et al*.(2009), Zuccaro and Leone (2011) |
| Interconnections | Perles Rosello´ and Cantarero Prados (2010) |
| Interrelations | Delmonaco *et al*. (2006b), Greiving (2006) |
| Knock-on effects | European Commission (2011) |
| Multiple hazard | Hewitt and Burton (1971) |
| Synergic effects | Tarvainen *et al*. (2006) |
| Triggering effects | Marzocchi *et al*. (2009) |

For clarification, the interaction between multiple hazards can be divided into four types of relationships or effects (Duncan et al., 2013):

1) *Causation.* Whereby one hazard triggers another. Without the primary hazard, the secondary hazard would not have occurred. An example of this is earthquake shaking triggering a landslide.

2) *Association.* The probability of a secondary hazard occurrence is increased as a result of the primary hazard. For example, wildfires can cause an increase in probability of flooding occurrence as the interception of vegetation is reduced and the ground is less permeable.

3) *Coincidence.* When two (or more) hazards occur in the same spatial and temporal space. They may not have any causative link between them. An example of this is a volcanic eruption occurring at the same time as a hurricane.

4) *Amplification.* Whereby one hazard exacerbates the effect of another hazard. An example could be a hurricane causing landslides which affects the area hit by the initial hurricane.

These four types are not mutually exclusive. For example, an earthquake can cause a volcanic eruption, it also increases the probability of a volcanic eruption, and the effects of the earthquake are amplified. These terms can help to understand the concept of interacting hazards.

### 5.1.1 Causation

The causation effect can also be described as serial chains, cascades or synergistic events; a succession of disaster events caused by a single hazard with the resultant disasters happening in turn (Shi, 2005; Marzocchi *et al*, 2009). The primary triggering event affects the physical system, causing a secondary hazard to occur. This secondary hazard can, in turn cause a tertiary hazard and so on. Most previous research into cascades has been conducted related to power grid failure (Motter, 2004) and industrial accidents (Glass *et al*, 2008). There have, however, been recent publications on the topic of cascades in relation to disaster management (Helbing *et al*, 2005; Helbing and Kuhnert, 2003); modelling disaster dynamics spreading in networks (Buzna *et al*, 2006); and efficient post-disaster response (Buzna *et al*, 2007 and Peters *et al*, 2008).

Many hazards are connected in pairs, whereby one can trigger the other (Figure 6). Examples of this are earthquake-induced landslides during the 1994 Northridge, California event (Harp and Jibson, 1996); volcano-induced tsunami from Tambora in Indonesia in 1815 (Oppenheimer, 2003); hurricane-induced storm surge and flooding in New Orleans during Hurricane Katrina (Fritz *et al*., 2007); hurricane-induced landslides from Hurricane Mitch in Central America in 1998 (Bucknam *et al*., 2001); and the 2004 Sumatra-Andaman earthquake-induced tsunami (Lay *et al*., 2005).

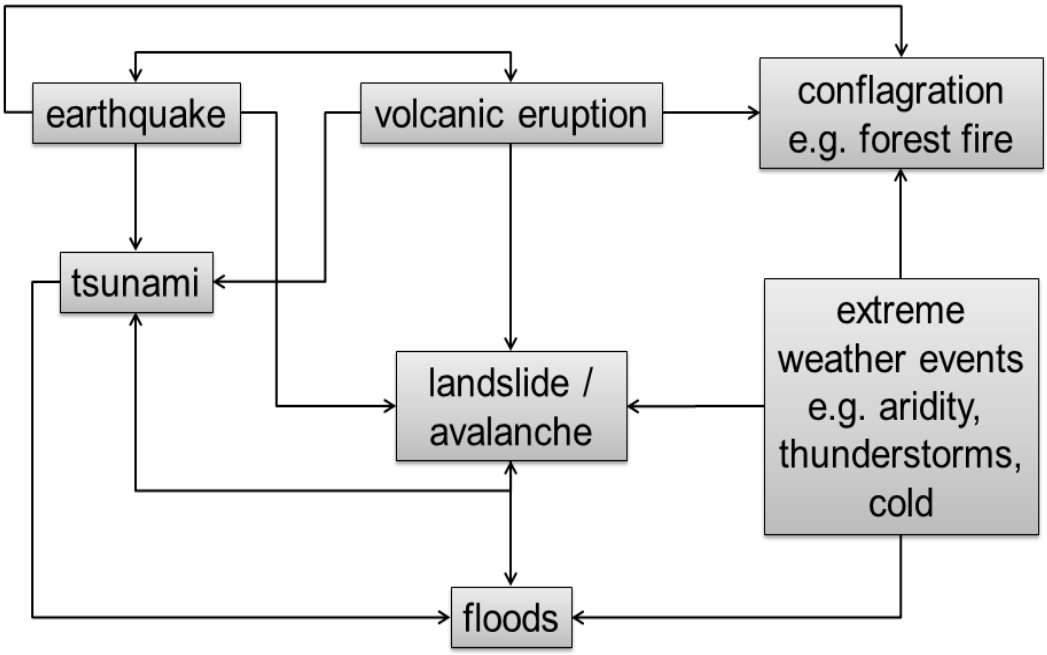


Figure 6. Diagram showing links between a selection of natural hazards.

### 5.1.2 Association

The association effect can in part be covered by the causation principle described above. However, the causation principle refers more exclusively to short term triggers – an almost immediate effect is seen when one hazard triggers another; for example earthquakes triggering a landslide. The idea behind the association of hazards is increasing the probability of one hazard as a result of another; this incorporates longer-term relationships such as wildfires increasing the probability of flooding (Jordan *et al*., 2006; Curran *et al*., 2006). De Graff *et al* (2007) describe the 'fire-flood cycle', whereby forest fires remove vegetation, increase runoff rates and sediment washout, causing an increase in subsequent floods and debris flows (in Kappes *et al*, 2010b).

Following a wildfire, several hydrological changes can occur which result in a higher probability of flooding (Jordan *et al*., 2006). The burning of the organic forest floor litter can create hydrophobic compounds to accumulate below the surface, creating water repellent soil conditions (Jordan *et al*., 2006; Curran *et al*., 2006). The removal of the forest canopy

and litter layer eliminates forest floor water storage capacity and the interception capacity (Jordan *et al*., 2006; Curran *et al*., 2006). Less evapotranspiration, increased snow accumulation and potentially higher groundwater levels and exposure of the underlying sediment to erosion can all cause hydrological changes (Jordan *et al*., 2006). During subsequent heavy rainfall, flooding is more likely to occur compared to the pre-fire conditions.

### 5.1.3 Coincidence

The coincidence of natural hazards refers to simultaneous events, when multiple hazards cluster at the same time and space and cause several disasters concurrently (Shi, 2005). There is not necessarily a direct causal relationship between the hazards, but they do interact with each other. An example of this is earthquakes and hurricanes; earthquakes do not cause hurricanes to form, yet they can occur in the same spatial and temporal location. Hurricane Irene hit Virginia and the Washington D.C area on August 27$^{th}$ 2011, just four days after a magnitude 5.8 earthquake occurred (Beavers *et al*., 2012; Jibson and Hart, 2012).

Similarly, hurricanes can exacerbate fires either caused by earthquakes or by natural processes despite the precipitation during the hurricane event. In Hokkaido, September 1954, 3300 buildings were destroyed due to hurricane generated winds spreading fires over Japan (Bryant, 2005). Similarly, 1100 buildings were destroyed in Niigata in October 1955 as a result of hurricane winds fanning fires caused by an earthquake (Bryant, 2005).

Determining between coincidence and causation is challenging to conclusively separate. Due to the complex nature of hazards and their effect on the physical environment, it is often difficult to establish a 'no-relationship' between various hazards. For example, it is not widely practiced to use hurricane or strong rain occurrences as an indicator for a volcanic eruption. However, some studies suggest that severe weather can trigger a volcanic eruption (Matthews *et al*., 2002; Elsworth *et al*., 2004). There appears to be a relationship between the wettest time of year and volcanic eruptions recorded at Yasur, Mt Etna, Mt St Helens and

Soufrière volcanoes (Elsworth *et al*., 2004; Matthews *et al*., 2002; Bryant, 2005). It is hypothesised that the rainwater seeps into the volcano and causes an eruption when it makes contact with the magma chamber as the water immediately turns into steam and causes a blast (Elsworth *et al*., 2004; Bryant, 2005).

Hurricanes have also been known to cause earthquakes due to the dramatic changes in pressure during a hurricane's passage (Bryant, 2005). A hurricane can cause a de-loading of the crust of 2.3 million tonnes per $km^2$ over a few hours (Bryant, 2005). A storm surge 6-7 m high from the hurricane can increase load on the crust up to 7 million tonnes per $km^2$ (Bryant, 2005). The total change in load over the Earth's crust from a hurricane can therefore measure 10 million tonnes per $km^2$, causing an earthquake (Bryant, 2005). The Pacific plate and plate boundaries in the Caribbean Sea are susceptible to this phenomenon. In Central America, the probability of an earthquake occurring given a hurricane event is greater than the sum of the probability of an earthquake and a hurricane separately (Bryant, 2005).

### 5.1.4 Amplification

The amplification effect of hazard chains, whereby the overall hazard and potential losses from causally linked processes is amplified in comparison to the aggregation of presumed independent hazards, is acknowledged as an important aspect of cascading hazards (Kappes *et al*, 2010b; Kappes *et al*., 2012; Greiving, 2006; Shi *et al*., 2010; Marzocchi *et al*., 2009; Zschau, 2010).

The amplification effect can either be due to chaining (whereby one hazard triggers and increases the effect of the next hazard) or a consequence of the spatial and temporal coincidence of both (Kappes *et al*, 2010b).

Tokyo experienced an earthquake in 1923 following a typhoon on 1st September (Visher, 1924; Bryant, 2005). The swift spread of fire (initiated by the earthquake shaking) is largely attributed to the hurricane winds fanning the flames (Visher, 1924). An estimation of

approximately three hundred thousand additional deaths were attributed to the hurricane winds increasing the severity of the fires (Visher, 1924). Visher (1924) noted the occurrence of the typhoon and severe earthquake together 'greatly augmented' the loss of life and property.

The aggregation procedure currently applied in multi-hazard and multi-hazard risk assessments does not take into account the interrelations between hazards and the possible 'exacerbating of ameliorating effects' of such interrelations (Greiving, 2006). The 'simple sum method or weighted sum method can hardly reflect objectively the losses arising from multiple hazards' (Shi *et al*., 2010). Considering each source of hazard as independent from the others using the aggregation of single risk indices could underestimate the potential risk arising from multiple hazards (Marzocchi *et al*., 2009). There is consensus among most literature assessing multi-hazards that the sum of the individual hazards or risks do not adequately account for the total risks from multiple hazards interacting (Greiving, 2006; Shi *et al*., 2010; Marzocchi *et al*., 2009; Kappes *et al*., 2010b; Kappes *et al*., 2012).

There are numerous acknowledgements in the multi-hazard literature of the occurrence and importance of the amplification effect and the need to consider and incorporate this effect into multi-hazard research (Greiving, 2006; Shi *et al*., 2010; Marzocchi *et al*., 2009; Kappes *et al*., 2010b; Kappes *et al*., 2012). However, few studies quantify or explicitly explore this principle. In Kappes *et al*.'s (2012) review of multi-hazard risk, it was noted that no studies exist which separate out the losses from separate hazards in a disaster chain; '…studies dealing with sequential damages and/or with the separation of the respective impact of each one of the processes (e.g., earthquake followed by tsunami or earthquake followed by landslide) have not been found' (Kappes *et al*., 2012). Kappes *et al*. (2012) suggest event trees can be used to study the amplification effects of interacting hazards in more detailed, local studies.

## 5.2 Vulnerability

Vulnerability determines the likelihood and scale of damage from the impact of a given hazard. The elements at risk such as people, buildings and infrastructure are vulnerable in different ways to different hazards. For example, the type of roof material has a significant contribution to the vulnerability of a building to wildfire, whereas it has no effect on the building's vulnerability to a flood (Table 2).

Table 2. Relative contribution of building characteristics to vulnerability (Granger *et al*. 1999; in Kappes *et al*., 2012). The number of stars reflects the significance of the contribution.

| **Characteristic** | **Flood** | **Wind** | **Hail** | **Fire** | **Quake** |
|---|---|---|---|---|---|
| Building age | *** | ***** | ** | ***** | ***** |
| Floor height or vertical regularity | ***** | * | | **** | ***** |
| Wall material | *** | *** | ***** | **** | **** |
| Roof material | | **** | ***** | **** | *** |
| Roof pitch | | **** | *** | * | |
| Large unprotected windows | ** | ***** | **** | ***** | ** |
| Unlined eaves | | *** | | ***** | |
| Number of stories | **** | ** | | * | ***** |
| Plan regularity | ** | ** | | *** | ***** |
| Topography | ***** | **** | | **** | *** |

As hazards overlap spatially and temporally, the hazard interactions may not only influence the severity of the hazard, but also the vulnerability of the elements at risk (Kappes *et al*., 2012). The vulnerability of a building can be altered by the simultaneous impacts of several hazards. For example, a building's ability to withstand seismic shaking is affected by whether the building is covered by ash or snow (Lee and Rosowsky, 2006 and Zuccaro *et al*., 2008, both in Kappes *et al*., 2012). Loading of the roof affects the structural properties of the building (Kappes *et al*., 2012). Summing of the individual vulnerabilities or separate analysis cannot capture the effect of these modifications (Kappes *et al*., 2012).

Temporal changes in vulnerability refer to the sequential impacts or the cumulative effect of multiple hazard impacts on a building (Kappes *et al*., 2012). This is where exposed elements are made more vulnerable to hazard B due to the previous hazard A. For example, an earthquake damaged building is more vulnerable to the succeeding landslide than it had been before the earthquake (Figure 7) (Zschau, 2010; Kappes *et al*, 2010b). As the structure has already been damaged by the initial earthquake shaking, the impact of the subsequent landslide will likely be greater than in the case of an intact building (Zuccaro *et al*., 2008; in Kappes *et al*., 2012).

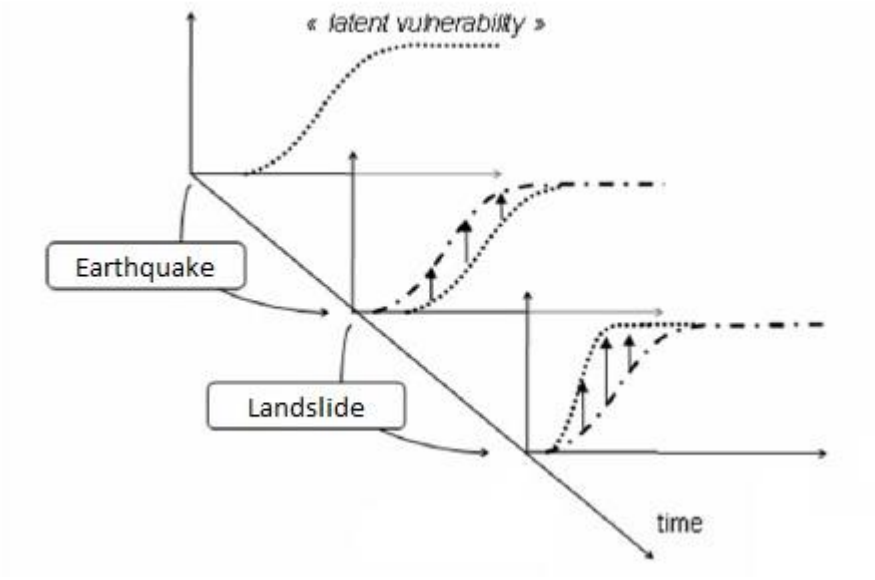


Figure 7. Temporal changes in vulnerability as a result of the primary hazard (earthquake), making it more vulnerable to the secondary hazard (landslide). Adapted from Zschau (2010), fig 2, p12.

## 5.3 Comparability of different hazards

A difficulty in multi-hazard assessment is that hazards have different measurements and scales (Zschau, 2010). Natural hazards all act differently, with disparities in their 'nature, intensity, return periods, and […] effects they may have on exposed elements' (Carpignano *et al*, 2009). Developing an overall scheme to compare hazards is therefore a major challenge (Kappes *et al*, 2010a and 2010b). The varieties of models used to examine hazards

are adapted for specific hazard characteristics, varying in type, applicability to scales and uncertainty of results (Kappes *et al*, 2010a).

Delmonaco *et al* (2007) argued that multi-hazard multi-risk assessment should not be implemented as a combination of hazard categories (e.g. superimposing individual hazard maps and summing the hazard degrees) as this assumes an equivalent level of hazard between types of hazards (e.g. 'high' flood hazard and 'high' earthquake hazard are assumed equal). This approach is often found in practical, state of the art applications, such as the Hotspots report (Delmonaco *et al*, 2007).

In order to create a harmonized assessment of multi-hazards, a comparable scheme needs to be created initially. Two approaches can be used to compare hazards: 1) creating units of hazard or risk, and 2) comparing the outcome of hazards.

### 5.3.1 Units of hazard

The choice of reference units to compare multiple hazards varies between 1) the classification of hazards (qualitative approach) and 2) the development of indices (semi-quantitative approach).

The qualitative approach uses intensity and frequency thresholds to classify hazards into a predefined number of classes, typically *high, medium,* or *low* hazard or risk (Delmonaco *et al*., 2007; Kappes *et al*., 2012). This method is used in the ARMONIA (Applied Multi Risk Mapping of Natural Hazards for Impact Assessment) project, the Swiss guidelines for analysis and evaluation of natural hazards, and the French risk prevention plans (Plan de Prévention des Risques naturales prévisibles, PPR) (Kappes *et al*., 2012). These classification schemes offer a simple way of comparing different natural hazards. However, they are designed for a specific situation, application or study and are restricted in their use (Kappes *et al*., 2012).

The indices approach offers a continuous standardisation of not directly comparable parameters. Classified single-hazard magnitudes, frequencies and proportions of the potentially affected area are used to create indices for each hazard. An example of this is the World Bank's Global Risk Analysis and the Simple Multi-hazard Index (Dilley *et al*, 2005). Single hazard risk analyses are divided into deciles, the first to fourth deciles indicate low, the fifth to seventh medium, and the eighth to tenth deciles indicate high hazard. In this way, the top deciles for each hazard are added together to create a map of multi-hazard risk (Dilley *et al*., 2005; Kappes *et al*., 2012).

Units of hazard or risk are useful tools in comparing single hazards and combining them into multi-hazard assessments (Kappes *et al*., 2012). However, the hazards are analysed separately, assuming independence from each other, summing individual hazards to create the overall hazard. This does not take into consideration the amplification effects of interacting natural hazards.

### 5.3.2 Hazard outcomes

Delmonaco *et al* (2007) suggested that the effects of hazards must be examined rather than the intensity of each hazard, in order to synthesise multi-hazards. It is easier to harmonize the effects of hazards, such as the expected damage to certain elements from each hazard, rather than estimate the size of hazards to compare for multi-hazard assessment (Delmonaco *et al*, 2007). Kappes *et al*. (2012) advocate using risk estimates as a method of comparing different hazards as, although emerging from different hazards, risk estimates are directly comparable.

## 5.4 Cascading Hazards in Cat Modelling

The type of secondary hazards or perils modelled in the three leading catastrophe modelling companies varies. The most common secondary hazards included are storm surge, fire following earthquakes, and precipitation-induced flooding during storms (AIR, 2014; RMS, 2014; EQECAT, 2014).

Typically, the risk modelling framework relies on the assumed independence of the hazard events (Atkinson et al., 2011). The model is characteristically run for a range of hazard types, and then combined to create a single EP curve (Atkinson et al., 2011). Understanding and accounting for the potential cascading/domino effects of multiple hazards interacting is rarely carried out (OECD, 2012). It is highlighted as an important need by many users by OECD (2012), yet requires specific modelling tools and a close cooperation and knowledge exchange between different fields of risk research (OECD, 2012). Standardised ways of dealing with cascading hazards globally in multiple hazard risk assessments is needed, but first rely on standardisation of data gathering and disaggregated data gathering to build databases of such events before this is achievable (Atkinson et al., 2011; OECD, 2012). Currently, only fire-following is treated in such a way (OECD, 2012).

There is little publicly available literature on the data, methodology, and source code used by cat risk modelling companies to compute risk assessments. Companies that develop risk models for in-house or licensing purposes keep their methods private for intellectual property reasons (Murnane et al., 2005). Therefore reviewing the strengths and weaknesses of the models is almost impossible to do from an outside perspective, particularly from an academic standpoint. Academic procedure requires the methodology and results to be available for public critique. However, in industry, the "black box" method is required to ensure secrecy against competition, with very little information about the inner details of the model released outside of the company (Pinho et al., 2008; Sarabandi, 2014; Latchman, 2014; Holland, 2014; Aita, 2014). In almost all cases detailed methodology and/or computer source code used to calculate risk is not publicly available (Murnane et al., 2005).

## 5.5 Multi-Hazards: Earthquakes and Landslides

Multi-hazard risk assessment has previously been neglected in favour of single-hazard risk analysis. Where multi-hazard risk assessment has been carried out, the risk posed by multiple hazards occurring in the same spatial location has been calculated by aggregating the single

hazard risk assessments for each hazard. This method does not take into consideration the symbiosis, interaction and cascading effects of natural hazards. There have been no studies that deal with 'sequential damages and/or with the separation of the respective impact of each' of the hazards in a cascading chain (Kappes *et al*, 2012).

Due to the time constraints of the PhD, it was impractical to research all interactions between all natural hazards. Therefore, developing on from the multi-hazard approach, the interaction between earthquakes and landslides was used as a focused example of cascading hazards. These phenomena have a sufficient body of research and available datasets to support further exploration of multi-hazard interactions.

## 6.0 Earthquakes

The death toll from earthquake events averages 10,000 people each year and causes US$400 million in property damage (Bryant, 2005). However, a single event can also kill many more than the yearly average (Bryant, 2005). Damage from earthquakes is not limited to shaking of the Earth causing damage to buildings and structures, which in turn can cause injury or death; there are several secondary or linked hazards which occur due to the initial earthquake event (Bryant, 2005). Earthquakes can lead to volcanic eruptions, landslides, liquefaction, tsunamis, fires and flooding from damaged dams or reservoirs (Bryant, 2005). Liquefaction or thixotropy can occur as a result of earthquakes when relatively firm clay-free soils and silts can behave like liquid due to the shaking from shear or compressional waves (Bryant, 2005).

Earthquakes can be compared based on the Richter scale developed in 1935. The magnitude of a local earthquake ($M_L$) is measured by the logarithm to base ten of the maximum seismic wave amplitude (to a thousandth of a millimetre) recorded on a seismograph 100 km from the epicentre of the earthquake (Bryant, 2005). Large seismic events require difference measuring scales. Seismic moment (Mw) is based on fault displacement surface area, average length of movement and rigidity of rocks fractured by the event (Bryant, 2005).

The measurement of surface magnitude requires seismographs. For occasions where these data are unavailable (due to lack of instrumentation or examining past occurrences), the Mercalli scale can be used (Bryant, 2005). The Mercalli scale is based on the damage inflicted by the earthquake at the epicentre, usually to the built environment (Bryant, 2005). The Mercalli scale can be loosely correlated with the Richter scale, as can be seen in Table 3.

Table 3. The Mercalli scale of earthquake intensity. Reproduced from Bryant (2005), p181, table 9.3.

| Scale | Intensity | Description of effect | Maximum Acceleration in mm $s^2$ | Corresponding Richter Scale |
|---|---|---|---|---|
| I | Instrumental | Detected only on seismographs | <10 | |
| II | Feeble | Some people feel it | <25 | |
| III | Slight | Felt by people resting; like a large truck rumbling by | <50 | <4.2 |
| IV | Moderate | Felt by people walking; loose objects rattle on shelves | <100 | |
| V | Slightly Strong | Sleepers awake; church bells ring | <250 | <4.8 |
| VI | Strong | Trees sway; suspended objects swing; objects fall of shelves | <500 | <5.4 |
| VII | Very Strong | Mild alarm; walls crack; plaster falls | <1000 | <6.1 |
| VIII | Destructive | Moving cars uncontrollable; chimneys fall and masonry fractures; poorly constructed buildings damaged | <2500 | |
| IX | Ruinous | Some houses collapse; ground cracks; pipes break open | <5000 | <6.9 |
| X | Disastrous | Ground cracks profusely; many buildings destroyed; liquefaction and landslides widespread | <7500 | <7.3 |
| XI | Very Disastrous | Most buildings and bridges collapse; roads, railways, pipes, and cables destroyed; general triggering of other hazards | <9800 | <8.1 |
| XII | Catastrophic | Total destruction; trees driven from ground; ground rises and falls in waves | >9800 | >8.1 |

Measurement of ground motion during an earthquake is useful in understanding the behaviour of buildings in earthquakes. Peak ground acceleration and peak ground velocity are the typical units of measurement to display spatial information about seismic shaking from an earthquake. Peak values of the horizontal amplitude of ground motion are used rather than the vertical component because on average, the vertical acceleration values are lower than the horizontal acceleration. Peak ground acceleration is measured in units of

percent-g (where g = acceleration due to the force of gravity = 9.8 m $s^{-2}$), peak ground velocity is measured in cm/sec.

ShakeMap produces maps of peak ground acceleration (as well as other seismic and loss information) for any significant earthquake event where the ShakeMap system is in place. Maps of shaking intensity can be combined with data on building infrastructure and population densities to produce estimates on losses and potential damage as a result of the earthquake shaking. These maps are vital for emergency responders in the immediate aftermath of an earthquake event for prioritising resources and response. ShakeMap uses empirically based ground-motion estimation in combination with geologically based simple frequency and amplitude-dependent site correction factors, providing a first-order correction for local amplification for regions without instruments. Peak ground acceleration and ground motion data are freely available in the USGS ShakeMap archive online for past significant earthquake events globally.

## 6.1 Shaking Software

The closed nature of cat models means researchers can only use them under limited circumstances, usually without the ability to modify their underlying methods, or be able to assess the methodology behind the black-box (Porter, 2007). Open source seismic hazard and risk models have recently been developed, allowing researchers to assess, modify, and use seismic hazard analysis (Porter, 2007).

### 6.1.1 Hazus-MH Earthquake Model

Hazus-MH is the Federal Emergency Management Agency's (FEMA) nationally applicable software program that estimates potential building and infrastructure losses as a result of multiple natural hazards in the United States. The model incorporates earthquakes, riverine and coastal floods, and hurricane winds. It uses ArcGIS to map and display hazard data, the

results of damage and economic loss analyses, and potential effects on area populations. It can be run in real time to support response and recovery actions following a disaster event.

The Hazus-MH earthquake module consists of three preliminary steps: (1) defining the earthquake hazard, (2) a catalogue of buildings and infrastructure, and (3) defining the relationship between ground shaking intensity and subsequent infrastructure damage (Remo and Pinter, 2012). The attenuation relationships describe the propagation of ground motion from the earthquake's epicentre to a specific location of interest (Remo and Pinter, 2012). Hazus-MH defines ground motion by two methods, using either: (1) probabilistic analysis, or (2) deterministic analysis. Probabilistic scenario earthquake hazard analysis is based on the USGS probabilistic hazard map data (Remo and Pinter, 2012). Deterministic analysis can be calculated using an "arbitrary earthquake scenario" or a "user-supplied hazard" (Remo and Pinter, 2012). For the "arbitrary earthquake scenario", the user selects their choice of attenuation function, event parameters (i.e. epicentre and magnitude), and soils data (Remo and Pinter, 2012). These are then used to apply the amplification factors and calculate peak ground acceleration spatially for the earthquake scenario (Remo and Pinter, 2012). The choice of input parameters can significantly affect the prediction of peak ground acceleration from an earthquake scenario (Figure 8) (Neighbors et al., 2013). The "user-supplied hazard" uses existing ground-motion data from the USGS ShakeMap archive (Remo and Pinter, 2012).

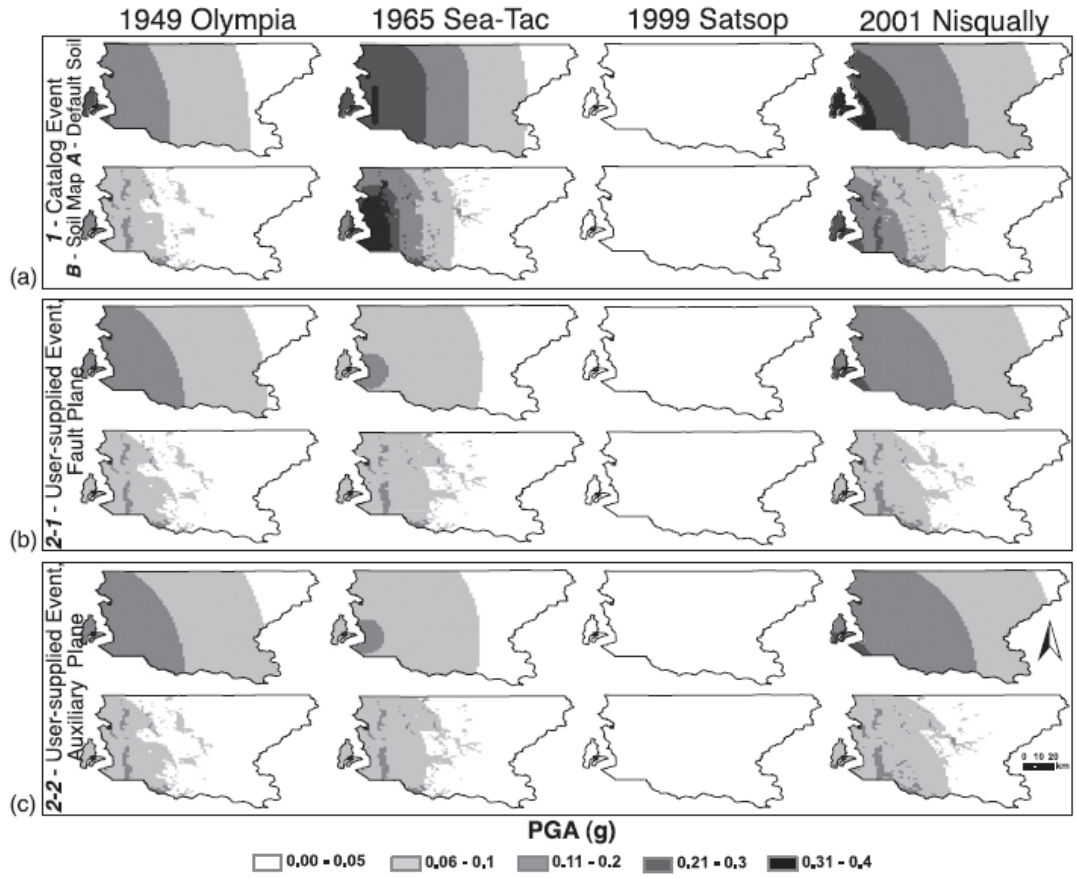


Figure 8. Maps of PGA for six HAZUS scenarios computed for each of three shallow earthquakes: (a) default source from HAZUS earthquake catalogue; (b) and (c) user-supplied sources with preferred fault-plane orientations and auxiliary fault-plane orientation, respectively (within each section, top row represents HAZUS default-site values, and bottom row represents user-supplied NEHRP site-specific soil conditions). Acquired from Neighbors et al., 2013, figure 6, page 140.

The model estimates the number of casualties from each hazard, however there is no indication of uncertainty or error within these calculated numbers; for example, Ploeger et al. (2010) estimated loss due to the scenario of a 6.5 magnitude earthquake in Ottawa using Hazus-MH. The simulation of the earthquake in Ottawa predicted 135 casualties (Ploeger et al., 2010). Remo and Pinter (2012) found earthquake damage, loss and casualty estimates are most sensitive to the seismic hazard data and selection of the attenuation function. Parameter selection can change loss estimates for a given earthquake scenario up to a factor of five (Neighbors et al., 2013; Kircher et al., 2006; Price et al, 2010; Remo and Pinter, 2012). Despite being openly available for use in the United States, the Hazus-MH model is not available for purchase or downloads outside the US.

### 6.1.2 Central American Probabilistic Risk Assessment: CAPRA

CAPRA was developed by the ERN-AL Consortium for the World Bank, the Inter-American Development Bank and the UN-ISDR to provide an open source model for governments to be able to assess hazard risks (Marulanda et al., 2013). The CAPRA model allows for evaluating losses on exposed elements using probabilistic metrics, useful for multi-hazard risk analyses (Marulanda et al., 2013). Software tools to model hazard frequency and intensity are contained in the hazard modules for a range of natural hazards: earthquakes, tsunamis, cyclone, floods, landslides and volcanic hazards. It permits a holistic evaluation of risk, not only the expected physical damage, but the conditions related to social fragility and lack of resilience (Marulanda et al., 2013).

The model was primarily developed for Central America, but since has been used to assess multi-hazard risk in case studies in the Caribbean, South America and in one case, Barcelona, Spain (Figure 9) (Marulanda et al., 2013). In the majority of cases, the model is used to estimate probabilistic losses on exposed elements using probabilistic metrics, but can also be used to estimate risk from a single event (Marulanda et al., 2013).

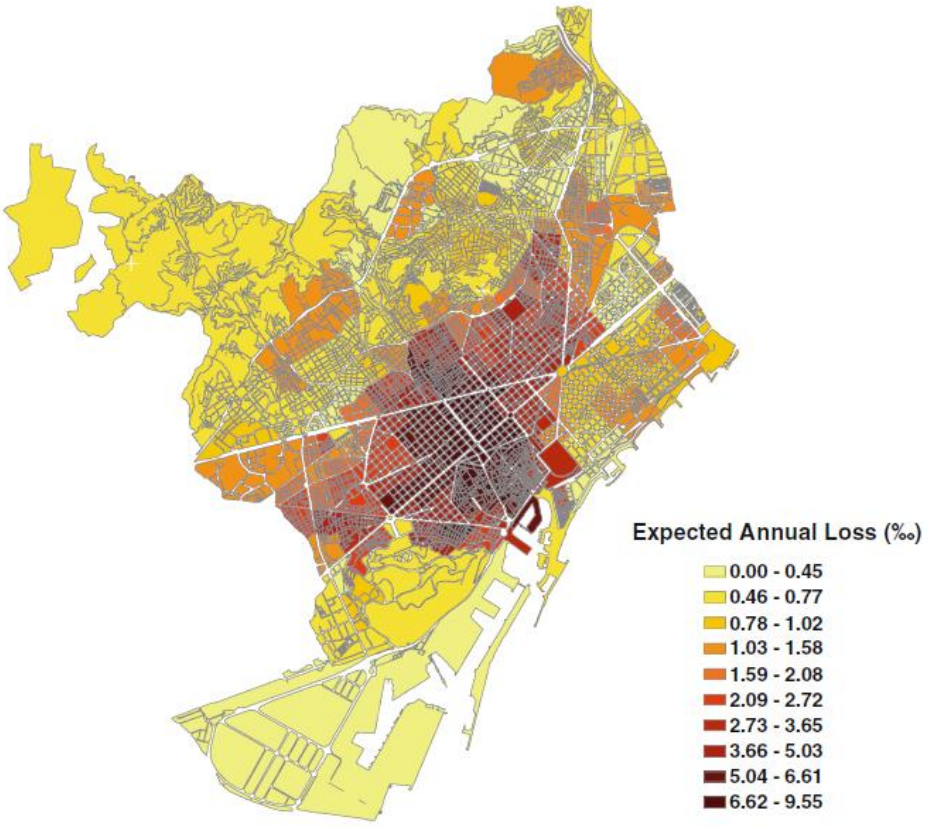


Figure 9. Expected economic annual loss for the basic statistical areas of Barcelona, calculated using CAPRA (Marulanda et al., 2013, figure 9, page 13).

The hazard module defines the frequency and severity of a peril, for example earthquakes, at a specific location, typically a city (Cardona et al., 2012). This is done by conducting an analysis of the historical event frequencies and a review of the scientific studies performed on the severity and frequencies in the region (Cardona et al., 2012). This analysis is performed at each new study site to develop hazard parameters specific to the study location. Then stochastic event sets are generated defining the frequency and severity of thousands of stochastic events (Cardona et al., 2012).

### 6.1.3 RiskScape

RiskScape is a software program developed to analyse potential impacts from various hazards in New Zealand (Reese et al., 2007). Five natural hazard modules are available for assessment in RiskScape: earthquake shaking, volcanic ashfall, river floods, wind storms, and tsunami (Reese et al., 2007). RiskScape was developed jointly by the National Institute

of Water and Atmospheric Research Ltd (NIWA) and the Institute of Geological and Nuclear Sciences (GNS Science) (Reese et al., 2007). A probabilistic approach is typically adopted when using the tool, but particular scenarios or historic events can also be simulated (Reese et al., 2007).

Earthquake hazard exposure fields are computed internally within the model (Reese et al., 2007). The earthquake model incorporates paleoseismic data, historical seismicity data, and attenuation relationships developed for New Zealand (Stirling, 2000). The attenuation relationships used in RiskScape are developed for 5% damped acceleration response spectra from a database of New Zealand earthquakes (Stirling, 2000). The models take into account the different tectonic types of earthquakes in New Zealand, such as crustal, subduction interface, and dipping slab (Stirling, 2000).

### 6.1.4 Earthquake Risk Model (EQRM)

Geoscience Australia's Earthquake Risk Model (EQRM) is an event-based tool for modelling the ground motion and loss associated with earthquakes (Dhu et al., 2008). It can be used in 'scenario mode' to model individual earthquake ground motion scenarios (Figure 10) and the financial loss due to building damage for an event of interest (Dhu et al., 2008). It can also be used in 'probabilistic mode' to generate a catalogue of synthetic events which are representative of 'plausible' events in the region, generating probabilistic seismic hazards (PSHA) and risk (PSRA) analysis (Dhu et al., 2008).

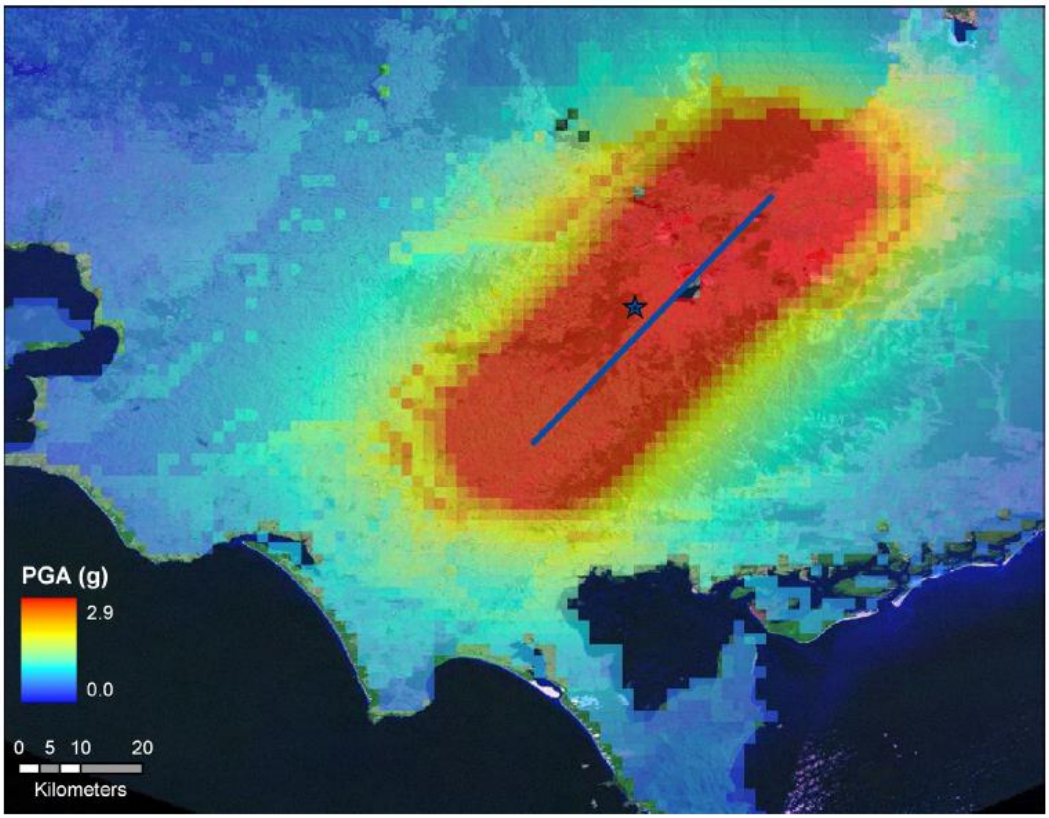


Figure 10. Modelled peak ground acceleration using EQRM for a Mw6.9 earthquake on the Morwell Moncline, Australia (Dhu et al., 2008, figure 1, page 4).

Local site conditions are incorporated using the site-class model and associated amplification factors of Dhu et al. (2002) to convert the bedrock ground motion to more realistic anticipated soil motions (Dhu et al., 2008). There are five attenuation models available for selection in EQRM (Table 4) (Robinson et al., 2006). Simulations of earthquake scenarios in the Latrobe Valley, Victoria, Australia and PSHA and PSRA modelling in the Newcastle, Australia region reveal the EQRM is sensitive to the choice of ground motion model(s) (Dhu et al., 2008).

Table 4. Attenuation models available in EQRM

| **EQRM Attenuation Relationships** |
|---|
| Gaull et al. (1990) |
| Toro et al. (1997) |
| Atkinson and Boore(1997) |
| Sadigh et al. (1997) |
| Somerville et al. (2001) |

### 6.1.5 OpenSHA

The OpenSHA application is an open-source, object-oriented (modular), multiplatform, web accessible, and graphical user interface (GUI) enabled computational infrastructure for seismic hazard analysis for anywhere worldwide (Field et al., 2005; Jordan and Field, 2006). It includes site effects by accounting for different soil types, hanging-wall effects, and basin depth responses, specific to each attenuation relationship (Field et al., 2005). By using GRID computing, the application accesses idle computers to expedite large computational problems (Jordan and Field, 2006). The goal of OpenSHA is to reduce the gap between cutting-edge geophysics and state-of-the-art hazard and risk evaluations (Jordan and Field, 2006).

The user can select either a point-source earthquake, or specify the rupture area for the earthquake scenario. An attenuation relationship must then be selected; the most basic attenuation relationship computes the ground motion as a function of magnitude and distance from the source, however many other parameters are included in other attenuation relationships, allowing for different site types (such as rock vs. soil) or styles of faulting. There are thirteen attenuation relationships which are available to be used in the OpenSHA tool (Table 29).

Table 5. Attenuation models available in OpenSHA

| **OpenSHA Attenuation Relationships** |
|---|
| Abrahamson and Silva (1997) |
| Abrahamson and Silva (2008) |
| Abrahamson (2000) |
| Boore and Atkinson (2008) |
| Boore, Joyner and Fumal (1997) |
| Campbell and Bozorgnia (2008) |
| Campbell (1997) |
| Chiou and Youngs (2008) |
| Field (2000) |
| Sadigh et al. (1997) |
| ShakeMap (2003) |
| Spudich et al. (1999) |
| USGS Combined (2004) |

Field et al. (2005) found when using OpenSHA to simulate earthquake events, the effect of different sediment types within the Puente Hills study site had an influence on ground motion within the model (Figure 11). The choice of ground motion model appears to be more influential on the peak ground acceleration outcome than the choice of input magnitude (Figure 11) (Field et al., 2005). Uncertainty from the ground shaking model accounted for at least a factor of two when used as the ground motion input to predict losses from the simulated earthquake event in the Puente Hills using the Hazus-MH model (Field et al., 2005).

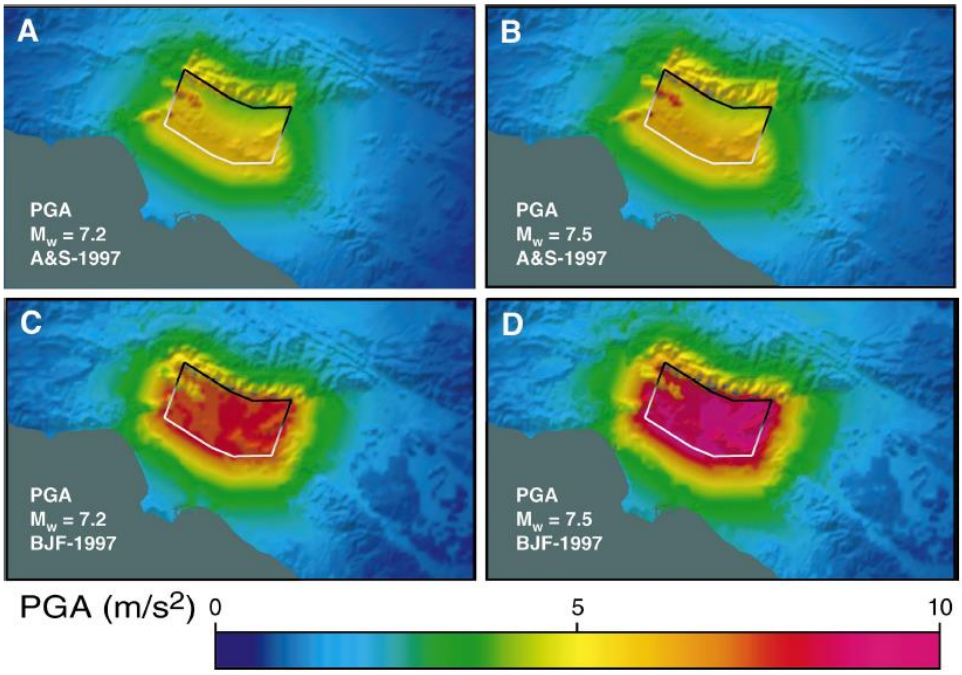


Figure 11. Earthquake shaking maps for some of the scenarios considered in the Field et al (2005) Puente Hills study. Mw is the earthquake magnitude, and the attenuation relationship labels are abbreviated: A&S-1997 represent Abrahamson and Silva (1997); BJF-1997 represents Boore, Joyner and Fumal (1997). The black and white line is the fault-rupture outline (dipping north). Acquired from Field et al., 2005, figure 1, page 3.

OpenSHA was chosen as the model to be used in the studies presented in this thesis to simulate earthquake ground shaking. This decision was based on several reasons, such as the freely available nature of the model; the model has been used to simulate multiple earthquake events in the United States, California in particular; and there are a large number of attenuation models available to choose from when simulating earthquake events. In

comparison, Hazus-MH is not available for use outside the United States. CAPRA, RiskScape, and EQRM were all developed initially for other countries or regions (South America, New Zealand, and Australia). A limited number of model simulations have been carried out in the United States using these models (none have been carried out using RiskScape). Lastly, OpenSHA has thirteen attenuation models to choose from, compared to the five available in EQRM. It has been observed that the choice of attenuation model has a significant effect on the generation of peak ground acceleration maps (Dhu et al., 2008; Field et al., 2005; Remo and Pinter, 2012). Thus, choosing shaking software which has a broad range of attenuation models available will allow for a greater chance of choosing the attenuation model which closest fits the observed peak ground acceleration data.

## 7.0 Landslides

Landslides are serious hazards which are common to many countries (Lu *et al*, 2007). Landslides globally cause thousands of deaths and billions of dollars of damage each year (Lu *et al*, 2007). During one event, thousands died in the Leyte province of the Philippines on 16$^{th}$ February 2006 due to a single debris flow triggered by heavy rainfall (Lu *et al*, 2007). Japan, India, Italy, Taiwan and the USA have an average yearly economic loss of billions of US dollars due to landslides; Canada, Nepal and Sweden have a loss of millions of US dollars (Metternicht *et al*, 2005).

Landslides occur mostly in five major types of terrain: upland areas subject to seismic shaking, mountainous environments with high relative-relief, areas of moderate relief suffering severe land degradation, areas with high rainfall, and areas covered with thick deposits of fine grained materials (Jones, 1995). There is a differentiation between the *preparatory* or *conditioning*, environmental factors which create a predisposed slope, and the *causative* or *triggering* factors of a landslide, which is the final event which causes failure (Figure 12) (Hervas and Bobrowsky, 2009). Conditioning factors making slopes susceptible to failure include geological conditions (such as soil/rock type, fractures in the rock), and

geomorphological character (such as slope angle, aspect, morphology) (Hervas and Bobrowsky, 2009).

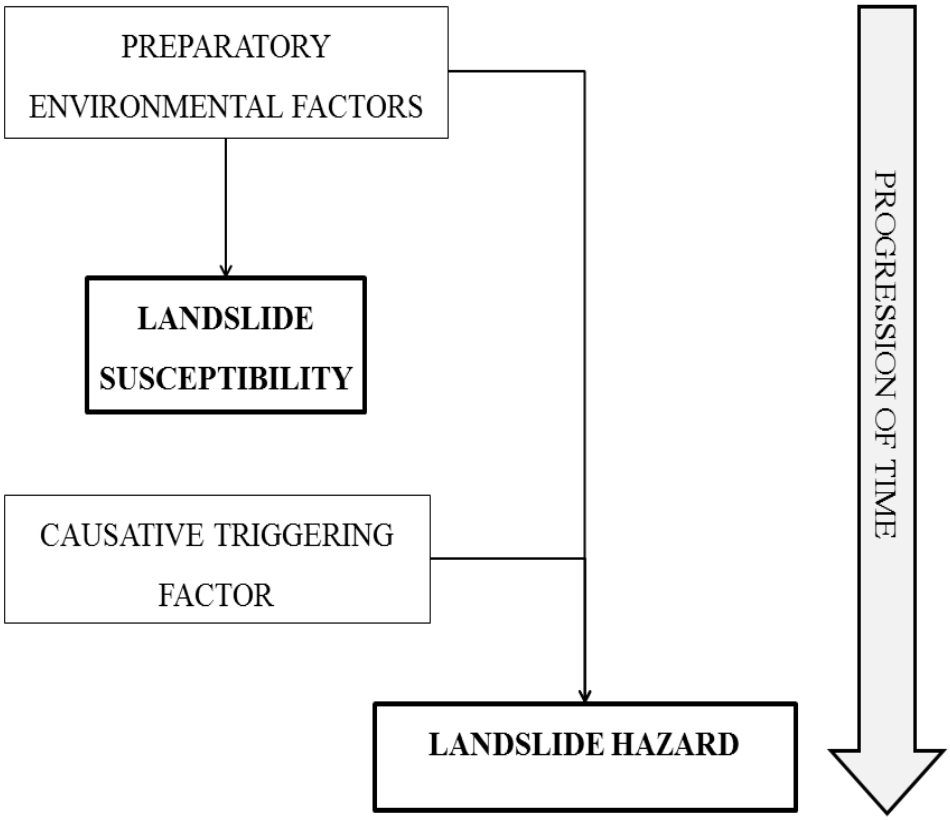


Figure 12. Conceptual diagram to clarify the distinction between preparatory landslide factors and landslide triggers. Based upon definition from Hervas and Bobrowsky, 2009).

## 7.1 Landslide Conditioning Factors

Slope gradient is a pre-requisite for any landsliding event to occur as without a gradient, land movement of the landsliding type is unable to occur. The definition of a 'landslide' inherently requires a slope to be present: "landslides are defined as a variety of processes that result in the *downward* and outward movement of slope-forming materials" (Sidle and Ochiai, 2006). Slope gradient can affect moisture concentration and pore pressure levels, indicating areas of instability (Ayalew and Yamagishi, 2005).

Aspect can exert an influence on landslide susceptibility as it affects hydrological processes such as evapotranspiration and, therefore, influences weathering processes and vegetation and root development (Chang et al., 2007; Sidle and Ochiai, 2006). In principle, north-facing slopes in the Northern Hemisphere could experience higher rates of rainfall-induced landsliding because they contain more moisture and are exposed to less frequent periods of wetting and drying compared to south-facing slopes (Sidle and Ochiai, 2006; Chauhan et al., 2010). The converse is true for the Southern Hemisphere. Similarly, aspect may be a common covariate significantly associated with landsliding, but the direction is typically site specific. Whilst slopes facing away from the influence of the sun will have greater soil moisture content and less frequent wetting and drying regimes, the most susceptible aspect will be the opposite for Northern Hemisphere slopes compared to Southern Hemisphere slopes. This underlying long-term susceptibility can also be undermined by influences such as the direction of frontal precipitation, direction of seismic propagation, lithological patterns, fault locations, and soil drainage patterns (Sidle and Ochiai, 2006).

Vegetation, particularly woody vegetation such as trees, can exert an influence on landslide susceptibility through reduction of soil moisture content through evapotranspiration, and/or through providing root cohesion to the soil mantle (Sidle and Ochiai, 2006; Dai et al., 2001). Land cover or land use can represent the vegetation type which can influence landslide susceptibility as previously covered. However, land cover also provides information on how the land is used, which can increase landslide susceptibility, such as clearing of forests and converting land to agriculture which reduces rooting strength and alters the soil regime (Sidle and Ochiai, 2006). Urban development can overload a slope with weak, poorly compacted material, remove support through excavation of hillsides, altering drainage patterns and removing or altering the root systems (Sidle and Ochiai, 2006).

Lithology defines the general physical characteristics of a rock or rock formation and can give an indication of the susceptibility of certain rock types to landsliding (Sidle and Ochiai,

2006). Lithology can influence landslide occurrence because rock types vary in strength and resistance against weathering (Das et al., 2010).

Elevation is associated with landsliding typically as an indicator of other factors such as slope gradient (steeper slopes in mountains which are high elevation), weathering, precipitation, ground motion (seismic amplification), soil thickness (thinner soils in higher elevations), and land use (Sidle and Ochiai, 2006).

Distance to drainage is typically associated with landsliding as it provides an indication of hydrological influences to landslides (Dai et al., 2001). Rivers can also increase susceptibility of proximal slopes due to undercutting of the hill toe (Suzen and Kaya, 2011;Bui et al., 2011).

### 7.2 Landslide Triggering Factors

In contrast to preparatory conditioning factors, triggering factors are the short-term processes which generate the landslide. Triggers of landslides include an increase in pore water pressure (typically from rainfall events), earthquake shaking and human activity (Smith and Petley, 2009; Bommer and Rodriguez, 2002). Rainfall-triggered landslides are strongly affected by four attributes: (1) total rainfall; (2) short-term intensity; (3) antecedent storm precipitation; and (4) storm duration (Sidle and Ochiai, 2006). These attributes influence the generation of pore water pressure in unstable hillslopes, leading to slope failure (Sidle and Ochiai, 2006). Earthquakes cause a shaking of the ground which can increase shear forces and reduce the resisting forces. The propagation of seismic waves result in horizontal acceleration of the soil mantle and cyclic loading and unloading of soils during an earthquake (Sidle and Ochiai, 2006; Hovius and Meunier, 2012). Hillslope failure occurs when the shear stress across a potential failure plane exceeds substrate strength (Hovius and Meunier, 2012). Human-triggered landslides occur for multiple reasons such as excavation into hillsides and removing support, removal of vegetation, concentration or redirection of

water into unsuitable locations, and placing poorly compacted fill materials on hillslopes (Sidle and Ochiai, 2006).

The triggering method has been shown to have a significant effect on the location and type of landslide; rainfall-triggered landslides occur in different locations to earthquake-triggered landslides. The trigger types are likely to be associated with different environmental factors, because their mechanisms and dynamics differ (Li et al., 2012; Chang et al., 2007). Taiwan is susceptible to both earthquake and rainfall induced landslides (Chang *et al*, 2007). Chang *et al* (2007) modelled earthquake triggered landslides and rainfall triggered landslides separately and assessed their accuracy based on observed data from the Hoshe basin in central Taiwan of landslides caused by four major typhoons between 1996 and 2005 and the Chi-Chi earthquake of 1999. They found earthquake-triggered landslides occurred in different locations to rainfall triggered landslides (Figure 13) (Chang *et al*, 2007).

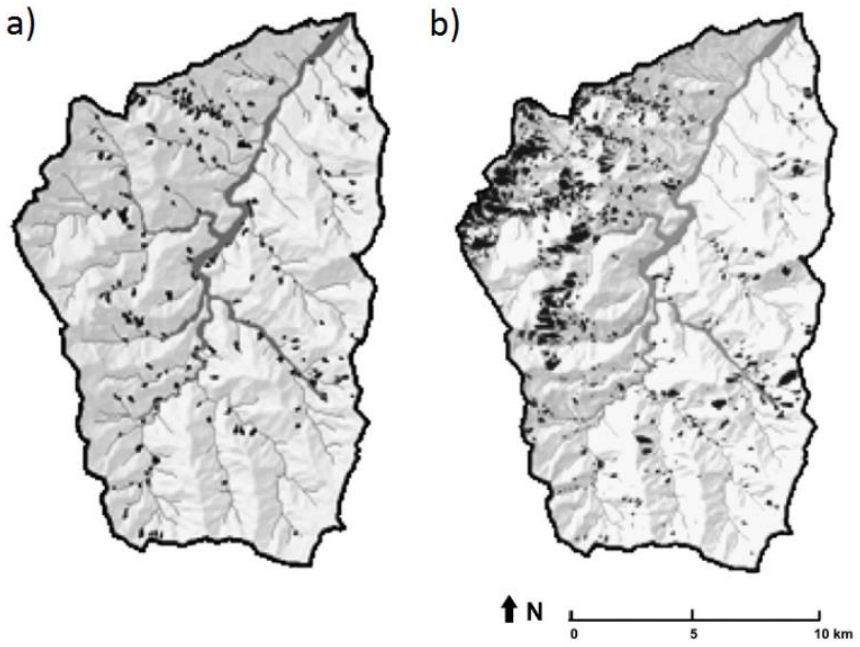


Figure 13. Distribution of landslides triggered by a) Typhoon Herb in 1996, and b) the Chi-Chi earthquake in 1999, taken from Chang *et al*, 2007, fig. 3, p339.

Earthquake induced landslides occurred near ridges, whereas rainfall-induced landslides occurred near streams (Chang *et al*, 2007). This pattern of coseismic landslides

predominantly detaching from upper hill slope portions is observed in other studies (Korup, 2010). This is attributed to topographic amplification of seismic shaking near these areas (Lin *et al*, 2008 in Korup, 2010). Chang *et al* (2007) suggests precipitation-induced landslides may have higher casualty rates compared to earthquake-induced landslides because they occur near streams and waterways, where people traditionally live, compared to ridges where earthquake-triggered landslides occur, which are typically less populated.

### 7.3 Physical Processes of Landslides

"Landslides occur when the shear strength of a soil layer in a slope becomes smaller than the shear stress acting on the soil, resulting in shear failure of the layer and movement of the slope along the slip surface or at the boundaries of soil layers" (Sidle and Ochiai, 2006). Factors affecting the shear strength of the soil and the shear stress acting on the soil cause landslides (Sidle and Ochiai, 2006). If all forces acting on the slope are balanced, the slope is stable and no landslide occurs (Figure 14). However, if there is a sufficient change in forces acting on the slope which exceeds a given threshold, landsliding occurs (Figure 14). The processes behind landslide generation include an increase in pore water pressure, increase in slope inclination, increase in slope weight, and earthquake ground motion. It is usually a combination of factors, rather than a single factor, which triggers a landslide.

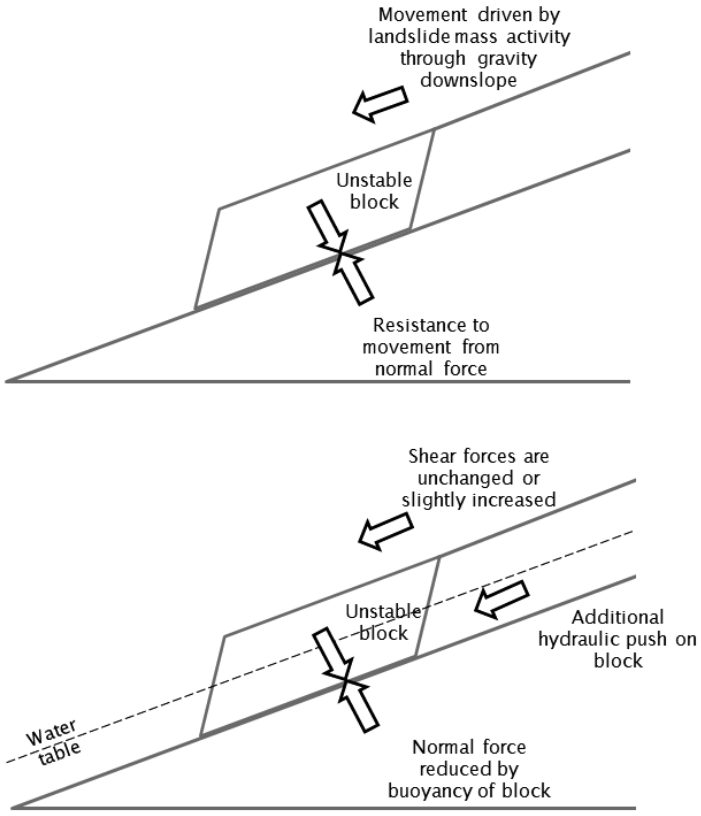


Figure 14. Resistance to, and causes of, movement in a slope system consisting of an unstable block.

Generally, a rise in groundwater and/or pore water pressure reduces the normal stress effect, thereby decreasing the shear resistance of the slide surface (Erener and Duzgun, 2010). When a slope is saturated with water and therefore the gaps between the particles are filled with water, the fluid pressure provides the block with buoyancy, reducing resistance to movement downslope (Figure 14). In some cases, such as groundwater flow, the fluid pressures can also provide a hydraulic push to the landslide, further decreasing its stability. In addition, water increases the weight of the slope, adding to the driving force and lowering the safety factor of rock-slope failures (Erener and Duzgun, 2010). Possible causes of an increase in pore pressure include infiltration from the surface, exfiltration from bedrock, preferential flow, and convergent flow; these all cause local accretion of groundwater levels (Sidle and Ochiai, 2006). Pore water pressure can also increase due to dynamic loading (Sidle and Ochiai, 2006).

An increase in the weight of the slope itself can be caused by various reasons, the two most common are overloading of the slope during earthworks, and rainfall inputs (Sidle and Ochiai, 2006). By increasing the weight of the block, the gravitational acceleration force downslope is increased, leading to movement of the block and landslide failure. Increases in soil weight as a result of prolonged rainfall has been cited as the cause of landslides for soil types with particularly high pore volumes, such as landslides in Shirasu deposits (Sidle and Ochiai, 2006).

An increase in slope inclination is also a trigger for landslide initiation, because the gravitational acceleration force increases downslope as the angle of the slope is increased. These changes in slope inclination are typically anthropogenically induced, such as cutting into hillslopes, and overloading potentially unstable or steep slopes (Sidle and Ochiai, 2006). Natural causes can be from erosion of the toe of the hillslope, such as by fluvial incision or glacial retreat (Sidle and Ochiai, 2006). Changes in slope inclination itself can lead to slope failure, but is often accompanied by pore water pressure accretion (Sidle and Ochiai, 2006).

Hillslope failure as a result of an earthquake trigger occurs when the shear stress across a potential failure plane exceeds substrate strength (Hovius and Meunier, 2012). Earthquake loading as a trigger for landsliding is complex because earthquake loads change dynamically (Sidle and Ochiai, 2006). Cyclical loading and unloading of soils during earthquakes occur as a result of earthquake strong ground motion added to the ambient gravitational acceleration of the slope (Sidle and Ochiai, 2006). Propagation of seismic waves causes horizontal acceleration of the soil mantle (Sidle and Ochiai, 2006). Earthquake strong ground motion reduces the strength of surface materials by progressive weakening (due to rock mass fracturing) and changes in the stresses in hillslopes (Hovius and Meunier, 2012). The greater the amplitude of the incoming seismic waves and the duration of shaking, the increased likelihood of failure on a slope (Hovius and Meunier, 2012). Cyclical loading of regoliths, particularly in soils with high moisture content, may also generate high pore water pressures that trigger landslides (Sidle and Ochiai, 2006).

## 8.0 Earthquake-triggered landslides

Earthquake-triggered landslides, also termed ‘coseismic landslides’ and ‘earthquake-induced landslides’ or ‘EILs’ are less common than rainfall-induced landslides (RILs) and as such there have been fewer opportunities to study the mechanisms of EILs compared to RILs (Sidle and Ochiai, 2006). Rodriguez *et al* (1999) argue earthquakes are one of the main triggers of landslides and ‘potentially the most destructive’ of secondary geotechnical hazards as a result of earthquakes. Horizontal ground acceleration from seismic shaking exerts additional transient shear stresses and increases ambient pore water pressures through cyclic gravitational loading, negatively affecting slope stability (Sidle and Ochiai, 2006 in Korup, 2010). The most prominent and abundant type of coseismic landslides are shallow (<2 m), disrupted slope failures (Keefer, 2002 in Korup, 2010).

Synthesis of worldwide and national data on earthquake-triggered landslides began in 1984, with Keefer’s key paper cataloguing 40 events between 1811 and 1980. Rodriguez *et al* (1999) updated Keefer’s (1984) earthquake-triggered landslide dataset which had previously covered 1811-1980, continuing it to 1997. This created a dataset of 76 earthquake-induced landslides from 1811 to 1997 containing information on each event. Keefer’s (1984) analysis of earthquake-induced landslides suggest earthquakes of magnitude 4.0 (Figure 15) and greater are able to trigger slope failure, and those above $M_L = 7.0$ are able to engender thousands of landslides in hilly areas (in Smith and Petley, 2009).

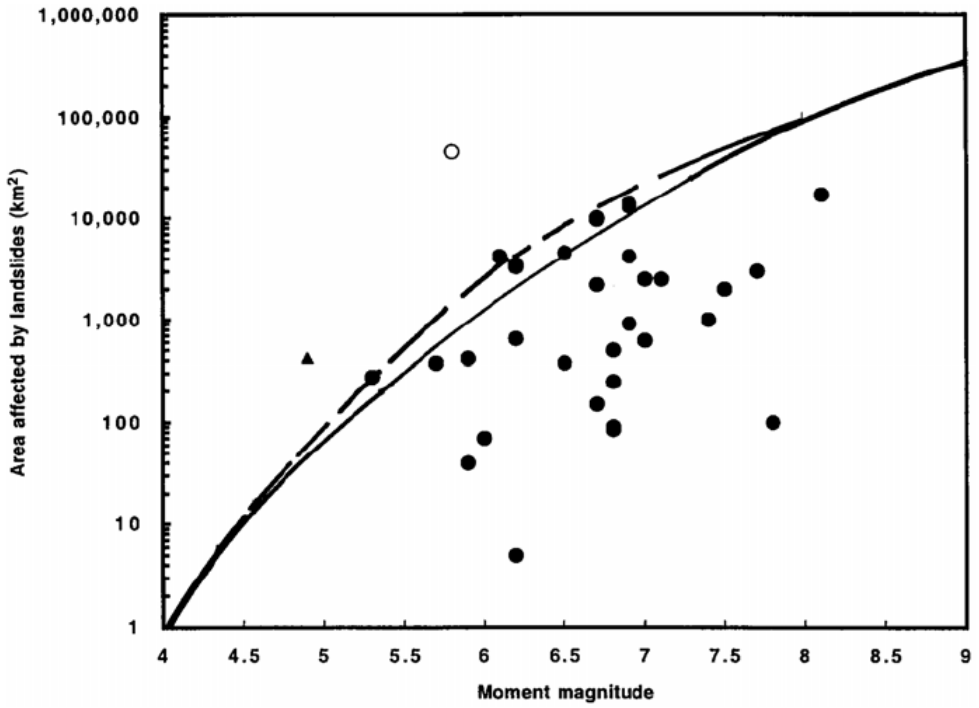


Figure 15. Relations between area affected by landslides and earthquake moment magnitude (after Keefer, 2002). Circles are data from earthquakes discussed by Rodriguéz *et al*. (1999), plotted using moment magnitude (*M*); open circle is 1988 Saguenay, Quebec earthquake. Solid line is upper bound of Keefer (1984). Dashed line is upper bound of Rodriguéz *et al*. (1999). Triangle is datum from 1963 Peria, New Zealand, earthquake, for which area exceeds upper bounds, plotted using Richter local magnitude (ML), from Hancox *et al*. (2002); after Keefer (2002). Acquired from Korup (2010, fig 6, p9).

Keefer (2002) proposed empirical curves based on the relationship between the total number of, and maximum area to be affected by, landslides in relation to earthquake magnitude (Figure 16). These empirical relationships are useful as rough estimates of the overall impact expected from an earthquake of given magnitude (Korup, 2010). However, these relationships differ between the regions they are derived for, and some recent earthquakes have resulted in fewer landslides than those predicted (Figure 15) (Korup, 2010).

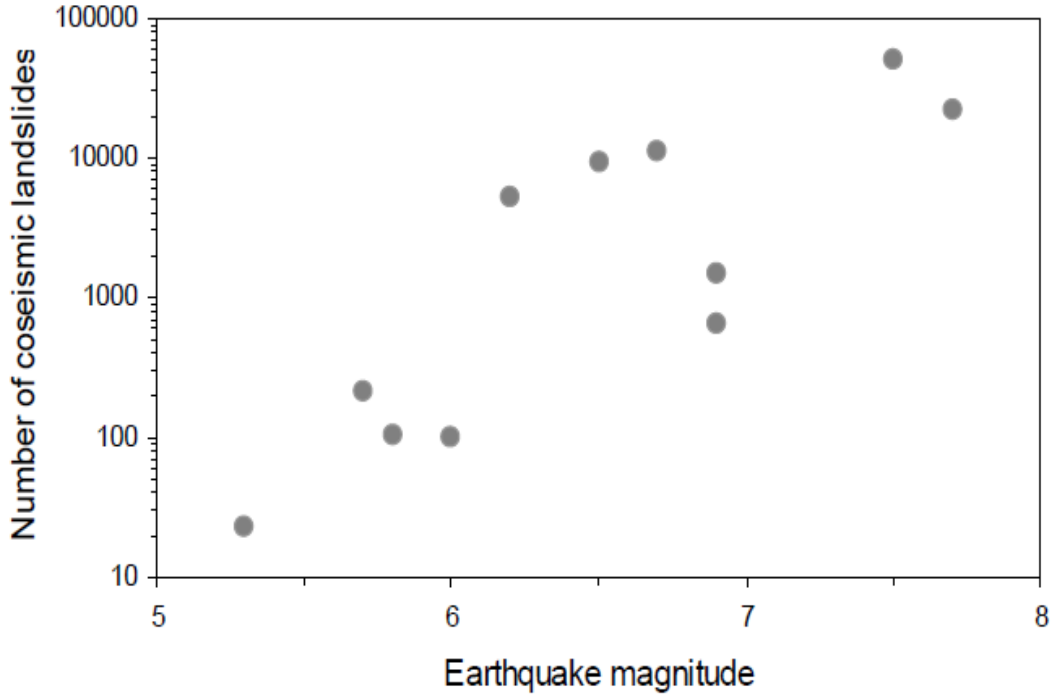


Figure 16. Relation between total number of reported landslides and earthquake magnitude for earthquakes with comprehensive, i.e. statistically robust, inventories of landslides (data from Keefer, 2002, in Korup, 2010, fig 5, p8).

Generally, deeply-weathered, sheared, intensely fractured or jointed, or saturated slope materials are particularly susceptible to failure due to earthquake shaking (Jibson, 2012). The dominant landslide type triggered by earthquakes are slides and falls (86%), with coherent slides constituting 8 percent, and lateral flows and spreads 6 percent (Jibson, 2012).

There appears to be a relationship between the earthquake magnitude, focal depth and distance from the epicentre, and the extent and intensity of landsliding (Sidle and Ochiai, 2006; Hovius and Meunier, 2012). Marano *et al*. (2010) found fatal earthquake-induced landslides generally occurred in areas of high topographic relief such as the Himalayas, Andes and Alps. This is consistent with other studies, which have shown coseismic spatial distribution is not random, but could be a function of distance to the epicentre, slope gradient, slope position, and rock type (Keefer, 2002; Meunier *et al*, 2007, both in Korup, 2010).

A spatial database of 2252 landslides were analysed from the 8th October 2005 Kashmir earthquake to determine the significance of event-controlling parameters in triggering landslides (Kamp *et al*, 2008). Data from the several thousand landslides were sourced from ASTER data (Kamp *et al*, 2008). GIS techniques were used to assess parameters such as lithology, faults, slope gradient, elevation, land cover, rivers and roads (Kamp *et al*, 2008). Lithology appeared to be the strongest influence on triggering landslides, especially when rock was highly fractured (Kamp *et al*, 2008). The proximity to faults, rivers and roads appeared to initiate failures, and landslides occur mainly at moderate elevations on south-facing slopes (Kamp *et al*, 2008). The study concluded that 'earthquake-triggered landslides are concentrated in specific zones associated with event-controlling parameters' (Kamp *et al*, 2008).

The 1989 Loma Prieta earthquake triggered landslides over 15,000 $km^2$ (Keefer, 2000). Keefer (2000) used distributional statistics (regression and one-way analysis of variance) to analyse the pattern of landslides caused by the earthquake. The concentration of landslides had a large inverse correlation with distance from earthquake source (Figure 17) and a large positive correlation with slope steepness (Keefer, 2000). There appeared to be a complex relationship between landslide occurrence and rock properties (Keefer, 2000).

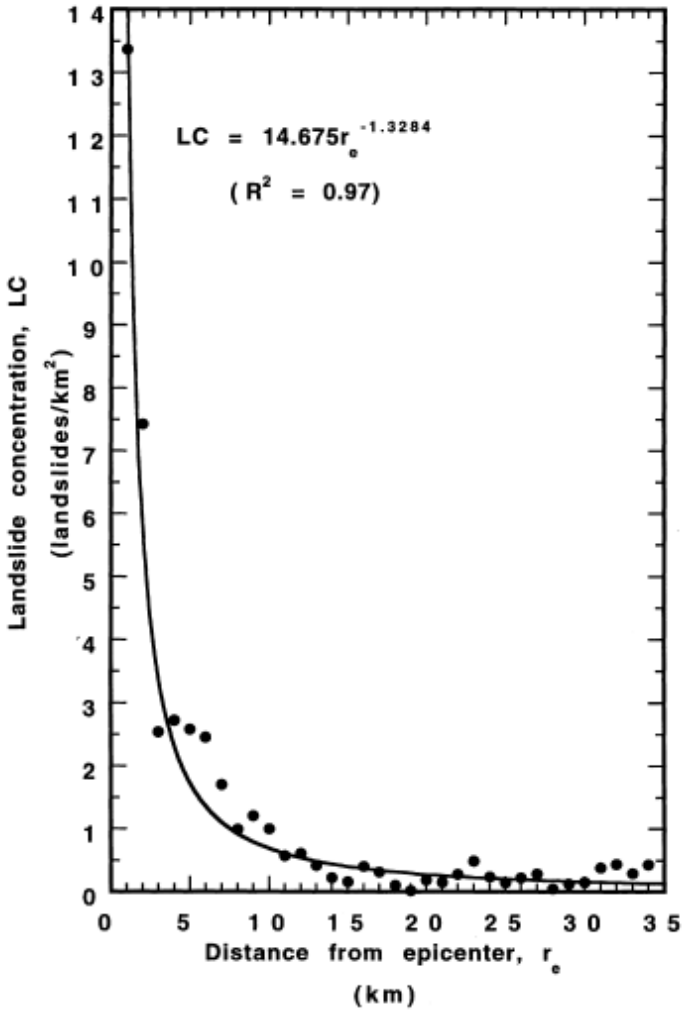


Figure 17. Landslide concentration vs. distance from earthquake epicentre. Solid line is best-fit regression line, which has power law form (Keefer, 2000, fig 3, p237).

## 8.1 Earthquake Ground Motion and EILs

The pattern of energy release, rather than the location of the epicentre should be considered when analysing earthquake-triggered landslides (Hovius and Meunier, 2012). Larger earthquakes ($M_w > 6$) tend to have more complex rupture patterns, leading to a more complex release of energy (Hovius and Meunier, 2012). Treating such earthquakes as a simple line or point source of energy can, therefore, lead to erroneous conclusions (Hovius and Meunier, 2012). Local topographic and geologic features can have significant impacts on the propagation of seismic waves. For example, sediment fills of basins and valleys can amplify ground waves significantly compared to bedrock (Hovius and Meunier, 2012;

Havenith et al, 2003). Similarly, topographic amplification of ground acceleration occurs along topographic ridges as the seismic waves are partially reflected back into the rock mass and diffracted (Hovius and Meunier, 2012). Patterns of earthquake ground motion are reflected in the densities of earthquake-triggered landslides (Hovius and Meunier, 2012; Meunier et al, 2008). To be able to predict the spatial location of potential landslides as a result of a given earthquake scenario, the pattern of ground motion should therefore be taken into consideration.

For many earthquake events which have triggered landslides, insufficient data exists on seismic ground motion and detailed landslide inventories to evaluate the relationship with landsliding (Hovius and Meunier, 2012; Hervas and Bobrowsky, 2009). However, where such detailed data do exist, there is clear evidence of a relationship between peak ground acceleration and landsliding (Marzorati et al, 2002; Carro et al, 2003; Dai et al, 2011; Hovius and Meuneir, 2012). Meunier et al (2007) analysed landslide densities triggered by the Northridge earthquake in California, the Chi-Chi earthquake in Taiwan, and two earthquakes on the Ramu-Markham fault in Papua New Guinea and found the highest landslide densities to be correlated with the highest peak ground acceleration values. Hovius and Meunier (2012) proposed that peak ground acceleration has a large correlation with landslide density and is "key to understanding the global attributes of regional and local patterns of earthquake-induced landsliding".

## 8.2 Seismic Parameters

Findings from multiple studies suggest regional patterns of earthquake-triggered landslides are associated with seismic parameters and the dissipation of seismic energy (Meunier et al., 2007; Keefer, 1984; 2000; 2002). For example, the landslide area percentage and landslide number density measures of landslides triggered by the 2008 Wenchuan earthquake were observed to have continuous correlations with distance from the epicentre, distance from the

surface fault rupture, seismic intensity, peak ground acceleration, and coseismic horizontal, vertical, and total surface displacement (Figure 18) (Xu et al., 2014).

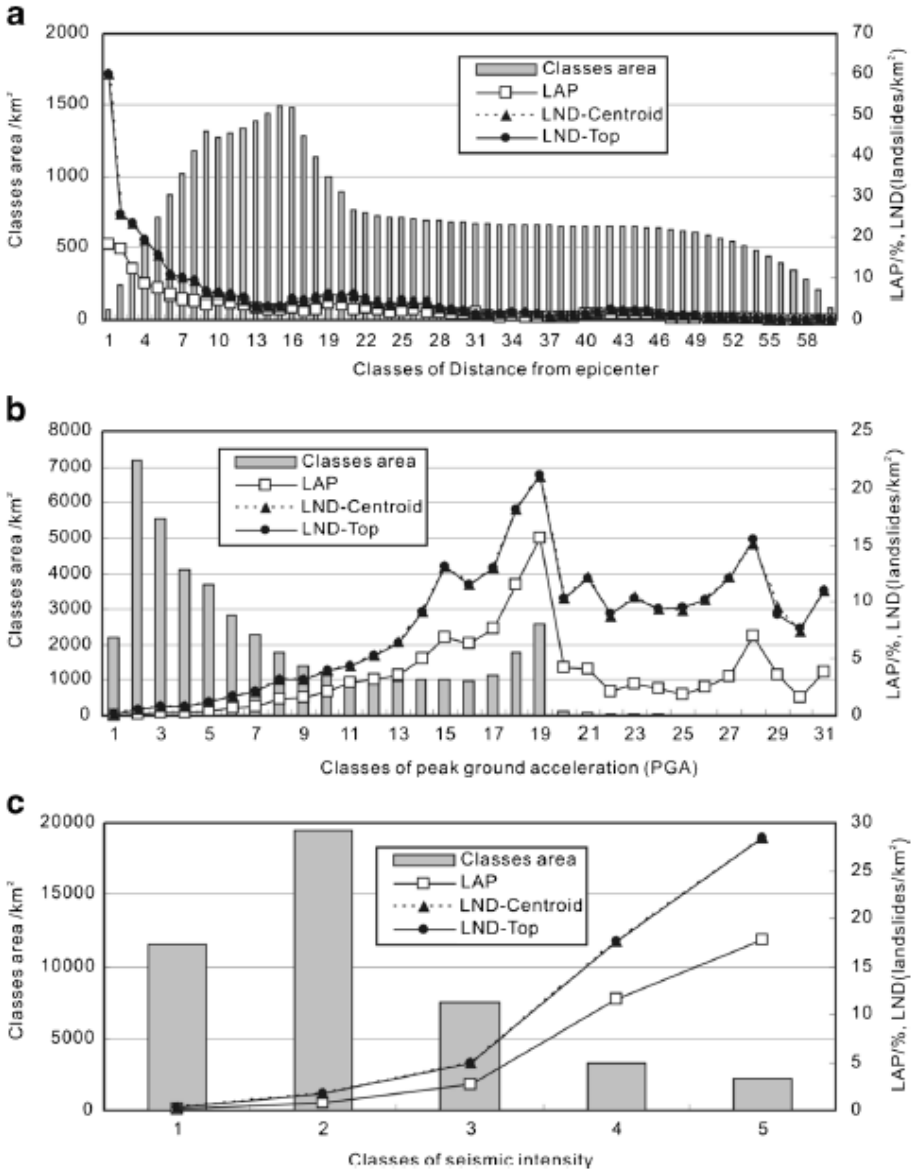


Figure 18. Relationships between landslide occurrence and seismic parameters for the Wenchuan 2008 earthquake: (a) distance from epicentre, 5 km intervals, 60 classes; (b) PGA; (c) seismic intensity (acquired from Xu et al., 2014, page 455, figure 11).

### 8.2.1 Distance from source

Keefer's (1984) review of earthquake-triggered landslides highlights distance from epicentre or fault rupture has a strong relation with landslide generation. The 1989 Loma Prieta earthquake generated landslides that have a strong inverse statistical relationship with

various measures of distance from the earthquake source (Keefer, 2000). The strongest correlation was between landslide concentration triggered by the Loma Prieta earthquake and epicentral distance, suggesting the seismic energy release during this earthquake event was concentrated near the epicentre, rather than uniformly distributed along the fault rupture (Keefer, 2000; Meunier et al., 2007). Meunier et al.'s (2007) study of the 1994 Northridge earthquake in California, the 1999 Chi-Chi earthquake in Taiwan, and two earthquakes on the Ramu-Markham fault in Papua New Guinea show landslide densities in each study to be greatest in the area of strongest ground motion and to decay with distance from the epicentre.

However, Keefer (1984) suggests maximum distance of landslides from fault-rupture zone may be a more refined relation rather than maximum epicentral distance because seismic energy is released throughout a zone of rupture, rather than from an isolated point. In general, the spatial distribution of earthquake-triggered landslides caused by the 2008 Wenchuan earthquake showed a good correlation with the distance from the main surface rupture (Xu et al., 2014).

However, the correlation between landslide occurrence and distance from epicentre or surface fault is not straightforward; for example, there was a lack of landslides near the epicentre of the Wenchuan earthquake (Xu et al., 2014). Not only does the seismic energy dissipate the further it gets from the epicentre or fault surface, but factors such as topography and geology can greatly affect the dissipation of energy, resulting in spatially varied ground motion.

### 8.2.2 Seismic intensity

There is no one universal measure of seismic intensity; measures of seismic intensity vary by country (Table 6). Unlike the Richter scale, which measures seismic energy released by the rupture and therefore is a record of magnitude, seismic intensity is a measurement of the perceived outcome of the seismic energy observed on the Earth's surface. It is not a mathematical measurement, but instead a qualitative ranking based on observed effects.

Table 6. Seismic intensity scale used by a selection of countries.

| Country | Seismic intensity scale used |
|---|---|
| China | Liedu Scale |
| Europe | European Macroseismic Scale |
| Hong Kong | Modified Mercalli Scale |
| India | Medvedev-Sponheuer-Karnik Scale |
| Israel | Medvedev-Sponheuer-Karnik Scale |
| Japan | Shindo Scale |
| Kazakhstan | Medvedev-Sponheuer-Karnik Scale |
| Russia | Medvedev-Sponheuer-Karnik Scale |
| Taiwan | Shindo Scale |
| United States | Modified Mercalli Scale |

The seismic intensity map produced by the China Earthquake Administration (CEA) during the Wenchuan earthquake showed a correlation with landslide area percentage and landslide number density (Xu et al., 2014). As the seismic grade intensity increases, landslide occurrence increases (Xu et al., 2014).

In a global review of earthquake-triggered landslides, minimum shaking intensities as measured on the Modified Mercalli (MMI) scale showed a relationship with landslide occurrence (Keefer, 1984; 2002). However, there is much scatter in the data, reflecting differences in application of the intensity scale by various investigators, and other factors (Keefer, 1984; 2002). Whilst seismic intensity shows significant correlation with earthquake generate landslides, the different rankings used worldwide make it an inconsistent attribute to use for measuring and comparing across multiple studies. Peak ground acceleration also maps the spatial distribution of the ground shaking, but is a quantitative measure of ground shaking which can be measured in any location globally with seismometers, and can be estimated using earthquake ground motion models.

### 8.2.3 Horizontal and Vertical PGA

Peak ground acceleration is a measure of maximum displacement of the ground during an earthquake: this can be vertical or horizontal displacement. Peak ground acceleration is measured in units of percent-g (where g = acceleration due to the force of

gravity = 981 cm/s/s) (USGS, 2014). Peak ground acceleration can vary greatly across the area affected by seismic shaking during an earthquake event. Horizontal peak ground acceleration is the more common measure; it is used for engineering applications to design building codes, and the USGS uses it as the peak ground acceleration variable in their ShakeMaps (USGS, 2014). This is because on average, the vertical component of peak ground acceleration is lower than the horizontal component (USGS, 2014).

Peak ground acceleration is shown to be significantly associated with landslide density or occurrence in many earthquake-triggered landslide studies, both the vertical and horizontal components (Figure 19) (Meunier et al., 2007; Yuan et al., 2013; Yin et al., 2009; Xu et al., 2014). The 1994 Northridge and 1999 Chi-Chi earthquakes both show linearity and high correlation between co-seismic landslide density and both the vertical and horizontal components of peak ground acceleration (Meunier et al., 2007).

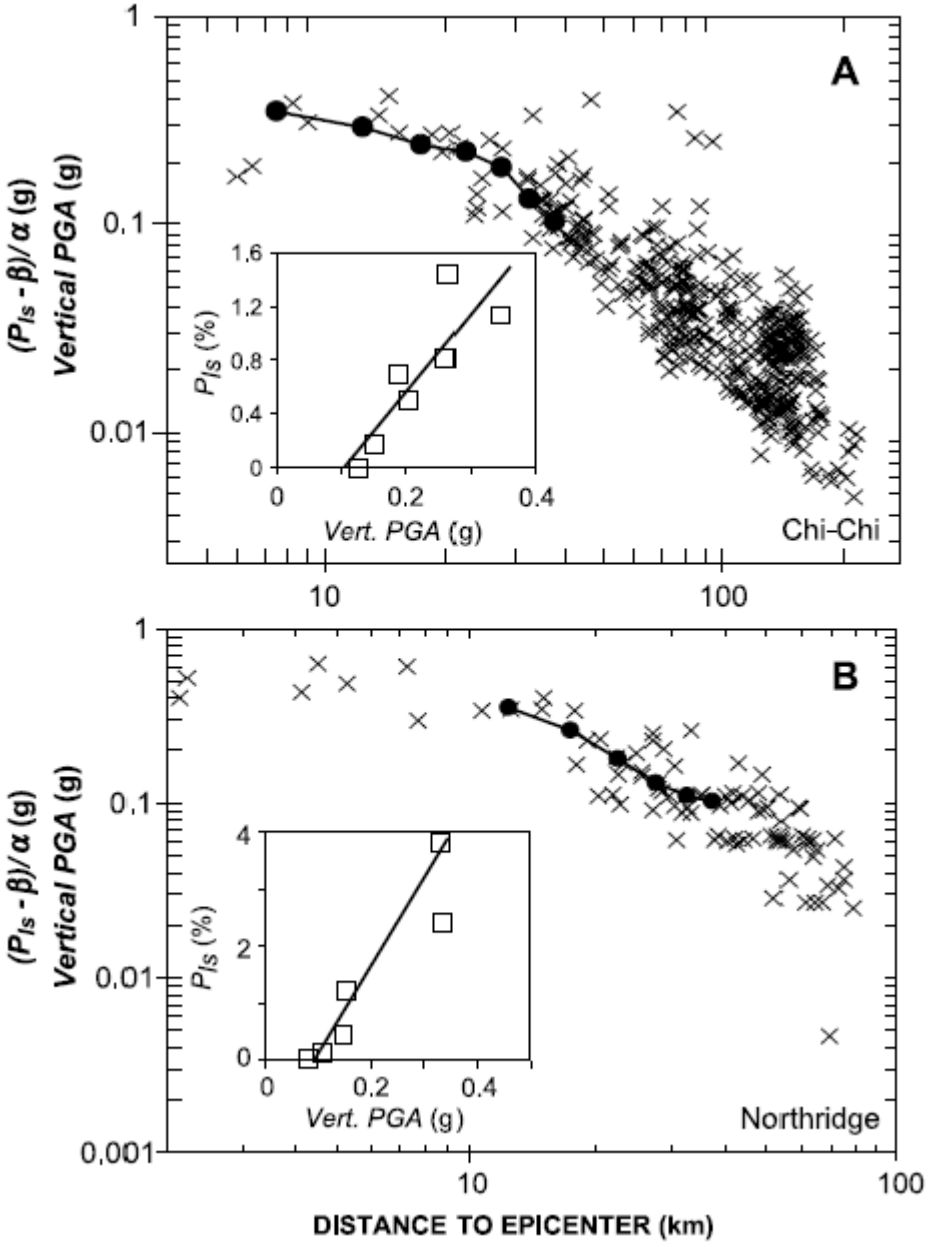


Figure 19. Landslide density (filled circles) and vertical PGA (crosses) plotted against distance from the epicentre for (a) the Chi-Chi earthquake (PGA data from Central Weather Bureau, Taipei, Taiwan), and (b) the Northridge earthquake (PGA data from Trifunac and Todorovska [1996]). For comparison with PGA, landslide densities were scaled linearly with help of trends shown in inset graphs. Inset graphs show average landslide density plotted against average vertical PGS for 5km windows parallel to the fault trend with least squares linear regressions. Figure acquired from Meunier et al. (2007), page3, figure 3.

The 2008 Wenchuan earthquake and triggered landslides have been studied extensively for relationship with seismic parameters (Yuan et al., 2013; Yin et al., 2009; Xu et al., 2014). Yuan et al. (2013) found peak ground acceleration to be significantly correlated with earthquake-triggered landslides caused by the Wenchuan earthquake (Figure 20). Thresholds

for landslide failure were estimated at 0.21g for average horizontal PGA and 0.12g for average vertical PGA (Yuan et al., 2013). In contrast to common findings, Yin et al. (2009) found vertical peak ground acceleration to be a predominant factor in landslide generation during the Wenchuan earthquake, compared to the horizontal component. However, the domination of the vertical component is not a common relationship found in other earthquake events (USGS, 2014); the vertical acceleration caused by the Wenchuan earthquake was significantly greater than the horizontal acceleration in the epicentre area of study (Yin et al., 2009). Horizontal, vertical and total surface displacement was used as a covariate in bivariate statistical analysis of the Wenchuan earthquake-triggered landslides by Xu et al. (2014). There was general correlation with the landslide area percentage and landslide number density, increasing landslide occurrence with increasing coseismic surface displacement (Xu et al., 2014). Out of the eight impact factors considered in the statistical analysis, peak ground acceleration and seismic intensity had the most significant effect on earthquake-triggered landslides, followed by lithology (Xu et al., 2014).

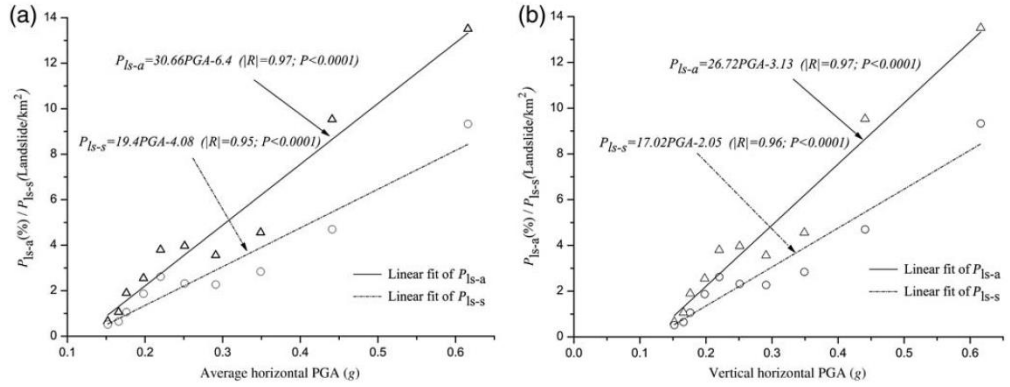


Figure 20. Average Pls-a/Pls-s of landslides plotted against average PGA for the Wenchuan 2008 earthquake, where Pls-a and Pls-s are the landslide area density and the source density at a distance from the rupture or the epicentre respectively (acquired from Yuan et al., 2013, page 2351, figure 8). Least-square linear regression lines, solid lines.

### 8.2.4 Arias Intensity

The Arias intensity ($I_a$) is a measurement used to characterise the shaking content of a strong-motion record. Arias (1970) defined this as:

$$I_a = \frac{\pi}{2g}\int_0^d [a(t)]^2 dt \qquad \text{Equation 2}$$

where *g* is the acceleration of gravity, *d* is the duration of the strong shaking, *a* is the ground acceleration, and *t* is time. The Arias intensity is sometimes considered a superior measure to peak ground acceleration, because it accounts for all acceleration peaks (not just the maximum), and, implicitly, for duration (Jibson, 2007). For the 1997 Umbria-Marche earthquake, landslide density correlated with Arias intensity (Meunier et al., 2007).

The Arias intensity provides a more complete representation of ground motion because it accounts for the entire process of earthquake shaking. If two similar slopes are subjected to the same peak ground acceleration, but the first slope is exposed to the maximum acceleration once for a limited duration and the second slope is subjected to the maximum ground acceleration multiple times, or for a longer duration, the second slope experiences greater cyclical loading and unloading. This puts the slope under more stress, thus making it more likely to fail. Whilst Keefer's (1984) review of earthquake-triggered landslides does not provide a detailed correlation of landslide generation related to seismic parameters, it highlights that shaking duration does have a significant effect on initiating landslides. The Arias intensity threshold for triggering landslide varies across landslide type (Table 7).

Table 7. Arias intensity thresholds for landslides (Table IV, page 502, in Keefer, 2002)

| Landslide category | Arias intensity threshold (M/s) | Reference |
|---|---|---|
| **Modelling studies** | | |
| Disrupted | 0.15 | Wilson and Keefer, 1985 |
| Disrupted | 0.11 | Keefer and Wilson, 1989 |
| Disrupted | 0.10 | Wilson, 1993 |
| Coherent | 0.5 | Wilson and Keefer, 1985 |
| Coherent | 0.32 | Keefer and Wilson, 1989 |
| Lateral spreads and flows | 0.5 | Wilson and Keefer, 1985 |
| Lateral spreads and flows | 0.54 | Keefer and Wilson, 1989 |
| **24 Oct. 1987 Superstition Hills, California earthquake** | | |
| Disrupted | 0.3 (mean) | Harp and Wilson, 1995 |
| Disrupted | 0.1-0.5 (range) | Harp and Wilson, 1995 |
| **1 Oct. 1987 Whittier Narrows, California earthquake** | | |
| Disrupted | 0.6-0.7 (weakly cemented sandstones and conglomerates) | Harp and Wilson, 1995 |
| Disrupted | 0.04 (mean, well-cemented rocks) | Harp and Wilson, 1995 |
| Disrupted | 0.01-0.07 (range, well-cemented rocks) | Harp and Wilson, 1995 |

Newmark's analysis uses the Arias measure to predict slope failure, treating the landslide as a rigid-plastic friction block having a known yield or critical acceleration (Jibson, 1993). The analysis calculates the permanent displacement of the block after subjected to the earthquake acceleration-time history, taking into account peak ground acceleration and duration of shaking (Jibson, 1993). However, using the Newmark analysis requires extensive detailed knowledge of the yield and critical acceleration properties of each slope and geological type in a study site, which are often difficult to obtain accurately over a large spatial area.

## 8.3 Assessing Risk from EILs

Quantitative approaches to landslide risk assessment uses mathematical methods to estimate probabilities such as loss of life or damage to structures or infrastructure due to landslides (Guzetti, 2005; Hervas and Bobrowsky, 2009). This is typically calculated by the generic risk equation (Equation 1).

In this case, *Hazard* is typically expressed as the probability of a landslide event occurring, the *Exposure* is expressed in terms of their amount or value (such as number of people or property value), and *Vulnerability* is the element's degree of potential loss (Hervas and

Bobrowsky, 2009). Assessing landslide *Risk* is still a complicated task, in particular because the precise information required to calculate quantitative landslide *Risk* may not be available (Hervas and Bobrowsky, 2009; van Westen et al, 2006).

Various methods exist for assessing earthquake-triggered landslide hazards such as the probability of the occurrence of a landslide, factor of safety of a slope, and the slope permanent displacement along a slip surface using Newmark type displacement methods or advanced numerical approaches (Hervas and Bobrowsky, 2009; SafeLand, 2011). However, whilst quantification of landslide hazard has received extensive attention, consequence analysis and vulnerability assessment to landslides has been limited (SafeLand, 2011). Assessing and understanding the vulnerability of elements to landslide hazard is vital in assessing landslide risk. The HAZUS multi-hazard loss estimation methodology is the closest model to estimate losses due to earthquake-triggered landslides. However, the fragility curves developed by HAZUS are derived exclusively from expert judgement, and so often carry a degree of subjectivity and simplification. An empirical landslide loss model currently does not exist in the literature.

## 8.4 Approaches to Landslide Susceptibility and Hazard Mapping

Most approaches assume future landslides will occur in locations similar to those they have occurred in the past (Sidle and Ochiai, 2006). Landslide hazard or susceptibility assessments therefore typically relate landslide hazard to measurable environmental attributes such as slope and geology. There are several approaches to landslide hazard and susceptibility mapping which can be divided into two main types: qualitative and quantitative methods. Quantitative methods can be further divided in to statistical and physically-based approaches.

Qualitative approaches are mainly direct (geomorphological) and weighting (indexing) approaches (Hervas and Bobrowsky, 2009). These are typically assessed by experts based on

geographical and environmental mapped features. As such, these maps are heavily subjective and directly relates to the experience of the analyst (Hervas and Bobrowsky, 2009).

Quantitative approaches to landslide susceptibility and hazard mapping typically rely on landslide inventory maps. Landslide inventory maps for an event are typically constructed from aerial photography and/or field observations (Van Den Eeckhaut et al. 2006). After an earthquake or rainfall event causes landslides, a landslide inventory is constructed to record the areas affected by landslides. This is typically in polygon formats, which can be converted easily into raster data at a later stage. However, sometimes the locations of the landslides are recorded as point data, indicating the source of the slip failure, or the origin of the landslide scar. In these cases a spatial distribution of landslide affected areas is not recorded. A buffer zone around the point of origin is typically used to delineate landslide source areas, and statistical analysis is used to determine the significant factors in these areas.

Long-term landslide inventories are also used, typically recorded in a national database of landslide occurrences, or inferred from aerial photography or satellite sensor imagery to determine the locations of past landslides over a specified time period. The trigger mechanism of these landslides is not recorded and these landslide inventory maps therefore represent a generic landslide hazard map. Often the dominant triggering method is generally known (e.g. the site is located in an area of high precipitation, or is known as a region of high seismic activity). However, as the records do not contain information on the specific triggering mechanism, it is not possible to stipulate directly the trigger type for these long-term landslide inventories.

Physically-based methods rely on physical laws influencing slope instability and are mostly based on slope stability analysis (Hervas and Bobrowsky, 2009). Physically-based models are typically used to assess the effect of a particular trigger or study a particular type of landslide (Hervas and Bobrowsky, 2009).

Statistical or probabilistic approaches to landslide hazard analysis correlate geo-environmental factors which could be conditioning or triggering factors to the distribution of past and current landslides recorded by landslide inventories. In bivariate statistical analysis, each factor map (such as slope, geology, aspect) is combined with the landslide distribution map and weighted based on densities calculated for each class of factor (Hervas and Bobrowsky, 2009). Multivariate analysis methods include logistic and multiple regression analysis, discriminant analysis, and artificial neural networks. Logistic regression (see 8.4.1) and discriminant analysis are the most popular of these methods (Hervas and Bobrowsky, 2009).

Discriminant Analysis (DA) determines the greatest separation for each independent variable between landslide occurrence and non-landslide occurrence (Pardeshi et al., 2013). Ideally, cells associated with landslide occurrence will have values far apart from cells associated with non-landslide occurrence (Santacana et al., 2003). After checking the discriminant function, it is applied to the rest of the site. The resultant susceptibility map is typically classified into failure and non-failure, or stable and unstable areas, or low, medium, and high susceptibility bands (Santacana et al., 2003).

The Artificial Neural Network (ANN) method has been compared in several studies with logistic regression method (Yesilnacar and Topal, 2005; Garcia-Rodriguez and Malpica, 2010; Pardeshi et al., 2013). It has been found to be a more effective method than logistic regression, with a greater accuracy in prediction; however, it has also been found to have no difference in overall predictive performance in other studies (Yesilnacar and Topal, 2005; Garcia-Rodriguez and Malpica, 2010; Pardeshi et al., 2013). This learning algorithm is a multi-layer neural network, consisting of an input layer, hidden layers and an output layer (Lee and Evangelista, 2006). ANN is a non-linear model and therefore is effective at modelling complex interrelated factors (Pardeshi et al., 2013).

### 8.4.1 Logistic Regression

Logistic regression analysis is one of the most popular methods for assessing landslide hazard and susceptibility (Atkinson et al., 1998; Hervas and Bobrowsky, 2009). Brenning (2005) demonstrated that logistic regression was the preferred method when comparing statistical methods used to model landslide susceptibility as it resulted in the lowest rate of error. Logistic regression is a useful tool for analysing landslide occurrence, where the dependent variable is categorical (e.g., presence or absence) and the explanatory (independent) variables are categorical, numerical, or both (Boslaugh, 2012; Chang et al., 2007; Atkinson et al., 1998).

In the case of landslide susceptibility mapping, logistic regression analysis can be used to find the best fitting model to describe the relationship between the presence or absence of a landslide (dependent variable) and a set of independent variables such as slope, aspect, vegetation, and geology (Akgun and Bulut, 2007). In logistic regression, the presence of a landslide is coded '1', and the absence of a landslide is coded '0' (Akgun and Bulut, 2007). The logistic model representing the maximum likelihood regression model can be expressed in its simplest form as:

$$P = \frac{1}{1+e^{-z}} \qquad \text{Equation 3}$$

where *P* is the probability of an event occurring. *P* is the estimated probability occurrence in the current situation (Akgun and Bulut, 2007). Since the z value varies from -∞ to +∞, the probability varies from 0 to 1 on an S-shaped curve (Akgun and Bulut, 2007). The logistic regression model has the form:

$$logit(y) = \beta_0 + \beta_1 x_1 + \beta_2 x_2 + \cdots + \beta_i x_i + e \qquad \text{Equation 4}$$

where $y$ is the dependent variable, $x_i$ is the $i$-th explanatory variable, $\beta_0$ is a constant, $\beta_i$ is the $i$-th regression coefficient, and $e$ is the error. The probability ($p$) of the occurrence of $y$ is

$$p = \frac{exp^{(\beta_0+\beta_1 x_1+\beta_2 x_2+\cdots+\beta_i x_i)}}{1+exp^{(\beta_0+\beta_1 x_1+\beta_2 x_2+\cdots+\beta_i x_i)}} \qquad \text{Equation 5}$$

The logistic regression model is most commonly fitted in a step-wise manner. In the backward step-wise method, bivariate models are fitted between the dependent variable and all covariates. The least significant covariate is then removed from the working model. At each further step, additional covariates are removed one at a time and the most significant covariates are retained in the working model. At a pre-determined confidence level, no further covariates are removed from the model.

The accuracy of a logistic regression model can be evaluated by several different methods (Brenning, 2005). A common method is calculating the receiver operating characteristic (ROC). The area under the ROC curve (AUC) is a statistic that measures the ability of the model to correctly classify cases of landslide and cases of stable area (Chang et al., 2007). When the total area is found to be 1, this indicates perfect accuracy.

Several studies have used logistic regression analysis to model secondary hazard probabilities. Goda et al. (2011) used logistic regression analysis with peak ground acceleration and earthquake magnitude covariates to calculate probabilistic liquefaction hazard maps for four Canadian cities. They found that including seismic hazard and magnitude as covariates had a direct impact on liquefaction potential assessment (Goda et al., 2011). Pradhan (2009) used topographic, geological, hydrological, land cover and precipitation data to construct a logistic regression flood hazard model for Malaysia's East coast. The model produced reasonable accuracy results, with an AUC value of 0.8476 (Pradhan, 2009). Jomelli et al. (2007) used precipitation and air temperature data to predict avalanche susceptibility using logistic regression analysis in the French Alps. Dong et al. (2011) used the logistic regression method to assess the failure probability of landslide dams for ten landslide dams (formed after the 1999 Chi-Chi earthquake, the 2008 Wenchuan earthquake, and 2009 Typhoon Morakot). Geomorphic variables such as peak flow, catchment area, dam height, width, and length were used to fit the several logistic regression models, with high accuracy results (AUC = 94.8%) (Dong et al., 2011). Preisler et al (2004) fitted a logistic regression model to weather-induced wildfires in the State of Oregon using a

range of weather and fuel indices. They suggested including the triggering mechanism of fire occurrences (namely, people-induced or lightning-induced) could increase the accuracy of the model (Preisler et al., 2004). This is supported by De Vasconcelos et al. (2001), who used logistic regression to predict fire ignition probabilities in central Portugal and found that the ignition type affected the significant covariates included in the model and the location of subsequent fires. They recommended the logistic regression method for improving the predictive capability of wildfires (De Vasconcelos et al., 2001).

## 8.5 Coseismic landslide fatalities

Systematic collection of landslide fatality data is typically poor for historical landslide events and multi-hazard databases typically classify by trigger rather than cause of death (Petley, 2012). Therefore, many landslide deaths are attributed to their trigger: earthquakes or hurricanes (Petley, 2012). Petley (2012) excluded coseismic landslides from his analysis of global fatalities due to landslides because of the high levels of uncertainty associated with landslide data for such events. In the 'chaotic aftermath' of large earthquakes, data are often not collected attributing cause of death, such that there are very high levels of uncertainty associated with data on the human impact from landsliding (Petley, 2012).

Keefer (2002) found that landslides were responsible for highly variable, but often significant numbers and proportions of casualties and levels of economic damage during an earthquake. Landslides triggered by the M7.8 Kansu, China earthquake in 1920 killed 240,000 people; the 1970 Peru earthquake induced a landslide killing 18,000 (Keefer, 2002).

Rapid soil flows, rock avalanches and rock falls together caused at least 90% of the reported landslide deaths in the 40 historical earthquakes analysed (Keefer, 1984). Most deaths caused by rapid soil flows and rock avalanches were located on gently sloping ground several kilometres from the landslide initiation sites (Keefer, 1984). Rockfalls were found to be the third leading cause of deaths in seismic events, occurring on all types of rock slopes steeper than 40° (Keefer, 1984).

Marano *et al* (2010) examined secondary hazards due to earthquakes from the Prompt Assessment of Global Earthquakes for Response CATalogue (PAGER-CAT) database of 18,807 earthquakes from 1968 to 2008. The USGS's Preliminary Determination of Epicenters (PDE) is the primary source of information on casualties due to secondary hazards from the PAGER-CAT database as it provides a breakdown of casualty types when possible. Marano *et al* (2010) found that while 21.5% of fatal earthquakes include deaths due to secondary (non-shaking) causes, 'only rarely are secondary effects the main cause of fatalities', but these rare events are significant and need researching.

After removal of deaths attributed to the 2004 Sumatra event, landslides were found to be the cause for 71.1% of all non-shaking deaths due to earthquakes, with tsunamis following second at 11.5% (Figure 21) (Marano *et al*, 2010).

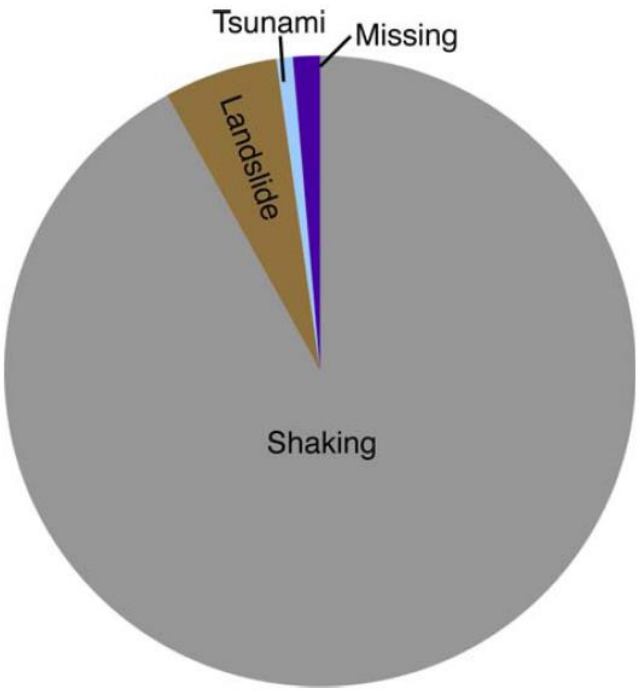


Figure 21. Fatality causes for all deadly earthquakes between September 1968 and June 2008, with deaths from the 2004 Sumatra event removed (Marano *et al*, 2010, fig 7, p325).

Of the 749 earthquakes in the PAGER-CAT database that caused at least one fatality, 276 triggered a landslide (1.47% of all events) and, of these, 43 were reported to have caused one or more deaths due to landslides (Figure 22) (Marano *et al*, 2010). Due to the

undifferentiated cause of deaths for some events, it is likely there are more events where deaths could be attributed to secondary hazards (Marano *et al*, 2010). Post-earthquake reconnaissance work is not always carried out, so often the cause of death remains ambiguous, and is often attributed to the initial triggering event (Marano *et al*, 2010).

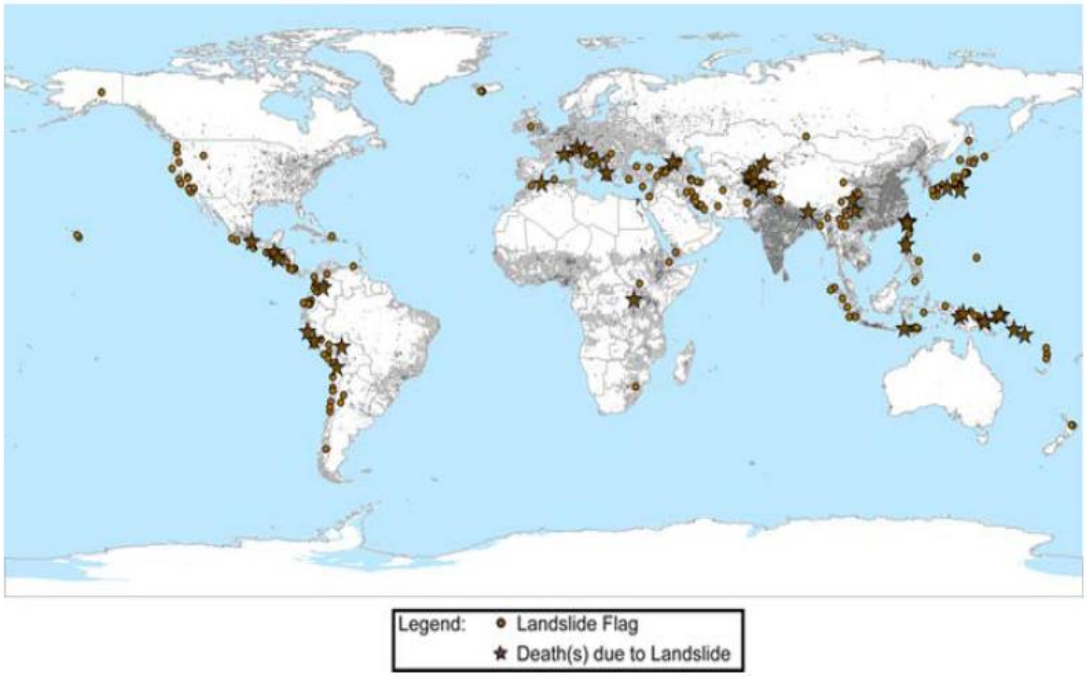


Figure 22. Epicentres of earthquake-induced landslides from September 1968 to June 2008. A star indicates events with deaths attributed to landslide (Marano *et al*, 2010, fig3, p323).

### 8.5.1 PAGER Secondary Losses

The USGS PAGER system provides near-real-time estimates of damages from earthquake events anywhere in the world for governmental and non-governmental relief organizations, and the media (Godt et al., 2008). The USGS's ShakeMap portrays the extent of potentially damaging shaking in the immediate aftermath of an earthquake. PAGER currently provides qualitative advisory statements following an earthquake event suggesting likely secondary hazards such as landslides, based on the history of the region (Wald et al., 2012). The secondary effects section of the PAGER Impact Estimates for the Chile 2014 M8.2 event read:

*"Recent earthquakes in this area have caused secondary hazards such as landslides that might have contributed to losses"*

Secondary hazards are highlighted as potential additional contributions to losses, currently unaccounted for in PAGER's shaking-based estimates (Wald et al., 2012). However, there is currently no quantitative coseismic landslide hazard model available to estimate the potential location of landslides as a result of earthquake shaking. The USGS is in the process of developing models to address this research gap (Nowicki et al., 2014b).

## 9.0 Summary

Millions of the world's population live in environments at risk from natural hazards. Often these areas at risk are affected by more than one natural hazard. Current multi-hazard risk assessments treat natural hazards as independent processes without accounting for the real-world interactions between them. This could potentially underestimate the calculated risk posed by the amplification effect of multiple hazards interacting. Current research into cascading, multi-hazards is in its infancy and requires further investigation. The interaction between earthquakes and triggered landslides has a sufficient body of research to support further investigation into the cascading effect of multi-hazards. Earthquakes often result in a variety of secondary hazards, landslides being one of the most common and damaging. Landslides are typically triggered by extreme rainfall, human causes, or earthquake shaking. The relationship between earthquake shaking and landsliding has been investigated; however, there has been limited research into predicting landslides as a direct result of earthquake shaking. An empirically-based earthquake-triggered landslide loss model does not currently exist.

The over-arching aim of this thesis was to model the earthquake-triggered landslide hazard (i.e., the probability of landsliding conditional upon possible earthquake hazard events) as an example of a cascading hazard, and to investigate the potential losses associated with the two sets of events (earthquakes and landsliding). The first paper of this thesis represents an initial

investigation into the relationship between *fatalities* and earthquake magnitude to establish whether there is an amplification of fatalities during events which triggered landslides compared to events where no subsequent landslides were triggered. The topic (i.e., predicting fatalities) was found to be challenging due to lack of high quality data, and was not pursued further in this thesis. Rather, the focus of attention shifted towards modelling the earthquake-triggered landslide *hazard*. The second paper in this thesis, therefore, provides a systematic review of all the published literature which uses logistic regression analysis to model landslide susceptibility and hazard. This provided a list of environmental preparatory covariates to include in the third paper, where two logistic regression models were developed for the Northridge 1994 earthquake event. The first *susceptibility* model used only preparatory covariates, whilst the second *hazard* model included ground motion covariates to account for the triggering factor. The fourth and final paper simulated earthquake scenarios of varying magnitudes and their subsequent probability of landsliding at Northridge, California. The potential exposure of current resident populations and infrastructure to such scenarios was estimated and compared to the 1994 event.

# 3. INTRODUCTION TO PAPER 1

## Earthquake-and-Landslide Events are Associated with More Fatalities than Earthquakes Alone

*This paper has been published in the Natural Hazards Journal*[1]*.*
*The full citation is:*

Budimir, M., Atkinson, P., and Lewis, H., (2014), 'Earthquake-and-Landslide Events are Associated with More Fatalities than Earthquakes Alone', *Natural Hazards*, Volume 72, Issue 2, Page 895-914.[2]

This paper provides an empirical investigation into the fatality data associated with earthquakes and earthquakes-and-landslide events to determine if there is any indication of the amplification effect. It aims to establish whether the numbers of fatalities in an event are significantly affected by whether an earthquake triggers a subsequent landslide or not. Other potential contributing factors which may affect fatalities are also included to untangle the effect of a cascading event on the subsequent severity of the event. This paper deals with the exposure and vulnerability components of the risk equation (Equation 1) for earthquakes and earthquake-and-landslide events (Figure 23).

---

[1] The paper has been edited from the published version: figure numbering has been changed to fit in sequentially with the thesis.

[2] When the unit 'pga' is used in this paper for peak ground acceleration values, it refers to the unit '%g'.


Figure 23. Diagram showing the focus of Paper 1 related to the risk equation.

**Paper 1 Research Questions**

*Is the total expected loss from earthquakes-and-landslides greater than the sum of the expected loss from earthquakes and earthquake-triggered-landslides combined?*

*Is the total expected loss from earthquake-and-landslides greater than earthquake only expected loss?*

# EARTHQUAKE-AND-LANDSLIDE EVENTS ARE ASSOCIATED WITH MORE FATALITIES THAN EARTHQUAKES ALONE

M.E.A. Budimir[1], P.M. Atkinson[1] and H.G. Lewis[2]

[1] *Faculty of Social and Human Sciences*

[2] *Faculty of Engineering and the Environment*

*University of Southampton, Highfield, Southampton, SO17 1BJ, UK*

## Abstract

Natural hazards are natural processes of the complex Earth system and may interact and affect each other. Often a single hazard can trigger a subsequent, different hazard, such as earthquakes triggering landslides. The effect of such cascading hazards has received relatively little attention in the literature. The majority of previous research has focused on single hazards in isolation, and even multi-hazard risk assessment currently does not account for the interaction between hazards, therefore ignoring potential amplification effects. Global earthquake and landslide fatality data were used to model cascading events to explore relationships between the number of fatalities during single and cascading events and covariates. A multivariate statistical approach was used to model the relationship between earthquake fatalities and several covariates. The covariates included earthquake magnitude, gross domestic product, slope, poverty, health, access to cities, exposed population to earthquake shaking, building strength and whether a landslide was triggered or not. Multivariate regression analysis showed the numbers of earthquake fatalities are significantly affected by whether a subsequent landslide is triggered or not.

## 1.0 Introduction

Approximately 19 % of the Earth's land area and over 50 % of its population are exposed to at least one natural hazard, including earthquakes, landslides, floods, volcanoes, cyclones and drought (Dilley et al., 2005). There is therefore great interest in efforts to map risks due to hazards globally. The United Nations defines risk as 'the probability of harmful consequences or expected loss of lives, people injured, property, livelihoods, economic activity disrupted (or environment damaged) resulting from interactions between natural or human induced hazards and vulnerable conditions' (UNDP, 2004). In particular, multi-risk approaches at the global level aim to identify the relative levels of overall risk, highlighting the nations where risk is highest (Carpignano et al., 2009).

State-of-the-art global multiple hazard and risk maps include Munich Re's World Map of Natural Hazards, the United Nations Development Program's (UNDP) Disaster Risk Index (DRI), the World Bank's Hotspots report and the UNU-EHS's World Risk Index (WRI) (Lerner-Lam, 2007; UNDP, 2004; Peduzzi et al., 2009; Dilley et al., 2005; UNU-EHS, 2011). An implicit assumption in all such global risk maps is that the risk sources are independent (Kappes et al., 2012). However, this assumption may be naive, leading to the neglect of possible interactions. In principle, a complete multi-hazard assessment should not be based solely on the superposition of distinct single hazard maps (Marzocchi, 2009). Natural processes are components of systems and as such are not independent and separated from each other (Kappes, 2010). Natural processes such as hazards are inter-connected, often in pairs or longer chains, whereby one can trigger the other (e.g. coseismic landslides, volcano-induced tsunamis, landslide-induced tsunamis, hurricane-induced flooding, hurricane-induced landslides, and earthquake-induced tsunamis).

Hazards acting in the natural system should not be seen as just the sum of a set of individual components, but instead as a net of interacting parts which therefore need to be examined using a more complex modelling approach (Kappes, 2010; Greiving, 2006; Marzocchi,

2009). Kappes et al. (2012) suggested that since there are only a few studies dealing with multi-hazard interactions, 'experience with associated problems is rare and standard approaches are not available'. Thus, the area of cascading natural hazards should be given greater attention by researchers.

## 1.1 Cascading hazards

The term 'cascading hazards' is used to describe the phenomenon whereby one hazard triggers another (Figure 24). Kappes et al. (2012) define the cascading hazard phenomenon as 'the triggering of one hazard by another, eventually leading to subsequent hazard events'. This phenomenon is also referred to as the 'avalanche' or 'domino' effect or a catastrophe 'chain' (Helbing and Kuhnert, 2003).

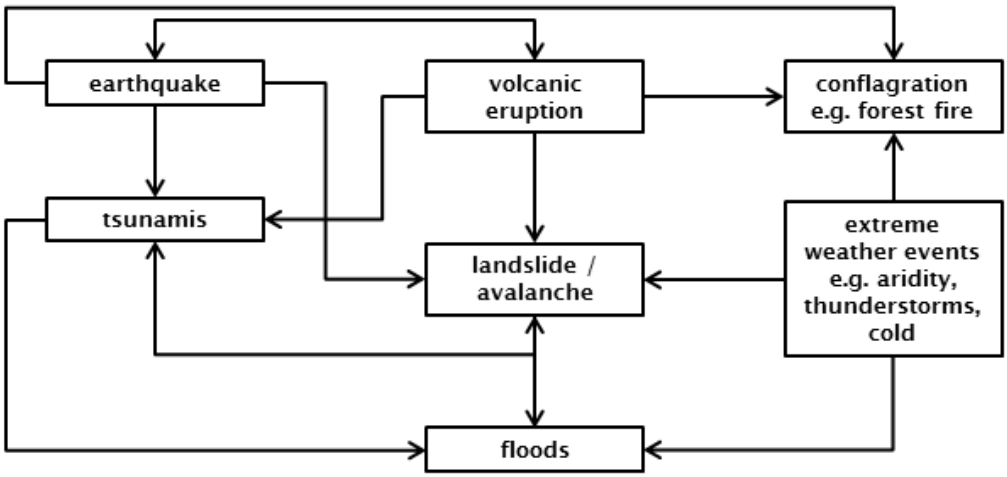


Figure 24. The interconnected network of one hazard affecting another. Adapted from Helbing et al. (2005, p14).

Shi (2005) divides 'disaster chains' into two separate types. Simultaneous chains occur when multiple hazards cluster at the same time and place and cause several disasters concurrently (Shi, 2005). Serial chains or synergistic events are a succession of disaster events caused by a single hazard with the resultant disasters occurring in turn (Shi, 2005; Marzocchi, 2009). Catastrophes are often typified by cascading failures disseminating in the system due to the causal dependencies between system constituents (Buzna et al., 2007). In such a case, one

strong initial event can trigger a failure avalanche, spreading in a cascade-like manner within a network, with large consequential impacts (Buzna et al., 2006).

The amplification effect of hazard chains, whereby the overall hazard and risk of causally linked processes is amplified in comparison with the aggregation of presumed independent hazards, is an important aspect of cascading hazards (Kappes, 2010, 2012; Marzocchi, 2009). The amplification effect can either be due to chaining (whereby one hazard triggers and increases the effect of the next hazard) or a consequence of the spatial and temporal coincidence of both (Kappes, 2010).

A difficulty in multi-hazard analysis arises due to the comparability of hazards as their characteristics are different (Carpignano et al., 2009; Marzocchi, 2009). For example, earthquakes are typically measured on the moment magnitude scale. Landslides are recorded by the area affected or the number of landslides in one event. Flooding is measured by, for example, the depth of water or area inundated. This makes the comparison of the severity of hazards and their interactions difficult. It is easier to compare earthquake events, for example, but more difficult to compare an earthquake event with a flood event as they vary spatially, temporally and in their effects and associated vulnerability. Classification and index schemes can help to overcome this problem, but remain applicable to the one purpose they are designed for and as such cannot be applied elsewhere (Kappes et al., 2012). A way to overcome this problem is by comparing the consequences of hazards such as loss of life, injury, and damage (Kappes et al., 2012; Marzocchi, 2009). In this paper, the number of fatalities was used to compare the severity of earthquakes, coseismic landslides and earthquake-and-landslide events.

### 1.2 Coseismic landslides

Coseismic landslides refer to topographical slope failure as a result of earthquakes because of the addition of gravitational and seismic accelerations causing short lived stressed in excess of the combined cohesive and frictional strength of the underlying rock and soils

(Meunier et al., 2007). Rodriguez et al. (1999) argued that landslides are potentially the most destructive of the secondary geotechnical hazards as a result of earthquakes. Horizontal ground acceleration from seismic shaking exerts additional transient shear stresses and increases to ambient pore water pressures through cyclic gravitational loading, negatively affecting slope stability (Sidle and Ochiai, 2006).

Keefer (1984) compiled a database of 40 historical earthquakes and their associated landslides from literature and field studies, chosen to sample a variety of climatic, geological and seismic settings of the Earth's major seismic regions. The database of 40 coseismic landslides showed that landslides were responsible for highly variable, but often significant numbers and proportions of casualties and high levels of economic damage (Keefer, 2002). Landslides triggered by the $M_w$7.8 Kansu, China, earthquake in 1920 killed 240,000 people; the 1970 Peru earthquake induced a landslide killing 18,000 people (Keefer, 2002).

Fatal coseismic landslides often occur in areas of high topographical relief such as the Himalayas, Andes and Alps (Keefer, 2002). This is consistent with other studies, which have shown that the coseismic spatial distribution is not random, but is a function of distance to the epicentre, slope gradient, slope position and rock type (Keefer, 2002; Meunier et al., 2007; both in Korup 2010).

Marano et al. (2010) examined secondary hazards due to earthquakes from the Prompt Assessment of Global Earthquakes for Response Catalog (PAGER-CAT) database of 18,807 earthquakes from 1968 to 2008. PAGER-CAT is a composite earthquake catalogue from published or online databases and reports; eight global earthquake catalogues are included in the database (Allen et al., 2009). The United States Geological Survey's (USGS) Preliminary Determination of Epicenters (PDE) dataset constitutes the main source of earthquake information. PAGER-CAT incorporates events with PDE's preferred magnitude M5.5 or greater and/or any events causing one or more fatalities or injuries (Allen et al., 2009). Events from non-tectonic sources (e.g. mining) were excluded from PAGER-CAT (Allen et

al., 2009). The PDE is the primary source of information on casualties due to secondary hazards providing a breakdown of casualty types when possible. Marano et al. (2010) found that of the 749 earthquakes in the PAGER-CAT database that caused at least one fatality, 276 triggered at least one landslide, and of these, 43 were reported to have caused one or more deaths due to landslides (Marano et al., 2010). Due to the undifferentiated cause of deaths for some events, it is likely that there are more events for which deaths could be attributed to secondary hazards (Marano et al., 2010). Post-earthquake reconnaissance work is not always carried out, so often the cause of death remains ambiguous and is often attributed to the initial triggering event (Marano et al., 2010). The 2004 Sumatra tsunami event contributed 227,000 fatalities of the total 238,385 fatalities as a result of all tsunamis during the time period. Marano et al. (2010) considered this an atypical event, which does not represent the non-shaking fatality distribution of events during the timeline. After the removal of deaths attributed to the 2004 Sumatra event, landslides were found to be the cause for 71.1 % of all non-shaking deaths due to earthquakes, with tsunamis following second at 11.5 % (Marano et al., 2010).

Kappes et al.'s (2012) review of multi-hazard risk stated that 'hazard relations and interactions may have unexpected effects and pose threats that are not captured by means of separate single-hazard analyses'. It is implicit throughout the literature that cascading hazards result in losses greater than the sum of the independent hazards (Helbing and Kuhnert, 2003; Kappes, 2010; Marzocchi, 2009). However, there have been no studies to date published in the literature to quantify or substantiate this claim.

This paper used fatality models based on regression analysis to determine which covariates significantly affect the number of fatalities during an earthquake. It is presumed in the literature that cascading events lead to an amplification of losses. The significance of a triggered event on fatalities is therefore of particular interest.

## 2.0 Data

A dataset of 248 global historical earthquakes from 1980 to 2000 where one or more fatalities was incurred was used to represent earthquake events. This dataset reports the number of fatalities along with the earthquake epicentre and moment magnitude. The dataset was compiled from the USGS earthquake database information and the Emergency Events Database (EM-DAT) fatality data from the Centre for Research on the Epidemiology of Disasters (CRED). Seventy-six historical earthquake events were selected randomly and used to assess the accuracy of the earthquake fatality model at a later stage. The remaining 172 global historical earthquakes were used to model earthquake fatalities.

Rodriguez et al.'s (1999) coseismic landslide dataset of 36 coseismic landslides from 1980 to 1997 was used to represent landslide events triggered by earthquakes. The landslides are described as earthquake or seismically induced and are therefore inferred to be caused directly be seismic shaking rather than by structural failure or geomorphic change. All references to 'earthquake-and-landslides' refer to an event when an earthquake has occurred and has triggered a coseismic landslide during that event. The number of fatalities recorded and referred to in the paper is the total fatalities recorded resulting from the earthquake *and* the landslide event combined. Rodriguez et al.'s (1999) coseismic landslide database was compiled from major seismological and geotechnical journals, symposia and conferences. The dataset contains information on the date, moment magnitude, focal depth, maximum intensity, area affected and number of landslides for each event. This was combined with the PAGER-CAT database to create a database with longitude and latitude of the epicentre of the triggering earthquake and the total number of recorded fatalities. The data were cleaned to remove events causing no fatalities, leaving a dataset which included 18 earthquake-and-landslides.

Information on other factors which may affect the number of fatalities due to earthquakes or earthquake-and-landslides was compiled from various sources (Table 8) and projected into a

GIS environment as a set of global maps. The covariates were chosen based on several factors including (1) typical covariates found in the literature for this type of model, (2) expectations based on the underlying processes and (3) availability of datasets.

Table 8. Description, spatial scale and source of data for the covariates used in multiple regression analysis to determine the factors affecting the number of fatalities during earthquake and earthquake-and-landslide events. Gridded population of the world data were used to estimate the number of people affected by different levels of earthquake shaking.

| Factor | Description | Spatial scale | Source |
|---|---|---|---|
| Gridded Population | Gridded Population of the World (version 3) per year 1990-2010. | 2.5 arc minutes ~5km at the equator | Columbia University Center for International Earth Science Information Network (CIESIN) and Centro International de Agricultura Tropical (CIAT). (CIESIN, 2005) |
| GDP 1990 | Gross Domestic Product in 1990 in millions of US dollars. | 15 arc minutes ¼ degree | Columbia University Center for International Earth Science Information Network (CIESIN), (Yetman, 2004) |
| GDP 2025 | Gross Domestic Product projected for 2025 in millions of US dollars. | 15 arc minutes ¼ degree | Columbia University Center for International Earth Science Information Network (CIESIN), (Yetman, 2004) |
| Slope | Derived from SRTM30+ and ETOPO DEM. | 1 arc minute 1/120 degree | Worldgrids.org (Hengl and Reuter, 2010) |
| Poverty | Percentage of population living below $1.25 per day in 2000. | Country | UNDP, World Bank (UNDP, 2013) |
| Health | Health expenditure as a percentage of GDP in 2000. | Country | UNDP, World Bank, World Health Organization National Health Account database (UNDP, 2013) |
| Access | Travel time to major cities. | 30 arc seconds | European Commission, World Bank. (Nelson, 2008) |
| Building strength | Building strength in 5 categories, from 1 (strongest) to 5 (weakest). | Country | USGS (Jaiswal and Wald, 2008) |

Global gridded population data were used to estimate the number of people living in the area affected by each earthquake (Table 8). Population estimates are provided for 1990, 1995 and 2000 and projected (in 2004, when GPWv3 was released) to 2005 and 2010. If global gridded population data were not available for the year of an earthquake, the population was estimated for the given year by weighted interpolation in time based on temporally neighbouring data. The population data were used to estimate the population exposed to shaking; the method of estimation is explained in more detail in the next section.

Gross Domestic Product (GDP) global grids for 1990 and 2025 were created using the country-level GDP for 1990 and 2025, and projections were downscaled based on the Special Report on Emission Scenarios (SRES) B2 scenario 1990-2100 dataset and Columbia University Centre for International Earth Science Information Network's (CIESIN) Gridded Population of the World, Version 2 (GPWv2) as a base map (Table 8) (Yetman, 2004).

Slope estimates, measured in percentage, were derived from a combination of global SRTM30+ and ETOPO DEM data at 1 arc min resolution (Table 8). Building strength data were sourced from the USGS Prompt Assessment of Global Earthquakes for Response (PAGER) project on a country-by-country basis (Table 8). The PAGER project divides building strength into five categories, from 1 (strongest) to 5 (weakest).

Access is a measure of travel time in minutes to the nearest major city with population over 50,000 in the year 2000 (Table 8) (Nelson, 2008). Accessibility was computed using a cost-distance algorithm which calculates the 'cost' of travelling between two positions on a raster grid (Nelson, 2008). Each cell is assigned a value representing the cost required to travel across them; this raster grid is often labelled a 'friction-surface'. The friction-surface contains information on transport network (road, railway, river and shipping lanes), environmental (land cover and slope), and political factors (national boundaries and border crossing) that affect travel times between locations (Nelson, 2008).

Poverty was defined as the percentage of population living below the international poverty line at $1.25 (in purchasing power parity in 2000) per day (Table 8). Data were based on primary household survey data obtained from government statistical agencies and the World Bank country departments. The source data from the UNDP were inconsistently recorded. Therefore, if data were missing, the poverty value was estimated using weighted interpolation in time based on temporally neighbouring data.

Health was defined as a measure of public health expenditure as a percentage of GDP in 2000 (Table 8). Public health expenditure consists of current and capital spending from

government budgets, external borrowings and grants, and social health insurance funds. Health expenditure data were downloaded at country level.

The required information for each covariate was extracted from the global covariate maps within a GIS environment using the longitude and latitude of the earthquake epicentre for each earthquake and earthquake-and-landslide event. For each epicentre location, the corresponding cell or country data were extracted and assigned to the event as a proxy for determining other factors which could affect the number of fatalities.

## 3.0 Estimation of exposed population

A key independent variable affecting the number of fatalities is the population potentially affected. The number of fatalities from an earthquake should be related to the number of people exposed to the shaking caused by the earthquake. If the epicentre of the earthquake is closer to highly dense populations, more people will be exposed and a higher number of fatalities is expected. If the epicentre of the earthquake is far from dense populations, less people will be exposed and a small number of fatalities are expected.

USGS ShakeMaps were used to calculate the area affected by different levels of shaking (3.9, 9.2, 18 and 34 pga) using 28 events between 2004 and 2009 ranging from 5.6 to 8.6 moment magnitude. Data were not available before this date except for the United States of America. The 28 events were selected from 78 earthquake events recorded in the PAGER-CAT database with one or more fatalities between 2004 and 2009. The selection from the 78 events was based on the availability of ShakeMaps for download from the USGS ShakeMap Archive.

The thresholds for the levels of shaking were taken from the USGS ShakeMap scale for moderate, strong, very strong and severe perceived shaking (Table 9). For each event, the peak ground acceleration (pga) point data recorded by seismometers were projected into a GIS environment and converted into the raster data format. The area affected by the different

thresholds of shaking was then estimated for each event (Figure 25). A best-fit model was developed from the empirical data relating earthquake moment magnitude to area affected (measured in degrees) and their 95 % confidence intervals for each of the different levels of shaking (Figure 26).

Table 9. The USGS ShakeMap scale. The USGS produces serveral ShakeMap types. The peak ground acceleration (pga) data were used to determine levels of shaking for estimated area affected. Peak ground acceleration at each station is contoured in units of percent-g (where g = acceleration due to the force of gravity). Thresholds of ≥3.9 pga (moderate perceived shaking), ≥9.2 pga (strong perceived shaking), ≥18 pga (very strong perceived shaking), and ≥34 pga (severe perceived shaking) were used to provide shaking levels for calculating exposed population to earthquake shaking.

| **PERCEIVED SHAKING** | Not felt | Weak | Light | Moderate | Strong | Very strong | Severe | Violent | Extreme |
|---|---|---|---|---|---|---|---|---|---|
| **POTENTIAL DAMAGE** | None | None | None | Very light | Light | Moderate | Moderate/ heavy | Heavy | Very heavy |
| **PEAK ACCELERATION (%g)** | < .17 | .17-1.4 | 1.4-3.9 | 3.9-9.2 | 9.2-18 | 18-34 | 34-65 | 65-124 | >124 |
| **PEAK VELOCITY (cm/s)** | <0.1 | 0.1-1.1 | 1.1-3.4 | 3.4-8.1 | 8.1-16 | 16-31 | 31-60 | 60-116 | >116 |
| **INSTRUMENTAL INTENSITY** | I | II-III | IV | V | VI | VII | VIII | IX | X+ |

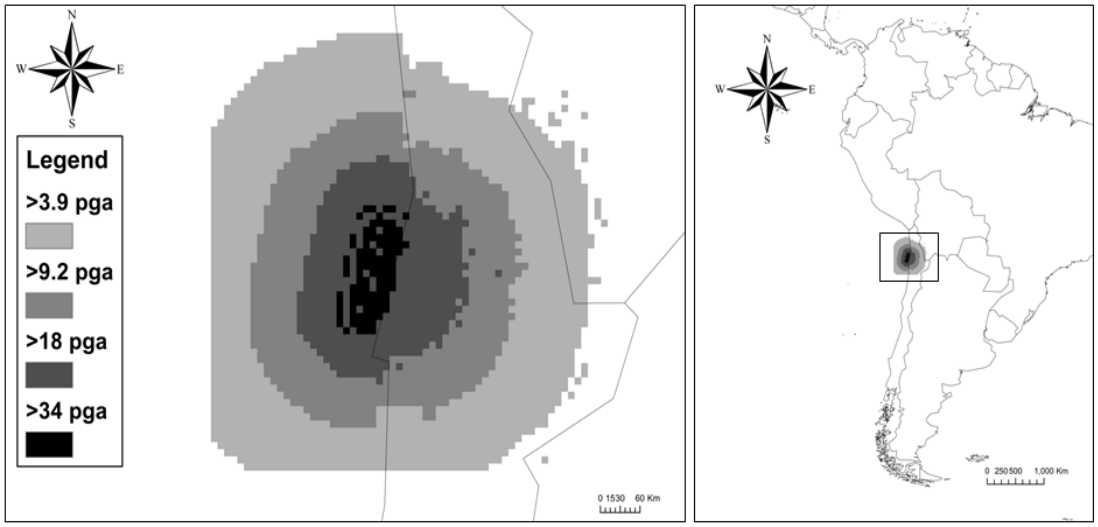


Figure 25. Example of a peak ground acceleration ShakeMap from the USGS archive representing the Chilean earthquake on 15th November 2007. Cell colours on a grey scale represent peak ground acceleration (%g) for thresholds of ≥3.9 pga, ≥9.2 pga, ≥18 pga, and ≥34 pga shaking. The area affected by each level of shaking was calculated for 28 events between 2004 and 2009 from the USGS ShakeMap archive. The data were ussed to create models to predict area affected by different levels of shaking given recorded earthquake moment magnitude at the epicentre.

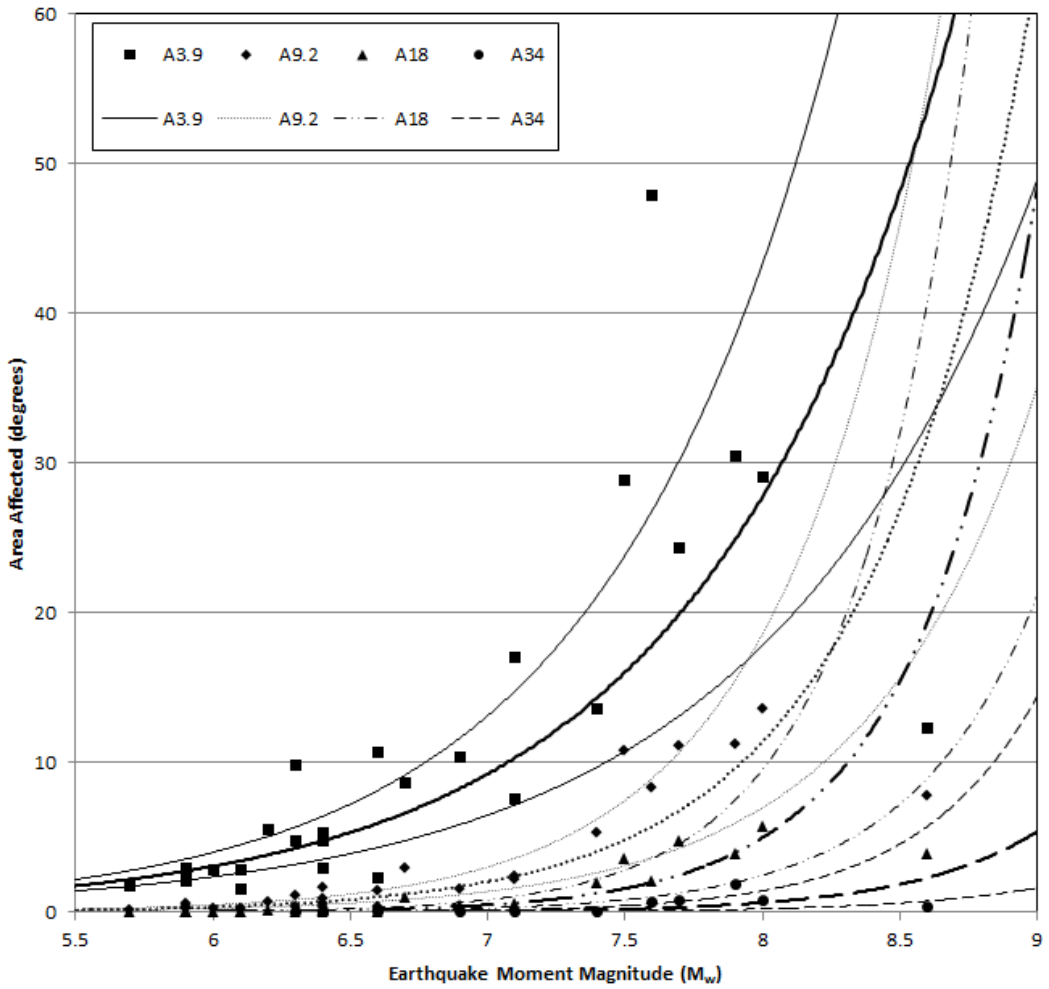


Figure 26. Area affected (degrees) for different levels of shaking (≥3.9 pga, ≥9.2 pga, ≥18 pga, and ≥34 pga) and models fitted to the data based on earthquake moment magnitude ($M_w$). The area affected by each level of shaking was estimated from 28 events between 2004 and 2009 from the USGS ShakeMap archive. The models were used to estimate population exposed to shaking to be used in the multiple regression analysis. Each model's 95% confidence limit is plotted using the same type of line as the best-fit model. The best-fit regression is shown in bold.

Four exponential models were fitted to the empirical data:

$$A_{3.9} = 0.0042e^{1.0992 \times M} \quad \text{Equation 6}$$

$$A_{9.2} = (1 \times 10^{-5})e^{1.7106 \times M} \quad \text{Equation 7}$$

$$A_{18} = (6 \times 10^{-8})e^{2.2792 \times M} \quad \text{Equation 8}$$

$$A_{34} = (3 \times 10^{-8})e^{2.1127 \times M} \quad \text{Equation 9}$$

Where,

$A_{3.9}$ = area affected by ≥3.9 pga shaking,

$A_{9.2}$ = area affected by ≥9.2 pga shaking,

$A_{18}$ = area affected by ≥18 pga shaking,

$A_{34}$ = area affected by ≥34 pga shaking, and

$M$ = earthquake magnitude.

Table 10 shows the upper and lower 95 % confidence intervals for the fitted models shown in Equations 5-8. The root mean square errors between model predictions and the estimated observed area affected were 10.29 for $A_{3.9}$, 3.92 for $A_{9.2}$, 3.02 for $A_{18}$ and 0.68 for $A_{34}$. The area affected was then calculated as a transform of the recorded earthquake magnitude for each historical earthquake event from the combined USGS and EM-DAT dataset. The radius $r$ of each area affected was calculated using:

$$r = \sqrt{\frac{A}{\pi}} \qquad \text{Equation 10}$$

Table 10. A table of estimated coefficients for Area Affected models seen in Equations 5-8. The upper and lower 95% confidence intervals for each fitted model are shown. This data is shown plotted in Figure 3.

| **Model** | **Covariate** | **Estimated coefficient** | **95% Confidence Interval** | |
|---|---|---|---|---|
| | | | **Lower limit** | **Upper limit** |
| **$A_{3.9}$** | Intercept | 0.0042 | 0.0056 | 0.0032 |
| | Earthquake Magnitude | 1.0992 | 1.0075 | 1.1909 |
| **$A_{9.2}$** | Intercept | $(1 \times 10^{-5})$ | $(2 \times 10^{-5})$ | $(9 \times 10^{-6})$ |
| | Earthquake Magnitude | 1.7106 | 1.6098 | 1.8113 |
| **$A_{18}$** | Intercept | $(6 \times 10^{-8})$ | $(9 \times 10^{-8})$ | $(4 \times 10^{-8})$ |
| | Earthquake Magnitude | 2.2792 | 2.1401 | 2.4184 |
| **$A_{34}$** | Intercept | $(3 \times 10^{-8})$ | $(5 \times 10^{-8})$ | $(1 \times 10^{-8})$ |
| | Earthquake Magnitude | 2.1127 | 1.9266 | 2.2987 |

Circular buffer zones around each event epicentre were generated based on the estimated radius of the affected area (Figure 27). The number of people living within the area exposed

to each level of shaking was estimated by intersecting the circular areas with the global gridded population data for the corresponding year from SEDAC.

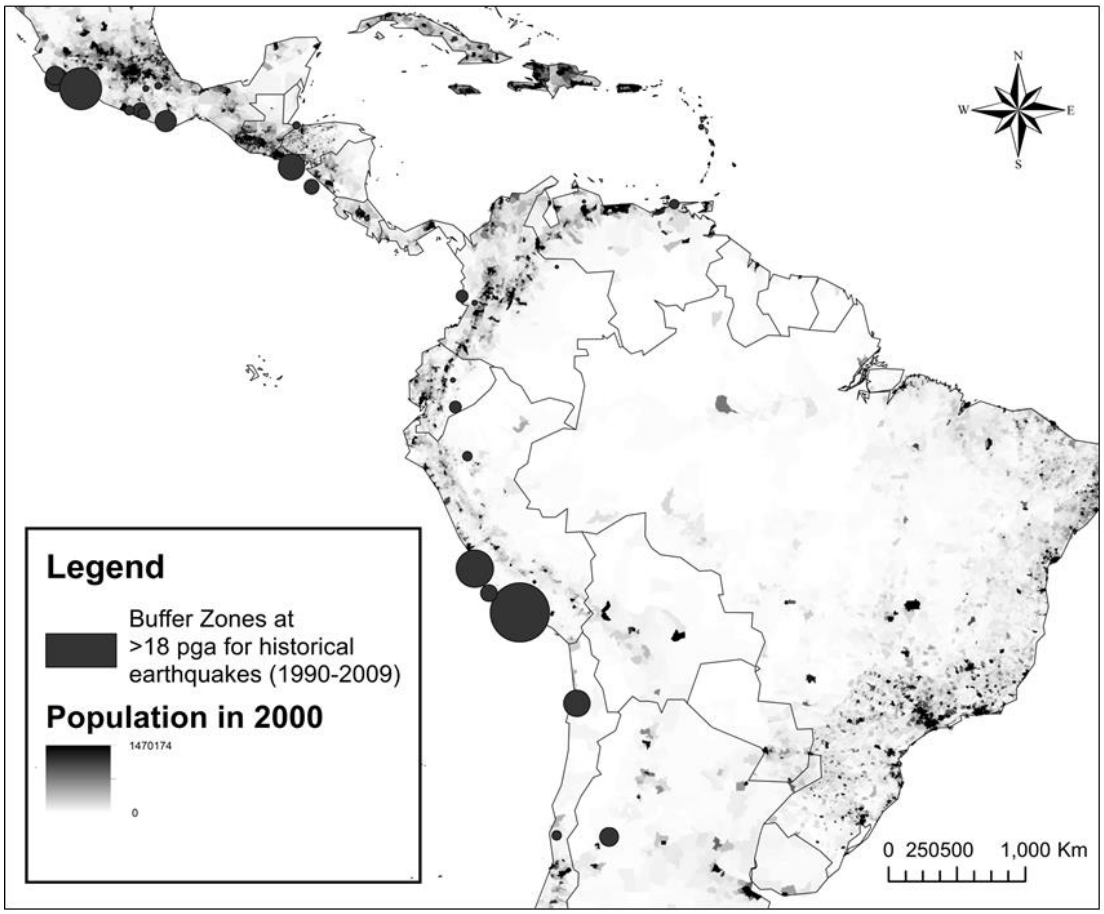


Figure 27. An example of buffer zones around historical earthquakes in Central and South America in the PAGER-CAT database causing one or more fatalities (1990-2009) using radius of area for ≥18 pga. The buffer zones were determined from the models for area affected for different levels of shaking (≥3.9 pga, ≥9.2 pga, ≥18 pga, and ≥34 pga) based on recorded epicentre moment magnitude data. Gridded Population of the World for 2000 data are also shown. The population data were used to count the number of people living within each buffer zone, providing the estimated population exposed to different levels of shaking, to be used in the multiple regression model.

## 4.0 Fatalities

The number of fatalities had a right-skewed distribution with a large number of smaller values and a tail of larger values with lower frequency. Therefore, the number of fatalities was transformed using the log function. Figure 28 shows a plot of number of fatalities against seismic magnitude where earthquakes are separated from earthquake-and-landslides. Figure 28 reveals an increase in the number of fatalities for earthquake-and-landslides compared with earthquake events with no landslides. It is also clear that the relationship

between number of fatalities from earthquakes and earthquake magnitude is nonlinear such that a log-transform of number of fatalities produces an approximately linear relation.

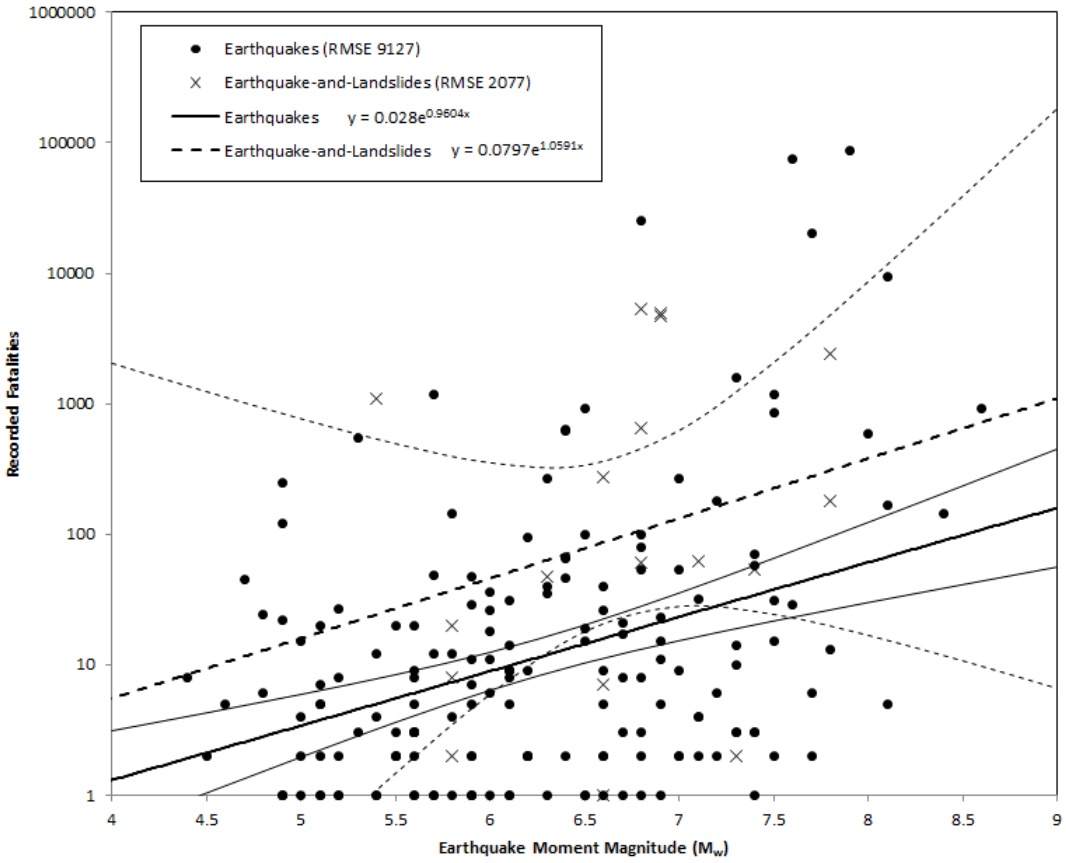


Figure 28. Log of the number of recorded historical fatalities with respect to moment magnitude for 172 earthquakes and 18 earthquake-and-landslides with fitted exponential models. Data were sourced from PAGER-CAT, EM-DAT and Rodriguez et al. (1999) datasets described in section *2.0 Data*. The best-fit regression for Earthquake and Earthquake-and-Landslide models are shown in bold. Each model's 95% confidence limit is plotted using the same type of line as the best-fit model.

Although an increase in the number of fatalities was predicted, and this seems to match expectations, the magnitude of the uplift in number of fatalities was not expected: the increase in number of fatalities appears to be by a factor of almost ten (Figure 28). The 95 % confidence intervals for each best-fit statistical model are shown in Figure 28, and the corresponding coefficients for the best-fit, upper and lower 95 % confidence models can be seen in Table 11.

Table 11. A table of estimated coefficients for the best-fit statistical model shown in Figure 5. The upper and lower 95% confidence intervals for each fitted model are shown. This data is shown plotted in Figure 5.

| Model | Covariate | Estimated coefficient | 95% Confidence Interval | |
|---|---|---|---|---|
| | | | Lower limit | Upper limit |
| Earthquake | Intercept | 0.028 | 0.0198 | 0.0396 |
| | Earthquake Magnitude | 0.9604 | 0.9184 | 1.0024 |
| Earthquake-and-Landslide | Intercept | 0.0797 | 0.0007 | 8.9187 |
| | Earthquake Magnitude | 1.0591 | 1.2645 | 0.8536 |

## 4.1 Multiple regression analysis

Multiple regression analysis was used to model the relationship between the number of fatalities and several independent covariates using the backward stepwise method. The covariates selected were: exposed population, earthquake magnitude, GDP, slope, poverty, health, access to cities, building strength and whether a landslide was triggered or not. Whether there is a landslide or not as a result of an earthquake was coded as a binary variable, representing presence (1) or absence (0) of landslides.

The significant (at the 95 % confidence level) covariates were earthquake magnitude (EQ.M), building strength (BS), population exposed to ≥18 pga (PopExp18) and whether a landslide was triggered or not (LS.NoLS). Table 12 shows the covariates in order of significance with their statistics generated by the R statistical software.

Table 12. A table of the significant covariates (at the 95% confidence level) associated with fatalities determined by backward stepwise multiple regression analysis. Covariates are shown in order of significance and with their associated statistics. The upper and lower limit at the 95% confidence interval for each covariate is also shown.

| Covariate | Estimated Parameter | Estimated Standard Error | *t*-value | P(>\|*t*\|) | 95% Confidence Interval | |
|---|---|---|---|---|---|---|
| | | | | | Lower Limit | Upper Limit |
| Intercept | -1.806 | $6.137 \times 10^{-1}$ | -2.944 | 0.00368 | -3.009153 | $-6.036567 \times 10^{-1}$ |
| PopExp18 | $2.123 \times 10^{-7}$ | $4.807 \times 10^{-8}$ | 4.415 | $1.75 \times 10^{-5}$ | $1.180359 \times 10^{-7}$ | $3.064799 \times 10^{-7}$ |
| LS.NoLS | $9.614 \times 10^{-1}$ | $2.310 \times 10^{-1}$ | 4.162 | $4.91 \times 10^{-5}$ | $5.085989 \times 10^{-1}$ | 1.414142 |
| EQ.M | $3.348 \times 10^{-1}$ | $8.148 \times 10^{-1}$ | 4.109 | $6.06 \times 10^{-5}$ | $1.750993 \times 10^{-1}$ | $4.944906 \times 10^{-1}$ |
| BS | $1.841 \times 10^{-1}$ | $7.028 \times 10^{-2}$ | 2.619 | 0.00957 | $4.633698 \times 10^{-2}$ | $3.218353 \times 10^{-1}$ |

The number of fatalities is highly correlated with the number of people exposed to earthquake shaking above 18 pga. The model shows clearly that the presence of a triggered coseismic landslide due to the initial earthquake significantly increases the number of resultant fatalities. The earthquake magnitude and the strength of the buildings affected by the shaking are also contributing factors to the number of fatalities caused. Weaker building structures are more likely to be damaged or collapse during an earthquake and thus result in a greater number of fatalities compared with stronger building structures.

The fitted multivariate regression model was:

$$\log(F_E) = -1.806 + 0.3348M + 0.1841BS + 0.9614LS + 0.0000002123PE_{18} \quad \text{Equation 11}$$

where $F_e$ is the number of fatalities from an earthquake, $M$ is the earthquake moment magnitude, $BS$ is the building strength, $LS$ is whether a landslide was triggered (1) or not (0) and $PE_{18}$ is the population exposed to ≥18 pga shaking, 95% Confidence Interval (-1.95, 0.47).

## 4.2 City fatality estimates

Fatalities due to earthquakes and earthquake-and-landslides for 68 cities around the world were estimated using the fatality model (Equation 10). The global distribution of earthquake risk and global distribution of landslide risk maps from the Hotspots report were used to create a map of areas at risk of both earthquakes and landslides (Figure 29) (Dilley et al., 2005). 68 cities within this zone were selected and the number of fatalities from an earthquake of varying magnitudes ($M_w$ 4, 5, 6, 7, and 8) was estimated using the model (Equation 10).

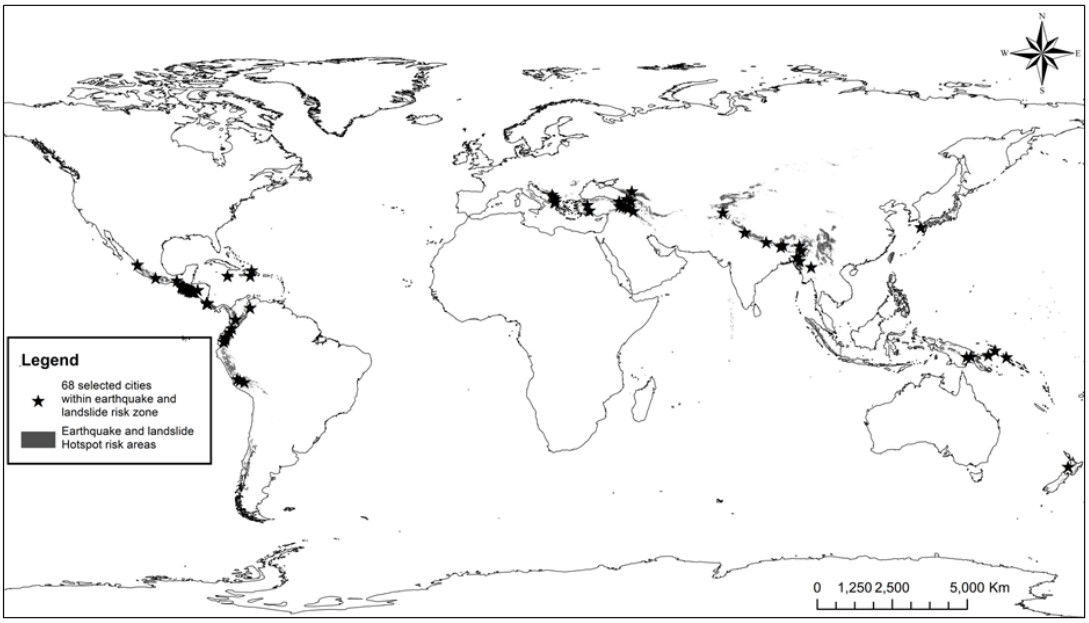


Figure 29. Areas at risk from both earthquakes and landslides. A map was produced from the overlap of the Global Distribution of Earthquake Risk of Mortality and Global Distribution of Landslide Risk of Mortality maps produced in the Hotspots report (Dilley et al., 2005). Starred points indicate the location of 68 cities within this at risk area which were used as the epicentres for simulated earthquakes. The number of fatalities estimated by the model for simulated earthquakes and earthquake-and-landslide events were recorded and are shown in Figure 30.

Global building strength data for each country from PAGER were used (Table 8); the area exposed to shaking above 18 pga was calculated using Equations 7 and 9 to create a circular buffer around each city epicentre for the different earthquake magnitudes. The number of people living within this area was counted using GPW for the year 2010 to estimate the population exposed to ≥18 pga shaking.

The number of fatalities from earthquakes alone and the increase in fatalities expected from landslides being subsequently triggered were estimated for the 68 cities. These fatality data can be seen in Figure 30. The variation in fatality estimates for each magnitude earthquake (Figure 30) arises due to the differences in the population exposed to shaking for each city and in building strength for each country. A selection of the 68 cities shown in Figure 30 was used to predict fatality values in each city using Equation 10 and the 95 % confidence intervals of the model for a $M_w8$ earthquake. This estimates a range of predicted fatalities for each city calculated from the model's 95 % confidence interval (seen in Table 13).

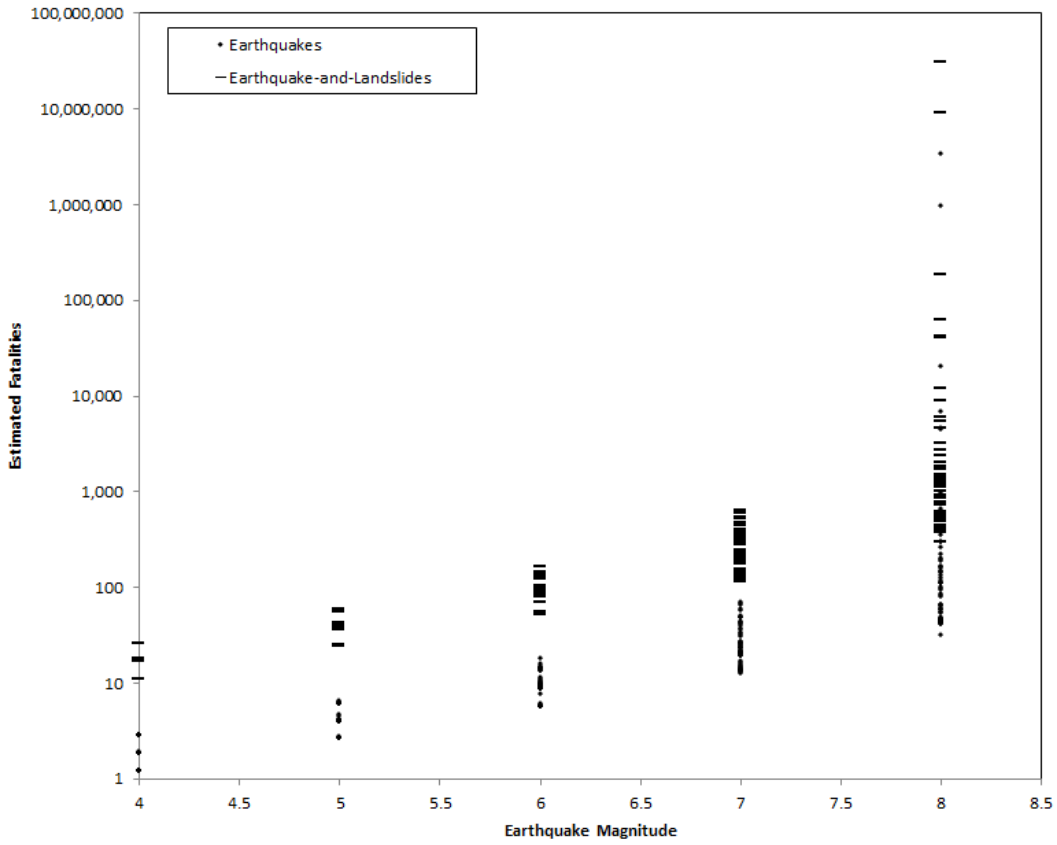


Figure 30. Plot of estimated number of fatalities for 68 cities given an earthquake at the city centre for magnitudes of $M_w$ 4, 5, 6, 7 and 8. Fatalities were estimated for earthquake-only and earthquakes-and-landslide scenarios.

Table 13. Predicted fatalities from earthquakes and earthquakes-and-landslides using the fatality model in Equation 10 when a $M_w$8 earthquake occurs for selected cities at risk from both earthquakes and landslides. The ranges of fatalities are calculated from the models 95% confidence intervals.

| City | Country | Predicted Earthquake Fatalities (and 95% confidence interval estimates) | Predicted Earthquake-and-Landslide Fatalities (and 95% confidence interval estimates) |
|---|---|---|---|
| Permet | Albania | 110 (1-323) | 1002 (11-2958) |
| Rreshen | Albania | 44 (0-129) | 400 (4-1180) |
| Manizales | Colombia | 4670 (53-13782) | 42728 (479-126099) |
| Cartago | Costa Rica | 352 (4-1038) | 3217 (36-9494) |
| Alajuela | Costa Rica | 8 (0-23) | 70 (1-207) |
| Guaranda | Ecuador | 604 (7-1783) | 5529 (62-16317) |
| La Tacunga | Ecuador | 204 (2-601) | 1864 (21-5500) |
| San Miguel | El Salvador | 43 (0-128) | 397 (4-1172) |
| Sonsonate | El Salvador | 196 (2-579) | 1794 (20-5295) |
| Antigua | Guatemala | 45 (1-134) | 415 (5-1226) |
| Solola | Guatemala | 44 (0-131) | 406 (5-1197) |
| Yuscaran | Honduras | 101 (1-298) | 922 (10-2711) |
| Nagasaki | Japan | 387 (4-1141) | 3537 (40-10437) |
| Haka | Myanmar | 111 (1-327) | 1013 (11-2989) |
| New Plymouth | New Zealand | 8 (0-23) | 72 (1-212) |
| Arawa | Papua New Guinea | 8 (0-25) | 77 (1-229) |
| Mendi | Papua New Guinea | 83 (1-246) | 762 (9-2249) |
| Abancay | Peru | 86 (2-255) | 790 (9-2333) |
| Nal'chik | Russia | 112 (1-329) | 1021 (11-3013) |
| Bitlis | Turkey | 97 (1-286) | 886 (10-2616) |
| Coruh | Turkey | 55 (1-164) | 507 (6-1497) |
| Merida | Venezuela | 164 (2-483) | 1496 (17-4416) |

The city fatality estimates represent the number of fatalities predicted given an earthquake at the centre of each city. The model predicts the number of fatalities given an earthquake of a given magnitude occurring at the city centre, and the numbers of fatalities if at least one landslide were to occur as a result of the earthquake. However, the model does not attempt to predict the probability of a landslide occurring given the earthquake.

### 4.3 Comparison with observed fatalities

The 76 historical earthquakes held back from the analysis were compared with model predictions. Building strength and the population exposed to ≥18 pga shaking were estimated

using the methods described previously. Of the 76 earthquakes, eight events resulted in triggered landslides.

The root mean square error for earthquake-only fatality estimates compared with the observed fatalities in the validation dataset is 52 fatalities. Two events stand out as outliers, with the number of observed fatalities higher than predicted by the model. For most of the fatal earthquakes in the sample, the estimated number of deaths is within one order of magnitude of those observed. While in the predictive sense such a large ratio of predicted to observed fatalities does not seem noteworthy, in practice the warning level accompanying such a prediction may be valuable and on target for deciding the appropriate level of response (Jaiswal and Wald, 2010).

The empirical model over-predicts fatalities during earthquake events with associated landsliding; the root mean square error for the earthquake-and-landslide events is 3,077 fatalities. This lack of predictive ability of the model is most likely due to the small sample size used for earthquake-and-landslide events. Unfortunately, very little data are available for earthquakes that have triggered landslide events. Until a more comprehensive fatality dataset is collated for landslides triggered by earthquakes, the model's predictive ability will remain limited.

## 5.0 Discussion

The model indicates the significant covariates affecting fatalities during earthquakes. Earthquake magnitude is a significant variable affecting the number of fatalities as expected; this is supported in the literature as the greater the shaking caused by the earthquake, the greater the damage to buildings and therefore the number of fatalities. The strength of the building also affects the number of fatalities; in countries with buildings more resistant to earthquake shaking, fewer fatalities are seen. The adage 'earthquakes don't kill people - buildings do' is applicable here. The number of people exposed to shaking also affects the number of fatalities during an event; the more people exposed to shaking, the more people

are at risk of death and more fatalities are experienced. Most interestingly, the triggering of landslides increases the risk of fatalities from the secondary hazard. If this landslide occurs where there is a built-up population, there is an associated increase in fatalities compared to if no landslide had occurred.

The selection of the data for each event was determined by the location of the epicentre. However, many of the covariates used in the fatality model were produced from source data representing a range of spatial resolutions. This variation in resolution may not adequately represent the conditions experienced by the area affected by the earthquake. Although the use of data defined at different spatial resolutions is necessary from a practical viewpoint, it may have implications for modelling as the relative importance of the independent variables may be affected. This should be taken into consideration when interpreting the results.

The method of calculating the area affected by different levels of shaking assumes that the area affected is circular, which provides a reasonable approximation for the purpose of estimating the area affected and the population exposed. However, the area affected is unlikely to be perfectly circular in practice, especially for higher levels of shaking and in areas of high relief. The geology of the area was also not included in the calculation of the area affected by shaking.

Poverty, health expenditure and building strength data were recorded at the country level. These country-level estimates were used as a proxy for the conditions present at the location of the earthquake epicenter. This assumes that these covariates are uniform within a country. In reality, this is not true. However, data at a finer resolution do not exist globally. Also, GDP per capita data for 1990 and 2025 were also originally estimated at the country level before being down-scaled to 15 arc min resolution using gridded population datasets.

The geology of the area could have a significant impact on the number of fatalities caused by an earthquake due to liquefaction and amplification effects through certain types of rock and soil, and on whether a landslide is triggered or not. Geology was not included in the multiple

regression analysis because a consistent global map with sufficient detail was not available. The geology of the area can affect shaking as a result of earthquakes because of the softness and thickness of the upper layer. Shaking increases in softer rocks, when the sediment above hard rock is thicker, and in soil near the surface.

Several high magnitude earthquake events exist in the dataset that were not recorded as having triggered a landslide. It is not guaranteed that these events did not trigger a subsequent landslide. It is, for example, possible that the area experiencing the earthquake was of low relief and slope. Alternatively, landslides may have occurred, but were not recorded, possibly because they did not cause any fatalities. Alternatively, it is highly unlikely that any landslides which caused a fatality directly went unrecorded.

The earthquake data were cleaned to remove any events below $M_w$4.0 shaking by the USGS. This could create bias in the sample as smaller earthquakes for which landslides may not be induced were excluded. Therefore, the model can only be applied to earthquake events above the $M_w$4.0 threshold. Below this level of shaking, the model has little usefulness; however, empirical evidence given by Keefer (1984) suggests few landslides are caused by earthquakes below $M_w$4.0.

Uncertainty in the model estimates particularly arise because it is unknown whether the landslides that occurred during these historical events affected any of the population. It is plausible that while landslides occurred during the events, they did not affect any human populations. The empirical model does not capture the population exposed to landslides. For this to be captured, the area (and associated exposed population) affected by historical coseismic landslides would have to be collated. Such a dataset does not currently exist and is beyond the scope of this investigation.

The association between landslides and increased fatalities is not necessarily directly causal (i.e. landslides cause fatalities adding to the total number of fatalities). It could arise, for example, because both outcomes (landslides, fatalities) are promoted by some underlying

common driver. For example, poorer (and therefore more vulnerable) communities are often located on steeper, less stable slopes (El-Masri, 1997; Kates and Haarmann, 1992). During an earthquake event, they may be more vulnerable to the shaking from earthquakes (e.g. because of poorer infrastructure) and could experience a higher proportion of fatalities while landslides also occur in these areas. Floodplains are often occupied by the wealthier population because of geographical access and proximity to rivers and estuaries as resources and centres of trade (Fleming, 2002). This wealthier component of the population is likely to be less vulnerable, but is spatially located in an area where landslides are unlikely to occur. Similarly, landslides could block roads and access routes, hampering rescue efforts following an earthquake. The first 24-48 h of search and rescue following an earthquake are especially important in saving lives. There is a dramatic drop-off in live finds during the 24-48 h post-earthquake timeframe, with very few live rescues after 10 days (Macintyre et al., 2006). In earthquake-and-landslide events, the landslide may not necessarily be the direct cause of fatalities, but could exacerbate the number of fatalities by reducing access to those trapped or requiring medical assistance in the immediate aftermath of an earthquake. Therefore, the increase in fatalities associated with earthquake-and-landslide events may be, but is not necessarily, directly causal.

To be able to differentiate between the above possibilities (i.e. landslides cause and increase fatalities; an underlying driver such as high slope promotes landslides and increases vulnerability), and ultimately attribute cause, data at a finer spatial resolution than used here would be required. The spatial distribution of each landslide occurrence would need to be correlated with a topographical map of slope and poverty indicators per household or neighbourhood. Although measures of these factors were used in this study to explore their statistical relations with fatalities, the spatial scale at which they were analysed prevented diagnosis of these potential causal links. Until within-country data are provided, for example on social vulnerability, it will remain an open question.

The uncertainty in hindcasting the total earthquake fatalities using the empirical model incorporates the variability that comes from (a) the uncertainty in the estimated population exposed, (b) the variability of building strengths within countries, (c) possible errors in the number of recorded deaths in the catalogue, and (d) uncertainty in the recorded factors affecting earthquake fatality data. Despite the limited predictive ability for earthquake-and-landslide fatalities, the model is useful in revealing the significant factors affecting fatalities during earthquakes; particularly, that landsliding is associated with an increase in the number of fatalities.

Further research should investigate whether economic losses, number of injured, ratio of injured to fatalities and building damage are greater for cascading hazards compared with single hazards. The signal within the data is very small when looking at global examples and when dealing with natural hazards as they are such complex phenomena, affected by many other factors. If we examine a range of hazard outcomes, the signal could be present in other consequences, which would strengthen the overall signal if the numbers involved are greater, or if the multiple outcomes can be analysed simultaneously. For example, whereas people can move their location, affecting fatality rates through evacuation and being outside or inside during an event, economic assets cannot be moved out of the affected area.

The utility of the available data on earthquake events for investigating cascading hazards is limited as records typically assign losses to the primary hazard event. To be able to determine whether cascading events result in greater losses than the sum of the constituent hazards, the fatalities caused by the coseismic landslide alone need to be separated from those caused by the triggering earthquake. This can be achieved by subtracting earthquake-only loss models from earthquake-and-landslide models. The difference between the models would account for those fatalities as a result of the coseismic landslides. The fatality estimates could be used to create a coseismic landslide model based on landslide magnitude.

### 6.0 Conclusions

The relationship between number of fatalities and earthquakes alone and earthquake-and-landslides was investigated. Regression analysis suggested that the presence of a triggered landslide significantly increases the number of fatalities caused by an earthquake event compared with if no landslide is triggered, independent of other factors including seismic magnitude, building strength and population affected. The model quantifies, for the first time, the effect of triggered landslides in increasing the number of fatalities. This pattern of increased losses as a result of cascading events has previously been referred to, but has been hitherto unsubstantiated, in the literature. The fitted earthquake fatality model can be used to predict the likely human losses as a result of earthquakes given the availability of earthquake magnitude, building strength and population data. Further research into cascading hazards is necessary, but will ultimately be constrained by data availability. Data collection and recording methods are becoming more detailed with wider coverage suggesting that improvements in terms of data quality to the model presented here will be possible in future.

## Acknowledgements

We would like to thank the Centre for Research on the Epidemiology of Disasters and U.S. Geological Survey for the provision of earthquake data.

## References

ALLEN, T. I., MARANO, K. D., EARLE, P. S. & WALD, D. 2009. PAGER-CAT: A composite earthquake catalog for calibrating global fatality models. Seismological Research Letters, 80, 57-62.

BUZNA, L., PETERS, K., AMMOSER, H., KUHNERT, C. & HELBING, D. 2007. Efficient response to cascading disaster spreading. Physical Review E, 75.

BUZNA, L., PETERS, K. & HELBING, D. 2006. Modelling the dynamics of disaster spreading in networks. Physica a-Statistical Mechanics and Its Applications, 363, 132-140.

CARPIGNANO, A., GOLIA, E., DI MAURO, C., BOUCHON, S. & NORDVIK, J. P. 2009. A methodological approach for the definition of multi-risk maps at regional level: first application. Journal of Risk Research, 12, 513-534.

CIESIN 2005. Gridded Population of the World, Version 3 (GPWv3). Palisades, NY: CIESIN, Columbia University.

DILLEY, M., CHEN, R. S., DEICHMANN, U., LERNERLAM, A. L. & ARNOLD, M. 2005. Natural Disaster Hotspots: A Global Risk Analysis. Natural Disaster Hotspots: A Global Risk Analysis, 1-134.
EL-MASRI, S., AND TIPPLE, G., 1997. Urbanization, poverty and natural disasters: vulnerability of settlements in developing countries. Reconstructing after Disasters, 12, 141-158.
FLEMING, G. 2002. Learning to live with rivers - the ICE's report to government. Proceedings of the Institution of Civil Engineers-Civil Engineering, 150, 15-21.
GREIVING, S. 2006. Integrated risk assessment of multi-hazards: a new methodology, Geological Survey of Finland.
HELBING, D. & KUHNERT, C. 2003. Assessing interaction networks with applications to catastrophe dynamics and disaster management. Physica a-Statistical Mechanics and Its Applications, 328, 584-606.
HENGL, T. & REUTER, H. I. 2010. Worldgrids - a public repository and a WPS for global environmental alyers: Slope Map [Online]. Available: http://worldgrids.org/doku.php?id=wiki:slpsrt3 [Accessed 9th February 2012].
JAISWAL, K. & WALD, D. 2008. Creating a Global Building Inventory for Earthquake Loss Assessment and Risk Management: Open-File Report 2008-1160: Appendix VII: PAGER_database_v1.4.xls [Online]. Available: http//pubs.usgs.gov/of/2008/1160/downloads/PAGER_database/ [Accessed 4th March 2012].
JAISWAL, K. & WALD, D. 2010. An Empirical Model for Global Earthquake Fatality Estimation. Earthquake Spectra, 26, 1017-1037.
KAPPES, M. S., KEILER, M., VON ELVERFELDT, K. & GLADE, T. 2012. Challenges of analyzing multi-hazard risk: a review. Natural Hazards, 64, 1925-1958.
KAPPES, M. S., KEILER, M., AND GLADE, T., (ed.) 2010. From single- to multi-hazard risk analyses: a concept addressing emerging challenges: Proceedings of the 'Mountain Risks' International Conference, Nov 2010.
KATES, R. W. & HAARMANN, V. 1992. Where the Poor Live - Are the Assumptions Correct. Environment, 34, 4-&.
KEEFER, D. K. 1984. Landslides Caused by Earthquakes. Geological Society of America Bulletin, 95, 406-421.
KEEFER, D. K. 2002. Investigating landslides caused by earthquakes - A historical review. Surveys in Geophysics, 23, 473-510.
LERNER-LAM, A. 2007. Assessing global exposure to natural hazards: Progress and future trends. Environmental Hazards, 7, 10-19.
MACINTYRE, A. G., BARBERA, J. A. & SMITH, E. R. 2006. Surviving collapsed structure entrapment after earthquakes: a "time-to-rescue" analysis. Prehospital Disaster Medicine, 21, 4-19.
MARANO, K. D., WALD, D. J. & ALLEN, T. I. 2010. Global earthquake casualties due to secondary effects: a quantitative analysis for improving rapid loss analyses. Natural Hazards, 52, 319-328.
MARZOCCHI, W., MASTELLONE, M.L., AND DI RUOCCO, A., 2009. Principles of multi-risk assessment: Interaction amongst natural and man-induced risks. European Comission, EU23615.
MEUNIER, P., HOVIUS, N. & HAINES, A. J. 2007. Regional patterns of earthquake-triggered landslides and their relation to ground motion. Geophysical Research Letters, 34.
NELSON, A. 2008. Travel time to major cities: A global map of accessibility [Online]. Ispra Italy. Available: http://www-tem.jrc.it/accessibility [Accessed 9th March 2012].
PEDUZZI, P., DAO, H., HEROLD, C. & MOUTON, F. 2009. Assessing global exposure and vulnerability towards natural hazards: the Disaster Risk Index. Natural Hazards and Earth System Sciences, 9, 1149-1159.
RODRIGUEZ, C. E., BOMMER, J. J. & CHANDLER, R. J. 1999. Earthquake-induced landslides: 1980-1997. Soil Dynamics and Earthquake Engineering, 18, 325-346.
SHI, P. 2005. Theory and practice on Disaster System Research. Ppaer for the Fifth Annual IIASA-DPRI Forum.
SIDLE, R. C. & OCHIAI, H. 2006. Landslides: Processes, Prediction, and Landuse, Water Resources Monograph.
UNDP 2004. Reducing Disaster Risk: A Challenge for Development. UNDP Bureau for Crisis Prevention and Recovery, New York, 146.
UNDP. 2013. International Human Development Indices: Data [Online]. Available: http://hdrstats.undp.org/en/tables/ [Accessed 1st March 2012].

UNU-EHS 2011. World Risk Report 2011.
YETMAN, G., GAFFIN, S. R. & XING, X. 2004. Global 15 x 15 Minute Grids of the Downscaled GDP Based on the SRES B2 Scenario, 1990 and 2025 [Online]. Available: http://sedac.ciesin.columbia.edu/data/set/sdp-downscaled-gdp-grid-b2-1990-2025 [Accessed 1st March 2012].

# Appendix 1

Table A1. A list of the acronyms used.

| Acronym | Description |
|---|---|
| CIESIN | Columbia University Centre for International Earth Science Information Network |
| CRED | Centre for Research on the Epidemiology of Disasters |
| DEM | Digital Elevation Model |
| DRI | Disaster Risk Index |
| EM-DAT | Emergency Events Database |
| ETOPO | Earth Topography Digital Dataset |
| GDP | Gross Domestic Product |
| GIS | Geographical Information System |
| GPW | Gridded Population of the World |
| PAGER | Prompt Assessment of Global Earthquakes for Response |
| PAGER-CAT | Prompt Assessment of Global Earthquakes for Response Catalog |
| PDE | Preliminary Determination of Epicentres |
| pga | Peak ground acceleration |
| SRES | Special Report on Emission Scenarios |
| SRTM | Shuttle Radar Topography Mission |
| UNDP | United Nations Development Program |
| USGS | United Stated Geological Society |
| WRI | World Risk Index |

# 4. INTRODUCTION TO PAPER 2

## A Systematic Review of Landslide Probability Mapping Using Logistic Regression

*A version of this paper has been accepted for publication in the Landslides Journal.*

*The citation is:*

Budimir, M.E.A., Atkinson, P.M., and Lewis, H.G., (2015), 'A Systematic Review of Landslide Probability Mapping Using Logistic Regression', *Landslides Journal*.

A difficulty experienced whilst conducting the research for Paper 1 was the lack of empirical data. Losses as a result of natural hazards are typically assigned to the primary hazard; separating out losses caused directly by secondary hazards is currently very difficult. It became apparent during the research process that is would not be possible to model multi-hazard *risk* (Figure 31), accounting for the interaction and potential amplification effects, due to data constraints. Therefore, the direction of the research was altered to concentrate upon the relation between earthquakes and the subsequent landslide *hazard* (Figure 31).


Figure 31. Diagram showing the focus of Paper 2 related to the risk equation.

In researching earthquake-triggered landslide hazards, it became apparent that there were multiple methods of assessing the landslide hazard (or susceptibility). Also, specific earthquake-triggered landslide studies were rarer than generic landslide studies. Logistic

regression analysis was the most frequently used method to assess landslide probability. However, the covariates used in the logistic regression analysis varied between studies.

Paper 2 therefore aims to consolidate the current published research on landslide occurrence using logistic regression analysis[3]. A systematic search method was used to amalgamate and evaluate the covariates used in logistic regression to predict landslides, and assessed for consistency for factors such as earthquake-triggered, rainfall-triggered, and landslide type. The covariates found to be significant in Paper 2 for all-landslide and in earthquake-triggered landslide studies were used as an inventory from which to select covariates for the logistic regression analysis models in Papers 3 and 4.

**Paper 2 Research Questions**

*What factors are significantly associated with landsliding in logistic regression analysis?*

*Do the significant factors associated with landsliding in logistic regression analysis change for landslide type and/or by triggering factor?*

[3] Paper 2 reviews papers published at the time of the search (15th February 2013 and 5th July 2013). Since the systematic search, a noteworthy paper has been published using peak ground acceleration in logistic regression analysis for landslide hazard assessment. The paper by Nowicki et al., (2014) is referred to in the Discussion chapter in relation to the results presented in the thesis.

# A SYSTEMATIC REVIEW OF LANDSLIDE PROBABILITY MAPPING USING LOGISTIC REGRESSION

M.E.A. Budimir[1], P.M. Atkinson[1] and H.G. Lewis[2]

[1] *Faculty of Social and Human Sciences*

[2] *Faculty of Engineering and the Environment*

*University of Southampton, Highfield, Southampton, SO17 1BJ, UK*

## Abstract

Logistic regression studies which assess landslide susceptibility are widely available in the literature. However, a global review of these studies to synthesise and compare the results does not exist. There are currently no guidelines for selection of covariates to be used in logistic regression analysis and as such, the covariates selected vary widely between studies. An inventory of significant covariates associated with landsliding produced from the full set of such studies globally would be a useful aid to the selection of covariates in future logistic regression studies. Thus, studies using logistic regression for landslide susceptibility estimation published in the literature were collated and a database created of the significant factors affecting the generation of landslides. The database records the paper the data were taken from, the year of publication, the approximate longitude and latitude of the study area, the trigger method (where appropriate), and the most dominant type of landslides occurring in the study area. The significant and non-significant (at the 95% confidence level) covariates were recorded, as well as their coefficient, statistical significance, and unit of measurement. The most common statistically significant covariate used in landslide logistic regression was slope, followed by aspect. The significant covariates related to landsliding varied for earthquake-induced landslides compared to rainfall-induced landslides, and

between landslide types. More importantly, the full range of covariates used was identified along with their frequencies of inclusion. The analysis showed that there needs to be more clarity and consistency in the methodology for selecting covariates for logistic regression analysis and in the metrics included when presenting the results. Several recommendations for future studies were given.

## 1.0 Introduction

Globally, landslides cause thousands of deaths and billions of dollars of damage each year (Dilley et al., 2005; Lu et al., 2007). Triggers of landslides include an increase in pore water pressure, earthquake shaking and human activity (Smith and Petley, 2009; Bommer and Rodriguez, 2002). Landslide hazards are one of the major life threats resulting from earthquakes, flooding and storm events in mountainous areas (Suzen and Kaya, 2011; Marano et al., 2010). Due to the interaction with other hazards and the spatially dispersed nature of landslide occurrences, it is necessary to map susceptibility to failure especially in areas with elements at risk (Bednarik et al., 2010). Landslide susceptibility can be mapped by fitting a statistical model to data on historical landslide occurrence and a set of covariates (Atkinson and Massari, 2011).

There have been many localised studies to determine the significant factors affecting landsliding, using either expert-dependent or data-driven methods (Suzen and Kaya, 2011). Data-driven methods aim to identify the statistically significant factors affecting landsliding based on data. Many data-driven methods have been applied in the literature, but the majority of research has tended towards multivariate statistical analysis such as discriminant analysis (Carrara et al., 1991; Santacana et al., 2003; Guzzetti et al., 2005), factor analysis (Ercanoglu et al., 2004) and logistic regression (Atkinson and Massari, 1998, 2011; Ohlmacher and Davis, 2003; Ayalew and Yamagishi, 2005; Das et al., 2010; Suzen and Kaya, 2011; Gorsevski, 2006).

Generally, the typical factors that influence the generation of landslides are known. For example, Suzen and Kaya (2011) recorded at least 18 different factors used in data-driven landslide hazard or susceptibility assessment procedures in a review of 145 articles between 1986 and 2007. These factors can be categorized into four major groups: geological, topographical, geotechnical and environmental (Table 14) (Suzen and Kaya, 2011). However, in any given situation, some of these factors may be important while others are irrelevant.

Table 14. Typical variables affecting landslide hazard or susceptibility grouped into four major types. From Suzen and Kaya (2011)

| **Grouping Type** | **Variables** |
|---|---|
| Environmental | Anthropogenic Parameters |
| | Position within Catchment |
| | Rainfall |
| | Land use / Land cover |
| Geotechnical | Soil Texture |
| | Soil Thickness |
| | Other Geotechnical Parameters |
| Topographical | Drainage |
| | Surface Roughness |
| | Topographic Indices |
| | Elevation |
| | Slope Aspect |
| | Slope Length |
| | Slope Angle |
| | Slope Curvature |
| Geological | Strata-Slope Interaction |
| | Lineaments / Faults |
| | Geology / Lithology |

Suzen and Kaya (2011) compared the factors used to predict landslide hazard or susceptibility found in the literature to those for a landslide inventory in the Asarsuyu catchment in northwest Turkey and found that some factors often used in landslide susceptibility mapping were not significant for the study site. This is most likely because the review covered all landslide types, which are most often derived from historical landslide inventories, with unspecified trigger types, whereas the study site in Turkey was predominantly prone to earthquake-induced landsliding. Most landslide susceptibility

mapping studies do not delineate between landslide type or the triggering event (van Westen et al., 2006; Nadim et al., 2006). Indeed, it is most common for studies to generate statistical relationships for all landslides types merged together and, as studies tend to be site-specific, the triggering factor is often ignored (van Westen et al., 2006).

The significant factors affecting landslides vary with trigger type (Suzen and Kaya, 2011; Korup, 2010; Meunier et al., 2008; Li et al., 2012; Chang et al., 2007). Thus, it is important to consider rainfall- and earthquake-triggered landslides separately as these trigger types are likely to be associated with different environmental factors, their mechanisms and dynamics (Li et al., 2012; Chang et al., 2007). Studies have found that earthquake-induced landslides (EILs) are often located near to ridges, faults, hanging walls and on convex hill slopes, whereas rainfall-induced landslides (RILs) are often distributed uniformly with respect to hill slope position, and are closer to streams, further from ridges and on concave hill slopes (Korup, 2010; Meunier et al., 2008; Li et al., 2012; Chang et al., 2007). This pattern of coseismic landslides predominantly detaching from upper hill slope portions is attributed to topographic amplification of seismic shaking near these areas (Korup, 2010; Meunier et al., 2008; Li et al., 2012). Chang et al. (2007) modelled landslides in the Hoshe basin of central Taiwan triggered by Typhoon Herb (1996) separately from those triggered by the Chi-Chi earthquake (1999) and found that the distribution differed according to trigger type (Figure 32).

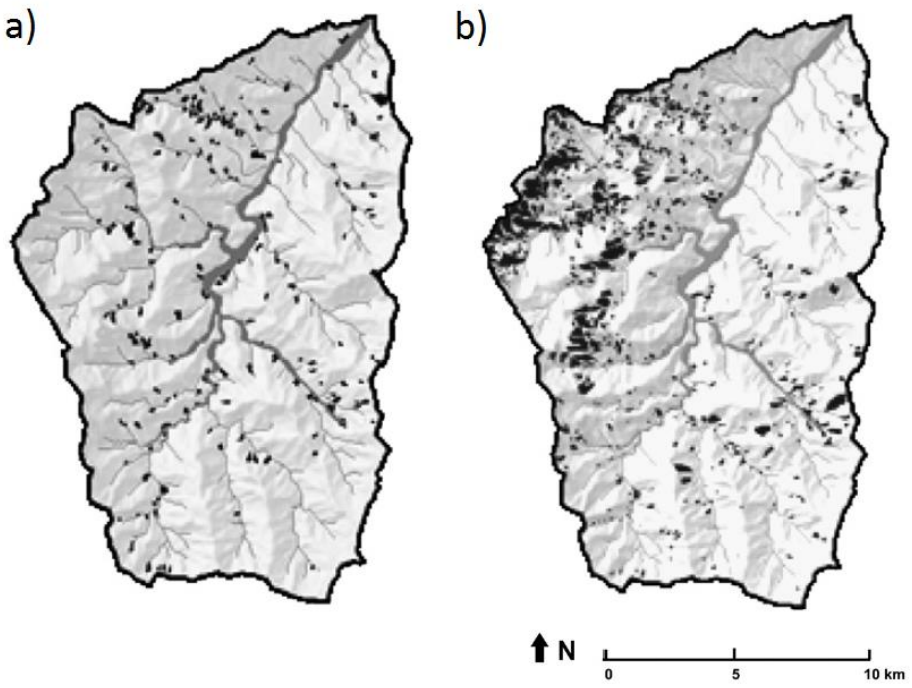


Figure 32. Distribution of landslides triggered by a) Typhoon Herb in 1996, and b) the Chi-Chi earthquake in 1999, taken from Chang et al. (2007, fig. 3, p. 339).

Beyond landslide type and trigger type, it is important to be clear about what is being predicted, being careful to distinguish between landslide susceptibility and landslide hazard. When modelling landslide susceptibility, the conditioning (preparatory) factors which make the slope susceptible to failure need to be considered (Hervas and Bobrowsky, 2009). When modelling landslide hazard, both the conditioning factors *and* triggering (causative) mechanisms, which initiate movement, should be considered (Dai and Lee, 2003; Hervas and Bobrowsky, 2009).

Commonly, several statistical methods are used to identify the significant factors affecting landslide susceptibility. In comparing statistical methods previously used to model landslide susceptibility, Brenning (2005) demonstrated that logistic regression was the preferred method as it resulted in the lowest rate of error. Logistic regression is a useful tool for analysing landslide occurrence, where the dependent variable is categorical (e.g., presence or absence) and the explanatory (independent) variables are categorical, numerical, or both

(Boslaugh, 2012; Chang et al., 2007; Atkinson et al., 1998). The logistic regression model has the form

$$logit(y) = \beta_0 + \beta_1 x_1 + \beta_2 x_2 + \cdots + \beta_i x_i + e \qquad \text{Equation 12}$$

where $y$ is the dependent variable, $x_i$ is the $i$-th explanatory variable, $\beta_0$ is a constant, $\beta_i$ is the $i$-th regression coefficient, and $e$ is the error. The probability ($p$) of the occurrence of $y$ is

$$p = \frac{exp^{(\beta_0+\beta_1 x_1+\beta_2 x_2+\cdots+\beta_i x_i)}}{1+exp^{(\beta_0+\beta_1 x_1+\beta_2 x_2+\cdots+\beta_i x_i)}} \qquad \text{Equation 13}$$

The logistic regression model is most commonly fitted in a step-wise manner. In the forward step-wise method, bivariate models are fitted between the dependent variable and each individual covariate. The most significant covariate is then added to the working model. At each further step, additional covariates are added one at a time and the most significant covariate is retained in the working model. Thus, each covariate added is modelled while the effects of the previously added covariates are controlled for. At a pre-determined confidence level, no further covariates are added to the model when none are found to be significant.

As logistic regression has become a popular method for assessing landslide susceptibility, and will foreseeably be a common method used in the future, a review of published studies using logistic regression should act as a useful guide for future research. There are currently no guidelines for the selection of covariates in modelling landslide susceptibility with logistic regression (Ayalew and Yamagishi, 2005). The choice of covariates selected for logistic regression analysis varies between published studies. This review consolidates previous studies and identifies common covariates and their frequency of inclusion, providing an inventory of covariates that future logistic regression studies can select from. The inventory also provides a basis of comparison to determine how comprehensive the choice of covariates is in published logistic regression studies. Recommendations to inform future landslide studies using logistic regression analysis are also provided.

We undertook a systematic review of the literature to assess the significant factors affecting landslide occurrence for all (unspecified) landslide types, including analysis of EILs and RILs separately, and analysis by landslide type. A database was created from the systematic literature search. Any commonalities or differences in significant covariates in the logistic regression models were identified and explored, and differences between EIL and RIL covariates and landslide type covariates were also examined.

Logistic regression was chosen as a constraint on the scope of the literature search (i.e., only papers using logistic regression were included) for several reasons: (i) it is one of the most common statistical methods used to model landslide susceptibility (the other being discriminant analysis) (Brenning, 2005), meaning that it was possible to generate a sufficiently large sample; (ii) in a limited study, Brenning's (2005) review of landslide susceptibility models determined logistic regression to result in the lowest rate of error, increasing confidence in the results of any review and comparison; (iii) logistic regression analysis generates a statistical significance value for each covariate in the model, which allows comparison of covariates between studies; and (iv) logistic regression analysis can generate probabilities of landslide susceptibility and hazard (rather than predicted categories as in discriminant analysis), which is of use in risk and loss assessments.

Four research questions were addressed by this study (i) what are the significant covariates affecting landslide occurrence in logistic regression studies; (ii) what are the covariates found to be not significant in determining landslide occurrence in logistic regression studies; (iii) how do the significant covariates in logistic regression studies vary for EILs compared to RILs; and (iv) how do the significant covariates in logistic regression studies vary by landslide type? The steps in the systematic literature review are outlined in the next section.

## 2.0 Method

### 2.1 Search Process

A manual systematic literature search was conducted following the structure of Figure 33 between 15 February 2013 and 05 July 2013. All papers were restricted to English language peer-reviewed journal articles with access rights granted by the University of Southampton. The bibliographic databases Web of Knowledge and Science Direct were used as the primary search tools, with later steps supplemented with journal searches of the key journals commonly publishing relevant literature. The key journals searched were *Landslides*, *Geomorphology* and *Engineering Geology*.

Papers using logistic regression to model landslide hazard or susceptibility with explicitly itemised covariates were included in the database. Papers were excluded from the database if they were qualitative, employed expert-driven models, if no statistical method was outlined, or if the method used to calculate significant factors was not stated.

Figure 33 presents a flow chart outlining the search terms and database selection process. For each step in the systematic search, papers were selected and downloaded based on a reading of the paper abstract and title online to determine if the paper was relevant. When conducting the searches, no papers were downloaded to be assessed in more detail if they had already been selected from the search result of a previous step. This avoided potential duplication of data. Of the selected and downloaded papers, only papers conforming to the aforementioned conditions were accepted into the database. The conformity of the paper to the conditions was determined by a more thorough reading of the downloaded paper.

Each journal article was reviewed by one researcher and the details in the paper recorded into a spreadsheet. The final four steps (Step 6, Step 7, Step 8, and Step 9 in Figure 33) of the systematic literature search did not yield any new papers to be added to the database because the papers relevant for the database had already been accepted into the database

from previous stages. See Appendix A for a full list of the reviewed references used to compile the database.

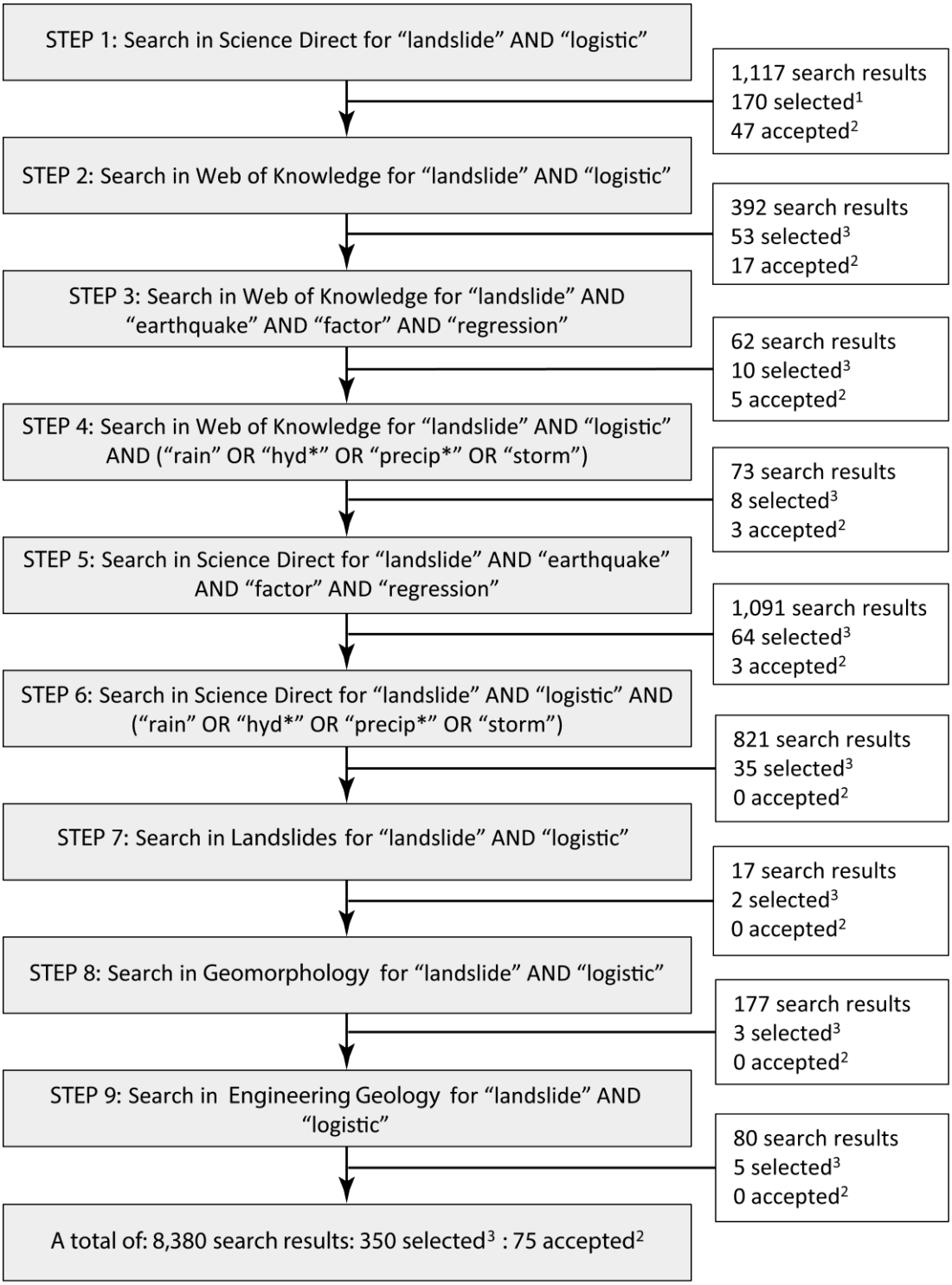


Figure 33. Flowchart describing the systematic literature review method and resulting actions. [1] from the search results, these papers were selected based on a reading of the paper abstract and title to determine if the paper was relevant. [2] these papers were accepted for the database from the previous selection (1 or 3) based on suitability for the database (for full details see main text). [3] these papers were selected based on the same principle as 1, but no duplicates of previously selected were selected.

## 2.2 Data Collection

The database records the source reference, the year of publication, the trigger method (or 'unspecified' when the information was not available) and the most dominant type of landslides occurring in the study area (if noted in the article). The significant and non-significant factors reported by the authors were recorded, as well as their coefficients, statistical significance, and unit of measurement where appropriate. Significance was determined at the 95% confidence level. A code associated with each factor was assigned (Table 15). The covariate 'Other' was used to combine covariates with a single occurrence incidence in the database; for a list of these covariates, see Appendix B.

Table 15. Covariates found in the literature search and their code used in this paper.

| Covariate Code | Description |
|---|---|
| ASP | Aspect |
| ASP_OTHER | Aspect properties not covered by aspect (e.g. tan of aspect) |
| CONC | Slope (concave) |
| CONT | Upslope contributing area |
| CURV | Slope curvature |
| DRAIN_DENS | Density of drainage / river / stream |
| DRAIN_DIST | Distance to drainage / river / stream |
| ELEV | Elevation |
| ELEV_RANGE | Elevation range |
| FAULT_DENS | Density of faults |
| FAULT_DIST | Distance to fault |
| FLOW_ACC | Accumulated flow |
| FLOW_DIR | Flow direction |
| GEOL | Geology |
| LAND | Land use / land cover |
| LIN_BUFFER | Buffer around lineament |
| LIN_DIST | Distance to lineament |
| LITH | Lithology / rock type |
| OTHER | Covariate used only once in studies. See Appendix B. |
| PGA | Peak ground acceleration |
| PL_CURV | Planform curvature |
| PR_CURV | Profile curvature |
| PPT | Precipitation |
| RIDGE_DIST | Distance to ridge |
| ROAD_DENS | Density of roads |
| ROAD_DIST | Distance to road |
| ROUGH | Terrain roughness / standard deviation of slope gradient |

| | |
|---|---|
| SED_TRANS | Stream sediment transport index or capacity |
| SL | Slope gradient |
| SL_OTHER | Slope properties not covered by slope gradient (e.g. slope$^2$) |
| SOIL | Soil type |
| SOIL_OTHER | Soil properties, not covered by soil type |
| SPI | Stream index or power (SPI) |
| TOPOG | Topography type, geomorphology, landform unit |
| TWI | Topographic wetness index (TWI) |
| VEG | Vegetation / NDVI |
| WEATH | Weathering |

The longitude and latitude of each study site was taken from details in the paper if available. If this information was not recorded in the paper, the approximate centre of the study area was estimated using details of the paper's study site, such as the site name, local landmarks, and the landslide inventory map. These details were then matched visually in Google Earth to select and record the central location of each study site.

The type of triggering event was determined by the type of landslide inventory map used in the logistic regression analysis. Each study was allocated as an 'earthquake' or 'rainfall' type if the landslide inventory map used in the logistic regression was constructed in the immediate aftermath of an earthquake or rainfall event causing landslides.

The type of triggering event was termed 'unspecified' if long-term landslide inventories were used, typically recorded in a national database of landslide occurrences, or inferred from aerial photography or satellite sensor imagery to determine the locations of past landslides over a specified time period. The trigger mechanism of these landslides is generally not recorded and these landslide inventory maps, therefore, represent the generic landslide hazard. Often the dominant triggering method can be surmised from the published paper (e.g. the site is located in an area of high precipitation, but not near any active faults). However, as the records do not specify directly the triggering mechanism, it was not possible to be certain about the trigger type for these long-term landslide inventories.

The literature search database was further divided into landslide type using the landslide classification scheme developed by Varnes (1978). Where the landslide type was recorded, the site was then classified in the database according to the main type of movement. For example, a debris slump would be categorised as a slide (Table 16). In some instances, there were multiple landslide types found at the site and included in the landslide inventory. In these cases, if there was a dominant landslide type present, it was recorded as the main landslide type; if there was not a clear dominant type, they were classified as complex slope movements.

Table 16. An abbreviated and modified version of the landslide classification scheme developed by Varnes (1978). Taken from Sidle and Ochiai (2006, p. 24, Table 2.1).

| **Type of movement** | | **Type of material** | | |
|---|---|---|---|---|
| | | **Bedrock** | **Engineering soils** | |
| | | | ***Coarse*** | ***Fine*** |
| **Falls** | | Rock fall | Debris fall | Earth fall |
| **Topples** | | Rock topple | Debris topple | Earth topple |
| **Slides** | **Rotational** | Rock slump | Debris slump | Earth slump |
| | **Translational** | Rock block slide; rock slide | Debris block slide; debris slide | Earth block slide; earth slide |
| **Lateral spreads** | | Rock spread | Debris spread | Earth spread |
| **Flows** | | Rock flow (deep creep) | Debris flow (soil creep) | Earth flow (soil creep) |
| **Complex slope movements** (i.e., combinations of two or more types) | | | | |

## 3.0 Results

The literature search yielded 75 papers (Figure 33). For nine of the papers, more than one site was studied and logistic regression modelling was applied separately for each site. Thus, from the 75 papers, 91 discrete study sites were recorded. Figure 34 shows the country where each study took place for all of the logistic regression studies.

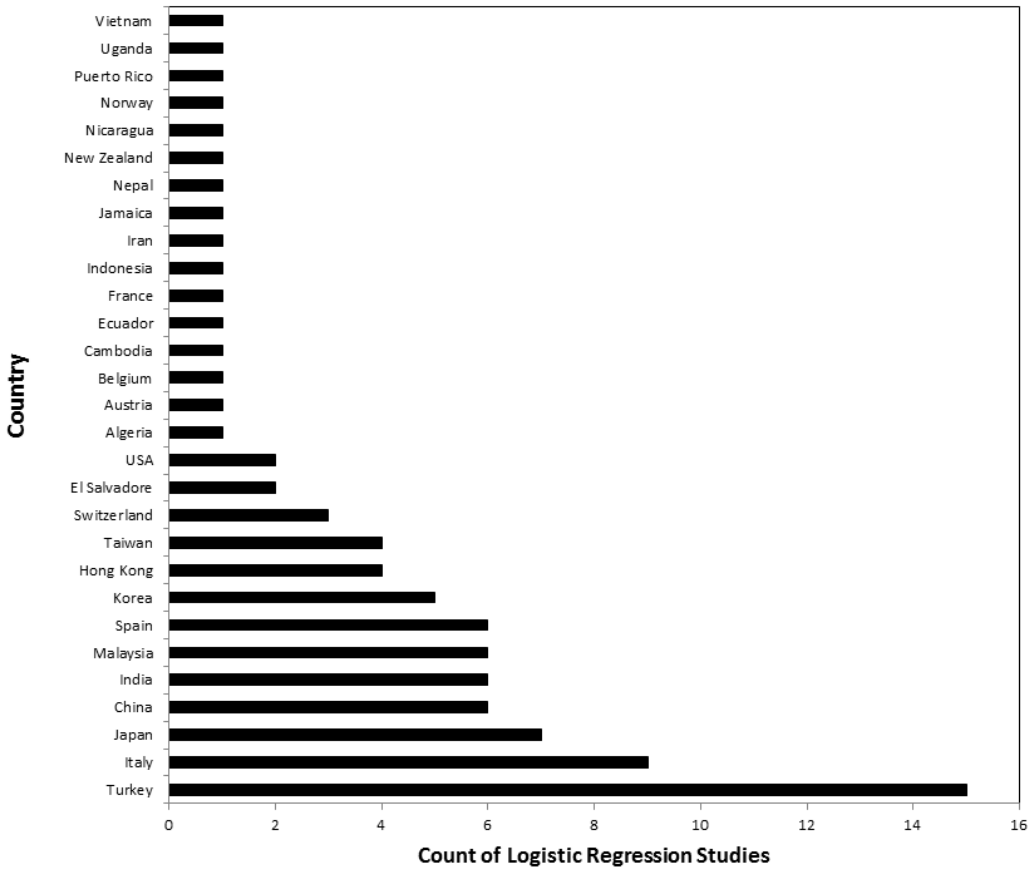


Figure 34. Plot of the country of origin for each logistic regression landslide study.

Figure 35 shows an increase in logistic regression landslide studies per year from 2001 to 2013. The number of published studies increased in 2005 and again in 2010, suggesting logistic regression analysis increasing in popularity as a method for assessing landslide susceptibility during these periods. This pattern also corresponds with the increased utilisation and availability of geographic information systems, which make fitting logistic regression models to landslide and environmental data increasingly less demanding.

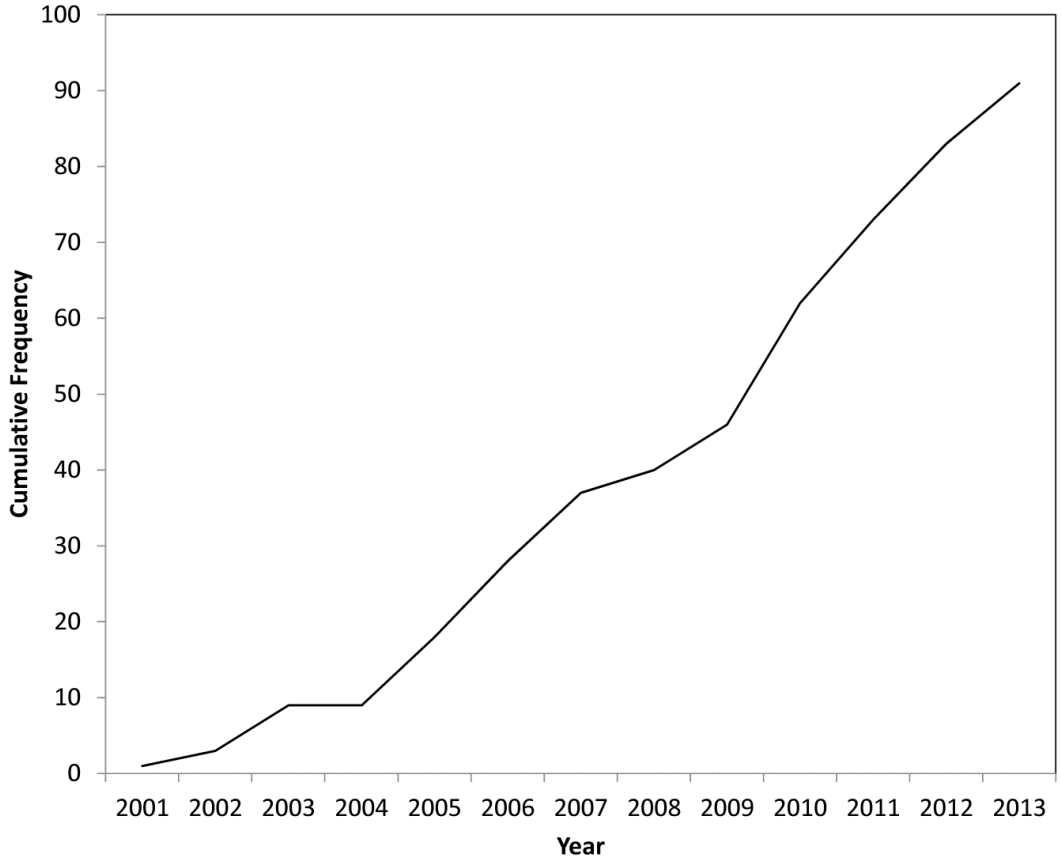


Figure 35. Cumulative frequency plot of study sites for the year of publication.

The main finding from the literature search was the lack of consistent and uniform approaches to the methodology, the selection of covariates included in the logistic regression model, and in the presentation of results. The statistical significance used to determine which covariate to include in the model was not published in all papers. In addition, presenting the coefficient of each significant covariate was not uniformly adopted across all studies; this practice was commonly excluded for categorized covariates.

There was a perceptible variation in the choice of covariates selected by authors in the logistic regression modelling of landslide probability. The literature search yielded 37 types of covariates, classified in Table 15. However, there are more than 37 covariates in total published in the studies. Covariates occurring only once in the search are classified under the coding ‘other’, and covariates representing additional properties or transformations of aspect, slope and soil are classified as ‘aspect_other’, ‘slope_other’ or ‘soil_other’. Whilst some

covariates appeared more frequently in the studies than others, the literature search does show that there is a wide range of potential covariates which can be used in landslide models. The method by which covariates are selected initially to fit the logistic regression model to is rarely published in the papers. With the exception of slope and aspect, there does not appear to be much commonality in the covariates selected across all studies.

Of the 91 study sites, 39 published covariates found not to be significantly associated with landsliding. The remaining 52 sites did not publish any non-significant covariates. This suggests either (1) the selection of the initial covariates to include in the modelling yielded only significant relationships with landsliding, or (2) the covariates found not to be significantly associated with landsliding were not published in the final paper, only including those covariates found to be statistically significant.

Landslide density for categorized covariates was presented as part of the results in 25% of the studies. Where this was performed, further analysis of the relationship between landsliding and significant covariates was carried out in more detail. This provides a more in-depth exploration of the relationship, which is useful for understanding the nature of the correlation and the processes that govern landslide initiation. However, this practice was not commonly carried out across all 91 studies.

60% of studies published details on the landslide type recorded in the landslide inventory. For 59 study sites, long-term landslide inventories were used; nine studies used an earthquake-induced landslide inventory, and 23 used a rainfall-induced landslide inventory. The majority of these EIL- and RIL-specific papers modelled landslide susceptibility, while four modelled landslide hazard (two studies included an earthquake trigger covariate, and two included a rainfall trigger covariate).

In logistic regression model fitting there are two common approaches to select the best model: backward stepwise fitting and forward stepwise fitting. The backward stepwise method begins with all covariates and eliminates the least significant variable at each step

until the best model is obtained. The forward stepwise model operates in reverse, beginning with no covariates, and adding the most significant variable at each step until the best model is fitted. Nine studies used the backward-stepwise fitting of the logistic model method, 21 used the forward-stepwise fitting method and the remaining 61 studies did not specify the direction method.

## 3.1 Search Results

Figure 36 shows a plot of common covariates and how often they were cited as significant or not significant in the literature review database as a percentage of the total number of sites. Slope was a statistically significant covariate in 95% of all landslide logistic regression studies. The next most common significant covariate was aspect (64%). There is a grouping of several covariates found to be significant in 35-45% of studies; these are vegetation, lithology, land cover, elevation and distance to drainage. In 10-25% of studies, the following covariates were significant: curvature, geology, distance to faults, soil type, distance to roads, topographic wetness index (TWI), precipitation, other soil properties, and stream power index (SPI). The remaining covariates were significant in less than 10% of the studies.

Distance to drainage, curvature and aspect were not statistically significant in 10-20% of studies. Elevation, distance to faults, upslope contributing area, and land cover were not significant in 5-10% of studies. The remaining covariates were not significant in less than 5% of the studies.

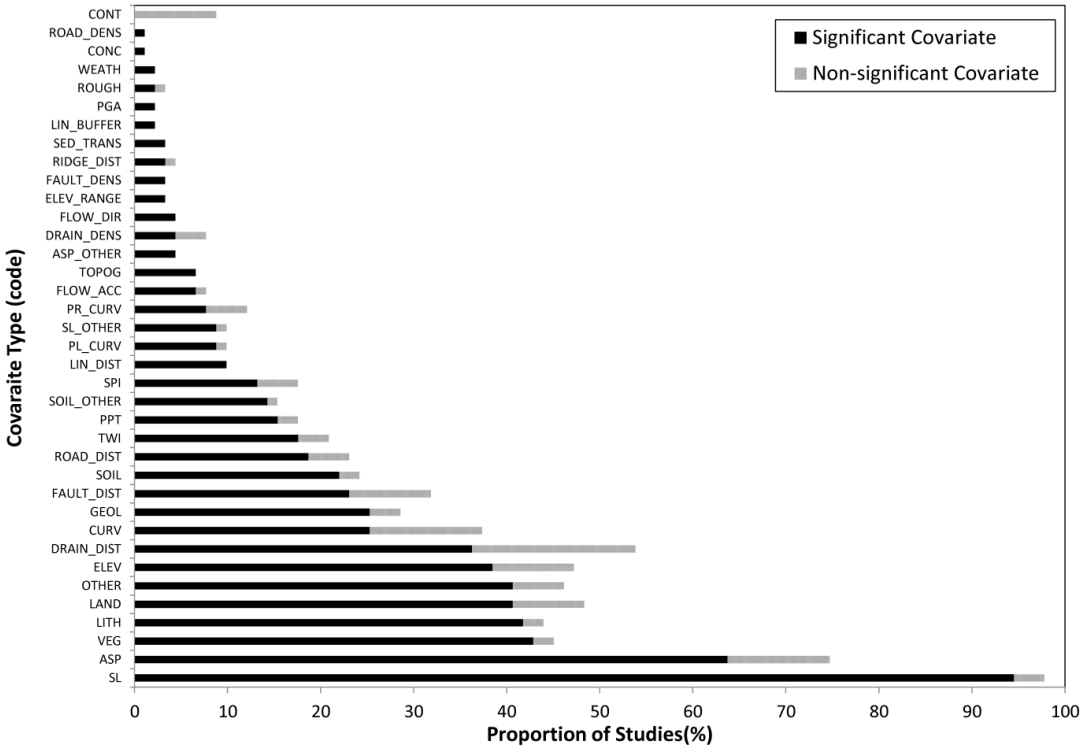


Figure 36. Percentage at which covariates were found to be significant or non-significant for all types of landslides in the literature review database. The description for each covariate type code is given in Table 15.

## 3.2 Search Results by Trigger

For 59 of the 91 study sites, the type of triggering event was not specified, nine were earthquake-induced landslides (EILs), and 23 were rainfall-induced landslides (RILs). The studies were split into earthquake-induced landslide (EIL) and rainfall-induced landslide (RIL) studies and the significant covariates (Figure 37) were compared.

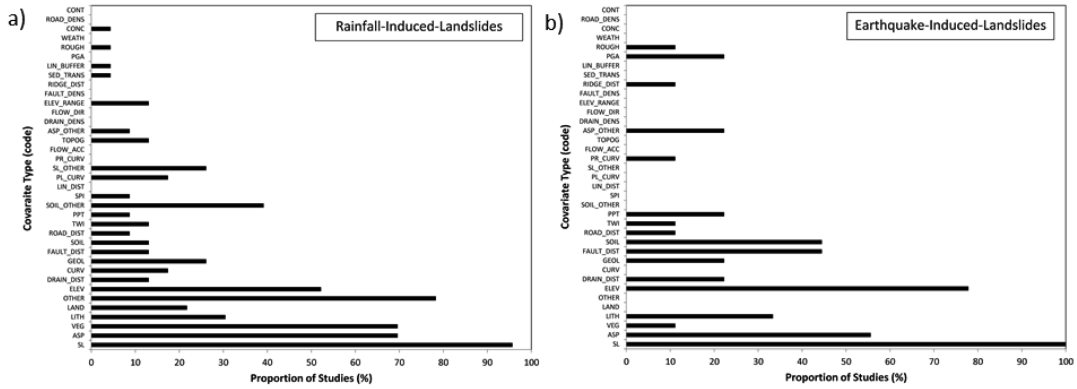


Figure 37. Percentage at which covariates were found to be significant for (a) rainfall-induced landslides and (b) earthquake-induced landslides in the literature review search. The description for each covariate type code is given in Table 15.

The most common significant covariate for both RIL and EIL studies was slope (95-100%), with aspect and elevation the next most common significant covariates, occurring in over 50% of studies. Geology and lithology were significant covariates in both RIL and EIL studies, occurring in 22-33% of studies. Topographic Wetness Index (TWI) was significant in 11-13% of studies.

In the RIL studies vegetation was a significant covariate in 69% of studies, compared to 11% for EIL studies. Soil properties were considered significant in 39% of RIL studies, but in 0% of EIL studies. Plan curvature, curvature, land cover/use, and slope properties were found to be significant in 17-26% of RIL studies, but in 0% of EIL studies. Similarly, elevation range and topography were found to be significant in 13% of RIL studies, but in 0% of EIL studies.

For the EIL studies soil type and distance to fault lines were significant in 44% of studies, but were only significant in 13% of RIL studies. Distances to ridge lines and profile curvature were found to be significant in 11% of EIL studies, but in 0% of RIL studies. Peak ground acceleration was only found to be significant in EIL studies (in 22% of studies).

## 3.3 Search Results by Landslide Type

Of the 91 sites, 55 published details of the landslide type. Of these 55 studies, there were two falls, 27 slides, six flows, 20 complex slides and no topples or lateral spreads. The following

section presents the significant covariates associated with each landslide type found in the literature search.

*Slides*

Slides were the most common landslide type found in the logistic regression studies. From the 27 studies investigating this landslide type, 18 covariates were found to be significantly related to landsliding (Figure 38). The two most common significant covariates were slope and aspect (Figure 38).

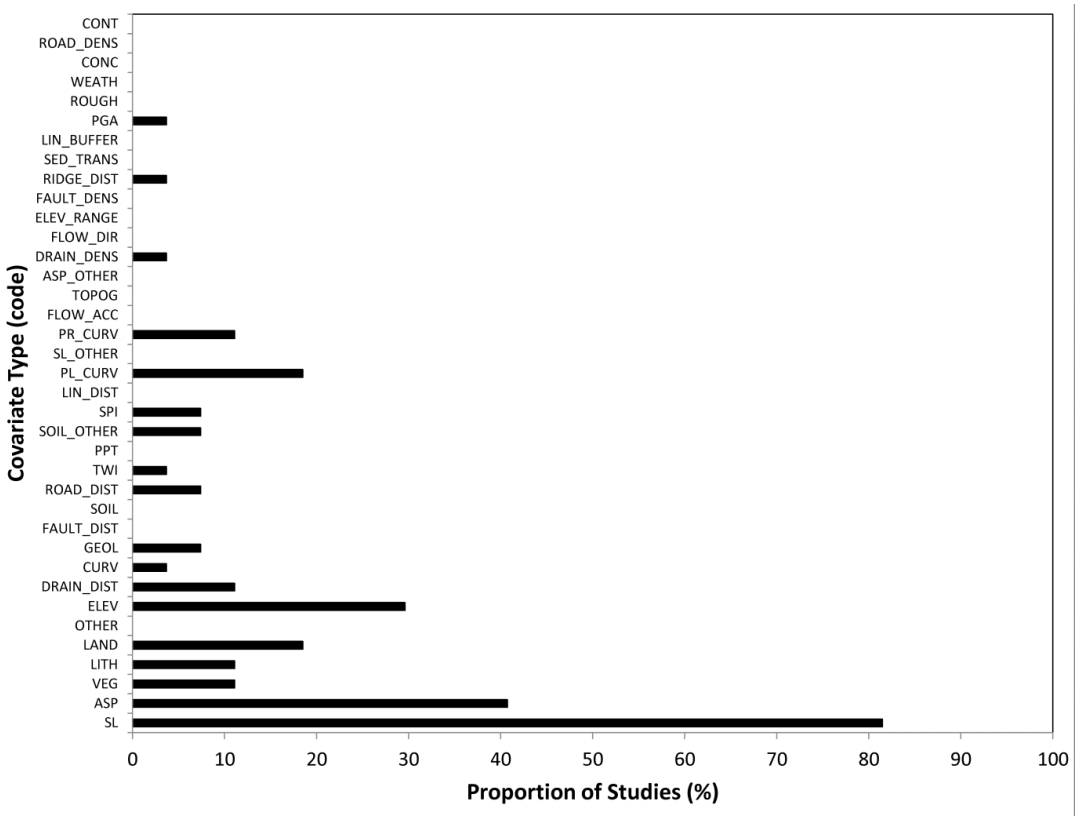


Figure 38. Plot of significant covariates associated with the slide type of landsliding.

*Complex Slope Movements*

Complex slope movements were the next most common type of landsliding after slides. 20 studies investigated complex slope movements using logistic regression analysis. From these studies, 24 covariates were found to be significantly associated with landsliding (Figure 39). Complex slope movements have a wider range of significant covariates than any other type

of landsliding. Slope and aspect were the two most common significant covariates found in the studies (Figure 39).

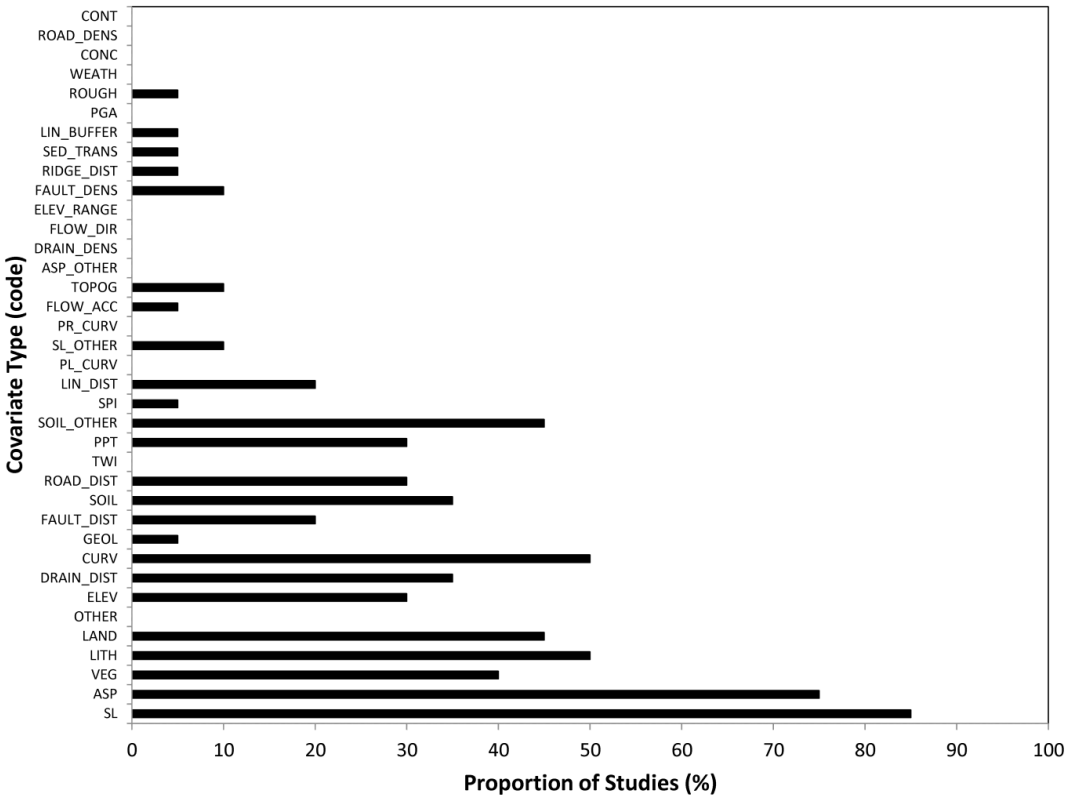


Figure 39. Plot of significant covariates associated with complex types of landsliding.

*Flows*

Six studies investigated flows as the dominant type at the site. Only seven covariates were found to be significantly associated with flows. In 50% of the studies, slope, aspect, and lithology were found to be significantly related to landsliding. In 30% of the studies, elevation, elevation range and vegetation were found to be significantly associated with landsliding. Topography was significant in 15% of cases. The significant covariates associated with flows are mostly topographical, with geological and environmental types (Table 14).

*Falls*

Two studies investigated falls as the dominant landslide type at the site. Only seven covariates were found to be significantly associated with falls. In both studies, slope was found to be a significant covariate related to landsliding. In 50% of the falls, fault distance, peak ground acceleration, curvature, distance to roads, geology and lithology were significantly associated with falls. The covariates are dominated by topographical and geological types in these studies (Table 14).

## 3.4 Slope

Slope was the most common significant covariate in all studies: of 91 studies, it was found to be significant in 95%. Of these, 23 sites published the landslide density for slope gradient classes. Landslide density is calculated by separating the study site into classes (in this case, slope gradient class) and calculating the area covered by landslides per class as a percentage of the total area for each class. A consistent method of grouping slope classes in the studies was not used; Figure 40 shows the landslide density found at each of the 23 sites grouped into nine slope gradient classes at 5° intervals ranging from 0° to 45°, with an additional class for those greater than 45°. There is significant spread in the landslide density for each slope gradient class as shown by the outliers in Figure 40.

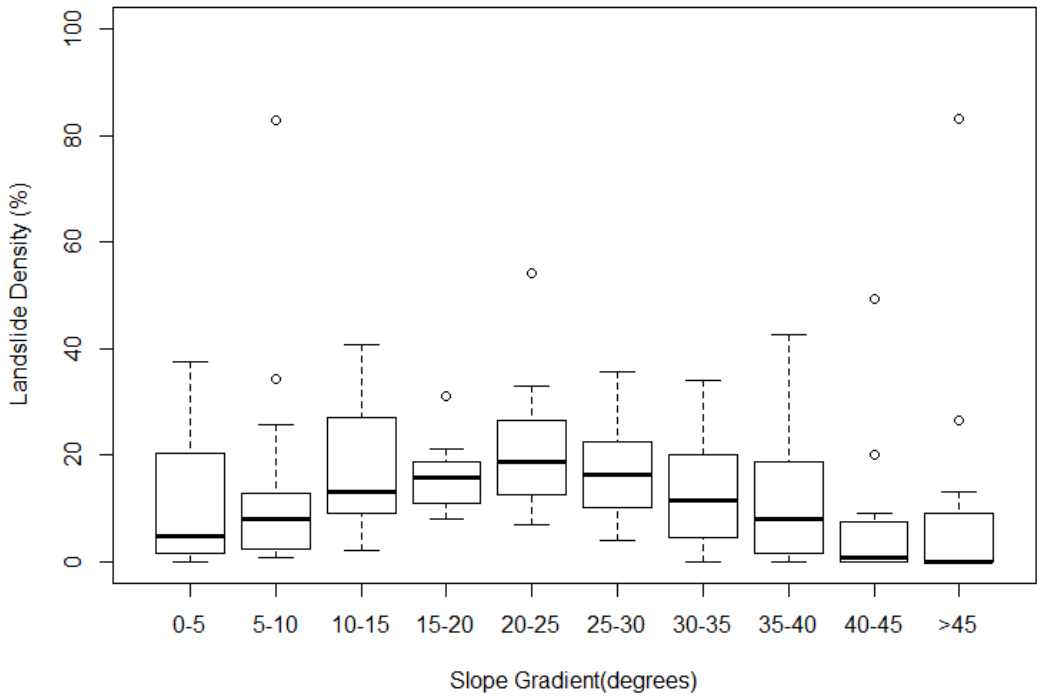


Figure 40. Box plot of landslide density published at 23 sites and grouped into slope gradient classes for consistency. The plot shows that there is significant spread with outliers for most of the slope gradient categories.

Figure 41 shows the landslide density for the same slope gradient classes for the six studies on the slide type of landsliding. There are less outliers in this plot than when all landslide types are combined as in Figure 40.

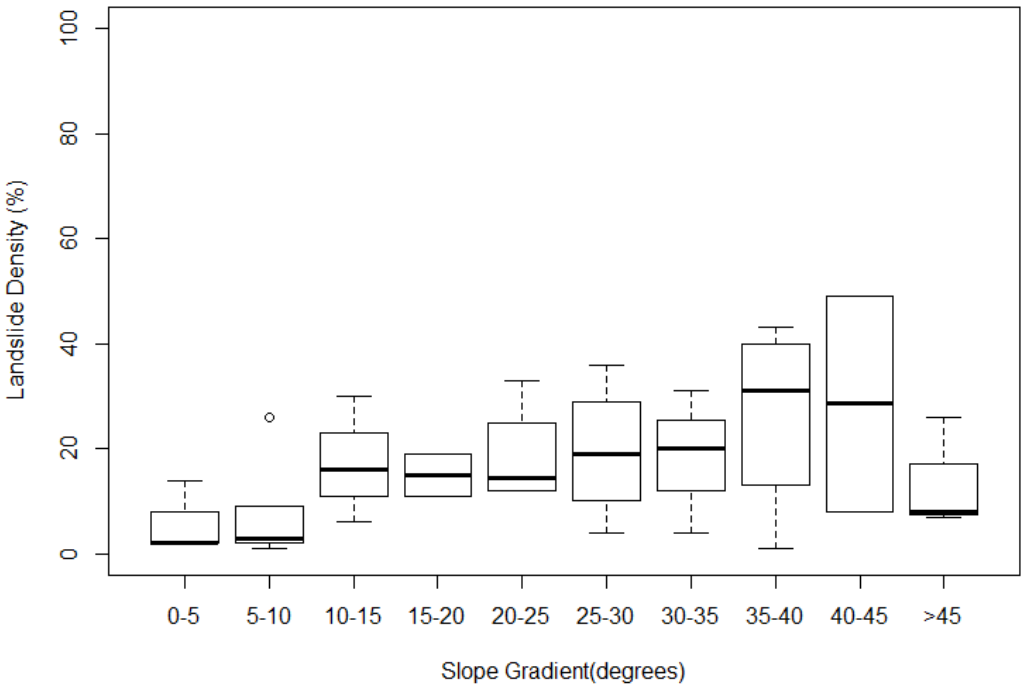


Figure 41. Box plot of landslide density for the slide type of landsliding published at 6 sites and grouped into slope gradient classes for consistency.

## 4.0 Discussion

This systematic literature review shows that there are several clear common significant covariates associated with all landsliding. These are slope, aspect, vegetation, lithology, land cover, elevation and distance to drainage. The significant covariates related to landsliding vary between earthquake-induced landslides compared to rainfall-induced landslides, and between landslide types.

## 4.1 Summary

Although there are common significant covariates associated with landsliding, the logistic regression models are site-specific. For the two most common significant covariates (slope and aspect), there is no consistent relation between landslide density and slope (or aspect) across the sites. For slope, this is because the slope gradient most susceptible to landsliding depends on the landslide type. Sidle and Ochiai (2006) suggest that "it is clear that debris slides, debris avalanches, and debris flows (shallow, rapid failure types) initiate on the

steepest slopes, while earthflows, slumps, and soil creep (generally deep-seated mass movements) typically initiate on gentler slopes". This can be seen in the difference between the landslide density per slope gradient class for all landslides compared to specifically slide types (Figure 40 and Figure 41). The all landslides slope gradient plot has a widely dispersed scattering of landslide percentage density, whilst slides have less scatter and greater landsliding at the higher slope gradient classes. However, there is still scatter within the slope gradient for the slide type of landslide, suggesting additional influences on landslide susceptibility other than slope gradient. Slope gradient should not be used as the sole indicator of landslide susceptibility as the landslide type significantly influences the most susceptible slope gradient and other factors significantly affect landslide susceptibility. Therefore, other geomorphic, geologic and hydrological processes must be taken into consideration as significant contributing factors of slope stability (Sidle and Ochiai, 2006).

There is a clear difference in the range and type of significant covariates associated with different landslide types. Whilst generalising across all landslide types will mask the patterns of significant covariates associated with a specific landslide type, the number of studies for specific landslide types using logistic regression analysis is fairly limited. Therefore, it was useful to examine all landslides together because they form a larger database from which to characterise the relations of interest. In addition, it was necessary to investigate the covariates associated by landslide type and by trigger. More studies of landslide susceptibility and hazard are required for specific landslide types and by trigger type in order to draw definitive conclusions about the significant covariates associated with specific landsliding processes and to model landslide susceptibility and hazard across different sites.

The review cannot act as a definitive guide to all covariates which might potentially influence landslide susceptibility for different landslide types because the sample size is not large enough. Thus, when conditioning the results to a particular landslide type or trigger, sampling variation will be large. Moreover, there may be several site-specific factors which determine the set of covariates that we could not control for. The results, however, remain

useful. The systematic review acts as a window, and it is for the reader to interpret these results bearing in mind the small sample sizes and inherent lack of control.

The covariates associated with EILs and RILs in this reported literature search were found to be different. This is likely because the triggering type determines the mechanistic processes, which are different for EILs compared to RILs. For example, vegetation is a common significant covariate associated with RILs, but much less so for EILs. This may be because RILs are driven by soil water content; vegetation types can significantly increase or decrease susceptibility to landsliding when the soil is saturated due to heavy precipitation by affecting the cohesion of the soil and infiltration rates.

Furthermore, the systematic literature search found that EILs were commonly associated with distance to faults, soil type, and distance to ridge lines in more instances than for RILs. Since the main driving force for EILs is the shaking intensity from an earthquake, susceptibility to landslides increases closer to the source of greatest shaking, which is likely to be related to faulting. Fault lines are the source of most earthquake ruptures and the location of the greatest amount of ground motion. Therefore, the distance from faults is a useful proxy for determining EILs. Weaker soil types can amplify seismic waves, as they have a low elastic modulus, and can undergo a greater displacement (Hovius and Meunier, 2012). Topographic amplification of ground acceleration occurs during earthquake events, as seismic waves are reflected and diffracted along the surface, causing higher levels of shaking near ridge lines (Hovius and Meunier, 2012). Therefore, distance to ridge lines provides another covariate related to EILs in logistic regression analysis.

### 4.2 Potential for selection bias

The range of significant covariates related to all landsliding and the recorded differences between EIL and RIL covariates and by landslide type could, in part be attributed to selection bias of the covariates by the authors. Landslide type and trigger could be a controlling factor not only in the choice of covariates to be entered into the model, but also

determining the significant covariates. From all the possible covariates to choose from with possible relations to landsliding, a section of these covariates are inherently relevant to the landslide type (e.g. geomorphological covariates may be important for rock falls), the geography of the study site (e.g. a region dominated by undercutting of hillslopes by river processes), or the triggering mechanism (e.g. peak ground acceleration for earthquake triggered landslides) (Figure 42). Authors select the covariates for input into the logistic regression model from this smaller subset of covariates, and from these, some are determined to be significantly associated with landsliding, and others may not be significantly related (Figure 42). This review of the literature is, therefore, limited to whether the covariates *selected by the authors* are determined significant or not significant through logistic regression. There is no way of determining whether the covariates not selected by the authors are significant or not significantly related to landsliding. Nevertheless, the choices made by the authors are informative in themselves, in relation to which of those covariates were found to be significant (see Figure 4; Figure 10).

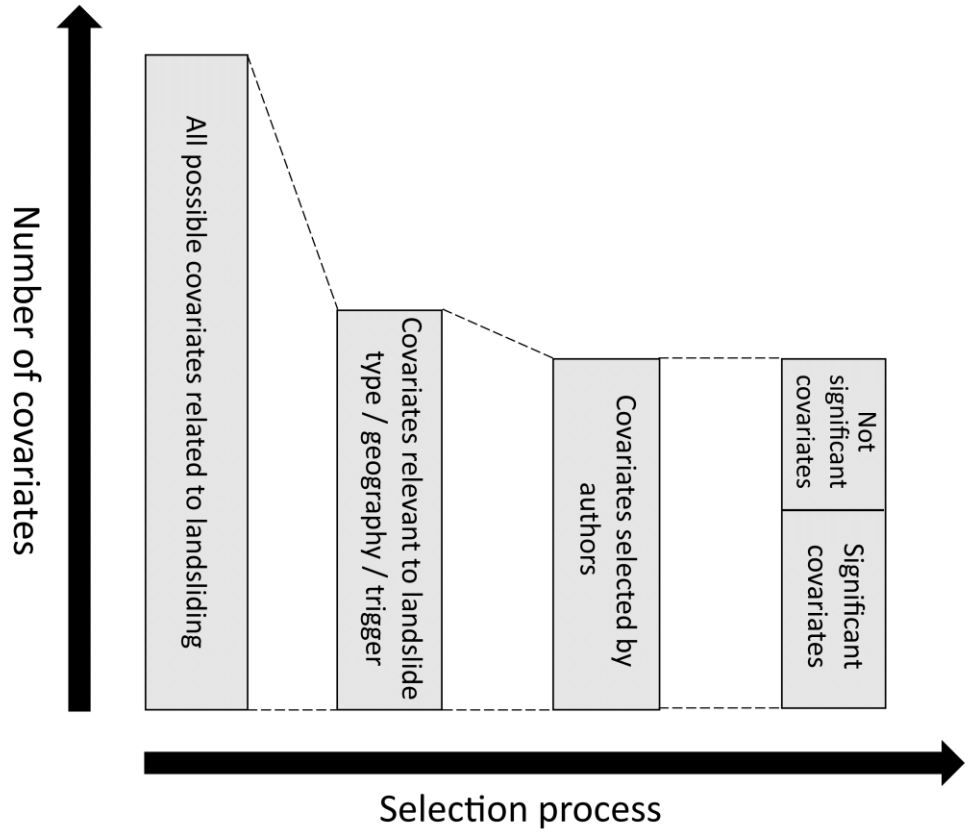


Figure 42. A diagram showing how the selection process determines the significant covariates in the logistic regression model.

### 4.3 A note on landslide hazard models

Logistic regression is used to analyse landslide occurrence for two purposes: to predict susceptibility and to predict hazard. Susceptibility refers to the pre-existing condition of the land; these studies use covariates which are relatively stable such as geology, slope, aspect, vegetation. These conditions can change over a longer time period (e.g. vegetation type and land cover), but are mostly stable conditions pre-existing in the landscape. Logistic regression modelling to predict landslide *hazard* must include the trigger mechanism (rainfall or ground shaking), which acts on a much shorter time frame.

Triggering covariates are rarely included in logistic regression analysis. Of the 23 studies specifically modelling RILs, only two studies (8%) used a precipitation covariate (Hadji et al., 2013; Dai and Lee, 2003). Of the nine studies specifically modelling EILs, only two studies (22%) included a peak ground acceleration covariate (Carro et al., 2003; Marzorati et

al., 2002). Both studies on EILs found the triggering mechanism to be significantly associated with EILs. Whilst this indicates the utility of including a triggering mechanism to model landslide probability, there are limitations in determining a suitable covariate to represent the trigger and the availability of such data. For example, no consistent covariate was used in logistic regression analysis of landslides to represent precipitation. Precipitation was used as a covariate in a total of 15 study sites, only two of which used specific RIL inventory maps. From the literature search, the following units of measurement were used: annual precipitation, mean rainy seasonal precipitation, mean annual precipitation, monthly variation in precipitation, 30 year annual average precipitation, maximum monthly rainfall, and rolling 24 hr rainfall. In addition, accurate maps of peak ground acceleration are rarely available, particularly in more remote locations.

Susceptibility modelling is more common in the literature as hazard modelling requires data on the trigger variable, which are frequently not available. However, landslide hazard models have the advantage that they can be used to predict the likely locations of landslides in future *conditional upon* the occurrence of a triggering event. In particular, hazard modelling of EILs, in contrast with susceptibility modelling, can represent the influence of non-uniform spatially distributed ground motion on landsliding.

Many more studies are needed which model landslide probability specifically as a result of earthquake or rainfall triggers to increase our understanding and prediction capability. Hovius and Meunier (2012) proposed that the correlation between landsliding and peak ground acceleration is the "key to understanding the global attributes of regional and local patterns of earthquake-induced landsliding". Similarly, greater understanding of the appropriate rainfall variable for landslide probability modelling is needed, particularly at a time when climate change could increase the frequency or intensity of rainfall events in susceptible locations.

## 4.4 Recommendations

It is apparent from the systematic literature review search that there is no consistent methodology for applying logistic regression analysis for landslide susceptibility and hazard mapping. There are no guidelines or universal criteria for selection of covariates in logistic regression modelling of landslide susceptibility (Ayalew and Yamagishi, 2005). Also, the methods of presenting the results from logistic regression in the literature are not consistent. Therefore, several suggestions for future publication of research on logistic regression analysis of landslide occurrence are identified here from the systematic literature review search:

1) Select covariates to be included in logistic regression in an informed and systematic way. The choice of covariates to include in the logistic regression analysis will naturally be dependent on data availability and a range of site-specific factors. However, a more comprehensive list of covariates should be initially included, before systematically eliminating the non-significant covariates through fitting the model. The systematic literature search undertaken here provides valuable information in the form of a list of previously selected and significant covariates which can be used as a starting point for selecting covariates to be included in any future logistic regression modelling.

2) Publish all the covariates entered into the logistic regression, whether or not they are found to be significant as a result of the logistic regression fitting. Reporting of non-significant covariates, not just significant covariates, is valuable in fully understanding the relations of environmental variables with landsliding.

3) Publish the statistical significance of covariates included in logistic regression models. The confidence level should be stated explicitly such that the results can be interpreted and potentially compared between studies.

4) Publish the coefficients for all covariates found to be significant in the logistic regression.

5) Publish the landslide types recorded in the landslide inventory because landslide type can affect which covariates are found to be significant in logistic regression. When multiple types are present, report the proportion of each type of landslide found in the study site.

6) Publish the landslide density for the covariates found to be significant in the logistic regression studies. This will provide a more in-depth understanding of the relationship between landsliding and covariates.

## 5.0 Conclusion

The literature search yielded over 37 covariates used in logistic regression modelling for landslide probability. Slope was the most frequently significant covariate for 95% of studies. The significant covariates associated with landsliding differed between earthquake-induced-landslides and rainfall-induced landslides. Landslide type also affected which covariates were found to be significantly related to landsliding. The selection of covariates to use in logistic regression modelling of landslide probability varied across the studies.

This systematic review provides guidelines and a list of covariates commonly found to be associated significantly with landslide occurrence which can be used in future logistic regression studies. This has the potential to increase the consistency of results published in the subject area and allow further comparison between studies and sites. Logistic regression analysis is a widely used method for landslide susceptibility mapping in the literature. However, there needs to be more clarity and consistency in the methodology for selecting covariates for the logistic regression analysis and in the presentation of the results.

## Acknowledgements

We would like to acknowledge all authors mentioned in the Appendix A reference list for their publications of logistic regression analysis of landslide susceptibility and hazard.

## References

ATKINSON, P. M. & MASSARI, R. 1998. Generalised linear modelling of susceptibility to landsliding in the central Apennines, Italy. Computers & Geosciences, 24, 373-385.

ATKINSON, P. M. & MASSARI, R. 2011. Autologistic modelling of susceptibility to landsliding in the Central Apennines, Italy. Geomorphology, 130, 55-64.

AYALEW, L. & YAMAGISHI, H. 2005. The application of GIS-based logistic regression for landslide susceptibility mapping in the Kakuda-Yahiko Mountains, Central Japan. Geomorphology, 65, 15-31.

BEDNARIK, M., MAGULOVA, B., MATYS, M. & MARSCHALKO, M. 2010. Landslide susceptibility assessment of the Kralovany-Liptovsky Mikulas railway case study. Physics and Chemistry of the Earth, 35, 162-171.

BOMMER, J. J. & RODRIGUEZ, C. E. 2002. Earthquake-induced landslides in central America. Engineering Geology, 63, 189-220.

BOSLAUGH, S. 2012. Statistics in a Nutshell, O'Reilly Media.

BRENNING, A. 2005. Spatial prediction models for landslide hazards: review, comparison and evaluation. Natural Hazards and Earth System Sciences, 5, 853-862.

CARRARA, A., CARDINALI, M., DETTI, R., GUZZETTI, F., PASQUI, V. & REICHENBACH, P. 1991. Gis Techniques and Statistical-Models in Evaluating Landslide Hazard. Earth Surface Processes and Landforms, 16, 427-445.

CARRO, M., DE AMICIS, M., LUZI, L. & MARZORATI, S. 2003. The application of predictive modeling techniques to landslides induced by earthquakes: the case study of the 26 September 1997 Umbria-Marche earthquake (Italy). Engineering Geology, 69, 139-159.

CHANG, K. T., CHIANG, S. H. & HSU, M. L. 2007. Modeling typhoon- and earthquake-induced landslides in a mountainous watershed using logistic regression. Geomorphology, 89, 335-347.

DAI, F. C. & LEE, C. F. 2003. A spatiotemporal probabilistic modelling of storm-induced shallow landsliding using aerial photographs and logistic regression. Earth Surface Processes and Landforms, 28, 527-545.

DAS, I., SAHOO, S., VAN WESTEN, C., STEIN, A. & HACK, R. 2010. Landslide susceptibility assessment using logistic regression and its comparison with a rock mass classification system, along a road section in the northern Himalayas (India). Geomorphology, 114, 627-637.

DILLEY, M., CHEN, R. S., DEICHMANN, U., LERNERLAM, A. L. & ARNOLD, M. 2005. Natural Disaster Hotspots: A Global Risk Analysis. Natural Disaster Hotspots: A Global Risk Analysis, 1-134.

ERCANOGLU, M., GOKCEOGLU, C. & VAN ASCH, T. W. J. 2004. Landslide susceptibility zoning north of Yenice (NW Turkey) by multivariate statistical techniques. Natural Hazards, 32, 1-23.

GORSEVSKI, P. V., GESSLER, P.E., FOLTZ, R.B., ELLIOT, W.J. 2006. Spatial prediction of landslide hazard using logistic regression and ROC analysis. Transactions in GIS, 10.

GUZZETTI, F., REICHENBACH, P., CARDINALI, M., GALLI, M. & ARDIZZONE, F. 2005. Probabilistic landslide hazard assessment at the basin scale. Geomorphology, 72, 272-299.

HADJI, R., BOUMAZBEUR, A., LIMANI, Y., BAGHEM, M., CHOUABI, A. & DEMDOUM, A. 2013. Geologic, topographic and climatic controls in landslide hazard assessment using GIS modeling: A case study of Souk Ahras region, NE Algeria. Quaternary International, 302, 224-237.

HERVAS, J. & BOBROWSKY, P. 2009. Mapping: Inventories, Susceptibility, Hazard and Risk. In: SASSA, K. & CANUTI, P. (eds.) Landslides: Disaster Risk Reduction. Berlin: Springer.

HOVIUS, N. & MEUNIER, P. 2012. Earthquake ground motion and the pattern of seismically induced landslides. In: CLEAGUE, J. J. & STEAD, D. (eds.) Landslides: Types, Mechanisms and Modeling. 2nd ed.: Cambridge University Press.

KORUP, O. 2010. Earthquake-triggered landslides - spatial patterns and impacts. COGEAR, Module 1a - Report.

LI, Y., CHEN, G., TANG, C., ZHOU, G. & ZHENG, L. 2012. Rainfall and earthquake-induced landslide susceptibility assessment using GIS and Artificial Neural Network. Natural Hazards and Earth System Sciences, 12, 2719-2729.

LU, G. Y., CHIU, L. S. & WONG, D. W. 2007. Vulnerability assessment of rainfall-induced debris flows in Taiwan. Natural Hazards, 43, 223-244.

MARANO, K. D., WALD, D. J. & ALLEN, T. I. 2010. Global earthquake casualties due to secondary effects: a quantitative analysis for improving rapid loss analyses. Natural Hazards, 52, 319-328.

MARZORATI, S., LUZI, L. & DE AMICIS, M. 2002. Rock falls induced by earthquakes: a statistical approach. Soil Dynamics and Earthquake Engineering, 22, 565-577.

MEUNIER, P., HOVIUS, N. & HAINES, J. A. 2008. Topographic site effects and the location of earthquake induced landslides. Earth and Planetary Science Letters, 275, 221-232.

NADIM, F., KJEKSTAD, O., PEDUZZI, P., HEROLD, C. & JAEDICKE, C. 2006. Global landslide and avalanche hotspots. Landslides, 3, 159-173.

OHLMACHER, G. C. & DAVIS, J. C. 2003. Using multiple logistic regression and GIS technology to predict landslide hazard in northeast Kansas, USA. Engineering Geology, 69, 331-343.

SANTACANA, N., BAEZA, B., COROMINAS, J., DE PAZ, A. & MARTURIA, J. 2003. A GIS-based multivariate statistical analysis for shallow landslide susceptibility mapping in La Pobla de Lillet area (Eastern Pyrenees, Spain). Natural Hazards, 30, 281-295.

SIDLE, R. C. & OCHIAI, H. 2006. Landslides: Processes, Prediction, and Landuse, Water Resources Monograph.

SMITH, K. & PETLEY, D. N. 2009. Environmental hazards: assessing risk and reducing disaster, Routledge.

SUZEN, M. L. & KAYA, B. S. 2011. Evaluation of environmental parameters in logistic regression models for landslide susceptibility mapping. International Journal of Digital Earth, 5, 338-355.

VAN WESTEN, C. J., VAN ASCH, T. W. J. & SOETERS, R. 2006. Landslide hazard and risk zonation - why is it still so difficult? Bulletin of Engineering Geology and the Environment, 65, 167-184.

VARNES, D. J. 1978. Slope movement types and processes. In: CLARK, M. (ed.) Landslide Analysis and Control. Washington, DC.

# Appendix A

List of papers accepted from the systematic literature search for analysis in this paper.

Akgun, A., and Bulut, F., (2007), 'GIS-based landslide susceptibility for Arsin-Yomra (Trabzon, North Turkey) region', *Engineering Geology*, 51, 1377-1387.

Akgun, A., Kincal, C., and Pradhan, B., (2012), 'Application of remote sensing data and GIS for landslide risk assessment as an environmental threat to Izmir city (west Turkey)'. *Environmental Monitoring Assessment*, 184, 5453-5470.

Akgun, A., (2012), 'A comparison of landslide susceptibility maps produced by logistic regression, multi-criteria decision, and likelihood ratio methods: a case study at Izmir, Turkey', *Landslides*, 9, 93-106.

Atkinson, P.M., and Massari, R., (2011), 'Autologistic modelling of susceptibility to landsliding in the Central Apennines, Italy', *Geomorphology*, 130, 55-64.

Ayalew, L., and Yamagashi, H., (2005), 'The application of GIS-based logistic regression for landslide susceptibility mapping in the Kakuda-Yahiko Mountains, Central Japan', *Geomorphology*, 65, 15-31.

Ayalew, L., Yamagashi, H., Marui, H., and Kanno, T., (2005), 'Landslides in Sado Island of Japan: Part II. GIS-based susceptibility mapping with comparisons of results from two methods and verifications', *Engineering Geology*, 81, 432-445.

Baeza, C., Lantada, N., and Moya, J., (2010), 'Validation and evaluation of two multivariate statistical models for predictive shallow landslide susceptibility mapping of the Eastern Pyrenees (Spain)', *Environmental Earth Sciences*, 61, 507-523.

Bai, S., Lu, G., Wang, J., Zhou, P., and Ding, L., (2011), 'GIS-based rare events logistic regression for landslide-susceptibility mapping of Lianyungang, China', *Environmental Earth Sciences*, 62, 139-149.

Bai, S.B., Wang, J., Lu, G.N., Zhou, P.G., Hou, S.S., and Xu, S.N., (2010), 'GIS-based logistic regression for landslide susceptibility mapping of the Zhongxian segment in the Three Gorges area, China', *Geomorphology*, 115, 23-31.

Begueria, S., (2006), 'Changes in land cover and shallow landslide activity: A case study in the Spanish Pyrenees', *Geomorphology*, 74, 196-206.

Bui, D.T., Lofman, O., Revhaug, I., and Dick, O., (2011), 'Landslide susceptibility analysis in the Hoa Binh province of Vietnam using statistical index and logistic regression', *Natural Hazards*, 59, 1413-1444.

Can, T., Nefeslioglu, H.A., Gokceoglu, C., Sonmez, H., and Duman, T.Y., (2005), 'Susceptibility assessments of shallow earthflows triggered by heavy rainfall at three catchments by logistic regression analyses', *Geomorphology*, 72, 250-271.

Carro, M., De Amicis, M., Luzi, L., and Marzorati, S., (2003), 'The application of predictive modelling techniques to landslides induced by earthquakes: the case study of the 26 September 1997 Umbria-Marche earthquake (Italy)', *Engineering Geology*, 69, 139-159.

Chang, K.T., Chiang, S.H., and Hsu, M.L., (2007), 'Modeling typhoon- and earthquake-induced landslides in a mountainous watershed using logistic regression', *Geomorphology*, 89, 335-347.

Chau, K.T., and Chan, J.E., (2005), 'Regional bias of landslide data in generating

susceptibility maps using logistic regression: Case of Hong Kong Island', *Landslides*, 2, 280-290.

Chauhan, S., Shama, M., and Arora, M.K., (2010), 'Landslide susceptibility zonation of the Chamoli region, Garwhal Himalayas, using logistic regression model', *Landslides*, 7, 411-423.

Choi, J., Oh, H.J., Lee, H.J., Lee, C., and Lee, S., (2012), 'Combining landslide susceptibility maps obtained from frequency ratio, logistic regression, and artificial neural network models using ASTER images and GIS', *Engineering Geology*, 124, 12-23.

Dai, F.C, and Lee, C.F., (2003), 'A spatiotemporal probabilistic modelling of storm-induced shallow landsliding using aerial photographs and logistic regression', *Earth Surface Processes and Landforms*, 28, 527-545.

Dai, F.C., Lee, C.F., Li, J., and Xu, Z.W., (2001), 'Assessment of landslide susceptibility on the natural terrain of Lantau Island, Hong Kong', *Environmental Geology*, 40, 3, 381-391.

Dai, F.C., and Lee, C.F., (2002), 'Landslide characteristics and slope instability modelling using GIS, Lantau Island, Hong Kong', *Geomorphology*, 42, 213-228.

Das, I., Sahoo, S., van Westen, C., Stein, A., and Hack, R., (2010), 'Landslide susceptibility assessment using logistic regression and its comparison with a rock mass classification system, along a road section in the northern Himalayas (India)', *Geomorphology*, 114, 627-637.

Das, I., Stein, A., Kerle, N., and Dadhwal, V.K., (2012), 'Landslide susceptibility mapping along road corridors in the Indian Himalayas using Bayesian logistic regression models', *Geomorphology*, 179, 116-125.

Devkota, K.C., Regmi, A.D., Pourghasemi, H.R., Yoshida, K., Pradhan, B., Ryu, I.C., Dhital, M.R., and Althuwaynee, O.F., (2013), 'Landslide susceptibility mapping using

certainty factor, index of entropy and logistic regression models in GIS and their comparison at Mugling-Narayanghat road section in Nepal Himalaya', *Natural Hazards*, 65, 135-165.

Dominguez-Cuesta, M.J., Jimenez-Sanchez, M., and Berrezueta, E., (2007), 'Landslides in the Central Coalfield (Cantabrian Mountains, NW Spain): Geomorphological features, conditioning factors and methodological implications in susceptibility assessment', *Geomorphology*, 89, 358-369.

Dominguez-Cuesta, M.J., Jimenez-Sanchez, M., Colubi, A., and Gonzalez-Rodriguez, G., (2010), 'Modelling shallow landslide susceptibility: a new approach in logistic regression by using favourability assessment', *International Journal of Earth Science*, 99, 661-674.

Duman, T.Y., Can, T., Gokceoglu, C., Nefeslioglu, H.A., and Sonmez, H., (2006), 'Application of logistic regression for landslide susceptibility zoning of Cekmece Area, Istanbul, Turkey', *Environmental Geology*, 51, 241-256.

Ercanoglu, M., and Temiz, F.A., (2011), 'Appliction of logistic regression and fuzzy operators to landslide susceptibility assessment in Azdavay (Kastamonu, Turkey)', *Environmental Earth Sciences*, 64, 949-964.

Erener, A., Sebnen, H., and Duzgun, B., (2010), 'Improvement of statistical landslide susceptibility mapping by using spatial and global regression methods in the case of More and Romsdal (Norway)', *Landslides*, 7, 55-68.

Falaschi, F., Giacomelli, F., Federici, P.R., Pucinelli, A., D'Amato Avanzi, G., Pchini, A., and Ribolini, A., (2009), 'Logistic regression versus artificial neural networks: landslide susceptibility evaluation in a sample area of the Serchio River valley, Italy', *Natural Hazards*, 50, 551-569.

Federici, P.R., Puccinelli, A., Cantarelli, E., Casarosa, N., Avanzi, G., Falaschi, F., Giannecchini, R., Pochini, A., Ribolini, A., Bottai, M., Salvati, N., and Testi, C., (2007),

‘Multidisciplinary investigations in evaluating landslide susceptibility – An example in the Serchio River valley (Italy)’, *Quaternary International*, 171-172, 52-63.

Fenghuan, S., Peng, C., Jianqiang, Z., and Lingzhi, X., (2010), ‘Susceptibility assessment of landslides caused by the Wenchaun earthquake using a logistic regression model’, *Journal of Mountain Science*, 7, 234-245.

Garcia-Rodriguez, M.J., Malpica, J.A., Benito, B., and Diaz, M., (2008), ‘Susceptibility assessment of earthquake-triggered landslides in El Salvador using logistic regression’, *Geomorphology*, 95, 172-191.

Ghosh, S., Carranza, E.J.M., van Westen, C.J., Jetten, V.G., and Bhattacharya, D.N., (2011), ‘Selecting and weighting spatial predictors for empirical modelling of landslide susceptibility in the Darjeeling Himalayas (India)’, *Geomorphology*, 131, 35-56.

Greco, R., Sorriso-Valvo, M., and Catalano, E., (2007), ‘Logistic Regression analysis in the evaluation of mass movements susceptibility: The Aspromonte case study, Calabria, Italy’, *Engineering Geology*, 89, 47-66.

Guns, M., and Vanacker, V., (2012), ‘Logistic regression applied to natural hazards: rare event logistic regression with replications’, *Natural Hazards and Earth System Sciences*, 12, 1937-1947.

Hadji, R., Boumazbeur, A., Limani, Y., Bagham, M., el Madjid Chouabi, A., and Demdoum, A., (2013), ‘Geologic, topographic and climatic controls in landslide hazard assessment using GIS modelling: A case study of Souk Ahras region, NE Algeria’, *Quaternary International*, 302, 224-237.

Jaiswal, P., van Westen, C.J., and Jetten, V., (2010), ‘Quantitative landslide hazard assessment along a transportation corridor in southern India’, *Engineering Geology*, 116, 236-250.

Kincal, C., Akgun, A., and Koca, M.Y., (2009), 'Landslide susceptibility assessment in the Izmir (West Anatolia, Turkey) city center and its near vicinity by the logistic regression method', *Environmental Earth Science*, 59, 745-756.

Knapen, A., Kitutu, M.G., Poesen, J., Breugelmans, W., Deckers, J., and Muwanga, A., (2006), 'Landslide in a densely populated county at the footslopes of Mount Elgon (Uganda): Characteristics and causal factors', *Geomorphology*, 73, 149-165.

Lee, S., and Pradhan, B., (2007), 'Landslide hazard mapping at Selangor, Malaysia using frequency ratio and logistic regression models', *Landslides*, 4, 33-41.

Lee, S., and Sambath, T., (2006), 'Landslide susceptibility mapping in the Damrei Romel area, Cambodia using frequency ratio and logistic regression models', *Environmental Geology*, 50, 6, 847-855.

Lee, S., Ryu, J.H., and Kim, I.S., (2007), 'Landslide susceptibility analysis and its verification using likelihood ratio, logistic regression, and artificial neural network models: case study of Youngin, Korea', *Landslides*, 4, 327-338.

Lee, S.T., Yu, T.T. Peng, W.F., and Wang, C.L., (2010), 'Incorporating the effects of topographic amplification in the analysis of earthquake-induced landslide hazards using logistic regression', *Natural Hazards and Earth System Sciences*, 10, 2475-2488.

Lee, S., (2005a), 'Application of logistic regression model and its validation for landslide susceptibility mapping using GIS and remote sensing data', *International Journal of Remote Sensing*, 26, 7, 1477-1491.

Lee, S., (2005b), 'Application and cross-validation of spatial logistic multiple regression for landslide susceptibility analysis', *Geosciences Journal*, 9, 1, 63-71.

Lee, S., (2007), 'Comparison of landslide susceptibility maps generated through multiple logistic regression for three test areas in Korea', *Earth Surface Processes and Landforms*,

32, 2133-2148.

Lepore, C., Kamal, S.A., Shanahan, P., and Bras, R.L., (2012), 'Rainfall-induced landslide susceptibility zonation of Puerto Rico', *Environmental Earth Sciences*, 66, 1667-1681.

Li, X.P., and Zhou, S.P., (2012), 'Application and Research of GIS-based Wushan County Slope Stability Evaluation Information System', *Procedia Engineering*, 29, 2296-2302.

Mancini, F., Ceppi, C., and Ritrovato, G., (2010), 'GIS and statistical analysis for landslide susceptibility mapping in the Daunia area, Italy', *Natural Hazards and Earth System Sciences*, 10, 1851-1864.

Marzorati, S., Luzi, L., and De Amicis, M., (2002), 'Rock falls induced by earthquakes: a statistical approach', *Soil Dynamics and Earthquake Engineering*, 22, 565-577.

Mathew, J., Jha, V.K., and Rawat, G.S., (2007), 'Application of binary logistic regression analysis and its validation for landslide susceptibility mapping in part of Garhwal Himalaya, India', *International Journal of Remote Sensing*, 28, 10, 2257-2275.

Menendez-Duarte, R., Marquinez, J., and Devoli, G., (2003), 'Slope instability in Nicaragua triggered by Hurricane Mitch: distribution of shallow mass movements', *Environmental Geology*, 44, 290-300.

Miller, S., Brewer, T., and Harris, N., (2009), 'Rainfall thresholding and susceptibility assessment of rainfall-induced landslides: application to landslide management in St Thomas, Jamaica', *Bulletin of Engineering Geology and Environment*, 68, 539-550.

Nandi, A., and Shakoor, A., (2009), 'A GIS-based landslide susceptibility evaluation using bivariate and multivariate statistical analyses', *Engineering Geology*, 110, 11-20.

Nefeslioglu, H. A., Duman, T.Y., and Durmaz, S., (2008), 'Landslide susceptibility mapping for a part of tectonic Kelkit Valley (Eastern Black Sea region of Turkey)', *Geomorphology*,

94, 401-418.

Oh, H.J., Lee, S., and Soedradjat, G.M., (2010), 'Quantitative landslide susceptibility mapping at Pemalang area, Indonesia', *Environmental Earth Sciences*, 60, 1317-1328.

Ohlmacher, G.C., and Davis, J.C., (2003), 'Using multiple logistic regression and GIS technology to predict landslide hazard in northeast Kansas, USA', *Engineering Geology*, 69, 331-343.

Ozdemir, A., and Altural, T., (2013), 'A comparative study of frequency ratio, weights of evidence and logistic regression methods for landslide susceptibility mapping: Sultan Mountains, SW Turkey', *Journal of Asian Earth Sciences*, 64, 180-197.

Park, S., Choi, C., Kim, B., and Kim, J., (2013), 'Landslide susceptibility mapping using frequency ratio, analytic hierarchy process, logistic regression, and artificial neural network methods at the Inje area, Korea', *Environmental Earth Sciences*, 68, 1443-1464.

Pradhan, B., and Youssef, A.M., (2010), 'Manifestation of remote sensing data and GIS on landslide hazard analysis using spatial-based statistical models', *Arab Journal of Geosciences*, 3, 319-326.

Pradhan, B., (2010), 'Remote sensing and GIS-based landslide hazard analysis and cross-validation using multivariate logistic regression model on three test areas in Malaysia', *Advances in Space Research*, 45, 1244-1256.

Schicker, R., and Moon, V., (2012), 'Comparison of bivariate and multivariate statistical approaches in landslide susceptibility mapping at a regional scale', *Geomorphology*, 161-162, 40-57.

Shirzadi, A., Saro, L., Joo, O.H., and Chapi, K., (2012), 'A GIS-based logistic regression model in rock-fall susceptibility mapping along a mountainous road: Salvat Abad case study, Kurdistan, Iran', *Natural Hazards*, 64, 1639-1656.

Suzen, M.L., and Kaya, B.S., (2012), 'Evaluation of environmental parameters in logistic regression models for landslide susceptibility mapping', *International Journal of Digital Earth*, 5, 4, 338-355.

Tasser, E., Mader, M., and Tappeiner, U., (2003), 'Effects of land use in alpine grasslands on the probability of landslides', *Basic and Applied Ecology*, 4, 271-280.

Van Den Eeckhaut, M., Vanwalleghem, T., Poesen, J., Govers, G., Verstraeten, G., and Vandekerckhove, L., (2006), 'Prediction of landslide susceptibility using rare events logistic regression: A case-study in the Flemish Ardennes (Belgium)', *Geomorphology*, 76, 392-410.

Van Den Eeckhaut, M., Marre, A., and Poesen, J., (2010), 'Comparison of two landslide susceptibility assessments in the Champagne-Ardenne region (France)', *Geomorphology*, 115, 141-155.

Von Ruette, J., Papritz, A., Lehmann, P., Rickli, C., and Or, D., (2011), 'Spatial statistical modelling of shallow landslides – Validating predictions for different landslide inventories and rainfall events', *Geomorphology*, 133, 11-22.

Wan, S., (2009), 'A spatial decision support system for extracting the core factors and thresholds for landslide susceptibility map', *Engineering Geology*, 108, 237-251.

Wang, L.J., Sawada, K., and Moriguchi, S., (2013), 'Landslide susceptibility analysis with logistic regression model based on FCM sampling strategy', *Computers and Geosciences*, 57, 81-92.

Yalcin, A., Reis, S., Aydinoglu, A.C., and Yomralioglu, T., (2011), 'A GIS-based comparative study of frequency ratio, analytical hierarchy process, bivariate statistics and logistics regression methods for landslide susceptibility mapping in Trabzon, NE Turkey', *Catena*, 85, 274-287.

Yesilnacar, E., and Topal, T., (2005), 'Landslide susceptibility mapping: A comparison of

logistic regression and neural networks methods in a medium scale study, Hendek region (Turkey)', *Engineering Geology*, 79, 251-266.

Yilmaz, I., (2009), 'Landslide susceptibility mapping using frequency ratio, logistic regression, artificial neural networks and their comparison: A case study from Kat landslides (Tokat – Turkey)', *Computers and Geosciences*, 35, 1125-1138.

Zhang, J., Cui, P., Ge, Y., and Xiang, L., (2012), 'Susceptibility and risk assessment of earthquake-induced landslides based on Landslide Response Units in the Subao River basin, China', *Environmental Earth Sciences*, 65, 1037-1047.

Zhu, L., and Huang, J.F., (2006), 'GIS-based logistic regression method for landslide susceptibility mapping in regional scale', *Journal of Zhejiang University SCIENCE A*, 7, 12, 2007-2017.

# Appendix B

Covariates assigned to the 'Other' label in the systematic literature search.

| |
|---|
| Bedrock depth |
| Bedrock-slope relationship |
| Convergence index |
| Crown density |
| Debris |
| Distance to drainage$^2$ |
| Distance to path |
| Distance to residential area |
| Elevation$^2$ |
| Exposition |
| Forest age |
| Forest degradation |
| Forest density |
| Forest diameter |
| Groundwater depth |
| Kinematic depth |
| Liquidity index |
| (Marly limestone) x (log of slope angle) |

| |
|---|
| Mean watershed angle |
| Potential radiation |
| Proximity to old rock slide |
| Regolith thickness |
| Relative permeability |
| Strata orientation |
| Tectonic uplift |
| Tree age |
| Tree diameter |
| Wood age |

# 5. INTRODUCTION TO PAPER 3

## Coseismic Landslide Hazard Probability Modelled as a Function of the Earthquake Trigger for the 1994 Northridge California Event

Of the 91 study sites reviewed in Paper 2, only two sites[4] considered peak ground acceleration in the logistic regression model; these were Marzorati et al.(2002) and Carro et al.(2003), both studies on the Umbria-Marche earthquake. Both found the peak ground acceleration covariate to be a significant factor in predicting landslide occurrence. This paper (Paper 3) develops on from Paper 2 by using logistic regression to model landslide hazard probability for the Northridge, California 1994 earthquake event (Figure 43).


Figure 43. Diagram showing the focus of Paper 3 related to the risk equation.

Two models are compared: the first is a *susceptibility* model, using only environmental preparatory factors; the second is a *hazard* model, which includes peak ground acceleration and peak ground velocity as factors in addition to the same environmental factors used in the

[4] At the time of the systematic review and the submission of Paper 2 and Paper 3 to academic journals, only 2 papers used peak ground acceleration as a covariate in logistic regression analysis for landslide assessment. Since submission of the papers to journals for review, the Nowicki et al. (2014) paper has been published, which also uses peak ground acceleration as a covariate in logistic regression analysis. This paper is referred to in the Discussion section of the thesis.

susceptibility model. The hazard model method is then used in Paper 4 to estimate the probability of landsliding as a result of seven earthquake scenarios of different magnitudes.

This paper (Paper 3) uses the inventory of covariates from Paper 2 as a starting point to select covariates to include in the logistic regression analysis. Of the 37 named covariates found to be significant in logistic regression studies more than once in Paper 2's systematic review, 22 were used in this paper. Table 15 shows the covariates from Paper 2, and which were used in each model in Paper 3.

Table 17. Covariates found in the literature search from Paper 2, and the covariates used in the logistic regression analysis for Paper 3's susceptibility and hazard model.

| **Covariates from Paper 2** | **Susceptibility Model** | **Hazard Model** |
|---|---|---|
| Aspect | Aspect | Aspect |
| Aspect properties not covered by aspect | | |
| Slope (concave) | | |
| Upslope contributing area | | |
| Slope curvature | Curvature | Curvature |
| Density of drainage / river / stream | Drainage Density | Drainage Density |
| Distance to drainage / river / stream | Distance to Drainage | Distance to Drainage |
| Elevation | Elevation | Elevation |
| Elevation range | | |
| Density of faults | Fault Density | Fault Density |
| Distance to fault | Distance to Fault | Distance to Fault |
| Accumulated flow | | |
| Flow direction | | |
| Geology | Geology | Geology |
| Land use / land cover | Land cover | Land cover |
| Buffer around lineament | | |
| Distance to lineament | | |
| Lithology / rock type | | |
| Peak ground acceleration | | Peak Ground Acceleration and Peak Ground Velocity |
| Planform curvature | Planform Curvature | Planform Curvature |
| Profile curvature | Profile Curvature | Profile Curvature |
| Precipitation | | |
| Distance to ridge | Distance to Ridgeline | Distance to Ridgeline |
| Density of roads | Road Density | Road Density |
| Distance to road | Distance to Road | Distance to Road |
| Terrain roughness / standard deviation of slope gradient | Roughness (3x3 and 5x5 cell sample) | Roughness (3x3 and 5x5 cell sample) |
| Stream sediment transport index or capacity | | |
| Slope gradient | Slope Gradient | Slope Gradient |

| | | |
|---|---|---|
| Slope properties not covered by slope gradient<br>Soil type | Soil Type | Soil Type |
| Soil properties, not covered by soil type<br>Stream index or power (SPI) | Stream Power Index | Stream Power Index |
| Topography type, geomorphology, landform unit<br>Topographic wetness index (TWI) | | |
| Vegetation / NDVI<br>Weathering | Vegetation Type | Vegetation Type |

**Research Questions**

*Does including peak ground acceleration as a variable in logistic regression improve the predictive ability of the landslide hazard assessment?*

*What factors are associated with earthquake-induced landsliding in the Northridge 1994 earthquake event?*

# COSEISMIC LANDSLIDE HAZARD PROBABILITY MODELLED AS A FUNCTION OF THE EARTHQUAKE TRIGGER FOR THE 1994 NORTHRIDGE, CALIFORNIA EVENT

M.E.A. Budimir[1], P.M. Atkinson[1] and H.G. Lewis[2]

[1] Faculty of Social and Human Sciences

[2] Faculty of Engineering and the Environment

University of Southampton, Highfield, Southampton, SO17 1BJ, UK

## Abstract

Earthquake-induced landslides are one of the most damaging secondary hazards associated with earthquakes and can cause significant loss of life and damage to exposed areas. The 1994 Northridge $M_w$6.7 earthquake triggered 11,000 landslides in the surrounding region, which were recorded in the immediate aftermath of the event. This unique landslide inventory was used in conjunction with spatial data of covariates known to be significantly associated with landslide occurrence to create a logistic regression model of probable landslide occurrence for the Northridge site. A *susceptibility* model was fitted based on preparatory environmental covariates only, and compared to a separate *hazard* model which included additional triggering covariates. The susceptibility model found aspect, elevation, fault density, distance to roads, road density, roughness, slope, geology, vegetation, land cover and soil type to be significant covariates in predicting landslide susceptibility. The hazard model found the same covariates to be significant in addition to distance to faults, peak ground acceleration and peak ground velocity. The inclusion of peak ground acceleration and peak ground velocity as covariates in the hazard model increased the successful identification of landslide locations compared to the susceptibility model. Using a

failure threshold of ≥0.9 probability of landsliding, the susceptibility model had a successful prediction rate of 75.79% for landslide cells compared to 80.87% for the hazard model. This hazard model can be utilised in further studies to detect probable locations of landslides as a result of earthquake scenarios in the Northridge study site, identifying areas at risk and potential damage to populations and infrastructure.

## 1.0 Introduction

The USGS's National Earthquake Information Center (NEIC) reports on more than 30,000 earthquakes per year, an average of 25 of which cause significant damage, injuries or fatalities (Godt et al., 2008). Earthquake strong ground motion can lead to slope failure due to cyclical changes in the normal and shear stresses of hill slopes (Hovius and Meunier, 2012). Earthquake-induced landslides are one of the most damaging secondary hazards associated with earthquakes (Jibson et al., 2000). The 7.6$M_w$ Chi-Chi earthquake in Taiwan in 1999 triggered an estimated 9270 large landslides, and the 7.6$M_w$ Kashmir earthquake in 2005 triggered at least 1300 large failures (Marui and Nadim, 2009). Approximately 5% of all earthquake-related fatalities arise as a result of seismically-induced landslides, and in some cases landsliding is the cause of the majority of non-shaking deaths (Marano et al., 2010). Damage to residential buildings caused by the 1994 Northridge $M_w$6.7 earthquake was three to four times greater when landsliding was involved than the average shaking-induced damage (Brown and Ghilarducci, 2013). In addition to causing large fatalities due to direct impact and burial, landslides can severely impede recovery and relief procedures in the immediate aftermath of earthquakes by obstructing transport paths and diverting important resources (Marui and Nadim, 2009).

Due to the spatially dispersed nature of landslide occurrences and their potentially damaging effects, it is necessary to map susceptibility to failure especially in areas with elements at risk (Bednarik et al., 2010). Landslide susceptibility maps are essential resources for land use

planning, engineering works design, and civil protection and risk reduction programmes (Hervas and Bobrowsky, 2009). Landslide susceptibility refers to "the propensity of an area to landslide occurrence". Landslide susceptibility maps are available for various regions, and also globally (Yin et al., 2010; Hong et al., 2007; Ercanoglu et al., 2004; Van Westen et al., 2003; Lee et al., 2004). However, typically these represent long-term susceptibility to landslides (Nadim et al., 2006), and the unique shaking distribution of an earthquake event is not taken into consideration (Atkinson and Massari, 2011).

When modelling landslide hazard, the conditioning (preparatory) factors, which make the slope susceptible to failure, and triggering (causative) mechanisms, which initiate movement, should be considered (Dai and Lee, 2003; Hervas and Bobrowsky, 2009). There is a temporal difference between landslide susceptibility and landslide hazard (Figure 12). Landslide susceptibility accounts for the inherent likelihood of landsliding based upon typically long-term factors such as geology, slope gradient and vegetation cover. These factors control the propensity of a slope to fail. Landslide hazard is dependent upon a triggering factor occurring, which could be severe rainfall, earthquake shaking or human activity. The likelihood of failure at this point is conditional upon the triggering event occurring. Landslide hazard is, therefore, a combination of the preparatory environmental factors and the causative triggering factors (Figure 1).

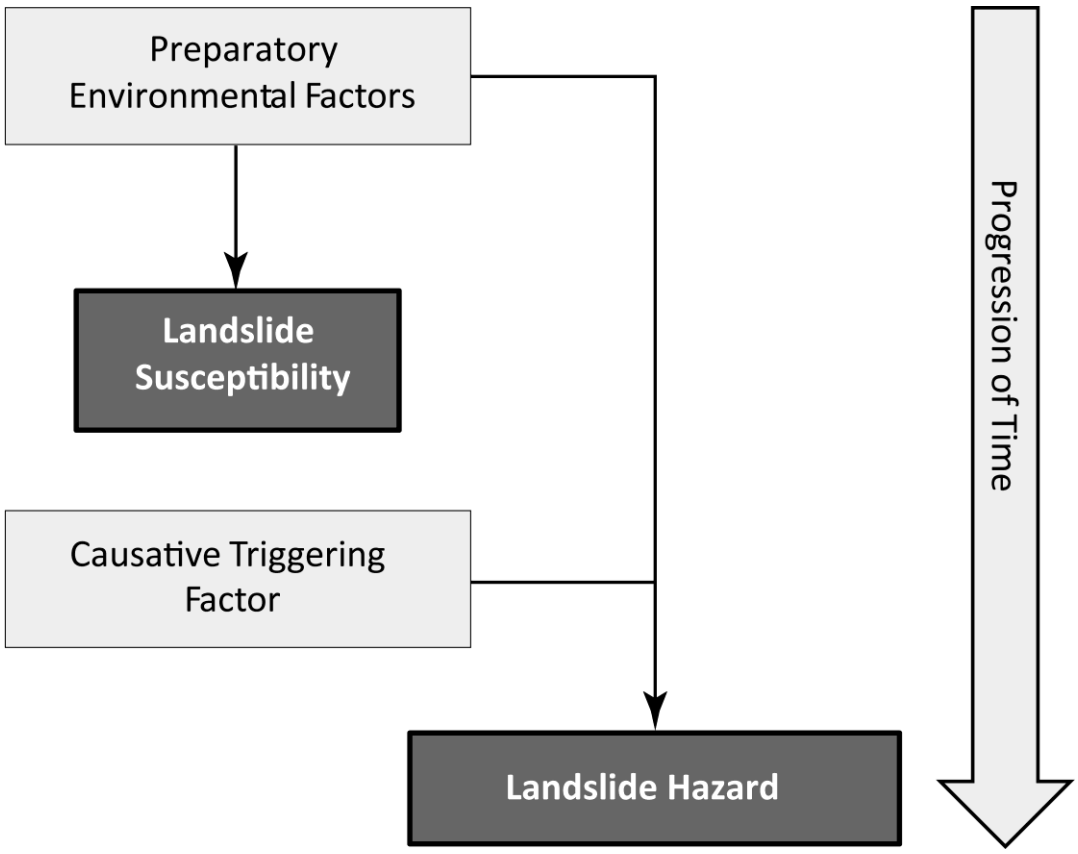


Figure 44. Conceptual diagram to clarify the distinction between susceptibility to landsliding and landslide hazard, conditional upon a triggering event occurring. Based upon definition from Hervas and Bobrowsky, 2009).

Predicting the location of landslides as a result of an earthquake trigger is important for understanding risk, but is rarely carried out in the published literature (Hovius and Meunier, 2012). A systematic search of the literature revealed that 91 studies used logistic regression to map landslide probability, of which only two used peak ground acceleration as a covariate (Budimir et al., 2015). This is partly attributed to a lack of sufficiently detailed shaking distribution data (Pradhan et al., 2010; Atkinson and Massari, 2011; Hovius and Meunier, 2012). Marzorati et al.(2002) and Carro et al.(2003) both considered peak ground acceleration in their logistic regression models for studies on the Umbria-Marche earthquake. Both found the peak ground acceleration covariate to be a significant factor in predicting landslide occurrence. Meunier et al. (2007) and Dai et al. (2011) found patterns of landsliding closely quantitatively related to ground shaking.

Despite the scarcity of published empirical evidence, Hovius and Meunier (2012) proposed that landslide density is correlated to peak ground acceleration and is "key to understanding the global attributes of regional and local patterns of earthquake-induced landsliding". Earthquake strong ground motion causes cyclical changes of the normal and shear stresses in hillslopes during earthquakes (Meunier et al., 2007; Meunier et al., 2008; Hovius and Meunier, 2012). When this shear stress across a potential failure plane exceeds substrate strength, failure occurs (Hovius and Meunier, 2012).

However, the peak ground acceleration field is not entirely concentric as topographic and geologic factors can influence this relationship (Geli et al., 1988). For example, softer sediments can increase the amplitude of earthquake ground motion because of lower elastic modulus than strong rocks (Aki, 1993; Field et al., 1997; Hovius and Meunier, 2012). Topographic amplification of ground acceleration can occur near ridges as the seismic waves are reflected and diffracted along ridges (Lin et al., 2008; Tibaldi et al., 1995; Hovius and Meunier, 2012). Therefore, whilst ground acceleration from earthquakes can influence landsliding, other factors must also be taken into consideration when predicting the likelihood of slope failure as a result of an earthquake event (Yin et al., 2010).

Approaches for quantifying landslide susceptibility include statistical approaches and physically-based models (Aleotti and Chowdhury, 1999; Yin et al., 2010; Hervas and Bobrowsky, 2009). Physically-based approaches are often data demanding and challenging to implement because of difficulties in estimating fundamental parameters. Statistical analysis correlates geo-environmental factors with the distribution of landslide occurrence, recorded by landslide inventories (Hervas and Bobrowsky, 2009). Statistical approaches have become popular with the increased availability of remotely sensed satellite sensor data, generation of digital elevation models, widely accessible state-of-the-art geographical information system (GIS) software tools and statistical software (Carrara et al., 1991; Wang et al., 2011; Hervas and Bobrowsky, 2009). Whilst statistical methods are restricted by the

availability of suitable data, and are unable to predict landslide paths, they are useful for land use and scenario planning (Hervas and Bobrowsky, 2009).

This paper uses a well-documented landslide inventory map, detailed peak ground acceleration data and environmental variables associated with landsliding to fit logistic regression models of probability of landslide occurrence for the 1994 Northridge earthquake event. Two models were fitted to the data: the first to model *susceptibility* to landsliding using geo-environmental pre-existing conditioning factors (such as slope gradient, geology); the second to model landslide *hazard* by including the earthquake triggering mechanism (peak ground acceleration and peak ground velocity). The accuracy of each model was compared to determine if the inclusion of the earthquake shaking data increased the accuracy of prediction.

## 2.0 Data

### 2.1 Study site

The San Fernando Valley and neighbouring mountains are part of the Transverse Ranges physiographic province, one of the most seismically active parts of the United States (Parise and Jibson, 2000). The region is located near the boundary between the Pacific Plate (the largest plate on the Earth's crust) and the continental North American Plate (He and Beighley, 2008). The mean elevation of the study site is 585 m, ranging between sea level and 2250 m. The slope gradient ranges between 0° and 55°.

In 1994, Northridge, in the San Fernando Valley, California, USA, roughly 30 km northwest of Los Angeles, experienced a magnitude 6.7 earthquake at 4:30 am local time (Parise and Jibson, 2000). 60 people were killed, more than 7,000 injured, 20,000 left homeless and more than 40,000 buildings damaged in Los Angeles, Ventura, Orange and San Bernardino Counties (USGS, 2012). Landslide damage from the Northridge earthquake was only moderate because the area of heaviest landslide activity was undeveloped at the time (Keefer

and Wilson, 2011). However, there are plans to develop dense residential areas in the Santa Susana Mountains in the future (Harp and Jibson, 1996; Keefer and Wilson, 2011).

Digital maps of more than 11,000 earthquake-induced landslides were recorded as a result of the event over a 1000 $km^2$ area, providing a dataset of unprecedented completeness for detailed study, and freely available for download from the USGS (Figure 45) (Harp and Jibson, 1996; Meunier et al., 2007). The study site, defined to encompass all the landslide events, lies between the latitudes 34°00' N and 34°67' N and longitudes 118°16' W and 119°07' W. The majority of the triggered landslides were shallow (1 m to 5 m), highly disrupted falls and slides (Harp and Jibson, 1996). High-altitude aerial photography immediately after the earthquake, and field observations were used to compile the landslide inventory map. For a more detailed description of the landslide data and the compilation of the inventory map, see Harp and Jibson (1996).

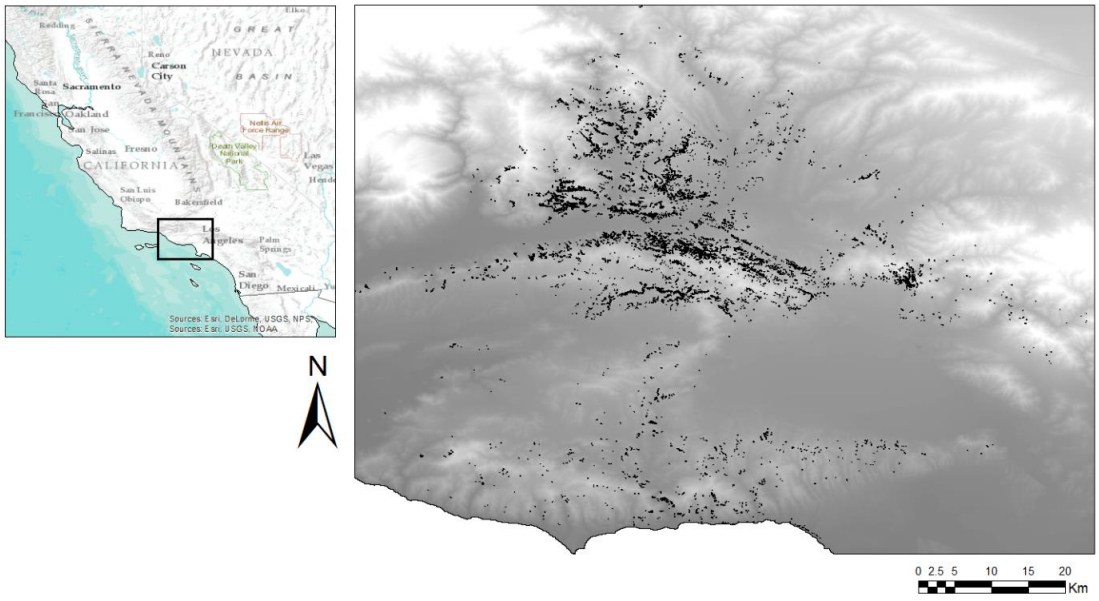


Figure 45. Site location (left) and landslide inventory map (right) of the 1994 Northridge earthquake event.

## 2.2 Environmental covariates

To develop the landslide models, a dependent variable separating landslide areas from non-landslide (stable) areas was created. A series of environmental covariates for use in the

logistic regression model was chosen based on common environmental covariates used in landslide logistic regression analysis in the literature, and the availability of the data (Table 18).

Table 18. Definitions and interpretation of the environmental covariates selected for use in logistic regression to predict landslide occurrence.

| Explanatory variable | Definition | Significance |
|---|---|---|
| Aspect | Slope azimuth | Solar insulation, evapotranspiration, flora and fauna distribution and abundance |
| Curvature | Representing morphology of the topography: a positive curvature indicates that the surface is upwardly convex at that pixel. A negative curvature indicates that the surface is upwardly concave at that pixel; a value of zero indicates that the surface is flat. | Retention of water and soil wetness |
| Drainage density | The density of drainage lines in the neighborhood of each output raster cell. Density is calculated in units of length per unit of area. | Increased percolation in low drainage density, higher slope instability and soil water content in high drainage density. |
| Distance to drainage | Euclidean distance to drainage | Streams undercut and destabilise slopes, soil water content |
| Elevation | Height above sea level | Climate, vegetation, potential energy |
| Fault density | The density of fault lines in the neighborhood of each output raster cell. Density is calculated in units of length per unit of area. | Source of shaking destabilised slope |
| Distance to fault | Euclidean distance to recorded fault line | Proximity to source of shaking destabilised slope |
| PGA | Peak ground acceleration | Vibration of ground and destabilising effect |
| PGV | Peak ground velocity | Vibration of ground and destabilising effect |
| Plan curvature | Contour curvature: perpendicular to the direction of maximum slope | Converging, diverging flow, soil water content, soil characteristics |
| Profile curvature | Slope profile curvature: direction of the maximum slope | Flow acceleration , erosion/deposition rate, geomorphology |
| Distance to ridgeline | Euclidean distance to ridgeline | Hanging wall effect |
| Road density | The density of road lines in the neighborhood of each output raster cell. Density is calculated in units of length per unit of area. | Destabilisation and undercutting of slopes by roads. |
| Distance to road | Euclidean distance to road | Destabilising and undercutting effect on slopes. |
| Roughness | Standard deviation of slope (3x3 and 5x5 cell sample) | Terrain ruggedness, affecting water retention and stability of slope |
| Slope gradient | Change in elevation divided by horizontal distance | Overland and subsurface flow velocity and runoff rate, precipitation, vegetation, geomorphology, soil water content, land capability class, stability and loading of slope |
| SPI | Stream power index | Erosive power of water flow |
| Geology | Type of geology beneath the soil layer | Shear strength |

| | | |
|---|---|---|
| Land cover | Type of vegetation or land use | Vegetation type and human alteration affects infiltration and soil water content |
| Soil type | Top most soil layer type | Shear strength, stability of cohesive/non-cohesive material |
| Vegetation | Vegetation type | Evapotranspiration, infiltration and soil water content, root system stabilisation |

Of the 21 environmental covariates entered into the logistic regression model, 15 were numerical or continuous in nature: curvature, drainage density, distance to drainage, elevation, fault density, distance to fault line, peak ground acceleration (PGA), peak ground velocity (PGV), plan curvature, profile curvature, distance to ridgeline, road density, distance to roads, roughness (standard deviation of elevation across 3 by 3 cells and 5 by 5 cells), slope gradient, and stream power index (SPI). Five environmental covariates were categorical: aspect, geology, land cover, soil type and vegetation. Table 19 shows the spatial resolution and data source for these covariates.

Table 19. Spatial resolution or scale and source for the independent environmental covariates used for each study site.

| | **Spatial resolution (or scale if given as a ratio)** | **Source** |
|---|---|---|
| **DEM** | 3 arc-seconds | GMTED2010 |
| **Drainage** | 3 arc-seconds | HydroSHEDS |
| **Faults and Geology** | 1:40,000,000 < scale < 1:5,000,000 | OneGeology Portal |
| **Land use** | 30 m | USGS Landcover Institute |
| **PGA** | 1.6 km | USGS |
| **PGV** | 1.6 km | USGS |
| **Roads** | 1:2,000,000 | GeoCommunities |
| **Soil** | 1:250,000 | GeoCommunities |
| **Vegetation** | 1 km | GeoCommunities |

*Elevation*

A digital elevation model (DEM) for the study site was obtained from the USGS Global Multi-resolution Terrain Elevation Data 2010 (GMTED2010). These data are defined at an approximate spatial resolution of 3 arc seconds, 0.00083 degrees, or roughly 90 m cells. From the elevation data, several topographic covariates were calculated using ArcGIS: aspect, curvature, plan curvature, profile curvature, distance to ridge line, roughness (3 by 3

cells and 5 by 5 cells), slope gradient, and SPI. The SPI was calculated using the following equation:

$$SPI = \ln[(FA + 0.001) * \left(\frac{SL}{100}\right) + 0.001] \quad \text{Equation 14}$$

where *SPI* is the stream power index value, *FA* is the flow accumulation, and *SL* is the slope gradient.

*Drainage*

The distance to drainage and drainage density covariates were compiled using drainage network data from HydroSHEDS (Hydrological data and maps based on Shuttle Elevation Derivatives at multiple Scales). HydroSHEDS data are available at a spatial resolution of 3 arc seconds globally, and can be downloaded free of charge via the USGS or World Wildlife Fund (WWF).

*Geology*

Geological and fault data were digitized in ArcGIS from the Geologic Map of North America, published by the Geological Society of America in 2005 and downloaded from the OneGeology portal (Reed et al., 2005). Digital geological data were compiled from source data at a scale of 1:5,000,000. The geology types present in the study site were coded with dummy variables for the logistic regression analysis (see Appendix Table A1 for a table of dummy variables and associated geology).

*Land cover*

Land cover for the Northridge area was obtained via the USGS National Land Cover Dataset compiled from Landsat Thematic Mapper (TM) imagery. The land cover data have a spatial resolution of 30 m and were compiled in 1992, before the Northridge earthquake. For a list of the land cover types and associated dummy variable codes, see Appendix Table A2.

*Shaking*

About 200 strong-motion recordings of the main shock were taken, producing one of the most comprehensive datasets at the time of the event (Parise and Jibson, 2000). Peak horizontal acceleration and peak velocity maps were obtained from the USGS ShakeMap Archive for the 1994 Northridge earthquake event. Peak horizontal acceleration at each station is contoured in units of percent-*g* (where *g* = acceleration due to the force of gravity = 981 cm $s^{-1}$ $s^{-1}$). Peak velocity values are contoured for the maximum horizontal velocity (in cm $s^{-1}$) at each station.

*Roads*

The distance to roads and road density covariates were calculated in ArcGIS using road line data from the Digital Chart of the World's (DCW) data repository. The DCW is an Environmental Systems Research Institute, Inc. (ESRI) product originally developed for the US Defense Mapping Agency (DMA) using DMA data. The US Defense Mapping Agency Operational Navigation Chart (ONC) series was the primary source of data for the DCW database.

*Soil*

The soil data were provided by the National Cooperative Soil Survey and sourced from the DCW. These data provide information about soil features on or near the surface of the Earth. The dataset was created by generalizing from more detailed soil survey maps. Where these more detailed soil survey maps did not exist, data on geology, topography, vegetation and climate were used with Landsat images to infer soil type. For a list of the soil types and associated dummy variable codes, see Appendix Table A3.

*Vegetation*

The vegetation data were sourced from the DCW data repository. An Advanced Very High Resolution Radiometer (AVHRR) image of the United States was used to identify vegetation types for use in the DCW data repository. The types of vegetation identified are classified in accordance with the Level II categories of the USGS Land Use and Land Cover Classification System (Anderson et al., 1976). The Northridge study site has five vegetation types; for a list of the vegetation types and associated dummy variable codes, see Appendix Table A4.

## 3.0 Methodology

A raster-based methodology was adopted for this study. A spatially random, equal number of landslide and non-landslide raster image cells were selected for logistic regression modelling, with a third of this initial sample retained for future accuracy assessment. Two logistic models were fitted: a susceptibility model containing only environmental preparatory data, and a landslide hazard model containing the additional causative triggering factors (peak ground acceleration and peak ground velocity). These models were used to map the probability of landsliding in the Northridge study site and the accuracy of each model was assessed and compared.

### 3.1 Sampling strategy

Data analysis for this study was based on raster image data with a spatial resolution (pixel size) of approximately 1 $km^2$, the same resolution as the DEM data. Thus, all covariate data were converted (rasterized) to the same spatial resolution as that of the DEM data. The landslide inventory maps were rasterized and coded with the value of 1 (landslide occurrence) and 0 (no landslide occurrence). At this spatial resolution, the 11,000 landslides were represented by 3,358 raster grid cells. To increase the certainty of selecting landslide-free grid cells outside a mapped landslide, a 1 km buffer zone was drawn around each landslide to prevent landslide cells from influencing the selection of non-landslide cells for the logistic regression analysis (Van Den Eeckhaut et al., 2010).

The total number of landslide cells was 3,358; after excluding the 1 km buffer around these cells, there remained 614,511 non-landslide cells. It is recommended in logistic regression to use equal proportions of 1 (landslide) and 0 (non-landslide) cells (Chang et al., 2007; Dai and Lee, 2002; Yesilnacar and Topal, 2005). Therefore, a selection of two thirds (2,518) of the landslide cells was selected and a further 2,518 non-landslide cells were generated randomly for model fitting. This left 840 landslide cells, a third of the total landslide cells, and 840 non-landslide cells taken from the remaining cells, without the 1 km buffer, to assess the accuracy of the models at a later stage (Van Den Eeckhaut et al., 2010; Brenning, 2005; Santacana et al., 2003).

## 3.2 Logistic regression

Several statistical methods are used commonly to determine the significant factors affecting landslide susceptibility and occurrence. In a limited study, Brenning (2005) demonstrated that logistic regression is the preferred method for modelling landslide susceptibility as it resulted in the lowest rate of error. Logistic regression is a useful tool for analysing landslide occurrence, where the dependent variable is categorical (e.g. presence or absence) and the explanatory (independent) covariates are categorical, numerical, or both (Atkinson and Massari, 1998; Chang et al., 2007; Ohlmacher and Davis, 2003). The logit model from a logistic regression has the following form:

$$logit(y) = \beta_0 + \beta_1 x_1 + \beta_2 x_2 + \cdots + \beta_i x_i + e \qquad \text{Equation 15}$$

where $y$ is the dependent variable, $x_i$ is the $i$-th explanatory variable, $\beta_0$ is a constant, $\beta_i$ is the $i$-th regression coefficient, and $e$ is the error term. The probability ($p$) of the occurrence of $y$ can be written as:

$$p = \frac{exp^{(\beta_0+\beta_1 x_1+\beta_2 x_2+\cdots+\beta_i x_i)}}{1+exp^{(\beta_0+\beta_1 x_1+\beta_2 x_2+\cdots+\beta_i x_i)}} \qquad \text{Equation 16}$$

The logistic regression model was fitted twice as described above. The logistic models were fitted automatically using the statistical software 'R', in a backward-stepwise manner, using the AIC value to determine the best fitting model.

### 3.3 Accuracy Assessment

A subset of the original data was set aside for assessing the accuracy of the model. These 840 landslide and 840 non-landslide data points were not used in the fitting of the model. The landslide probability value predicted for each cell was retained and analysed statistically for the susceptibility model and the hazard model.

The accuracy of the logistic regression models was evaluated by calculating the receiver operating characteristic (ROC). The ROC is a graphical plot which illustrates the performance of a binary classifier system as its discrimination threshold is varied (Gorsevski et al., 2006). The area under the ROC curve (AUC) is a statistic that measures the ability of the model to correctly classify cases of landslide and cases of stable area (Chang et al., 2007). When the total area is found to be 1, this indicates perfect accuracy. In addition to the ROC AUC, the percentage of correctly and incorrectly predicted landslides and non-landslide cells for various levels of failure threshold probability values for both the susceptibility and hazard models were calculated and compared.

## 4.0 Analysis

### 4.1 Susceptibility Model

Table 20 shows the regression coefficients and their significance levels (*P*-value) for the environmental covariates of the susceptibility model. The susceptibility model found aspect, elevation, fault density, distance to roads, road density, roughness (3 by 3 cells), slope, geology, vegetation, land cover and soil type to be significant covariates in predicting landslide susceptibility (Table 20). Of the environmental covariates input into the regression analysis, ten numeric covariates were eliminated from the susceptibility model: curvature,

plan curvature, profile curvature, SPI, drainage density, distance to drainage, distance to fault, road density, distance to ridge lines, and roughness (5 by 5 cells).

Table 20. Logistic regression coefficients and the associated p-value for environmental covariates in the susceptibility model. The coefficients and p-values for the categorical explanatory variables (aspect, geology, vegetation, land cover and soil type) are shown separately in Table A5 of the Appendix.

| **Environmental covariates** | **Susceptibility model** | |
|---|---|---|
| | **Coefficients** | ***p*-value** |
| *(Intercept)* | *-5.896* | - |
| Road distance | -34.810000 | 0.000000 |
| Slope | 0.074290 | 0.000000 |
| Elevation | -0.002755 | 0.000000 |
| Road density | -0.045640 | 0.000000 |
| Fault density | 0.031790 | 0.000007 |
| Roughness (3x3) | 0.500800 | <2.00E-16 |

Using equations 14 and 15, and the coefficients from Table 20 and Table A5, the probability of landslide occurrence was predicted spatially using the susceptibility model (Figure 46). A visual comparison between the landslide inventory map (Figure 45) and the landslide probability map (Figure 46) indicate a close agreement between areas with mapped landslides and areas with high probability of landsliding. Additionally, areas with a high probability of landsliding are present in areas beyond the extent of the recorded landslides. This indicates that the logistic regression model is able to portray areas of landslide susceptibility (i.e., potential hazard).

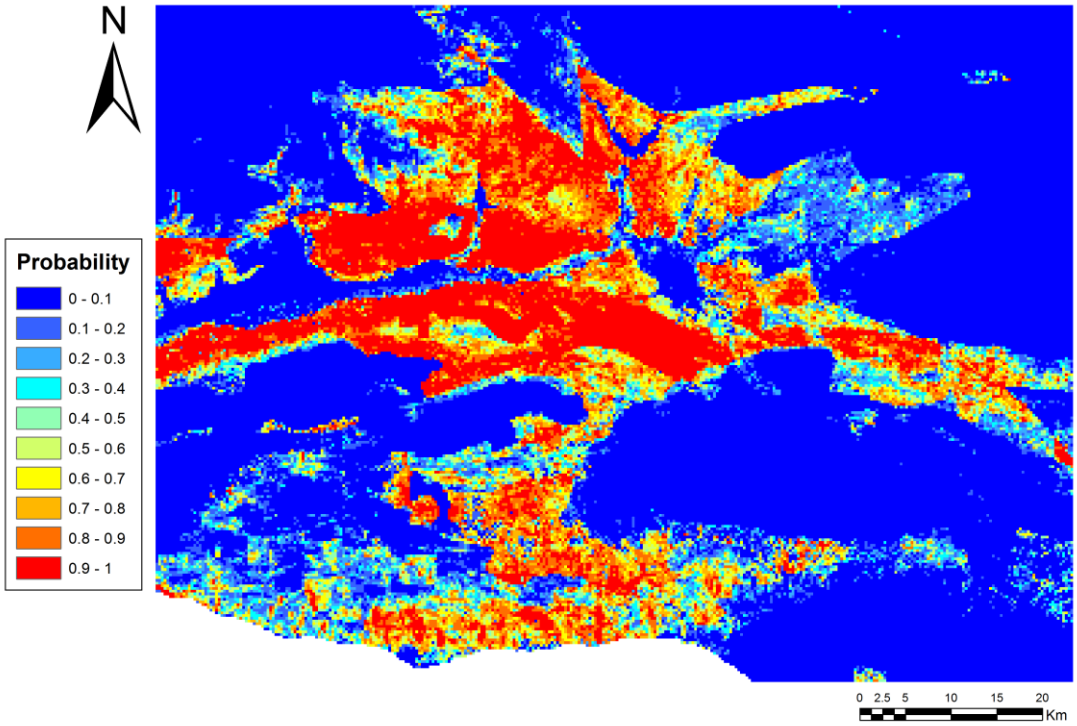


Figure 46. Landslide probability map predicted using the landslide susceptibility model.

## 4.2 Hazard Model

Table 21 shows the regression coefficients and the significance level (*p*-value) of the environmental covariates in the landslide hazard model. In the hazard model the same covariates were found to be significant as for the susceptibility model. However, additionally distance to faults, peak ground acceleration, and peak ground velocity were found to be significant. Of the environmental covariates input into the regression analysis, six continuous covariates were eliminated from the hazard model: curvature, plan curvature, profile curvature, SPI, drainage density and distance to drainage.

Table 21. Logistic regression coefficients and the associated p-value for environmental covariates in the hazard model. The coefficients and p-values for the categorical explanatory variables (aspect, geology, vegetation, land cover and soil type) are shown separately in Table A5 of the Appendix.

| **Environmental covariates** | **Hazard model** | |
|---|---|---|
| | **Coefficients** | **P-value** |
| *(Intercept)* | *-7.560000* | - |
| Elevation | -0.003211 | 0.000000 |
| PGV | 0.091680 | 0.000000 |
| Slope | 0.077890 | 0.000000 |
| Road density | -0.047680 | 0.000000 |
| Roughness (3x3) | 0.460100 | 0.000000 |
| Fault density | 0.034860 | 0.000487 |
| Road distance | -14.440000 | 0.000565 |
| Fault distance | 9.356000 | 0.013772 |
| Ridge distance | -52.730000 | 0.024898 |
| Roughness (5x5) | 0.215800 | 0.025570 |
| PGA | 0.038200 | 0.053880 |

Using equations 14 and 15, and the coefficients from Table 21 and Table A5, the probability of landslide occurrence was predicted spatially using the landslide hazard model (Figure 47). A visual comparison between the landslide inventory map (Figure 45) and the landslide probability map (Figure 47) again indicate close agreement between areas with mapped landslides and areas with high probability of landsliding.

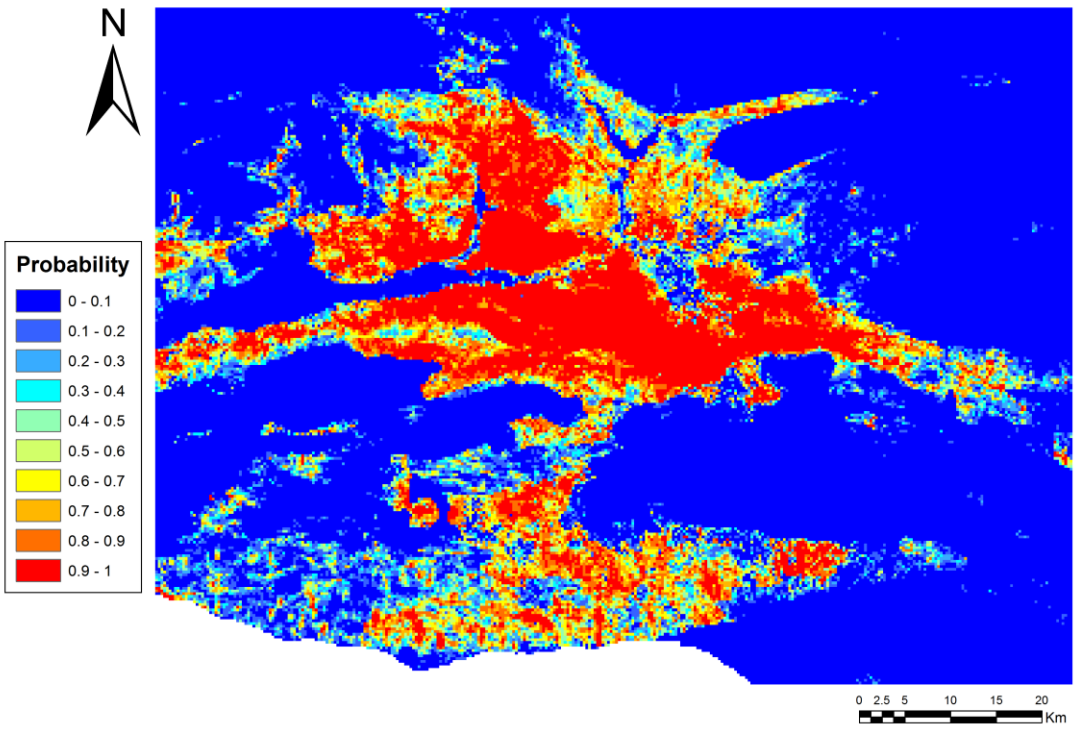


Figure 47. Landslide probability map predicted using the landslide hazard model.

## 4.3 Comparison of Models

A visual comparison of the probability maps created from the susceptibility and hazard models reveals a reasonably similar distribution of probability estimates for both models (Figure 46 and Figure 47). However, there is a difference in the models. The susceptibility model predicts a higher probability (0.9-1) of landsliding in a thin band from East to West across the middle of the site between Fillmore and the Simi Valley, whereas the hazard model predicts a higher concentration of landsliding in the centre of the site, with high probability in Santa Clarita, close to the San Fernando Valley. Figure 48 shows the difference between the two maps when the hazard map is subtracted from the susceptibility map. The red areas show where the hazard map predicted higher levels of probability to landsliding than the susceptibility model (i.e., more specific hazard, less general susceptibility). The green areas show where the hazard model predicted lower levels of probability to landsliding than the susceptibility model (i.e., more general susceptibility, less

specific hazard). In line with expectations, the hazard model predicted higher probability of landsliding closer to the epicentre of the earthquake, near the San Fernando Valley.

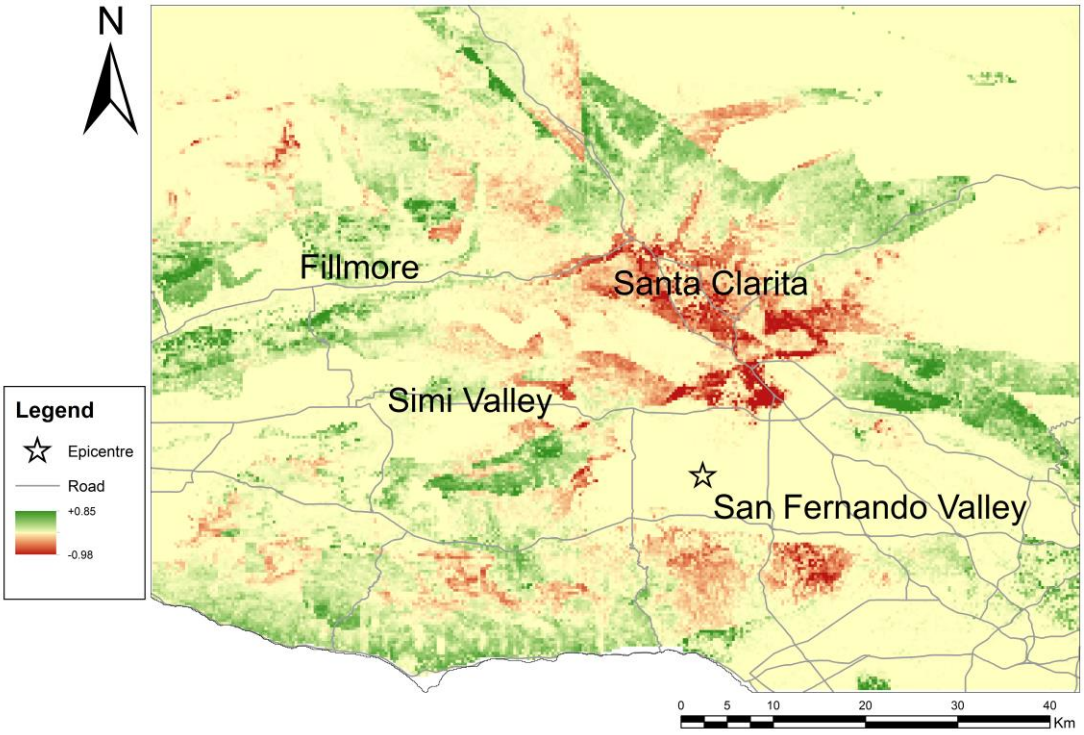


Figure 48. Map of the difference between the two landslide probability maps (hazard map subtracted from the susceptibility map). Positive values indicate greater general susceptibility than specific hazard related to the 1994 Northridge event. Negative values indicate greater specific hazard than general susceptibility. The earthquake epicentre, San Fernando Valley, Fillmore, Santa Clarita and Simi Valley are indicated on the map.

## 4.4 Accuracy Assessment

Figure 49 shows a plot of the ROC for both the susceptibility and hazard models. The susceptibility model has an ROC AUC statistic of 0.8648; the hazard model has a value of 0.8731. This suggests that the model including shaking covariates has a slightly greater predictive ability than one without shaking covariates. However, the difference in the AUC values is not statistically significant (Hanley and Mcneil, 1983). As the ROC is calculated based upon multiple thresholds of failure, the AUC values do not reflect if a model has a greater predictive ability at a specific threshold of failure. The ROC curves suggest that the hazard model has greater prediction ability at higher threshold values (>0.8).

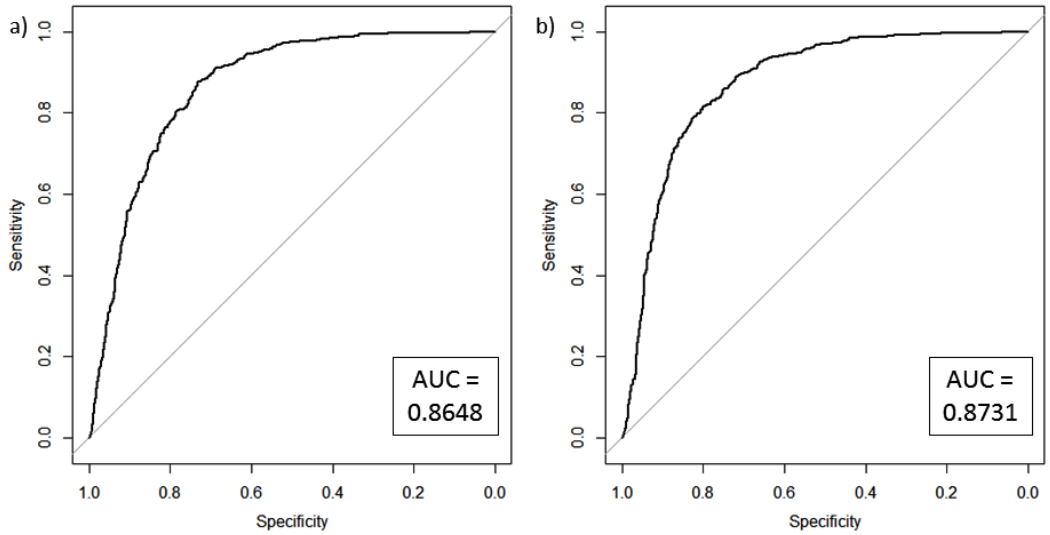


Figure 49. ROC plots for (a) the susceptibility logistic model, and (b) the hazard logistic model.

From Figure 50 it can be seen that the landslide presence values are clustered around the higher probability values for both models. Therefore, the percentage of correctly and incorrectly predicted landslides and non-landslide cells for various levels of threshold values ($P \geq 0.5$, 0.7, 0.9, and 0.95) for both the susceptibility and hazard models were calculated and compared (Table 22).

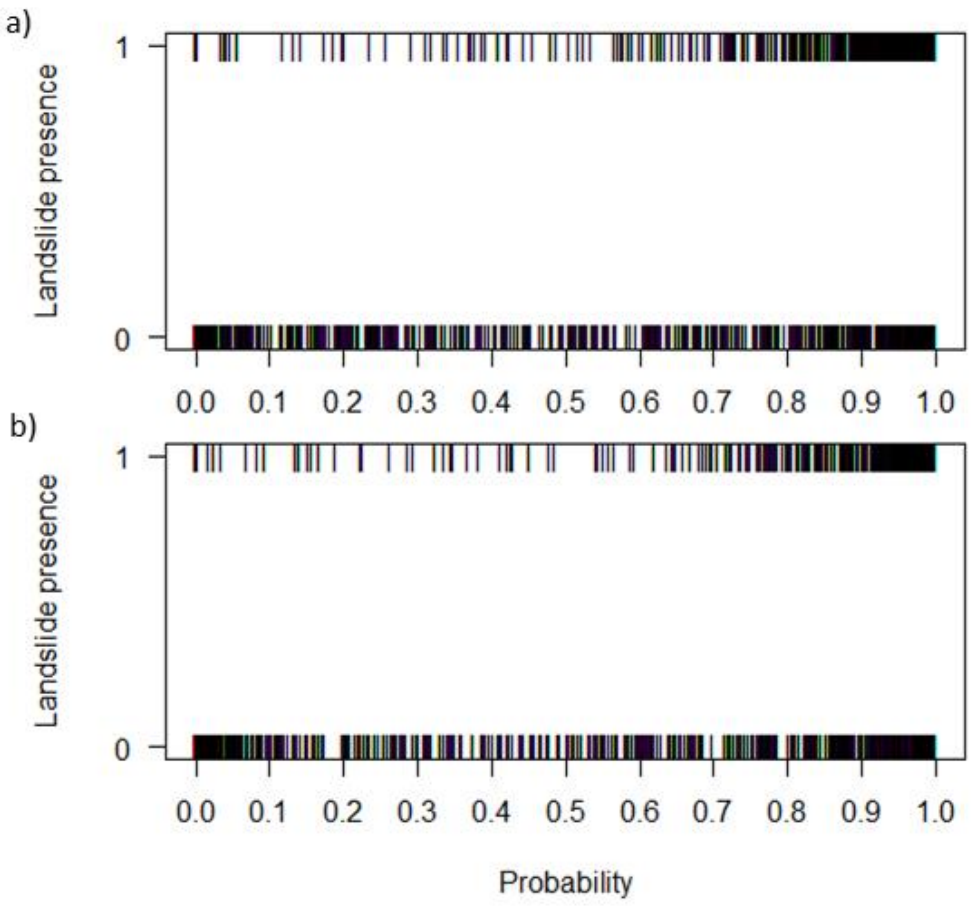


Figure 50. Plots of observed values against predicted probability values showing the separation between landslide and non-landslide points for (a) the susceptibility logistic model, and (b) the hazard logistic model.

The percentage of correctly and incorrectly predicted landslide and non-landslide cells based on landslide failure at $P \geq 0.5$ for both models is similar (Table 22). The models both have a high rate of predicting landslide cells correctly (96%), but have a high negative misclassification rate, over-predicting landslide occurrence in approximately 42-43% of cases. As the threshold of failure probability is increased, the hazard model produces greater accuracy in predicting landslide cells compared to the susceptibility model (Table 22). Using a failure threshold of $P \geq 0.9$ probability of landsliding, the susceptibility model had a successful prediction rate of 77% for landslide cells compared to 81.23% for the hazard model. For a failure threshold of $P \geq 0.95$, the hazard model is more accurate by 10.9% compared to the susceptibility model. For the hazard model, there is an overall increase in

prediction accuracy compared to the $P \geq 0.5$ threshold of 22.52% for non-landslide cells, but a reduction in prediction accuracy for landslide cells of -22.52%.

Table 22. Percentage of correctly and incorrectly predicted landslide (LS) and non-landslide (NoLS) cells for four different threshold failure probability values (0.5, 0.7, 0.9 and 0.95) for both the susceptibility and hazard models.

| | | **Failure = $P \geq 0.5$** | | **Failure = $P \geq 0.7$** | | **Failure = $P \geq 0.9$** | | **Failure = $P \geq 0.95$** | |
|---|---|---|---|---|---|---|---|---|---|
| | | **Present** | **Absent** | **Present** | **Absent** | **Present** | **Absent** | **Present** | **Absent** |
| **Susceptibility** | **LS** | 96.49 | 42.37 | 92.62 | 33.29 | 77.00 | 19.01 | 62.59 | 12.47 |
| **Model** | **NoLS** | 3.39 | 57.51 | 7.26 | 66.59 | 22.88 | 80.87 | 37.29 | 87.41 |
| **Hazard** | **LS** | 96.01 | 43.17 | 93.46 | 34.26 | 81.23 | 19.61 | 73.49 | 14.16 |
| **Model** | **NoLS** | 3.87 | 56.71 | 6.42 | 65.62 | 18.64 | 80.27 | 26.39 | 85.71 |

## 4.5 Landslide Occurrence

Landslide occurrence was calculated as a percentage of the total number of landslide cells (3,358) for each covariate found to be statistically significant in the susceptibility and hazard models. Table 23 shows the percentage of landslides in each class of aspect, elevation, fault distance, fault density, peak ground acceleration, peak ground velocity, distance to ridge line, distance to roads, road density, roughness (3 by 3 and 5 by 5), slope gradient, geology, land use, soil and vegetation type in the Northridge site. From Table 23, it can be seen that landsliding is particularly frequent on the south and southwest facing slopes. Geology type 7 has very high percentage of landslide occurrence (79.22%). This geology is Miocene sedimentary. Soil type 14 (San Benito, Castaic, Calleguas, Balcom and Badland soil types) also has high percentage of landslide occurrence (42.39%).

Table 23. Part A. Landslide percentage for each class for the numeric covariates: slope gradient, fault distance, PGA, PGV, roughness (3x3, and 5x5), road density, road distance, ridge distance and fault density.

| Covariate Class | Landslide Density (%) |
|---|---|
| *Slope Gradient (°)* | |
| 0-5 | 5 |
| 5-10 | 17 |
| 10-15 | 25 |
| 15-20 | 22 |
| 20-25 | 18 |
| 25-30 | 9 |
| 30-35 | 3 |
| 35-40 | 1 |
| >40 | 0 |
| *Roughness (3x3)* | |
| 0-1 | 0 |
| 1-2 | 1 |
| 2-3 | 7 |
| 3-4 | 16 |
| 4-5 | 22 |
| 5-6 | 22 |
| 6-7 | 15 |
| 7-8 | 9 |
| 8-9 | 4 |
| >9 | 3 |
| *Ridge Distance (km)* | |
| 0-0.001 | 13 |
| 0.001-0.002 | 0 |
| 0.002-0.003 | 25 |
| 0.003-0.004 | 13 |
| 0.004-0.005 | 49 |
| 0.005-0.006 | 28 |
| 0.006-0.007 | 0 |
| 0.007-0.008 | 5 |
| 0.008-0.009 | 9 |
| 0.009-0.01 | 3 |
| >0.01 | 5 |

| Covariate Class | Landslide Density (%) |
|---|---|
| *Fault Distance (km)* | |
| 0-0.02 | 36 |
| 0.02-0.04 | 43 |
| 0.04-0.06 | 13 |
| 0.06-0.08 | 1 |
| 0.08-0.1 | 2 |
| 0.1-0.12 | 2 |
| 0.12-0.14 | 2 |
| 0.14-0.16 | 1 |
| >0.16 | 0 |
| *Roughness (5x5)* | |
| 0-1 | 0 |
| 1-2 | 0 |
| 2-3 | 5 |
| 3-4 | 10 |
| 4-5 | 20 |
| 5-6 | 25 |
| 6-7 | 22 |
| 7-8 | 10 |
| 8-9 | 5 |
| >9 | 4 |
| *Fault Density* | |
| 0-5 | 58 |
| 5-10 | 3 |
| 10-20 | 13 |
| 20-30 | 26 |
| >30 | 1 |

| Covariate Class | Landslide Density (%) |
|---|---|
| *PGA (%g)* | |
| 0-10 | 0 |
| 10-20 | 1 |
| 20-30 | 29 |
| 30-40 | 32 |
| 40-50 | 22 |
| 50-60 | 13 |
| 60-70 | 4 |
| >70 | 1 |
| *Road Density* | |
| 0-5 | 72 |
| 5-10 | 2 |
| 10-15 | 4 |
| 15-20 | 5 |
| 20-25 | 7 |
| 25-30 | 8 |
| 30-35 | 1 |
| 35-40 | 1 |
| 40-45 | 1 |
| >45 | 0 |

| Covariate Class | Landslide Density (%) |
|---|---|
| *PGV (cm/sec)* | |
| 0-10 | 0 |
| 10-20 | 8 |
| 20-30 | 27 |
| 30-40 | 13 |
| 40-50 | 20 |
| 50-60 | 12 |
| 60-70 | 6 |
| 70-80 | 7 |
| 80-90 | 6 |
| >90 | 0 |
| *Road Distance (km)* | |
| 0-0.01 | 9 |
| 0.01-0.02 | 15 |
| 0.02-0.03 | 18 |
| 0.03-0.04 | 23 |
| 0.04-0.05 | 14 |
| 0.05-0.06 | 9 |
| 0.06-0.07 | 3 |
| 0.07-0.08 | 2 |
| 0.08-0.09 | 3 |
| >0.09 | 3 |

Table 6. Part B. Landslide as a percentage for each class for the categorical covariates: soil type, land cover, vegetation type, geology and aspect.

| Covariate Class | Landslide Density (%) |
|---|---|
| *Soil Type* | |
| SOIL1 | 0.11 |
| SOIL5 | 16.19 |
| SOIL6 | 0.11 |
| SOIL9 | 10.18 |
| SOIL11 | 0.20 |
| SOIL13 | 0.53 |
| SOIL14 | 42.39 |
| SOIL15 | 16.58 |
| SOIL16 | 1.25 |
| SOIL17 | 0.05 |
| SOIL18 | 1.16 |
| SOIL19 | 2.61 |
| SOIL20 | 0.98 |
| SOIL21 | 0.74 |
| SOIL26 | 1.25 |
| SOIL27 | 0.02 |
| SOIL29 | 2.29 |
| SOIL30 | 3.15 |

| Covariate Class | Landslide Density (%) |
|---|---|
| *Land Cover* | |
| LAND1 | 0.35 |
| LAND3 | 0.20 |
| LAND4 | 3.66 |
| LAND7 | 0.95 |
| LAND8 | 11.67 |
| LAND9 | 2.38 |
| LAND10 | 59.06 |
| LAND12 | 21.19 |
| LAND13 | 0.26 |
| LAND15 | 0.11 |
| *Vegetation* | |
| VEG1 | 11.84 |
| VEG3 | 30.27 |
| VEG4 | 34.86 |
| VEG5 | 21.73 |

| Covariate Class | Landslide Density (%) |
|---|---|
| *Geology* | |
| GEOL1 | 4.58 |
| GEOL2 | 0.50 |
| GEOL3 | 0.08 |
| GEOL4 | 0.41 |
| GEOL5 | 0.14 |
| GEOL6 | 1.51 |
| GEOL7 | 79.22 |
| GEOL8 | 0.02 |
| GEOL9 | 5.77 |
| GEOL10 | 5.50 |
| GEOL11 | 1.25 |
| GEOL12 | 0.74 |

| Covariate Class | Landslide Density (%) |
|---|---|
| *Aspect* | |
| N | 6 |
| NE | 5 |
| E | 6 |
| SE | 10 |
| S | 25 |
| SW | 22 |
| W | 14 |
| NW | 11 |

## 5.0 Discussion

The most appropriate method of testing the accuracy of a logistic regression model for predicting landslide probability is a point of contention in the literature. Multiple methods are used to assess the accuracy of such models, and each has its own limitations. A limitation of using the same study site to assess the predictive accuracy of a model is that the results can be overly optimistic (Brenning, 2005). The alternative is to use the model to predict landsliding at another site and assess its accuracy for the unobserved site. The limitation with this method is that the differences between sites make inferences from one site's model to another site flawed. Covariates in logistic regression analysis that are significant at one site may be different to those at any other site (Brenning, 2005). Even when the significant covariates remain constant across sites, the estimated parameters (i.e., coefficients) may

differ between sites. Therefore, using data from site B to test a model from site A may be overly pessimistic. Obtaining sufficiently consistent landslide inventory maps from the same trigger type in another location, with adequate peak ground acceleration and peak ground velocity data is typically difficult. Whilst using the same study site to assess the accuracy of the model can make the model appear overly optimistic, this method does not require additional data of similar quality to the study site. Therefore, the method used in this study to assess the accuracy of the susceptibility and hazard models is adequate as long as the results are considered as site-specific.

The inclusion of peak ground acceleration as a covariate in the hazard model was initially expected to have a much greater impact on predicting landslide occurrence than found in the assessment. Whilst the inclusion of shaking covariates has been shown to increase the model's predictive ability at higher thresholds of failure, the statistical insignificance between the ROC AUC values requires further attention. The lack of statistically significant difference between the models when comparing the ROC AUC values could be because the highest level of shaking for the 1994 Northridge event was concentrated in the flat-lying lands in the San Fernando Valley (Figure 48). This could reduce the strength of the correlation between peak ground acceleration and landslide occurrence as there were instances where high levels of shaking did not result directly in landslide occurrence because these locations were on flat ground. Whilst slow-moving landslides can occur on the lower ranges of slope gradients, earthquake-induced landslides typically occur on steeper slopes (Table 23) (Sidle and Ochiai, 2006). The flat lands are more susceptible to liquefaction rather than landsliding as a result of earthquake shaking. The relation between landsliding and peak ground acceleration might exhibit a larger correlation if the study area were to be extended to the surrounding region affected by less ground motion, further from the flat epicentre of the earthquake. In this rougher terrain, the number of landslides triggered should reduce as peak ground acceleration decreases from the epicentre, which has been seen in other earthquake studies (Hovius and Meunier, 2012). However, the landslide inventory

collected from the Northridge 1994 event is limited to the area studied in this paper. It is impossible to say definitively that no landslides were triggered outside of the study area. The influence of the triggering mechanism is also reflected in other preparatory environmental factors used in the susceptibility model known to be associated with earthquake-triggered landslides.

Geology type and soil type were found to be statistically significant in the susceptibility model and are known to be related to peak ground acceleration. The type of geology most associated with landsliding in the Northridge site is Miocene sedimentary type (Geol7) (Table 23). The type of soil most associated with landsliding is Soil14, a mixture of San Benito, Castaic, Calleguas, Balcom and Badland soil types. These soils are silty, clay, loamy types, typically weathered from sedimentary rock. Earthquake shaking can cause greater displacement for weak soil and geologic materials compared to stronger types (Hovius and Meunier, 2012). This is reflected in the Northridge site, where the weaker sedimentary geology and soil type is associated with high percentages of landsliding (Table 23). Whilst the geology and soil type makes those slopes more susceptible to landsliding, the addition of the earthquake shaking amplifies this effect, making those materials more likely to fail in an earthquake event than other classes. The susceptibility model, therefore, predicts higher landslide probabilities in locations which are highly influenced by earthquake shaking by using proxy covariates such as geology and soil type.

Distance to ridge line is rarely used in landslide probability logistic regression analysis. A systematic search of the literature on mapping landslide probability using logistic regression analysis revealed that four of the 91 studies used distance to ridge line as a covariate (Budimir et al., 2015). However, it can be seen that in the hazard model this covariate has a large correlation with landslide occurrence in the Northridge site (Table 21 and Table 23). This is because topographic amplification of ground acceleration occurs during earthquake events, as seismic waves are reflected and diffracted along the surface, causing higher levels of shaking near ridge lines. This pattern of peak ground acceleration is not captured in

shaking distribution maps because the spatial distribution of seismic recording stations is insufficiently dense. The distance to ridgeline factor may, therefore, act as a proxy in the hazard model for some patterns of shaking unrepresented in the peak ground acceleration and peak ground velocity data.

The inclusion of peak ground acceleration and peak ground velocity in logistic regression model prediction of landslide probability is rarely seen in the literature, as stated previously (Hovius and Meunier, 2012; Budimir et al., 2015). This is partly due to the lack of sufficiently detailed (i.e., sufficiently fine spatial resolution) shaking maps for past earthquake events. However, recent advances mean that shaking maps for earthquake events are now much more widely available. The United States Geological Survey (USGS) provides a service in which ShakeMaps are created for specific earthquake events and scenarios available on request. OpenSHA is a tool which can be downloaded freely and used to create peak ground acceleration and peak ground velocity maps for earthquake scenarios globally. The wider availability of shaking maps means that logistic regression analysis can be conducted for past earthquake events when landslide inventory maps are available to create hazard models.

Developing landslide hazard models for specific regions prone to coseismic landsliding is important as they afford the ability to predict landsliding for hypothetical future earthquake events. This is because only the *hazard* model, in contrast with the *susceptibility* model, captures the relation between landsliding and peak ground acceleration and velocity, which are spatially distributed across the area exposed to earthquake shaking. The variation in ground motion across the field provides a sampling of the range of possible values of acceleration and velocity that may be associated with earthquakes of *different* magnitudes. Thus, once the hazard model is fitted, it becomes possible to map the probability of landsliding for (i) different spatially constant levels of peak ground acceleration and velocity, or (ii) specific hypothetical earthquake events where spatial maps of ground motion can be generated for use in the hazard model. This is an exciting prospect as it provides the ability

to explore landslide probability conditional upon “what-if” scenarios, which is likely to be of considerable interest to planners.

The hazard model developed in this paper can be used to model the probability of landslide occurrence in future ‘what-if’ earthquake scenarios for the Northridge site. By simulating earthquake shaking distribution for specific earthquake magnitude scenarios, the peak ground acceleration output maps can be used as the peak ground acceleration covariate input for the landslide hazard model to predict landslide probability as a result of a given earthquake event. Northridge is a location at risk from potential future earthquakes of similar or increased magnitude (Brown and Ghilarducci, 2013). Since 1994, the area has undergone urban expansion, particularly in the Santa Clarita and Simi Valley regions. These developments could be at risk of damage from future earthquakes and landslides. Whilst earthquake awareness in the region is fairly advanced, preparation for and knowledge about potential landslide effects as a result of an earthquake event have not been explored fully (Brown and Ghilarducci, 2013). California’s Multi-Hazard Mitigation Plan calls for increased research to increase our predictive understanding of landslide processes and triggering and for more comprehensive and systematic loss assessment (Brown and Ghilarducci, 2013). The hazard model from this paper could be used in conjunction with OpenSHA or USGS ShakeMap simulations and current data on assets such as population distribution, road networks and building footprints to assess the potential damage that landslides could cause in the local area.

## 6.0 Conclusion

Logistic regression was applied to model the relation between landsliding and environmental covariates using the exceptionally extensive landslide inventory associated with the 1994 Northridge earthquake. Two models were fitted: a landslide susceptibility model based on intrinsic factors only and a landslide hazard model which predicted the probability of landslide occurrence as a result of an earthquake trigger. While the use of logistic regression

in landslide susceptibility mapping is common, its use in hazard modelling is rare. The inclusion of peak ground acceleration and peak ground velocity as covariates in the hazard model increased predictive accuracy compared to that of the susceptibility model. Using a failure threshold of $P \geq 0.9$, the susceptibility model had a successful prediction rate of 75.79% for landslide cells compared to 80.87% for the hazard model. In line with expectations, the hazard model predicted greater landsliding close to the earthquake epicentre, although the difference between the two predicted maps was not as large as anticipated given such precise knowledge of the earthquake trigger. The unique pattern of peak ground acceleration in relation to slope gradient at the Northridge site in 1994 may have reduced the significance of ground motion as a covariate in the hazard model.

Importantly, the hazard model developed here can be utilised in further studies to predict probable locations of landslides as a result of earthquake scenarios in the Northridge study site, identifying areas at risk and potential damage to populations and infrastructure. In future, the relation between landsliding and peak ground acceleration should be investigated for other earthquake and coseismic landslide events where recorded ground motion data are available.

## References

AKI, K. 1993. Local Site Effects on Weak and Strong Ground Motion. Tectonophysics, 218, 93-111.

ALEOTTI, P. & CHOWDHURY, R. 1999. Landslide hazard assessment: summary review and new perspectives. Bull Eng Geol Env, 58, 21-44.

ANDERSON, J. R., HARDY, E. E., ROACH, J. T. & WITMER, R. E. 1976. A Land Use And Land Cover Classification System For Use With Remote Sensor Data. U.S. Geol. Survey Prof. Paper 964 28.

ATKINSON, P. M. & MASSARI, R. 1998. Generalised linear modelling of susceptibility to landsliding in the central Apennines, Italy. Computers & Geosciences, 24, 373-385.

ATKINSON, P. M. & MASSARI, R. 2011. Autologistic modelling of susceptibility to landsliding in the Central Apennines, Italy. Geomorphology, 130, 55-64.

BEDNARIK, M., MAGULOVA, B., MATYS, M. & MARSCHALKO, M. 2010. Landslide susceptibility assessment of the Kralovany-Liptovsky Mikulas railway case study. Physics and Chemistry of the Earth, 35, 162-171.

BRENNING, A. 2005. Spatial prediction models for landslide hazards: review, comparison and evaluation. Natural Hazards and Earth System Sciences, 5, 853-862.

BROWN, E. G. J. & GHILARDUCCI, M. S. 2013. 2013 State of California Multi-Hazard Mitigation Plan. In: SERVICES, C. G. S. O. O. E. (ed.). Mather, California.

BUDIMIR, M. E. A., ATKINSON, P. M. & LEWIS, H. G. 2015. A systematic review of landslide probability mapping using logistic regression. Landslides.

CARRARA, A., CARDINALI, M., DETTI, R., GUZZETTI, F., PASQUI, V. & REICHENBACH, P. 1991. Gis Techniques and Statistical-Models in Evaluating Landslide Hazard. Earth Surface Processes and Landforms, 16, 427-445.

CARRO, M., DE AMICIS, M., LUZI, L. & MARZORATI, S. 2003. The application of predictive modeling techniques to landslides induced by earthquakes: the case study of the 26 September 1997 Umbria-Marche earthquake (Italy). Engineering Geology, 69, 139-159.

CHANG, K. T., CHIANG, S. H. & HSU, M. L. 2007. Modeling typhoon- and earthquake-induced landslides in a mountainous watershed using logistic regression. Geomorphology, 89, 335-347.

DAI, F. C. & LEE, C. F. 2002. Landslide characteristics and, slope instability modeling using GIS, Lantau Island, Hong Kong. Geomorphology, 42, 213-228.

DAI, F. C. & LEE, C. F. 2003. A spatiotemporal probabilistic modelling of storm-induced shallow landsliding using aerial photographs and logistic regression. Earth Surface Processes and Landforms, 28, 527-545.

DAI, F. C., XU, C., YAO, X., XU, L., TU, X. B. & GONG, Q. M. 2011. Spatial distribution of landslides triggered by the 2008 Ms 8.0 Wenchuan earthquake, China. Journal of Asian Earth Sciences, 40, 883-895.

ERCANOGLU, M., GOKCEOGLU, C. & VAN ASCH, T. W. J. 2004. Landslide susceptibility zoning north of Yenice (NW Turkey) by multivariate statistical techniques. Natural Hazards, 32, 1-23.

FIELD, E. H., JOHNSON, P. A., BERESNEV, I. A. & ZENG, Y. H. 1997. Nonlinear ground-motion amplification by sediments during the 1994 Northridge earthquake. Nature, 390, 599-602.

GELI, L., BARD, P. Y. & JULLIEN, B. 1988. The Effect of Topography on Earthquake Ground Motion - a Review and New Results. Bulletin of the Seismological Society of America, 78, 42-63.

GODT, J., SENER, B., VERDIN, K., WALD, D., EARLE, P., HARP, E. & JIBSON, R. 2008. Rapid assessment of earthquake-induced landsliding. Proceedings of the First World Landslide Forum, United Nations University, Tokyo, 4.

GORSEVSKI, P. V., GESSLER, P. E., FOLTZ, R. B. & ELLIOT, W. J. 2006. Spatial Prediction of Landslide Hazard using Logistic Regression and ROC Analysis. Transactions in GIS, 10, 395-415.

HANLEY, J. A. & MCNEIL, B. J. 1983. A Method of Comparing the Areas under Receiver Operating Characteristic Curves Derived from the Same Cases. Radiology, 148, 839-843.

HARP, E. L. & JIBSON, R. W. 1996. Landslides triggered by the 1994 Northridge, California, earthquake. Bulletin of the Seismological Society of America, 86, S319-S332.

HE, Y. P. & BEIGHLEY, R. E. 2008. GIS-based regional landslide susceptibility mapping: a case study in southern California. Earth Surface Processes and Landforms, 33, 380-393.

HERVAS, J. & BOBROWSKY, P. 2009. Mapping: Inventories, Susceptibility, Hazard and Risk. In: SASSA, K. & CANUTI, P. (eds.) Landslides: Disaster Risk Reduction. Berlin: Springer.

HONG, Y., ADLER, R. & HUFFMAN, G. 2007. Use of satellite remote sensing data in the mapping of global landslide susceptibility. Natural Hazards, 43, 245-256.

HOVIUS, N. & MEUNIER, P. 2012. Earthquake ground motion and the pattern of seismically induced landslides. In: CLEAGUE, J. J. & STEAD, D. (eds.) Landslides: Types, Mechanisms and Modeling. 2nd ed.: Cambridge University Press.

JIBSON, R. W., HARP, E. L. & MICHAEL, J. A. 2000. A method for producing digital probabilistic seismic landslide hazard maps. Engineering Geology, 58, 271-289.

KEEFER, D. & WILSON, R. 2011. Effects from Earthquake-Triggered Landslides [Online]. USGS. Available: http://pubs.usgs.gov/of/1995/ofr-95-0213/EFFECTS.HTML [Accessed 10/07/2013].

LEE, S., RYU, J. H., WON, J. S. & PARK, H. J. 2004. Determination and application of the weights for landslide susceptibility mapping using an artificial neural network. Engineering Geology, 71, 289-302.

LIN, G. W., CHEN, H., HOVIUS, N., HORNG, M. J., DADSON, S., MEUNIER, P. & LINES, M. 2008. Effects of earthquake and cyclone sequencing on landsliding and fluvial sediment transfer in a mountain catchment. Earth Surface Processes and Landforms, 33, 1354-1373.

MARANO, K. D., WALD, D. J. & ALLEN, T. I. 2010. Global earthquake casualties due to secondary effects: a quantitative analysis for improving rapid loss analyses. Natural Hazards, 52, 319-328.

MARUI, H. & NADIM, F. 2009. Landslides and multi-hazards. In: SASSA, K. & CANUTI, P. (eds.) Landslides: Disaster risk reduction. Berlin: Springer.

MARZORATI, S., LUZI, L. & DE AMICIS, M. 2002. Rock falls induced by earthquakes: a statistical approach. Soil Dynamics and Earthquake Engineering, 22, 565-577.

MEUNIER, P., HOVIUS, N. & HAINES, A. J. 2007. Regional patterns of earthquake-triggered landslides and their relation to ground motion. Geophysical Research Letters, 34.

MEUNIER, P., HOVIUS, N. & HAINES, J. A. 2008. Topographic site effects and the location of earthquake induced landslides. Earth and Planetary Science Letters, 275, 221-232.

NADIM, F., KJEKSTAD, O., PEDUZZI, P., HEROLD, C. & JAEDICKE, C. 2006. Global landslide and avalanche hotspots. Landslides, 3, 159-173.

OHLMACHER, G. C. & DAVIS, J. C. 2003. Using multiple logistic regression and GIS technology to predict landslide hazard in northeast Kansas, USA. Engineering Geology, 69, 331-343.

PARISE, M. & JIBSON, R. W. 2000. A seismic landslide susceptibility rating of geologic units based on analysis of characteristics of landslides triggered by the 17 January, 1994 Northridge, California earthquake. Engineering Geology, 58, 251-270.

PRADHAN, B., LEE, B. & BUCHROITHNER, M. F. 2010. Remote Sensing and GIS-based Landslide Susceptibility Analysis and its Cross-validation in Three Test Areas Using a Frequency Ratio Model. Photogrammetrie Fernerkundung Geoinformation, 17-32.

REED, J. C., WHEELER, J. O. & TUCHOLKE, B. E. 2005. Geologic Map of North America, South Sheet, Geological Society of America Continent-Scale Map 001,, 1:5000000.

SANTACANA, N., BAEZA, B., COROMINAS, J., DE PAZ, A. & MARTURIA, J. 2003. A GIS-based multivariate statistical analysis for shallow landslide susceptibility mapping in La Pobla de Lillet area (Eastern Pyrenees, Spain). Natural Hazards, 30, 281-295.

SIDLE, R. C. & OCHIAI, H. 2006. Landslides: Processes, Prediction, and Landuse, Water Resources Monograph.

TIBALDI, A., FERRARI, L. & PASQUARE, G. 1995. Landslides Triggered by Earthquakes and Their Relations with Faults and Mountain Slope Geometry - an Example from Ecuador. Geomorphology, 11, 215-226.

USGS. 2012. Historic Earthquakes: Northridge California, 1994 [Online]. Available: http://earthquake.usgs.gov/earthquakes/states/events/1994_01_17.php [Accessed 03/09/2013].

VAN DEN EECKHAUT, M., MARRE, A. & POESEN, J. 2010. Comparison of two landslide susceptibility assessments in the Champagne-Ardenne region (France). Geomorphology, 115, 141-155.

VAN WESTEN, C. J., RENGERS, N. & SOETERS, R. 2003. Use of geomorphological information in indirect landslide susceptibility assessment. Natural Hazards, 30, 399-419.

WANG, L., SAWADA, K. & MORIGUCHI, S. 2011. Landslide Susceptibility Mapping by Using Logistic Regression Model with Neighborhood Analysis: A Case Study in Mizunami City. International Journal of Geomate, 1, 99-104.

YESILNACAR, E. & TOPAL, T. 2005. Landslide susceptibility mapping: A comparison of logistic regression and neural networks methods in a medium scale study, Hendek region (Turkey). Engineering Geology, 79, 251-266.

YIN, J. H., CHEN, J., XU, X. W., WANG, X. L. & ZHENG, Y. G. 2010. The characteristics of the landslides triggered by the Wenchuan M-s 8.0 earthquake from Anxian to Beichuan. Journal of Asian Earth Sciences, 37, 452-459.

# Appendix

Table A1. Geology type and characteristics and associated dummy variable code used in logistic regression for Northridge study site.

| Dummy variable | Unit Abbreviation | Rock Type | Lithology | Minimum Age | Maximum Age |
|---|---|---|---|---|---|
| Geol1 | MZg | Plutonic | undivided granitic rocks | Mesozoic | Mesozoic |
| Geol2 | eT | Sedimentary | Null | Eocene | Eocene |
| Geol3 | pCAx | Metamorphic and undivided crystalline | undivided crystalline rocks (seafloor units may include a variety of metamorphosed | Precambrian | Precambrian |

| | | | | | |
|---|---|---|---|---|---|
| | | | rock) | | |
| Geol4 | nT | Sedimentary | Null | Neogene | Neogene |
| Geol5 | KTsv | Volcanic | interlayered sedimentary and volcanic rocks | Tertiary | Cretaceous |
| Geol6 | Q | Sedimentary | Null | Quaternary | Quaternary |
| Geol7 | mT | Sedimentary | Null | Miocene | Miocene |
| Geol8 | TRg | Plutonic | undivided granitic rocks | Triassic | Triassic |
| Geol9 | Kg | Plutonic | undivided granitic rocks | Cretaceous | Cretaceous |
| Geol10 | JK | Sedimentary | Null | Cretaceous | Jurassic |
| Geol11 | Tv | Volcanic | undivided volcanic rocks | Tertiary | Tertiary |
| Geol12 | JKsv | Volcanic | interlayered sedimentary and volcanic rocks | Cretaceous | Jurassic |
| Geol13 | Q | Sedimentary | Null | Quaternary | Quaternary |

Table A2. Land cover type and associated dummy variable code used in logistic regression for Northridge study site.

| **Dummy Variable Code** | **Land Cover Type** | **Description** |
|---|---|---|
| Land1 | Low intensity residential | Areas with a mixture of constructed materials and vegetation. Constructed materials account for 30% to 80% of the cover. Vegetation may account for 20% to 70 % of the cover. These areas most commonly include single-family housing units. Population densities will be lower than in high intensity residential areas. |
| Land2 | High intensity residential | Areas highly developed where people reside in high numbers. Examples include apartment complexes and row houses. Vegetation accounts for less than 20% of the cover. Constructed materials account for 80% to100% of the cover. |
| Land3 | Commercial/industrial/transportation | Areas of infrastructure (e.g. roads, railroads, etc.) and all highly developed areas not classified as High Intensity Residential |
| Land4 | Bare rock/sand/clay | Perennially barren areas of bedrock, desert pavement, scarps, talus, slides, volcanic material, glacial debris, beaches, and other accumulations of earthen material. |
| Land5 | Quarries/strip mines/gravel pits | Areas of extractive mining activities with significant surface expression. |
| Land6 | Transitional barren | Areas of sparse vegetative cover (less than 25% of cover) that are dynamically changing from one land cover to another, often because of land use activities. Examples include forest clear cuts, a transition phase between forest and agricultural land, the temporary clearing of vegetation, and changes due to natural causes (e.g. fire, flood, etc.). |
| Land7 | Deciduous forest | Areas dominated by trees where 75% or more of the tree species shed foliage simultaneously in |

| | | |
|---|---|---|
| | | response to seasonal change. |
| Land8 | Evergreen forest | Areas dominated by trees where 75% or more of the tree species maintain their leaves all year. Canopy is never without green foliage. |
| Land9 | Mixed forest | Areas dominated by trees where neither deciduous nor evergreen species represent more than 75% of the cover present. |
| Land10 | Shrubland | Areas dominated by shrubs; shrub canopy accounts for 25 to 100% of the cover. Shrub cover is generally greater than 25% when tree cover is less than 25%. Shrub cover may be less than 25% in cases when the cover of other life forms (e.g. herbaceous or tree) is less than 25% and shrubs cover exceeds the cover of the other life forms. |
| Land11 | Orchards/vineyards/other | Orchards, vineyards, and other areas planted or maintained for the production of fruits, nuts, berries, or ornamentals. |
| Land12 | Grassland/herbaceous | Areas dominated by upland grasses and forbs. In rare cases, herbaceous cover is less than 25%, but exceeds the combined cover of the woody species present. These areas are not subject to intensive management, but they are often utilized for grazing. |
| Land13 | Pasture/hay | Areas of grasses, legumes, or grass-legume mixtures planted for livestock grazing or the production of seed or hay crops. |
| Land14 | Row crops | Areas used for the production of crops, such as corn, soybeans, vegetables, tobacco, and cotton. |
| Land15 | Small grains | Areas used for the production of graminoid crops such as wheat, barley, oats, and rice. |
| Land16 | Fallow | Areas used for the production of crops that do not exhibit visible vegetation as a result of being tilled in a management practice that incorporates prescribed alternation between cropping and tillage. |
| Land17 | Urban/recreational grasses | Vegetation (primarily grasses) planted in developed settings for recreation, erosion control, or aesthetic purposes. Examples include parks, lawns, golf courses, airport grasses, and industrial site grasses. |
| Land18 | Woody wetlands | Areas where forest or shrubland vegetation accounts for 25% to 100 % of the cover and the soil or substrate is periodically saturated with or covered with water. |
| Land19 | Emergent herbaceous wetlands | Areas where perennial herbaceous vegetation accounts for 75% to 100% of the cover and the soil or substrate is periodically saturated with or covered with water. |

Table A3**.** Soil type and associated dummy variable code used in logistic regression for Northridge study site.

| **Dummy Variable Code** | **Soil Type** |
|---|---|
| Soil 1 | Los Gatos-Gamboa (s936) |
| Soil 2 | Oak Glen-Gullied land-Gorman-Gaviota-Cushenbury (s1034) |
| Soil 3 | Marpa-Hilt-Arrastre (s935) |

| | |
|---|---|
| Soil 4 | Gaviota-Cieneba-Capistrano-Caperton (s1055) |
| Soil 5 | Sobrante-Exchequer-Cieneba (s1054) |
| Soil 6 | Water (s8369) |
| Soil 7 | Modjeska family-Coarsegold-Aramburu variant (s934) |
| Soil 8 | Wilshire-Soboba-Oak Glen-Avawatz (s1047) |
| Soil 9 | Millsholm-Millerton-Lodo (s933) |
| Soil 10 | Xerofluvents-Oak Glen-Dotta (s937) |
| Soil 11 | Stonyford-Rock outcrop-Chilao (s1056) |
| Soil 12 | Sobrante-Lodo (s1057) |
| Soil 13 | Vista-Cieneba-Andregg (s899) |
| Soil 14 | San Benito-Castaic-Calleguas-Balcom-Badland (s912) |
| Soil 15 | Rock outcrop-Lithic Xerorthents-Calleguas-Badland (s914) |
| Soil 16 | Sespe-Millsholm-Malibu-Lodo-Hambright (s913) |
| Soil 17 | Soper-Chesterton (s911) |
| Soil 18 | Rock outcrop-Lithic Xerorthents-Hambright-Gilroy (s915) |
| Soil 19 | San Andreas-Arujo-Arnold (s902) |
| Soil 20 | Zamora-Urban land-Ramona (s1033) |
| Soil 21 | Xerofluvents-Salinas-Pico-Mocho-Metz-Anacapa (s909) |
| Soil 22 | Oceano-Dune land-Baywood (s904) |
| Soil 23 | Pacheco-Hueneme-Camarillo (s910) |
| Soil 24 | Wasco-Rosamond-Cajon (s1024) |
| Soil 25 | Ramona-Hanford-Greenfield (s1009) |
| Soil 26 | Pismo-Etsel family-Cieneba-Caperton (s1059) |
| Soil 27 | Urban land-Sorrento-Hanford (s1026) |
| Soil 28 | Vista-Fallbrook-Cieneba (s1011) |
| Soil 29 | Urban land-Lithic Xerorthents-Hambright-Castaic (s1042) |
| Soil 30 | Urban land-Rock outcrop-Millsholm (s1035) |
| Soil 31 | Urban land-Delhi (s1028) |

Table A4**.** Vegetation type and associated dummy variable code used in logistic regression for Northridge study site.

| **Dummy Variable Code** | **Level II Category** | **Description** |
|---|---|---|
| Veg1 | 31 | Herbaceous rangeland |
| Veg2 | 32 | Shrub and bush rangeland |
| Veg3 | 33 | Mixed rangeland |
| Veg4 | 42 | Evergreen forest land |
| Veg5 | 99 | other |

Table A5**.** Categorical environmental covariates coefficients and *p*-values for both susceptibility and hazard logistic regression models.

| **Categorical environmental covariates** | **Class** | **Susceptibility model** | | **Hazard model** | |
|---|---|---|---|---|---|
| | | **Coefficients** | ***P*-value** | **Coefficients** | ***P*-value** |
| Aspect | East | 0.616500 | 0.021888 | 0.924300 | 0.004138 |
| | Southeast | 0.679700 | 0.001482 | 1.180000 | 0.000012 |
| | South | 0.694300 | 0.000146 | 1.172000 | 0.000001 |
| | Southwest | 0.971100 | 0.000001 | 1.632000 | 0.000000 |
| | West | 1.419000 | 0.000000 | 2.150000 | 0.000000 |
| | Northwest | - | - | 0.569700 | 0.042744 |
| Geology | geol1 | -0.927500 | 0.006771 | -4.310000 | 0.000017 |
| | geol2 | -4.656000 | <2.00E-16 | -7.017000 | 0.000000 |
| | geol3 | -4.891000 | 0.000000 | -6.668000 | 0.000000 |
| | geol4 | -3.935000 | 0.000000 | -4.844000 | 0.000014 |
| | geol5 | - | - | -1.929000 | 0.132000 |
| | geol6 | -2.037000 | 0.000000 | -4.772000 | 0.000002 |
| | geol7 | - | - | -3.937000 | 0.000042 |
| | geol8 | -6.192000 | 0.000000 | -6.984000 | 0.000002 |
| | geol9 | -1.280000 | 0.000056 | -3.401000 | 0.000755 |
| | geol10 | -2.704000 | 0.000000 | -6.775000 | 0.000000 |
| | geol11 | -0.845300 | 0.057239 | -4.595000 | 0.000020 |
| | geol12 | -0.926000 | 0.048420 | -5.343000 | 0.000000 |
| Vegetation | veg1 | 4.233000 | <2.00E-16 | 3.382000 | 0.000000 |
| | veg3 | 2.918000 | <2.00E-16 | 3.178000 | 0.000000 |
| | veg4 | 2.154000 | 0.000000 | 2.531000 | 0.000000 |
| | veg5 | 2.083000 | 0.000000 | 2.031000 | 0.000062 |
| Land cover | land1 | 2.238000 | 0.025162 | 1.857000 | 0.121254 |
| | land3 | 3.327000 | 0.002015 | 3.347000 | 0.013177 |
| | land4 | 4.719000 | 0.000000 | 4.565000 | 0.000045 |
| | land7 | 4.636000 | 0.000009 | 4.583000 | 0.000193 |
| | land8 | 5.010000 | 0.000000 | 4.815000 | 0.000009 |
| | land9 | 5.058000 | 0.000000 | 4.830000 | 0.000025 |
| | land10 | 4.847000 | 0.000000 | 4.775000 | 0.000006 |
| | land12 | 4.580000 | 0.000000 | 4.579000 | 0.000018 |
| | land13 | 3.013000 | 0.004864 | 2.129000 | 0.114149 |
| | land15 | 2.558000 | 0.039912 | 2.385000 | 0.096102 |
| Soil Type | soil1 | -4.780000 | 0.000031 | -4.397000 | 0.000135 |
| | soil4 | -18.540000 | 0.976828 | -18.320000 | 0.977315 |
| | soil5 | - | - | -2.580000 | <2.00E-16 |
| | soil6 | - | - | -2.133000 | 0.071510 |
| | soil7 | -16.070000 | 0.992132 | -16.660000 | 0.992214 |
| | soil9 | 0.720500 | 0.027386 | - | - |
| | soil11 | - | - | -2.182000 | 0.006398 |
| | soil12 | -20.360000 | 0.981688 | -22.990000 | 0.976297 |
| | soil13 | - | - | - | - |

| | | | | | |
|---|---|---|---|---|---|
| | soil14 | 0.390500 | 0.072369 | - | - |
| | soil15 | 1.699000 | 0.000027 | -1.091000 | 0.010030 |
| | soil16 | -3.652000 | <2.00E-16 | -3.079000 | 0.000000 |
| | soil17 | -19.350000 | 0.983197 | -18.300000 | 0.984482 |
| | soil18 | -3.786000 | <2.00E-16 | -3.197000 | 0.000000 |
| | soil19 | 17.390000 | 0.988562 | 15.260000 | 0.989764 |
| | soil20 | - | - | -5.142000 | 0.000000 |
| | soil21 | -2.498000 | 0.000000 | -3.997000 | <2.00E-16 |
| | soil23 | -19.620000 | 0.990915 | -19.910000 | 0.990334 |
| | soil25 | -18.180000 | 0.989462 | -16.590000 | 0.990102 |
| | soil26 | -2.494000 | <2.00E-16 | -4.303000 | <2.00E-16 |
| | soil27 | -1.692000 | 0.106901 | -7.459000 | 0.000002 |
| | soil29 | - | - | -0.878000 | 0.076965 |
| | soil30 | -2.056000 | 0.000000 | -2.070000 | 0.000002 |

# 6. INTRODUCTION TO PAPER 4

## Seismically-Induced Landslide Hazard and Exposure Modelling in Southern California Based on the 1994 Northridge, California Earthquake Event

*A version of this paper has been published in the Landslides Journal.*

*The full citation is:*

Budimir, M.E.A., Atkinson, P.M., and Lewis, H.G., (2015), 'Seismically-Induced Landslide Hazard and Exposure Modelling in Southern California Based on the 1994 Northridge, California Earthquake Event', *Landslides Journal*.

This paper (Paper 4) utilised the inventory of covariates from Paper 2, and the logistic regression hazard model method from Paper 3 to predict landslide hazard probability as a result of seven earthquake scenarios at the Northridge, California study site (Figure 51). The potential exposure of assets such as population, housing and infrastructure to landsliding and high levels of shaking are estimated for each scenario of different magnitudes (Figure 51). The increase in exposure as a result of developments in the region since the 1994 earthquake is also examined.

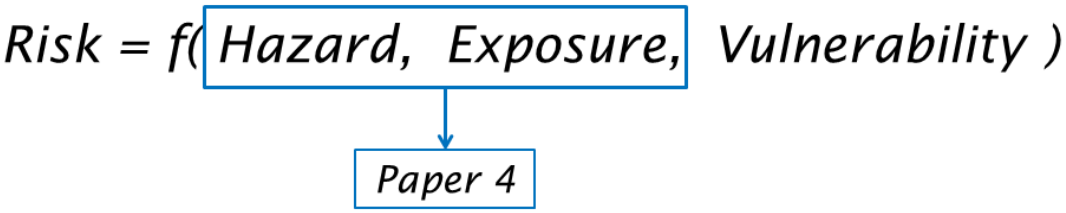


Figure 51. Diagram showing the focus of Paper 4 related to the risk equation.

*Hazard Model*

A simplified version of the logistic regression landslide hazard model used in Paper 3 was used to estimate landslide probability for seven earthquake scenarios of different magnitude. As the aim of this paper was to determine the exposure of assets to landslides and shaking, some of the covariates from the original model were removed from the logistic regression model used in Paper 3 if they were considered an asset. The covariates removed from the model were distance to roads, road density, and land cover (urban land cover type was used as an asset in this paper). The simplified landslide hazard model was then used to calculate landslide probability for the seven scenarios. The accuracy of the simplified hazard model used in this paper (Paper 4) is assessed here in comparison with the original landslide hazard model used in Paper 3 and the recorded landslide occurrence from the 1994 Northridge event.

The accuracies of the logistic regression models were evaluated by calculating the receiver operating characteristic (ROC). The ROC for the two landslide hazard models were calculated for: (i) the original landslide hazard model used in Paper 3 (AUC = 0.9825), and (ii) the simplified landslide hazard model used in Paper 4 (AUC = 0.983). The difference in AUC values between the original landslide hazard model and the simplified landslide hazard model, using the original peak ground acceleration variable, is not statistically significant (Hanley and McNeil, 1983). The percentage of correctly and incorrectly predicted landslide and non-landslide cells based on landslide failure at $P \geq 0.9$ for the original landslide hazard and the simplified landslide hazard models are also approximately the same (Table 24).

Table 24. Percentage of correctly and incorrectly predicted landslide (LS) and non-landslide (NoLS) cells the threshold failure probability value of 0.9 for the original landslide hazard model and the simplified hazard model.

| | | **Present** | **Absent** |
|---|---|---|---|
| **Original Landslide Hazard Model** | **LS** | 81.07 % | 1.43 % |
| | **NoLS** | 18.83 % | 98.57 % |
| **Simplified Landslide Hazard Model** | **LS** | 79.88 % | 2.14 % |
| | **NoLS** | 20.02 % | 97.85 % |

*Threshold Choice*

The exposure of assets to high levels of shaking and high probabilities of landsliding for each scenario was estimated above a threshold in this paper. The threshold for seismic shaking was ≥0.18 g. This threshold was determined to be the most significant level of shaking associated with fatalities for estimating the population affected in earthquake and landslide fatality modelling (Paper 1: Budimir et al., 2014). The threshold for high landslide probability was ≥0.9. This threshold was chosen as the level to determine landslide failure based on the high (and almost equal) accuracies of predicting landslide occurrence of 80.87% and non-landslide occurrence of 79.78% at this threshold (in Paper 3).

**Research Questions**

*Are assets in the Northridge area more exposed to potential earthquake-induced landslides now, than in 1994?*

*What locations are exposed to earthquake-induced landslides in larger magnitude scenarios in the Northridge region?*

# SEISMICALLY-INDUCED LANDSLIDE HAZARD AND EXPOSURE MODELLING IN SOUTHERN CALIFORNIA BASED ON THE 1994 NORTHRIDGE, CALIFORNIA EARTHQUAKE EVENT

M.E.A. Budimir[1*], P.M. Atkinson[1] and H.G. Lewis[2]

[1] *Geography and Environment, Faculty of Social and Human Sciences*

[2] *Engineering Sciences, Faculty of Engineering and the Environment*

*University of Southampton, Highfield, Southampton, SO17 1BJ, UK*

## Abstract

Quantitative modelling of landslide hazard, as opposed to landslide susceptibility, as a function of the earthquake trigger is vital in understanding and assessing future risk of landsliding. Logistic regression analysis is a method commonly used to assess susceptibility to landsliding; however, predicting landslide hazard as a result of an earthquake trigger is rarely undertaken. This paper utilises a very detailed landslide inventory map and a comprehensive dataset on peak ground acceleration for the 1994 $M_w$6.7 Northridge earthquake event to fit a landslide hazard logistic regression model. The model demonstrates a high success rate for predicting landslides as a result of earthquake shaking. Seven earthquake magnitude scenarios were simulated using the OpenSHA application to predict peak ground acceleration, a covariate of landsliding, for each event. The exposure of assets such as population, housing and roads to high levels of shaking and high probabilities of landsliding were estimated for each scenario. There has been urban development in the Northridge region since 1994, leading to an increase in prospective exposure of assets to the earthquake and landslide hazards in the event of a potential future earthquake. As the

earthquake scenario magnitude increases, the impact from earthquake shaking becomes saturated, but potential losses from landslides increase at a rapid rate. The modelling approach, as well as the specific model, developed in this paper can be used to predict landslide probabilities as a result of an earthquake event for any scenario where the peak ground acceleration variable is available.

## 1.0 Introduction

The United States Geological Survey's (USGS) National Earthquake Information Center (NEIC) reports more than 30,000 earthquakes per year, of which an average of 25 cause significant damage, injuries or fatalities (Godt et al., 2008). Seismically-induced landslides are one of the most damaging secondary hazards associated with earthquakes (Jibson et al., 2000). Approximately 5% of all earthquake-related fatalities are a result of seismically-induced landslides, and in some cases landsliding is the main cause of non-shaking deaths (Nowicki et al., 2014; Marano et al., 2010). There are also instances where earthquake-triggered landslides cause the majority of fatalities; 585 fatalities of the total 844 fatalities in the 13$^{th}$ January 2001 El Salvador earthquake were due to landslides (Bommer et al., 2002).

Many statistical methods are available to map the landslide hazard quantitatively based on explanatory variables or covariates. These include classical regression-type approaches such as logistic regression (Atkinson and Massari, 1998) and a range of machine-learning approaches (Pardeshi et al., 2013; Santacana et al., 2003; Yesilnacar and Topal, 2005). Logistic regression is used commonly to determine the significant factors affecting landslide hazard, and is the method recommended by Brenning (2005). Logistic regression is a useful tool for analysing landslide occurrence, where the dependent variable is binary (i.e., presence or absence) and the covariates are categorical, numerical, or both (Boslaugh, 2012; Chang et al., 2007; Atkinson et al., 1998). The logistic regression model has the form

$$logit(y) = \beta_0 + \beta_1 x_1 + \beta_2 x_2 + \cdots + \beta_i x_i + e \qquad \text{Equation 17}$$

where $y$ is the dependent variable, $x_i$ is the $i$-th covariate, $\beta_0$ is a constant, $\beta_i$ is the $i$-th regression coefficient, and $e$ is the error. The probability ($p$) of the occurrence of $y$ is given by:

$$p = \frac{exp^{(\beta_0+\beta_1 x_1+\beta_2 x_2+\cdots+\beta_i x_i)}}{1+exp^{(\beta_0+\beta_1 x_1+\beta_2 x_2+\cdots+\beta_i x_i)}} \quad \text{Equation 18}$$

A common difficulty with performing logistic regression analysis is acquiring sufficiently detailed landslide inventory maps, particularly for events which have not resulted in casualties, not caused significant damage or occur in remote, unpopulated terrain (Hervas and Bobrowsky, 2009). Moreover, the majority of logistic regression studies model underlying, long-term *susceptibility*, not accounting for the triggering factor (Budimir et al., 2015). For example, ground motion is rarely considered as a covariate in logistic regression analysis to predict landsliding (Nowicki et al., 2014; Carro et al., 2003; Marzorati et al., 2002).

When modelling landslide *hazard*, the preparatory or intrinsic factors (such as geology, slope, vegetation) and the causative or extrinsic factors (precipitation or shaking) must be considered (Dai and Lee, 2003; Hervas and Bobrowsky, 2009). Hovius and Meunier (2012) proposed that the relationship between landslides and peak ground acceleration is key to understanding the global attributes of regional and local patterns of seismically-induced landsliding. The unique shaking distribution from an earthquake event is required because the treatment of the earthquake as a simple line or point source of energy can lead to erroneous conclusions (Geli et al., 1988; Hovius and Meunier, 2012). Ground motion varies spatially not only because of distance from the epicentre, but also due to soil and bedrock characteristics and topographic site effects (Meunier et al., 2008; Sidle and Ochiai, 2006; Hovius and Meunier, 2012; Brown and Ghilarducci, 2013; Field et al., 1997; Tibaldi et al., 1995). Thus, a major limitation to coseismic landslide hazard modelling is the requirement for ground motion data, which are typically difficult to acquire (Pradhan et al., 2010; Atkinson and Massari, 2011; Hovius and Meunier, 2012).

Since 2007, the USGS has produced near-real-time ShakeMaps of ground motion through the Prompt Assessment of Global Earthquakes for Response (PAGER) programme following significant global earthquakes. These peak ground acceleration maps can be used in landslide hazard modelling to predict landslide hazard as a result of an earthquake trigger. When peak ground acceleration data are unavailable for a particular earthquake event, it is possible to simulate the data using attenuation models. The Open Source Seismic Hazard Analysis (OpenSHA) application is an open source application developed by the Southern California Earthquake Center (SCEC) in collaboration with the USGS, the California Geological Survey (CGS), and other partners, which can simulate any earthquake scenario. The application uses complex earthquake rupture forecasts and ground-motion models to produce peak ground acceleration maps, given the hypocentre location and earthquake magnitude (Field et al., 2003; Field et al., 2005).

This study investigates the landslide hazard at Northridge, California, utilizing an unprecedented landslide inventory taken in the immediate aftermath of the 1994 $M_w$6.7 earthquake (Harp and Jibson, 1996; Harp and Jibson, 1995). In addition, approximately 200 strong-motion recordings of the main shock were taken, producing one of the most comprehensive datasets at the time of the event, providing the peak ground acceleration data for this study (Parise and Jibson, 2000). These two key datasets were used in logistic regression modelling to create a model to predict landslide hazard given a set of environmental covariates (intrinsic factors) and the earthquake trigger (extrinsic factor). Seven earthquake events of different magnitudes were simulated using the OpenSHA program and the associated peak ground acceleration patterns were predicted. Using the fitted logistic model, the probability of landsliding in the region conditional upon these events was estimated. Finally, the utility of the modelling approach as a decision-support tool for hazard planning and emergency management is discussed.

## 2.0 Background

On 17th January 1994, a $M_w$ 6.7 earthquake struck Northridge, California. The causative fault of the Northridge earthquake is part of a broad system of thrust faults at the Big Bend of the San Andreas fault, resulting from the left step in the Pacific-North American plate boundary (Jones et al., 1994). The fault was not mapped before the event and did not extend to the surface (Jones et al., 1994). The greater Los Angeles region has a fairly active tectonic history; since 1920, 18 moderate ($M_w$4.8-6.7) earthquakes have occurred in the area (Jones et al., 1994). The 1971 San Fernando $M_w$6.7 earthquake epicentre was located northeast of the Northridge earthquake (Jones et al., 1994). The hypocentre was 18 km beneath the city of Northridge in the San Fernando Valley on a blind thrust fault striking N58°W and dipping 42°southward (Harp and Jibson, 1996). On average, the peak ground acceleration recorded for the event was larger in magnitude compared to other recorded reverse-faulting events (Jones et al., 1994).

The Northridge earthquake caused the greatest damage since the 1906 San Francisco earthquake (Wald et al., 1996). More than 1,500 people were seriously injured and 57 fatalities were recorded (Aurelius, 1994). Approximately 12,500 structures were moderately-to-severely damaged, leaving thousands of people temporarily homeless (Aurelius, 1994). The earthquake triggered more than 11,000 landslides which were recorded as digital landslide maps immediately following the earthquake (Figure 45) (Harp and Jibson, 1996; Harp and Jibson, 1995).

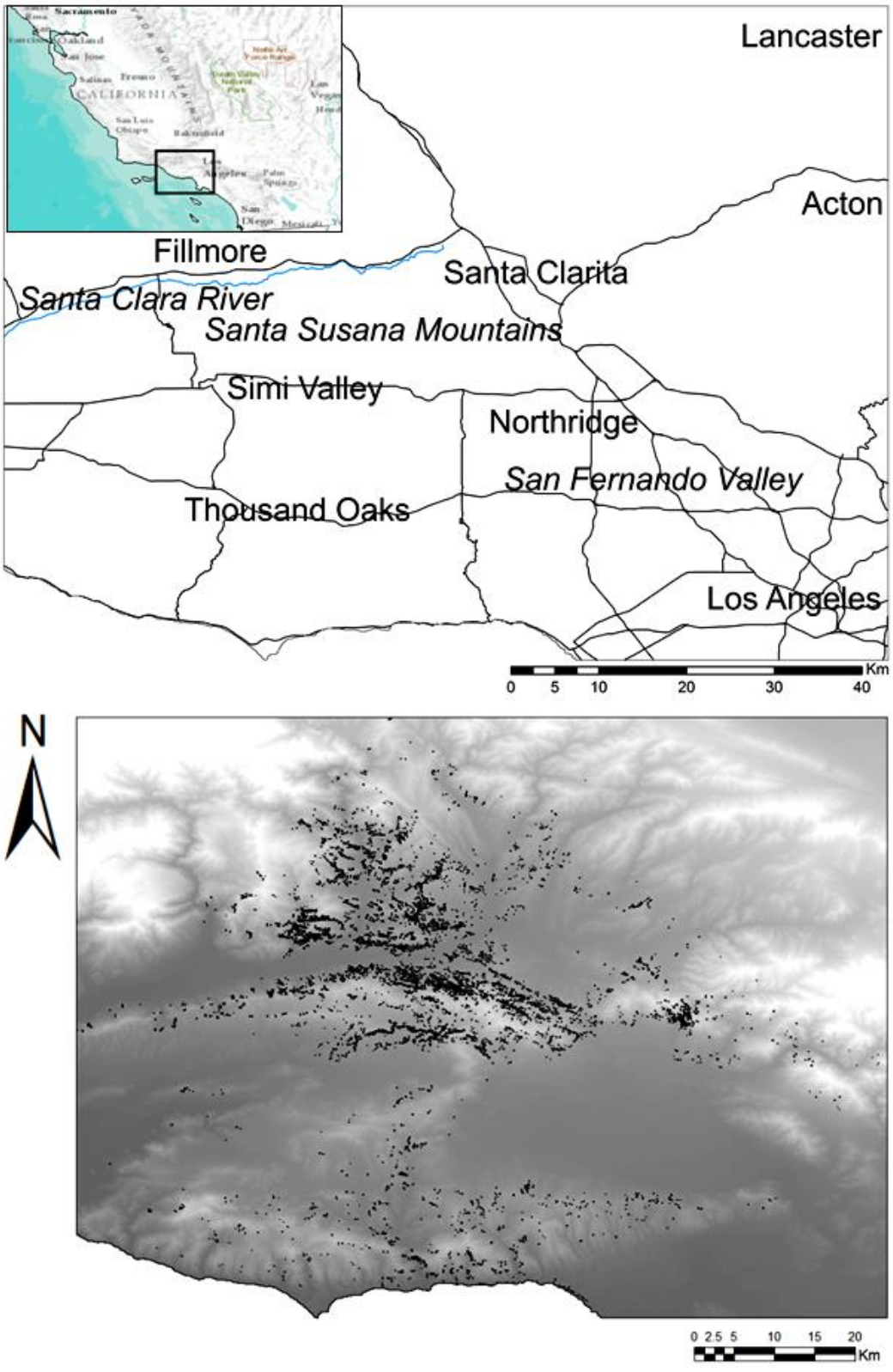


Figure 52. Site location and landslide inventory maps of the Northridge 1994 earthquake event (Harp and Jibson, 1996; Harp and Jibson, 1995).

The majority of the landslides were concentrated in a roughly concentric 1000 $km^2$ area north and northwest of the epicentre, including the Santa Susana Mountains and the mountains north of the Santa Clara River valley (Harp and Jibson, 1996). The maximum distance of the observed landslides to the epicentre was approximately 70 km (Harp and Jibson, 1996). The majority of landslides were shallow, highly disrupted slides and falls, composed of weakly cemented Tertiary and Pleistocene clastic sediments (Harp and Jibson, 1996). The average volumes of these triggered landslides were less than 1000 $m^3$, but many exceeded 100,000 $m^3$ (Harp and Jibson, 1996). There were approximately tens-to-hundreds of deeper triggered rotational slumps and block slides, a few of which were larger than 100,000 $m^3$ in volume (Harp and Jibson, 1996).

Damage to residential buildings was three to four times greater when landslides were involved than the average damage due to shaking (Brown and Ghilarducci, 2013). The area principally affected by coseismic landslides during the event had plans to develop dense residential areas at the time of the event (Harp and Jibson, 1996; Keefer and Wilson, 2011). In particular, since 1994, Santa Clarita and Simi Valley have been developed into much denser residential suburbs.

## 3.0 Methods

This paper uses a well-documented landslide inventory map, detailed peak ground acceleration data and environmental parameters associated with landsliding to fit a logistic regression model of probability of landslide occurrence for the 1994 Northridge earthquake event. The probability of coseismic landslide occurrence was then predicted using the logistic regression model for seven earthquake scenarios in Northridge, California. Peak ground acceleration (PGA) maps were produced for each scenario using OpenSHA, an open source application that makes use of distributed grid computing (Field et al., 2003; Field et al., 2005). The seven scenarios chosen were $M_w$6.0, $M_w$6.7, $M_w$6.9, $M_w$7.0, $M_w$7.2, $M_w$7.5, and $M_w$8.0. The selection of these earthquake magnitudes was based on the 1994 recorded

$M_w$6.7 moment magnitude and the forecasted 30 year magnitude probability distributions calculated for the Northridge 1994 event fault type in southern California using the Uniform California Earthquake Rupture Forecast (UCERF) II Report (Field et al., 2008).

The exposure of infrastructure and the population in the study site to high levels of earthquake shaking and landslide probability above a determined threshold was estimated for each scenario. In this context, exposure is a verb which has a binary outcome (exposed or not) applied to the elements present in the study site, that are thereby subject to potential losses (Allen et al., 2009; UNISDR, 2007). The set of assets within these high levels of shaking or areas of landslide hazard are termed exposed assets (Figure 53). The threshold adopted for potentially impactful seismic shaking was ≥0.18 g, taken from the USGS ShakeMap scale for moderate potential damage and very strong perceived shaking. The exposure of infrastructure and the population in the Northridge site to landslide hazard above 0.9 probability of occurrence was also calculated.

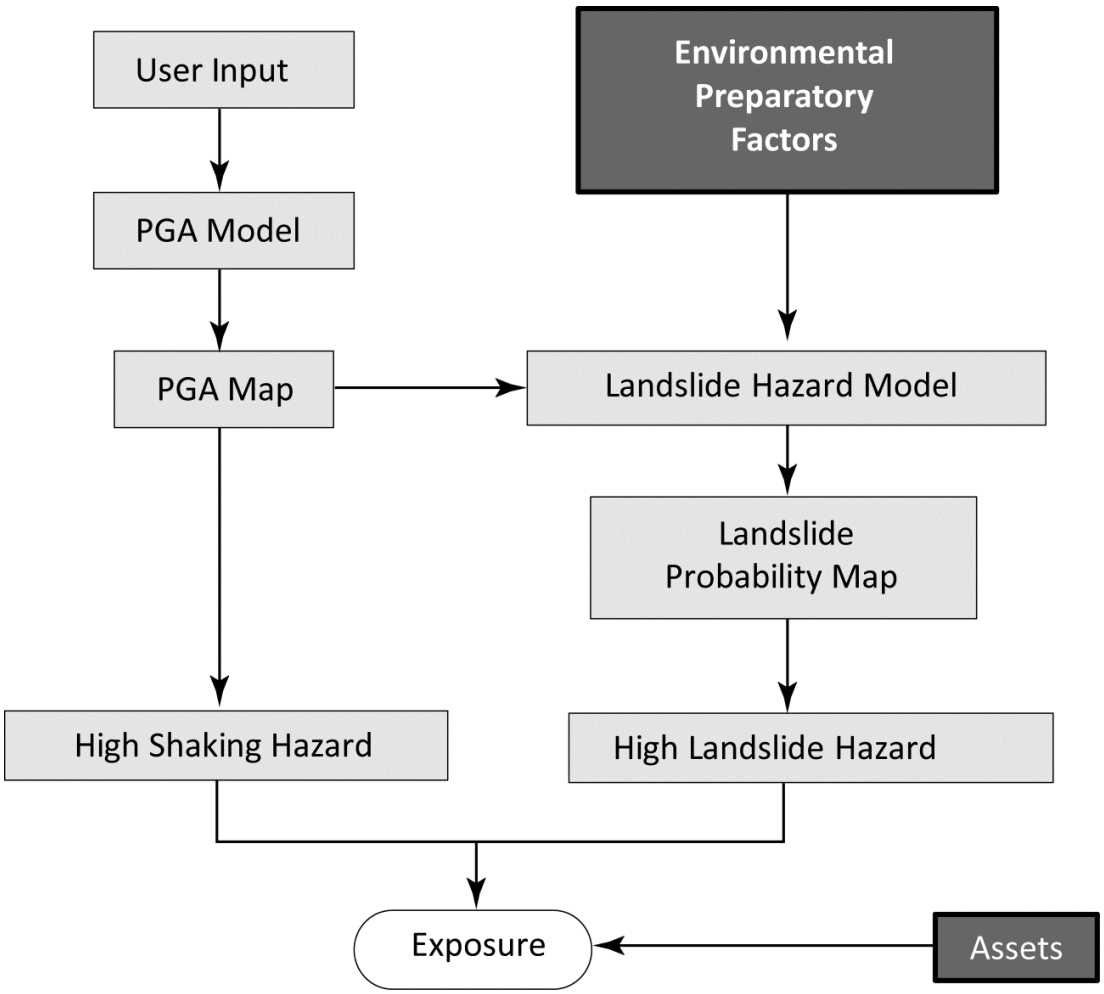


Figure 53. Conceptual diagram illustrating the method used to determine the exposure of assets to earthquake shaking and coseismic landslide hazard for seven scenarios at the Northridge site.

The accuracy of the logistic regression model was evaluated by calculating the area under the curve (AUC) for the receiver operating characteristic (ROC), based on a subset of the original data not used in the development of the model. The ROC curve is drawn by plotting the true positive rate and false positive rate as the *x* and *y* axes, respectively. The AUC is a statistic that measures the ability of the model to correctly classify cases of landslide and stable area (Chang et al., 2007). When the total area is found to be 1, this indicates perfect accuracy. In addition to this, the percentage of correctly and incorrectly predicted landslides and non-landslide cells for a failure threshold of ≥0.9 probability of landsliding were calculated. To assess the accuracy of the peak ground acceleration maps generated by the OpenSHA program, the recorded peak ground acceleration map from the 1994 Northridge event was compared to the OpenSHA modelled output for the $M_w$6.7 scenario. The accuracy

of the landslide hazard model using the OpenSHA-generated peak ground acceleration was also compared to the landslide hazard model generated using the recorded peak ground acceleration.

## 3.1 Landslide Hazard Model

A logistic regression model was fitted to the relation between landslide occurrence and several environmental covariates, including peak ground acceleration due to earthquake shaking, for the 1994 Northridge event. At a spatial resolution of 1 $km^2$, the 11,000 landslides were represented by 3,358 raster grid cells. Two thirds of these landslide cells (2,518) were selected randomly and an equal number (2,518) of non-landslide raster image cells were selected for use in logistic regression to predict landslide occurrence. One third of the initial sample (840 cells per class) was retained for future accuracy assessment.

The continuous covariates used as an input into the logistic regression analysis were: curvature, drainage density, distance to drainage, elevation, fault density, distance to fault line, peak ground acceleration, plan curvature, profile curvature, distance to ridgeline, roughness (at 3 and 5 cell radius standard deviation of elevation), slope gradient, and stream power index (SPI) (Table 25). An additional four categorical variables were included: aspect, geology, soil type and vegetation (Table 25). The logistic model was fitted automatically using the statistical software 'R', in a backward-stepwise manner, using the Akaike Information Criterion (AIC) value to determine the best-fitting model.

Table 25. Description and source of data for the preparatory environmental covariates selected for use in logistic regression to predict landslide occurrence.

| Explanatory variable | Description | Source of original data |
|---|---|---|
| Aspect | Slope azimuth from DEM | GMTED2010 |
| Curvature | Representing morphology of the topography: a positive curvature indicates that the surface is upwardly convex at that pixel. A negative curvature indicates that the surface is upwardly concave at that pixel; a value of zero indicates that the surface is flat. Calculated from DEM | GMTED2010 |

| | | |
|---|---|---|
| Drainage density | The density of drainage lines in the neighborhood of each output raster cell. Density is calculated in units of length per unit of area. | HydroSHEDS |
| Distance to drainage | Euclidean distance to drainage | HydroSHEDS |
| Elevation | Height above sea level from DEM | GMTED2010 |
| Fault density | The density of fault lines in the neighborhood of each output raster cell. Density is calculated in units of length per unit of area. | OneGeology Portal |
| Distance to fault | Euclidean distance to recorded fault line | OneGeology Portal |
| Plan curvature | Contour curvature: perpendicular to the direction of maximum slope. Calculated from DEM | GMTED2010 |
| Profile curvature | Slope profile curvature: direction of the maximum slope. Calculated from DEM | GMTED2010 |
| Distance to ridgeline | Euclidean distance to ridgeline. Ridgeline determined from DEM | GMTED2010 |
| Roughness | Standard deviation of slope (3x3 and 5x5 cell sample) from DEM | GMTED2010 |
| Slope gradient | Change in elevation divided by horizontal distance from DEM | GMTED2010 |
| SPI | Stream power index from DEM | GMTED2010 |
| Geology | Type of geology beneath the soil layer | OneGeology Portal |
| Soil type | Top most soil layer type | GeoCommunities |
| Vegetation | Vegetation type | GeoCommunities |

## 3.2 Peak Ground Acceleration Model

The earthquake peak ground acceleration shaking maps for each of the seven scenarios were computed using the OpenSHA application (freely available at http://www.OpenSHA.org). OpenSHA can simulate any earthquake scenario, given the hypocentre location and earthquake magnitude; using complex earthquake rupture forecasts and ground-motion models the application can produce peak ground acceleration maps. The fault point source coordinate data for the simulations in this paper (34.213 N, -118.536 E) were taken from the USGS Advanced National Seismic System (ANSS) ShakeMap for the Northridge 1994 event.

The attenuation model was selected from the available models in the OpenSHA program; specifically, the eleven models which use the CGS/Wills Site Classification map (2006) as site data. The OpenSHA application was run for the eleven attenuation models using the Northridge 1994 $M_w$6.7 epicentre coordinates, at a selection of depths (5-30 km deep). The

simulated peak ground acceleration maps produced were compared to the recorded peak ground acceleration variable for the event and the root mean square error (RMSE) was calculated. Campbell et al.'s (1997 with erratum 2000 changes) attenuation model at 30 km depth produced the smallest RMSE (0.16g) and was selected as the attenuation model for all seven scenarios in this paper.

### 3.3 Asset Data

Data for estimating the potential exposure of assets to earthquake shaking and high landslide probabilities were obtained from various sources, as outlined in the following section. An ideal dataset would provide data for each asset in 1994 *and* 2014 to both assess the impact of an event occurring now or in the near future, and provide the opportunity to compare the result to the 1994 event. However, this was not available. Therefore, the nearest existing data to 1994 and 2014 were used in this paper. The exact date or time frame for each asset dataset is stated in the following section. Each dataset was clipped in ArcGIS to the Northridge site extent.

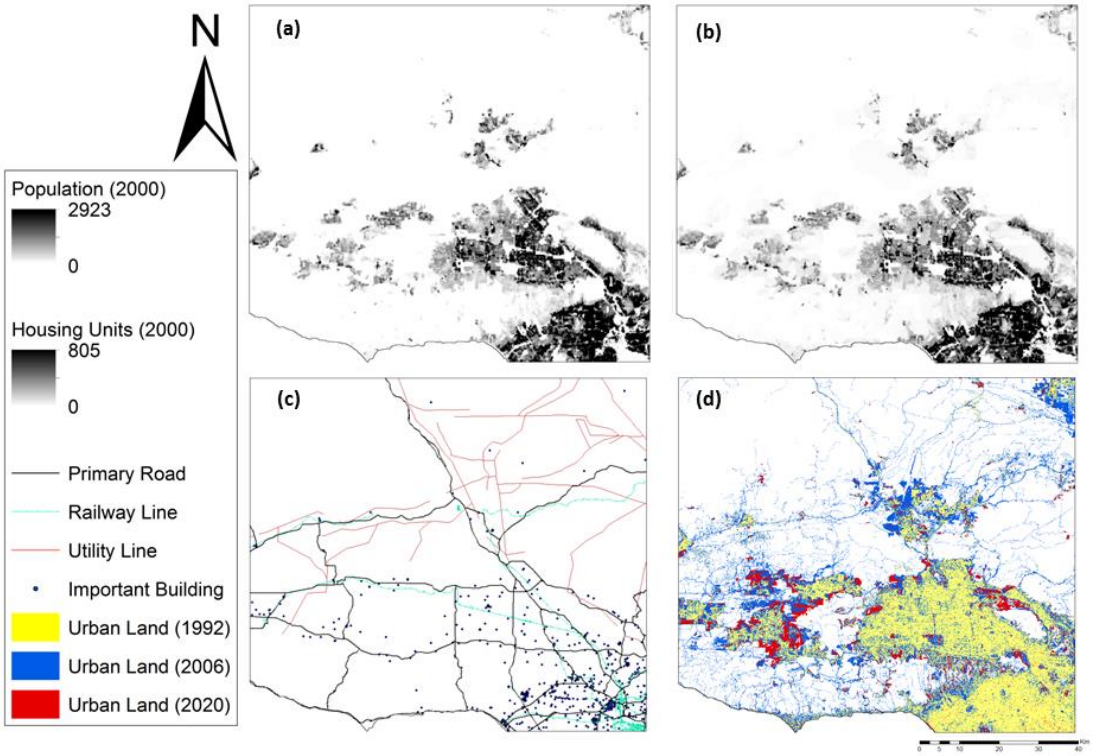

Figure 54. Maps of the asset data used to estimate exposure to high levels of shaking and landslide probability for the earthquake scenarios: (a) population density at the census grid scale (250 m) for the year 2000; (b) housing units at the census grid scale (250 m) for the year 2000; (c) primary roads, railway lines, utility lines, and important buildings within the Northridge site; and (d) classified urban land cover for 1992 and 2006, and projected to 2020.

Gridded population and housing unit data for the United States were obtained at a fine spatial resolution of approximately 250 m for the years 1990 and 2000 (Figure 54) (Seirup and Yetman, 2006; Seirup et al., 2012). The gridded variables are based on census block geography from the Census 1990 Topologically Integrated Geographic Encoding and Referencing (TIGER)/Line Files and produced by Columbia University Centre for International Earth Science Information Network (CIESIN) for California. Point data on important buildings were obtained from the Economic and Social Research Institute (ESRI) ArcCatalog BaseMap of North America. These data are part of a nationwide building base map of the USA and include major buildings, excluding churches, hospitals and schools.

Two types of road data were used to assess the impact of earthquake shaking and landslides on road assets: primary roads and all roads. Primary road line data were sourced from the Digital Chart of the World's (DCW) data repository for the state of California (Figure 54). The DCW is an ESRI product originally developed for the US Defense Mapping Agency (DMA) using DMA data.

All road data for Ventura County and Los Angeles County were obtained from the US Census Bureau's Master Address File (MAF)/TIGER database. The all roads shapefile includes primary roads, secondary roads, local neighbourhood roads, rural roads, city streets, vehicular trails, ramps, service drives, walkways, stairways, alleys, and private roads. The most recent version of data for 2011 was used in the paper.

Utility line data were obtained from the DCW's data repository for the state of California. Utilities recorded as line shapefiles included power transmission lines, telephone or

telegraph lines, above-ground pipelines, and underground pipelines (Figure 54). Railway line data are credited to ©OpenStreetMap contributors, with the data automatically extracted from the most recently available version from Geofabrik's free download server (Figure 54). The data were available for the entire North America region.

Three land cover maps were used in this paper to estimate the impact on urban land features (Figure 54). The 1992 land cover map was obtained via the USGS National Land Cover Dataset compiled from Landsat satellite Thematic Mapper (TM) imagery with a spatial resolution of 30 m. The 2006 land cover map was compiled by the Multi-Resolution Land Characteristics (MRLC) Consortium (Fry et al., 2011). Projected urban land cover data for 2020 were downloaded from Cal-Atlas, the original data provided by the California Environmental Resource Evaluation System (CERES). Urban land cover projections were made based on extrapolation of current population trends and recent urban development trends.

## 4.0 Results

### 4.1 Changes since 1994

Census data with a spatial resolution of 250 m collected in 1990 and 2000 show that there were increases in both the number of housing units and the population between these dates. Population increased from 477,924 to 542,384 people (a 12% increase); while the number of housing units increased from 121,528 to 125,884 houses (a 3% increase) in the study site. Locally, there was an increase in population in the San Fernando Valley and the outskirts of Los Angeles in the southeast corner of the study site. Development also occurred along the primary roads in the hillier northern region of the site, particularly at Santa Clarita.

Urban land cover in the study site increased from 1,320 $km^2$ to 2,125 $km^2$ (a 38% increase) between 1992 and 2006 (Figure 54). The main urban regions of Northridge, Santa Clarita, Simi Valley, Thousand Oaks, Fillmore and Lancaster clearly expanded since 1992, and the

regions in-between are beginning to be developed (Figure 54 and Figure 45). Projected urban area for the year 2020 suggest further development in Northridge, Thousand Oaks and Simi Valley, in particular (Figure 54 and Figure 45).

## 4.2 Simulation Results

The landslide logistic regression hazard model found peak ground acceleration, roughness (3 x 3 cells), elevation, slope, fault density, drainage distance, ridge distance, aspect, geology, vegetation and soil type to be significant covariates in predicting landslide hazard. The logistic regression model was used with these covariates to calculate the probability of landsliding for each earthquake simulation using the OpenSHA peak ground acceleration variables seen in Figure 55.

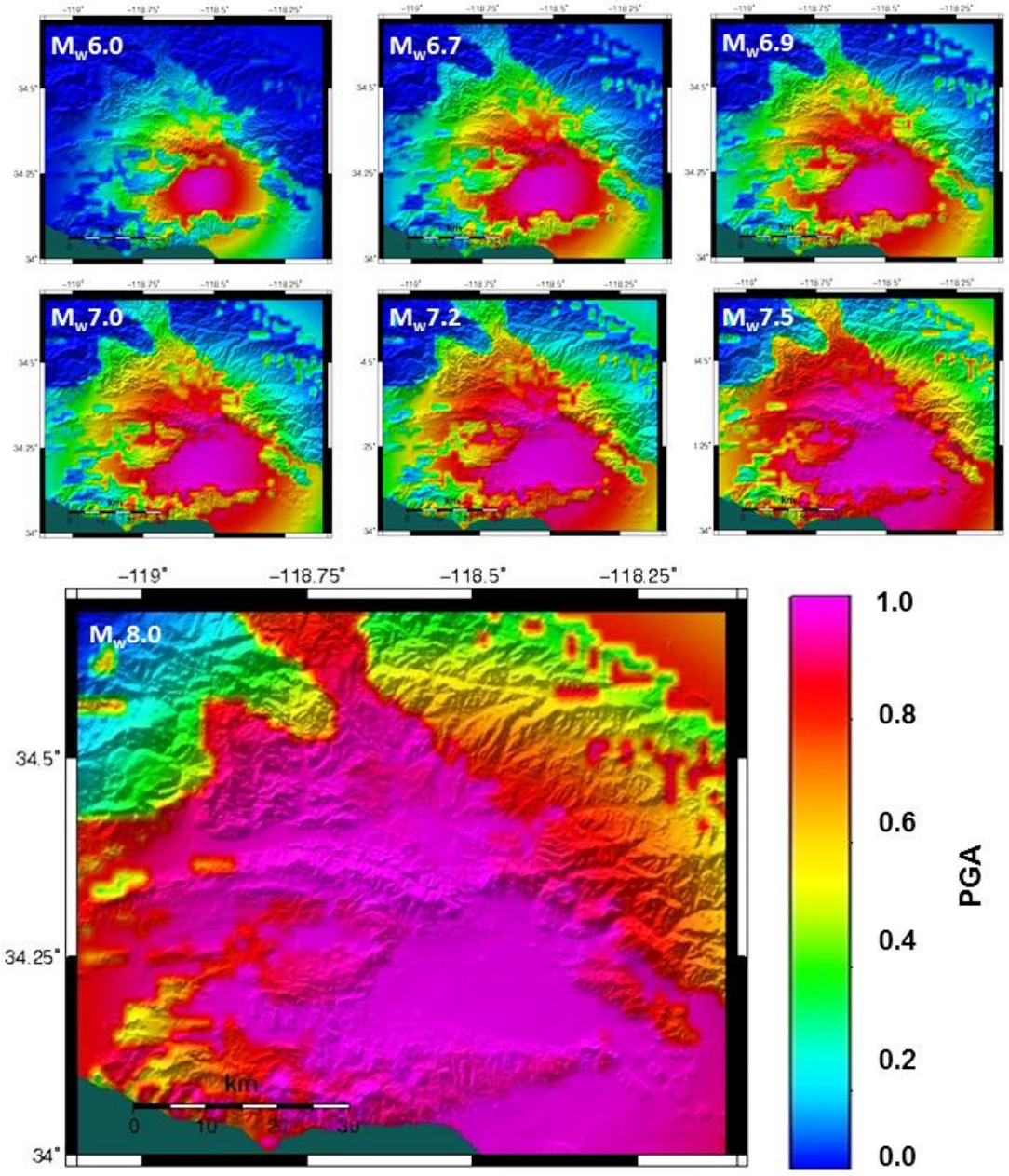


Figure 55. Maps of peak ground acceleration calculated using OpenSHA for seven seismic magnitude scenarios for Northridge (Mw6.0, Mw6.7, Mw6.9, Mw7.0, Mw7.2, Mw7.5, and Mw8.0).

Figure 56 shows the areas predicted to be affected by ≥0.9 probability of landsliding and ≥0.18 g for the seven earthquake scenarios in which the Northridge event is repeated, but with varying magnitudes ($M_w$6.0, $M_w$6.7, $M_w$6.9, $M_w$7.0, $M_w$7.2, $M_w$7.5, and $M_w$8.0), simulated using the OpenSHA application and the landslide hazard model. As earthquake magnitude increases, the area affected by high levels of shaking spreads outwards from the epicentre, affecting a greater area. As the initial earthquake magnitude is increased, the area

affected by high probability of landsliding also increases. Santa Clarita, Fillmore, Simi Valley, Thousand Oaks and the outskirts of Northridge become more likely to be affected by landsliding as earthquake magnitude increases. For the $M_w$8.0 scenario, the majority of the study site is affected by very strong perceived shaking and moderate potential damage.

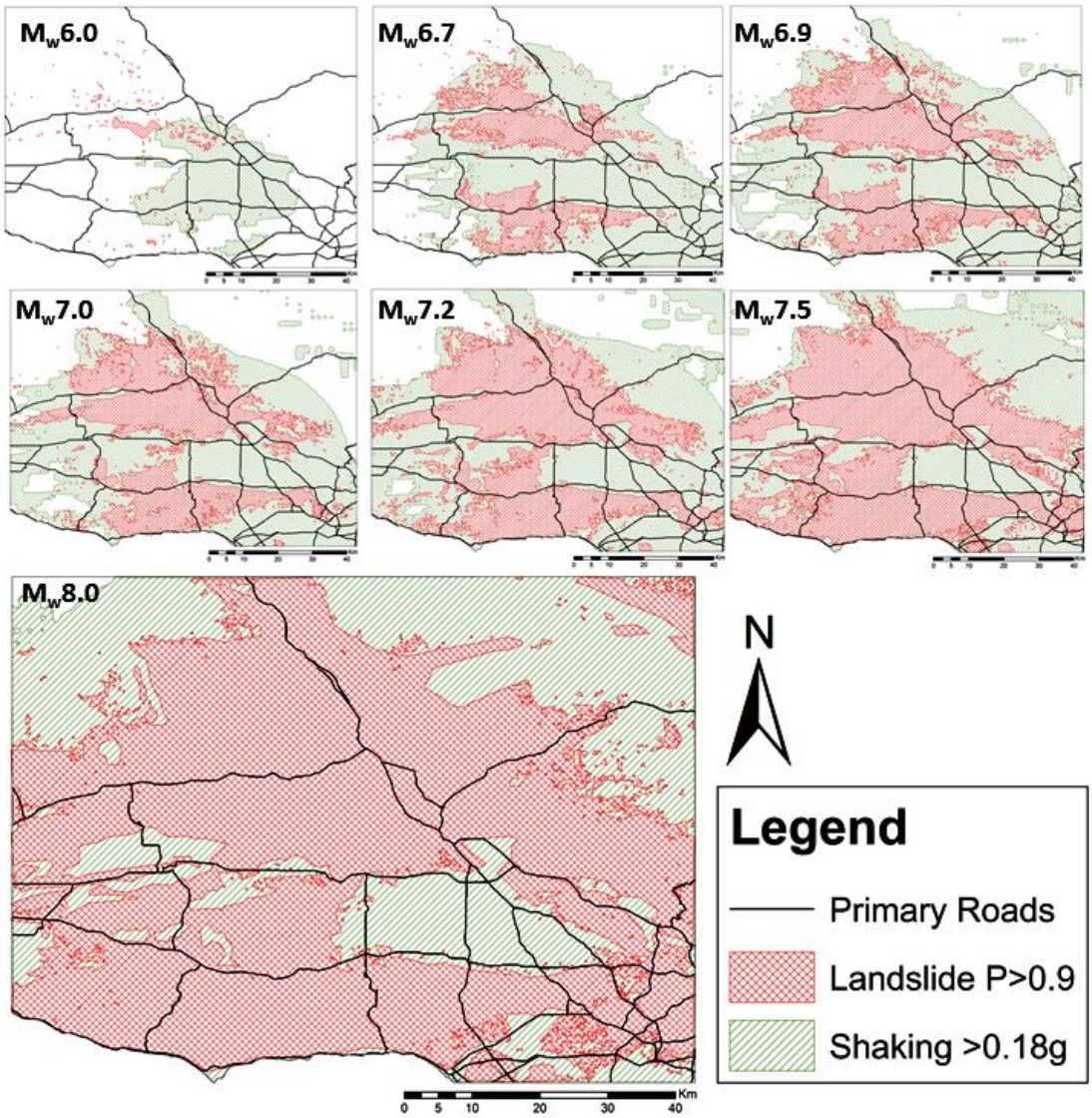


Figure 56. Area affected by ≥0.9 probability of landsliding (red) and ≥0.18 g shaking (green) for the seven earthquake magnitude scenarios. Primary roads (black lines) are shown on each map for spatial reference.

## 4.3 Validation of the Landslide Hazard Model

A subset of 840 landslide and 840 non-landslide data points were not used in the fitting of the logistic regression landslide hazard model. For each of the cells, the probability of

landslide occurrence was selected and used to assess the accuracy of the hazard model in predicting landsliding. The accuracy of the logistic regression model was evaluated by calculating the area under the curve (AUC) for the receiver operating characteristic (ROC). The ROC AUC for the landslide hazard model using the recorded peak ground acceleration from the 1994 Northridge event was 0.974. This indicates very high prediction accuracy.

The percentages of correctly and incorrectly predicted landslide and non-landslide cells based on landslide failure at $P \geq 0.9$ for the landslide hazard model were also calculated. The model shows good predictive ability in separating landslide cells from non-landslide cells using the ≥0.9 probability of failure threshold value, with a 77.26% successful prediction of landslide cells and 97.62% successful prediction of non-landsliding.

### 4.4 Validation of Peak Ground Acceleration Model

The recorded peak ground acceleration data for the Northridge 1994 $M_w$6.7 event were compared to the OpenSHA estimated peak ground acceleration maps to calculate the error in simulating the peak ground acceleration variable. The difference between observed shaking and modelled shaking varies between +0.39g and -0.47g (Figure 57). The RMSE between the observed and modelled peak ground acceleration using the OpenSHA program for the $M_w$6.7 scenario is 0.16 g.

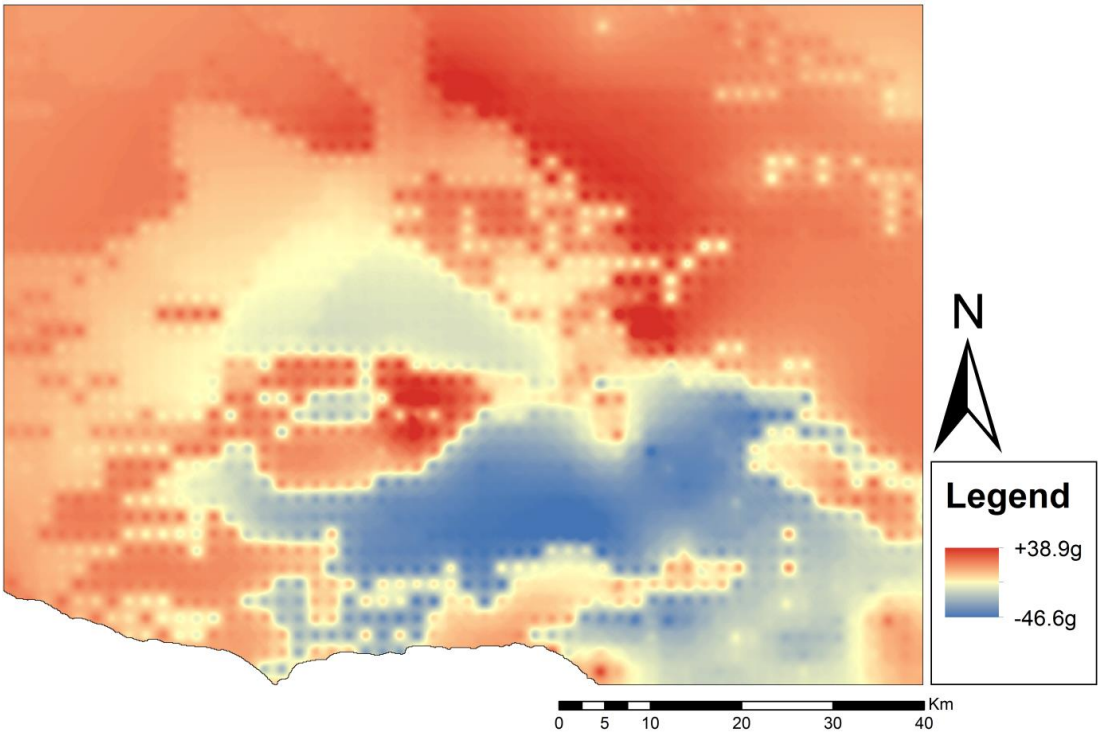


Figure 57. Error between peak ground acceleration recorded during the 1994 Mw6.7 Northridge earthquake, and the scenario Mw6.7 simulated by OpenSHA. Red areas show where the OpenSHA over-predicts peak ground acceleration, blue areas show where OpenSHA under-predicts peak ground acceleration.

The impact of using the simulated peak ground acceleration variable on the prediction of landslide hazard probability was also tested. The model used in predicting landslide probability for the six scenarios has a high AUC value of 0.974, demonstrating a high degree of accuracy in predicting landslide occurrence for this study site. There was no difference in ROC AUC values between using the original PGA variable and the OpenSHA generated PGA variable (Hanley and Mcneil, 1983).

Similarly, when the percentage of correctly and incorrectly predicted landslide and non-landslide cells based on a landslide failure at $P \geq 0.9$ for the original peak ground acceleration variable and simulated $M_w$6.7 peak ground acceleration variable were compared, there was only a small loss in successful prediction of landsliding. The original PGA variable model achieved a 79.88% successful prediction of landslide cells and a 97.85% successful prediction of non-landsliding. The simulated PGA variable model achieved a 70.12% successful prediction of landslide cells and a 96.66% successful prediction of non-

landsliding. This indicates that the OpenSHA generated peak ground acceleration variable does not introduce significant error into the landslide hazard model prediction relative to using the observed peak ground acceleration data.

## 4.5 Asset Exposure to Earthquake Shaking and Landsliding

Asset exposure to earthquake shaking ≥0.18 g and to landslide probability ≥0.9 for each of the seven earthquake scenarios was calculated by overlaying the asset variables on the shaking and landsliding data layers and estimating the total number or quantity of assets within these regions. This was conducted within the study site for the following assets: primary roads, utility lines, railway lines, all roads, urban land cover (1994, 2006, 2020), population at the census block spatial resolution (1990, 2000), housing units (1990, 2000), and important buildings (Figure 58 to Figure 60).

*Roads, Railway lines and Utilities*

Primary roads and all roads have a similar pattern of exposure to high levels of earthquake shaking and landslide probability as earthquake magnitude increases between simulations, despite the total length of roads exposed being different (Figure 58). Roads exposed to ≥0.18 g show a concave pattern, with a rapid increase and tapering off in the length exposed as earthquake magnitude increases (Figure 58). Roads exposed to ≥0.9 probability of landsliding show a steady increase in exposure as earthquake magnitude increases (Figure 58).

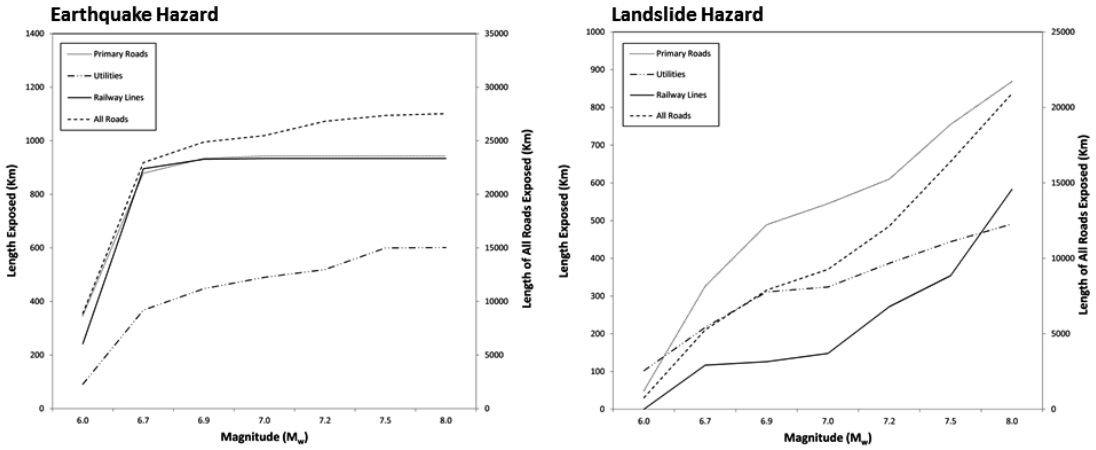


Figure 58. Assets (primary roads, utilities, railway lines and all roads) within the Northridge site exposed to (left) earthquake shaking ≥0.18 g, and (right) landslide probability ≥0.9, modelled using the OpenSHA program and the logistic regression model for the seven magnitude scenarios.

Railway lines are most densely clustered in the southeast corner of the site in Los Angeles. This area is not exposed to high landsliding probability, but is exposed to high levels of earthquake shaking at $\geq M_w6.7$, explaining the steep gradient of the exposed railway line affected by earthquake shaking before $M_w6.7$ (Figure 58). Utility lines are most densely clustered in the north of the study site, which is gradually exposed to ≥0.18 g as earthquake magnitude increases (Figure 58). The utility lines are concentrated in the landslide prone area of the study site, showing a steady increase in the length of utility lines exposed to high landslide probability as earthquake magnitude increases (Figure 58).

*Urban Land Cover*

The urban area exposed to high earthquake shaking and high landslide probability does not increase greatly as earthquake magnitude increases in the scenarios (Figure 59). This is because, even at a low magnitude earthquake event of $M_w6.0$, the majority of the urban land cover is exposed to shaking and a high probability of landsliding (Figure 56). As the area affected by increasing magnitude events expands, only a small proportion of urban land cover is newly incorporated into the exposed regions (Figure 59).

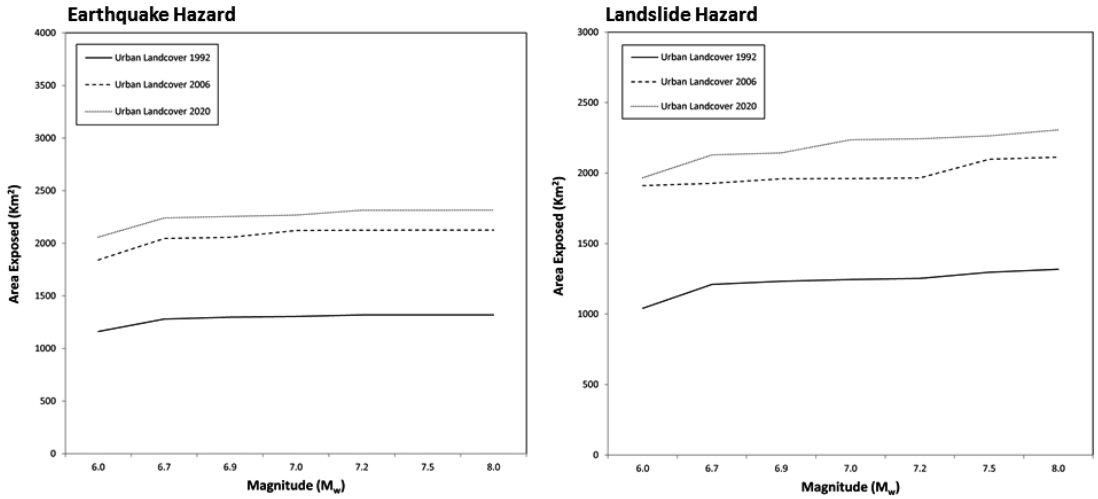


Figure 59. Urban land cover exposed to (left) earthquake shaking ≥0.18 g; and (right) landslide probability ≥0.9 modelled using the OpenSHA program and the logistic regression model for the seven magnitude scenarios for the years 1994, 2006 and 2020 within the Northridge site.

A clear increase can be seen in the total area of urban land cover exposed to high levels of earthquake shaking and landslide probability between 1992 and 2006. For the low magnitude event of $M_w$6.0, the urban area affected by high earthquake shaking increases by 680 km$^2$; and for high landslide probability by 870 km$^2$.

*Population and Buildings*

Population and buildings exposed to ≥0.18 g increase rapidly between $M_w$6.0 and $M_w$6.7, levelling off at the greater magnitude scenarios, while population and buildings exposed to ≥0.9 landslide probability rapidly increase as earthquake magnitude increases (Figure 60). This is because population density and housing units are clustered most densely in the centre and southeast of the site in Northridge and Los Angeles. The epicentre of the earthquake is in the centre of the San Fernando Valley, so as the earthquake magnitude increases the area exposed to high levels of shaking expands out from this centre (Figure 56). By the $M_w$6.7 scenario, the majority of the densest population and housing is exposed to earthquake shaking; above this magnitude, less dense population and housing is exposed in the remainder of the site.

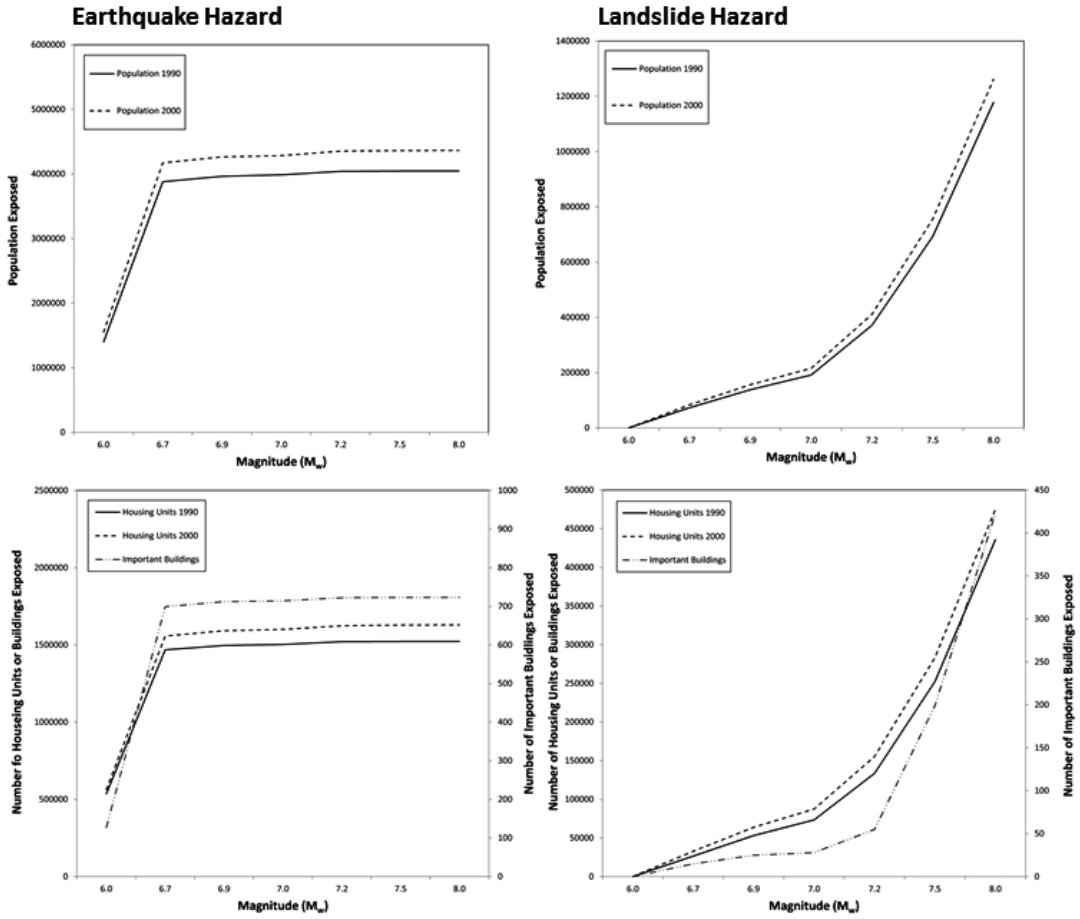


Figure 60. Assets exposed to (left) earthquake shaking ≥0.18 g; and (right) landslide probability ≥0.9 modelled using the OpenSHA program and the logistic regression model for the seven magnitude scenarios for (top) population and (bottom) buildings within the Northridge site. Population exposed was calculated for 1990 and 2000 using census data. Buildings exposed were calculated for housing units in 1990 and 2000 from census data, and important buildings within the Northridge site.

The area exposed to ≥0.9 landslide probability increases exponentially with increasing earthquake magnitude (Figure 58) because at lower magnitude scenarios, the area exposed to high landslide probability is mostly in the steeper slopes where the population and housing is less dense. However, as earthquake magnitude increases through the scenarios, this exposed area spreads quickly outwards to affect more residential areas such as Santa Clarita, Simi Valley, Thousand Oaks and the region between Northridge and Los Angeles (Figure 56).

## 5.0 Discussion

Landslide susceptibility assessment using logistic regression analysis is a common approach in the literature; however, using peak ground acceleration in logistic regression analysis to estimate landslide hazard probability is rare (Nowicki et al., 2014; Marzorati et al., 2002;

Carro et al., 2003). This study utilised two very detailed datasets – a landslide inventory map and recorded peak ground acceleration map – for the 1994 $M_w$6.7 Northridge earthquake to fit a logistic regression landslide hazard model. The landslide hazard model has a high level of accuracy in predicting landslide locations using the ≥0.9 probability threshold of failure. The freely available OpenSHA application was then used to generate peak ground acceleration maps for seven earthquake magnitude scenarios for the Northridge study site. The seven scenarios show an increase in the number of exposed assets since the 1994 Northridge earthquake, and an increase in exposed assets as earthquake magnitude is increased.

The earthquake scenarios chosen for this study assume the same fault type scenario occurring in the future as recorded during the 1994 Northridge earthquake event. The likelihood of such an event occurring in exactly the same way as in 1994 is not evaluated in this study. However, the parameters provided by the USGS ShakeMap archive provide input variables for the OpenSHA model to estimate the peak ground acceleration variable. This is required to fit the landslide hazard model and also assess the uncertainty in using the OpenSHA model to estimate peak ground acceleration. Therefore, whilst the exact future fault scenario is not accounted for in this paper, the landslide hazard model can be used with any peak ground acceleration variable as input to estimate the landslide probability and exposed assets to specific scenarios in the Northridge area.

There was a discrepancy between the OpenSHA peak ground acceleration estimates and those recorded during the 1994 Northridge event for the same scenario. However, the ROC AUC for the $M_w$6.7 scenario using the OpenSHA PGA variable was not significantly different from that for the original PGA variable, and the accuracy of correctly predicting landslide occurrence was only minimally reduced (Hanley and Mcneil, 1983). The error between the OpenSHA model-predicted peak ground acceleration and the recorded peak ground acceleration was mostly confined to the San Fernando Valley, which is not affected by landsliding and, thus, does not greatly affect the predictive ability of the landslide hazard

model. The confinement of the majority of error to the San Fernando Valley could indicate the difficulty of predicting ground amplifications in basin soils. Alternatively, the input parameters used in the OpenSHA application might not represent sufficiently accurately the fault process observed during the 1994 Northridge earthquake. The difference between the recorded peak ground acceleration and that predicted by OpenSHA could arise from several sources such as the choice of attenuation model, and the uncertainty in the original recorded data.

The attenuation model and fault parameters were chosen to match the ShakeMap 1994 Northridge scenario as closely as possible. Fault parameters were chosen as a point source of shaking located at the epicentre because accurate data of the real fault surface were not available. Campbell et al.'s (1997 with erratum 2000 changes) attenuation model produced the smallest RMSE; and, therefore, as the best available attenuation model, it was selected for this study. Alternative attenuation models would have resulted in greater error in predicting peak ground acceleration.

The recorded 1994 peak ground acceleration variable itself is not without uncertainty. Of the 200+ recording stations used to record the Northridge earthquake shaking, very few were located in steeply sloping areas where landslides occurred. The field evidence of topographic amplification suggests that the shaking in the mountains was much higher than would have been predicted by interpolating between flat land sites. The ShakeMap for the Northridge 1994 event was generated using the recorded ground motions from seismometers in Ventura and Los Angeles Counties and interpolated between stations using the attenuation model and ground amplification factors of Borcherdt (1994). The OpenSHA generated peak ground acceleration model is not calibrated to observed data, which can account for some of the error observed in this paper.

The thresholds of earthquake shaking (≥0.18 g) and landslide hazard (≥0.9 probability) were selected to represent earthquake shaking at 'moderate potential damage' described by the

USGS and to represent landslide hazard as a suitably accurate predictive threshold of failure from the 1994 Northridge event. These thresholds do not convey the spatial distribution of, and exposure to, higher or lower levels of hazard, masking patterns of exposure occurring outside the chosen thresholds, and resulting in a loss of some information. However, these thresholds provide a measuring level against which asset exposure can be calculated and compared between different scenarios.

As the scenario magnitude increases, earthquake shaking impact increases, but saturates rapidly above $M_w$6.7; however, landslide hazard impact increases rapidly. This is because the earthquake shaking centre is located in the highest density of the population, whilst landslide hazard radiates out from mountainous areas as earthquake magnitude increases, where there is lower density of population. In potential future earthquake events, emergency planners should be aware that as the magnitude of the earthquake increases, the effect of the earthquake shaking may not increase greatly, but the risk from landslide hazards will be much greater, and cover a wider spatial region. Long-term landslide susceptibility assessments do not incorporate the increased risk from triggered landslides by a higher magnitude earthquake event because they are based on long-term, typically rainfall-induced landslide occurrences. In the USGS Prompt Assessment of Global Earthquakes for Response (PAGER) reports, earthquake shaking damage is estimated in near-real-time following an earthquake event; however, damage and losses from secondary hazards such as landslides are not calculated (Wald et al., 2012). Awareness of the potential for a rapid increase in landslide risk as earthquake magnitude increases can help emergency planners prepare for potential landslide damage and losses, such as blocking roads, which can disrupt relief efforts.

Whilst every effort was made to obtain the most recent version of the asset data, the population, housing units and land cover data are not up-to-date representations of the assets in 2014. Considering the development in the study site between 1990 and 2000, it can be presumed that the area has developed further since the last census in 2000. However,

extrapolation to current levels of population and housing units would introduce an additional source of uncertainty in estimating exposed assets. The scenarios, therefore, provide an estimation of the relative increases in exposed assets as earthquake magnitude increases, rather than exact quantification of exposure in 2014. An increase was observed in the total number of assets within the study site since the Northridge 1994 earthquake. Therefore, the analysis suggests that if the same earthquake occurred tomorrow, more assets would be exposed to earthquake shaking and landsliding compared to the 1994 event.

In future research, the relation between landsliding and peak ground acceleration should be investigated for other earthquake and coseismic landslide events where recorded ground motion data and landslide inventory maps are available. Recent developments of ShakeMap peak ground acceleration maps and landslide inventory maps for past earthquake events can be used to develop quantitative landslide hazard models. Logistic regression analysis provides a quick and robust method of fitting landslide probability models for such events. The increased collation of landslide loss data in recent years could also be utilised with these logistic regression models to estimate potential losses from coseismic landslides in the future.

The method presented in this paper represents a new and powerful approach to landslide hazard modelling by linking landsliding to the trigger factor, spatially distributed as peak ground acceleration. The landslide *hazard,* rather than *susceptibility,* can be estimated for *any* earthquake in the greater Northridge area because it is a function of ground motion, which can be simulated for any earthquake event (earthquake magnitude, epicentre location and fault type). Thus, such a modelling approach represents a useful decision-support tool for planning and emergency management by predicting the distribution of risk of landsliding given the occurrence of an earthquake, whether real or hypothetical.

### 6.0 Conclusion

If the Northridge earthquake occurred tomorrow, exactly as in 1994, the event would likely result in more losses and damage than the 1994 event due to increases in human population and infrastructure since 1994. If the earthquake occurred with a higher recorded moment magnitude then exposure and, thus, potential losses from landslides would increase at a rapid rate, as quantified in this paper. The scenario maps produced here can be used by land use and emergency planners as a reference for those areas at risk of landsliding and high levels of earthquake shaking during a similar event to the Northridge 1994 earthquake.

Including ground motion as a variable in logistic regression analysis to predict landsliding is rare in the published literature. Including a ground motion variable can increase the accuracy of landslide prediction, but more importantly, the model can be utilised to predict probable locations of landslides as a result of *any* reasonable earthquake scenario, identifying areas at risk and, thus, the potential for damage to populations and infrastructure. The method and model used in this paper can be used to predict landslides as a result of earthquake shaking using OpenSHA-generated peak ground acceleration maps, or future ShakeMaps as a result of *potential* future earthquake events. In future, the relation between landsliding and peak ground acceleration should be investigated for other earthquake and coseismic landslide events where recorded ground motion data are available.

## Acknowledgements

The authors would like to thank the U.S. Geological Survey, OneGeology, GeoCommunities, OpenSHA, and Columbia University Center for International Earth Science Information Network for the provision of data.

# References


ALLEN, T. I., MARANO, K. D., EARLE, P. S. & WALD, D. 2009. PAGER-CAT: A composite earthquake catalog for calibrating global fatality models. Seismological Research Letters, 80, 57-62.

ATKINSON, P. M. & MASSARI, R. 2011. Autologistic modelling of susceptibility to landsliding in the Central Apennines, Italy. Geomorphology, 130, 55-64.

AURELIUS, E. 1994. The January 17, 1994 Northridge, CA earthquake: An EQE International Summary Report. Houston, TX: EQE International.

BOMMER, J. J., BENITO, M. B., CIUDAD-REAL, M., LEMOINE, A., LOPEZ-MENJIVAR, M. A., MADARIAGA, R., MANKELOW, J., DE HASBUN, P. M., MURPHY, W., NIETO-LOVO, M., RODRIGUEZ-PINEDA, C. E. & ROSA, H. 2002. The El Salvador earthquakes of January and February 2001: context, characteristics and implications for seismic risk. Soil Dynamics and Earthquake Engineering, 22, 389-418.

BORCHERDT, R. D. 1994. Estimates of site-dependent response spectra for design (methodology and justification). Earthquake Spectra, 10, 617-653.

BOSLAUGH, S. 2012. Statistics in a Nutshell, O'Reilly Media.

BRENNING, A. 2005. Spatial prediction models for landslide hazards: review, comparison and evaluation. Natural Hazards and Earth System Sciences, 5, 853-862.

BROWN, E. G. J. & GHILARDUCCI, M. S. 2013. 2013 State of California Multi-Hazard Mitigation Plan. In: SERVICES, C. G. S. O. O. E. (ed.). Mather, California.

CAMPBELL, K. W. 1997. Empirical Near-Source Attenuation Relationships for Horizontal and Vertical Components of Peak Ground Acceleration, Peak Ground Velocity, and Pseudo-Absolute Acceleration Response Spectra. Seismological Research Letters, 68, 154-179.

CAMPBELL, K. W. 2000. Erratum: Empirical Near-source Attenuation Relationships for Horizontal and Vertical Components of Peak Ground Acceleration, Peak Ground Velocity, and Pseudo-absolute Acceleration Response Spectra. Seismological Research Letters, 71, 352-354.

CARRO, M., DE AMICIS, M., LUZI, L. & MARZORATI, S. 2003. The application of predictive modeling techniques to landslides induced by earthquakes: the case study of the 26 September 1997 Umbria-Marche earthquake (Italy). Engineering Geology, 69, 139-159.

CHANG, K. T., CHIANG, S. H. & HSU, M. L. 2007. Modeling typhoon- and earthquake-induced landslides in a mountainous watershed using logistic regression. Geomorphology, 89, 335-347.

DAI, F. C. & LEE, C. F. 2003. A spatiotemporal probabilistic modelling of storm-induced shallow landsliding using aerial photographs and logistic regression. Earth Surface Processes and Landforms, 28, 527-545.

FIELD, E. H., DAWSON, T. E., FELZER, K. R., FRANKEL, A. D., GUPTA, V., JORDAN, T. H., PARSONS, T., PETERSON, M. D., STEIN, R. S., WELDON II, R. J. & WILLS, C. J. 2008. The Uniform California Earthquake Rupture Forecast, Version 2 (UCERF 2). Open-File Report. USGS.

FIELD, E. H., GUPTA, V., GUPTA, N., MAECHLING, P. & JORDAN, T. H. 2005. Hazard Map Calculations Using Grid Computing. Seismological Research Letters, 76, 565-573.

FIELD, E. H., JOHNSON, P. A., BERESNEV, I. A. & ZENG, Y. H. 1997. Nonlinear ground-motion amplification by sediments during the 1994 Northridge earthquake. Nature, 390, 599-602.

FIELD, E. H., JORDAN, T. H. & CORNELL, C. A. 2003. OpenSHA: A Developing Community-Modeling Environment for Seismic Hazard Analysis. Seismological Research Letters, 74, 406-419.

FRY, J. A., XIAN, G., JIN, S. M., DEWITZ, J. A., HOMER, C. G., YANG, L. M., BARNES, C. A., HEROLD, N. D. & WICKHAM, J. D. 2011. National Land Cover Databse for the Conterminous United Sates. Photogrammetric Engineering and Remote Sensing, 77, 859-864.

GELI, L., BARD, P. Y. & JULLIEN, B. 1988. The Effect of Topography on Earthquake Ground Motion - a Review and New Results. Bulletin of the Seismological Society of America, 78, 42-63.

GODT, J., SENER, B., VERDIN, K., WALD, D., EARLE, P., HARP, E. & JIBSON, R. 2008. Rapid assessment of earthquake-induced landsliding. Proceedings of the First World Landslide Forum, United Nations University, Tokyo, 4.

HANLEY, J. A. & MCNEIL, B. J. 1983. A Method of Comparing the Areas under Receiver Operating Characteristic Curves Derived from the Same Cases. Radiology, 148, 839-843.

HARP, E. L. & JIBSON, R. 1995. Inventory of landslides triggered by the 1994 Northridge, California earthquake. U.S. Geological Survey Open-File Report 95-213.

HARP, E. L. & JIBSON, R. W. 1996. Landslides triggered by the 1994 Northridge, California, earthquake. Bulletin of the Seismological Society of America, 86, S319-S332.

HERVAS, J. & BOBROWSKY, P. 2009. Mapping: Inventories, Susceptibility, Hazard and Risk. In: SASSA, K. & CANUTI, P. (eds.) Landslides: Disaster Risk Reduction. Berlin: Springer.

HOVIUS, N. & MEUNIER, P. 2012. Earthquake ground motion and the pattern of seismically induced landslides. In: CLEAGUE, J. J. & STEAD, D. (eds.) Landslides: Types, Mechanisms and Modeling. 2nd ed.: Cambridge University Press.

JIBSON, R. W., HARP, E. L. & MICHAEL, J. A. 2000. A method for producing digital probabilistic seismic landslide hazard maps. Engineering Geology, 58, 271-289.

JONES, L., AKI, K., BOORE, D., CELEBI, M., DONNELLAN, A., HALL, J., HARRIS, R., HAUKSSON, E., HEATON, T., HOUGH, S., HUDNUT, K., HUTTON, K., JOHNSTON, M., JOYNER, W., KANAMORI, H., MARSHALL, G., MICHAEL, A., MORI, J., MURRAY, M., PONTI, D., REASENBERG, P., SCHWARTZ, D., SEEBER, L., SHAKAL, A., SIMPSON, R., THIO, H., TINSLEY, J., TODOROVSKA, M., TRIFUNAC, M., WALD, D. & ZOBACK, M. L. 1994. The Magnitude-6.7 Northridge, California, Earthquake of 17-January-1994. Science, 266, 389-397.

KEEFER, D. & WILSON, R. 2011. Effects from Earthquake-Triggered Landslides [Online]. USGS. Available: http://pubs.usgs.gov/of/1995/ofr-95-0213/EFFECTS.HTML [Accessed 10/07/2013].

MARANO, K. D., WALD, D. J. & ALLEN, T. I. 2010. Global earthquake casualties due to secondary effects: a quantitative analysis for improving rapid loss analyses. Natural Hazards, 52, 319-328.

MARZORATI, S., LUZI, L. & DE AMICIS, M. 2002. Rock falls induced by earthquakes: a statistical approach. Soil Dynamics and Earthquake Engineering, 22, 565-577.

MEUNIER, P., HOVIUS, N. & HAINES, J. A. 2008. Topographic site effects and the location of earthquake induced landslides. Earth and Planetary Science Letters, 275, 221-232.

NOWICKI, A. M., WALD, D. J., HAMBURGER, M. W., HEARNE, M. & THOMPSON, E. M. 2014. Development of a Globally Applicable Model for Near Real-Time Prediction of Seismically Induced Landslides. To be submitted to Engineering Geology.

PARDESHI, S. D., AUTADE, S. E. & PARDESHI, S. S. 2013. Landslide hazard assessment: recent trends and techniques. SpringerPlus, 2, 523.

PARISE, M. & JIBSON, R. W. 2000. A seismic landslide susceptibility rating of geologic units based on analysis of characteristics of landslides triggered by the 17 January, 1994 Northridge, California earthquake. Engineering Geology, 58, 251-270.

PRADHAN, B., LEE, B. & BUCHROITHNER, M. F. 2010. Remote Sensing and GIS-based Landslide Susceptibility Analysis and its Cross-validation in Three Test Areas Using a Frequency Ratio Model. Photogrammetrie Fernerkundung Geoinformation, 17-32.

SANTACANA, N., BAEZA, B., COROMINAS, J., DE PAZ, A. & MARTURIA, J. 2003. A GIS-based multivariate statistical analysis for shallow landslide susceptibility mapping in La Pobla de Lillet area (Eastern Pyrenees, Spain). Natural Hazards, 30, 281-295.

SEIRUP, L. & YETMAN, G. 2006. U.S. Census Grids (Summary File 1), 2000: Metropolitan Statistical Areas. In: (SEDAC), N. S. D. A. A. C. (ed.). Palisades, NY.

SEIRUP, L., YETMAN, G. & RAZAFINDRAZAY, L. 2012. U.S. Census Grids (Summary File 3), 1990: Metropolitan Statistical Areas. In: (SEDAC), N. S. D. A. A. C. (ed.). Palisades, NY.

SIDLE, R. C. & OCHIAI, H. 2006. Landslides: Processes, Prediction, and Landuse, Water Resources Monograph.

TIBALDI, A., FERRARI, L. & PASQUARE, G. 1995. Landslides Triggered by Earthquakes and Their Relations with Faults and Mountain Slope Geometry - an Example from Ecuador. Geomorphology, 11, 215-226.

UNISDR. 2007. Terminology [Online]. Available: http://www.unisdr.org/we/inform/terminology [Accessed 08/07/2014].

WALD, D. J., HEATON, T. H. & HUDNUT, K. W. 1996. The slip history of the 1994 Northridge, California, earthquake determined from strong-motion, teleseismic, GPS, and leveling data. Bulletin of the Seismological Society of America, 86, S49-S70.

WALD, D. J., JAISWAL, K. S., MARANO, K. D., GARCIA, D., SO, E. & HEARNE, M. 2012. Impact-based earthquake alerts with the U.S. Geological Survey's PAGER system: what's next? The 15th World Conference on Earthquake Engineering: September 24-28, 2012, Lisbon, Portugal.

YESILNACAR, E. & TOPAL, T. 2005. Landslide susceptibility mapping: A comparison of logistic regression and neural networks methods in a medium scale study, Hendek region (Turkey). Engineering Geology, 79, 251-266.

# 7. DISCUSSION

## 1.0 Summary

Multi-hazard risk assessments traditionally do not account for interaction effects between natural hazards (Kappes et al., 2012; Kappes, 2010). It is theorized in the literature that the total risk associated with multiple hazards is greater than the sum of the single hazard risks. Paper 1 establishes that there is an increase in fatalities for cascading events compared to single events. This paper focuses on the exposure and vulnerability component of the risk equation (Figure 61).

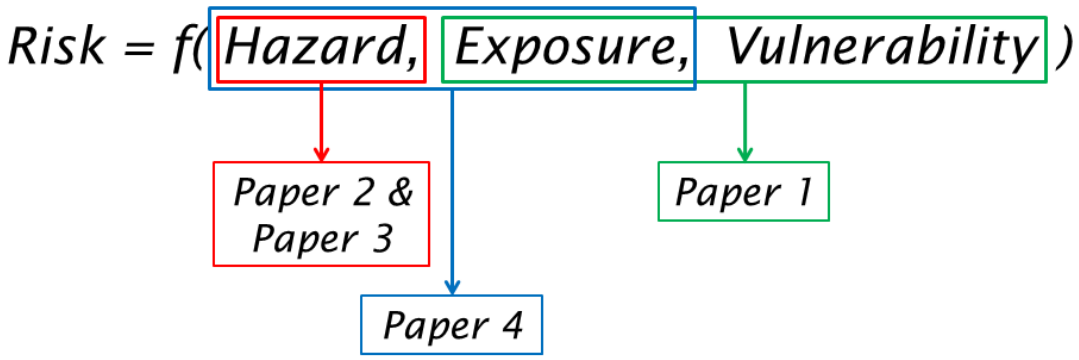


Figure 61. Diagram of how each paper presented in the thesis relates to the overall risk equation.

The amplification effect of multiple hazards interacting could not be quantified in this thesis because the separation of losses due to primary and secondary hazards is not currently available. The remainder of the thesis focused on developing an earthquake-triggered landslide hazard model and estimating the exposure of assets to high levels of earthquake and landslide hazard (Figure 61).

Logistic regression studies are one of the most popular methods of assessing landslide probabilities in the literature (Hervas and Bobrowsky, 2009; Nowicki et al., 2014b; Atkinson and Massari, 1998; Brenning, 2005). A systematic search of the literature revealed there are insufficient studies (or details within the published studies) from which to create a global

logistic regression landslide hazard model. Paper 2 showed that models for earthquake-induced landslides and rainfall-induced landslides include different covariate sets, reflecting the fact that the factors affecting susceptibility to landsliding vary by trigger. Paper 2 provided an inventory of covariates associated with landsliding in general, and specifically for earthquake-induced landslides, supporting the selection of covariates for Paper 3's logistic regression analysis.

Including peak ground acceleration in logistic regression analysis changes a landslide susceptibility model to a landslide hazard model. Peak ground acceleration was shown to have a significant relationship with earthquake-triggered landslides in Papers 3 and 4 and should be considered in landslide hazard mapping. The landslide hazard model in Paper 4 can be used with different peak ground acceleration inputs to calculate landslide and shaking hazard for any earthquake scenario. Paper 1's model has a high level of uncertainty associated with the prediction of fatalities as a result of an earthquake, so was not used to calculate losses in Paper 4. However, the exposure of assets to high landslide probability and earthquake shaking was calculated for a variety of earthquake magnitude scenarios in Paper 4. The next step required in multi-hazard risk analysis is creating fragility curves and loss functions specifically for earthquake-induced landslides in order to develop a multi-hazard risk model accounting for interacting effects.

## 2.0 Limitations

### 2.1 Limitations of the Landslide Hazard Model

Of the 37 named covariates types found to be significant in logistic regression studies more than once in Paper 2's systematic review, 22 covariates were used to develop the landslide hazard model in Paper 3 and in Paper 4 (Table 26). There were several reasons why some of the covariates were not included in the development of the landslide hazard model.

Table 26. Covariates found in the literature search from Paper 2, and the covariates used in the logistic regression analysis for Paper 3's hazard model.

| Covariates from Paper 2 | Covariates used to develop the Hazard Model |
|---|---|
| Aspect | Aspect |
| Aspect properties not covered by aspect | |
| Slope (concave) | |
| Upslope contributing area | |
| Slope curvature | Curvature |
| Density of drainage / river / stream | Drainage Density |
| Distance to drainage / river / stream | Distance to Drainage |
| Elevation | Elevation |
| Elevation range | |
| Density of faults | Fault Density |
| Distance to fault | Distance to Fault |
| Accumulated flow | |
| Flow direction | |
| Geology | Geology |
| Land use / land cover | Land cover |
| Buffer around lineament | |
| Distance to lineament | |
| Lithology / rock type | |
| Peak ground acceleration | Peak Ground Acceleration and Peak Ground Velocity |
| Planform curvature | Planform Curvature |
| Profile curvature | Profile Curvature |
| Precipitation | |
| Distance to ridge | Distance to Ridgeline |
| Density of roads | Road Density |
| Distance to road | Distance to Road |
| Terrain roughness / standard deviation of slope gradient | Roughness (3x3 and 5x5 cell sample) |
| Stream sediment transport index or capacity | |
| Slope gradient | Slope Gradient |
| Slope properties not covered by slope gradient | |
| Soil type | Soil Type |
| Soil properties, not covered by soil type | |
| Stream index or power (SPI) | Stream Power Index |
| Topography type, geomorphology, landform unit | |
| Topographic wetness index (TWI) | |
| Vegetation / NDVI | Vegetation Type |
| Weathering | |

Six of the covariates were not included because another covariate was used to represent the same type (Table 27). The covariate included in developing the model was selected in preference based on the frequency of use and significance in other logistic regression models. In addition, some of these covariates not included are difficult to obtain, for example soil properties not covered by soil type; this would require field studies to determine the properties of each soil type in the study area.

Table 27**.** Six covariates not included in the landslide hazard model development, and the similar covariate type chosen to be included in the model development in their stead.

| **Covariate not included** | **Covariate included** |
|---|---|
| Aspect properties not covered by aspect | Aspect |
| Slope (concave) | Slope gradient |
| Elevation range | Elevation |
| Lithology | Geology |
| Slope properties not covered by slope gradient | Slope gradient |
| Soil properties not covered by soil type | Soil type |

Another six covariates were not included in developing the model because they were covariates more associated with rainfall-induced landslides, rather than earthquake-induced landslides, which was the focus of the study. These covariates were: accumulated flow, flow direction, precipitation, stream sediment transport index or capacity, and topographic wetness index.

A further four covariates were not included due to the difficulty in defining the covariate itself. These were: buffer around lineament, distance to lineament, topography type/geomorphology/landform unit, and weathering. In addition, it was considered geology, slope gradient, and aspect would likely account for the relationship these covariates have with landsliding.

By not including all of the 37 covariates found to be significantly associated with landsliding in Table 26, the model could be excluding covariates which are significantly associated with landslide events in the 1994 Northridge study site. Whilst the most commonly significant covariates are included, it could be that other variations of the same type of parameter have a

stronger relationship with landsliding than the ones included in developing the model. Ideally, all 37 covariates would have been included in the model, and the most significant relationships would have been selected by backward stepwise regression modelling. However, this was not carried out in practice for Paper 3 or Paper 4, and as such, it is unknown whether the covariates not included in the model development have or do not have a significant relationship with landsliding caused by the Northridge earthquake.

The spatial resolution of the datasets used to develop the landslide hazard model varied (Table 19). However, all variables were rasterised to a 1km spatial resolution for consistency in the model development. This included the landslide inventory map. A cell was therefore assigned a 'landslide' or 'non-landslide' status based on what the majority of the cell was covered in. Some of the landslides caused by the 1994 Northridge earthquake were smaller than 1km, and as such, when rasterised many of the landslide occurrences were not represented as a 'landslide' cell in the final dataset used in the model. The 11,000 recorded landslide events were represented by 3,358 landslide cells. Many of the landslide occurrences were missing and automatically classified as a 'non-landslide' cell because they covered a small spatial area. The landslide hazard model therefore was developed using 'non-landslide' cells which could have contained a landslide event. This has implications for the training of the model, and the accuracy of the model and results. Some of the error in the model can be attributed to this. To minimise the influence of this, a buffer zone of 1km was placed around each landslide cell, and only cells outside of these buffer zones were drawn on to randomly select non-landslide cells which were used in the development of the model.

Table 28. Spatial resolution or scale and source for the independent environmental covariates used for each study site.

| **Covariate** | **Spatial resolution (or scale if given as a ratio)** |
|---|---|
| DEM | 30 arc-seconds (approx. 1km) |
| Drainage | 3 arc-seconds (approx. 1m) |
| Faults and Geology | 1:40,000,000 < scale < 1:5,000,000 |
| Land use | 30 m |
| PGA | 1.6 km |
| PGV | 1.6 km |
| Roads | 1:2,000,000 |

| | |
|---|---|
| Soil | 1:250,000 |
| Vegetation | km |

## 2.2 OpenSHA Peak Ground Acceleration Generation

The OpenSHA tool generated peak ground acceleration maps using attenuations models. There are two ways to input the initiating event: point-source input variables, or defining the fault rupture zone (either manually, or by selecting previously recorded events in the OpenSHA database). The tool then calculates the peak ground acceleration based on the selected ground motion attenuation model, and the soil map input variable. There are thirteen attenuation models that are available to be used by the tool (Table 29); the attenuation relationship must be chosen by the user.

Table 29. Attenuation models available in OpenSHA

| **OpenSHA Attenuation Relationships** |
|---|
| Abrahamson and Silva (1997) |
| Abrahamson and Silva (2008) |
| Abrahamson (2000) |
| Boore and Atkinson (2008) |
| Boore, Joyner and Fumal (1997) |
| Campbell and Bozorgnia (2008) |
| Campbell (1997) |
| Chiou and Youngs (2008) |
| Field (2000) |
| Sadigh et al. (1997) |
| ShakeMap (2003) |
| Spudich et al. (1999) |
| USGS Combined (2004) |

Campbell's (1997) attenuation model was selected based on least RMSE compared to observed data for use in Paper 4 to generate the peak ground acceleration variable. It was developed as a combination of attenuation relationship previously developed by the author from 1990 to 1994 (Campbell, 1997). These were specifically developed to predict horizontal and vertical components of peak ground acceleration, peak ground velocity and 5% damped pseudo-absolute acceleration response spectra in the near-source region of moderate-to-large earthquakes (Campbell, 1997). The strong motion database used to

develop the attenuation relationships (Figure 62) was compiled from worldwide earthquakes of moment magnitude ($M_w$) ≥5 and sites with distances to seismogenic rupture ≤60km in active tectonic regions (Campbell, 1997). Moment magnitude was used to define earthquake magnitude as it avoids the "saturation" of other band-limited measures at large seismic moments (Campbell, 1997). Various styles of faulting were considered as a variable in the attenuation model such as strike-slip faulting, reverse, thrust, reverse-oblique, and thrust-oblique faulting (Figure 62) (Campbell, 1997). Local site conditions such as alluvium or firm soil, soft rock, and hard rock were also used to determine attenuation relationships (Figure 62) (Campbell, 1997).

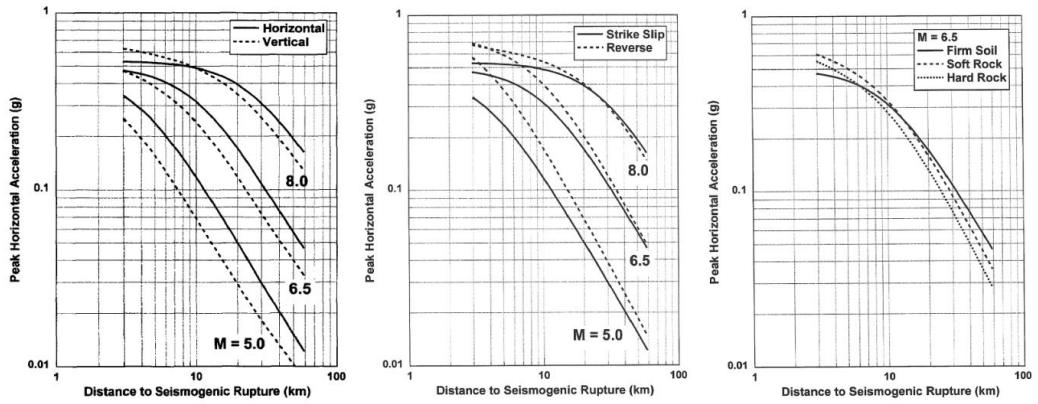


Figure 62. Scaling of peak ground acceleration with magnitude, distance, ground motion, style of faulting, and local site conditions predicted by the attenuation relationship developed by Campbell et al. (1997). Acquired from Campbell et al. (1997, figures 8, 9, and 10, pages 172-173).

The method for determining the earthquake input parameters was a point-source event, rather than determining the fault surface. Delineating the fault surface was beyond the scope of this thesis. Rather, the location and magnitude of the epicentre of the earthquake event was input into OpenSHA, and the peak ground acceleration variable used to estimate landslide probability and exposure of assets to earthquake shaking calculated using Campbell's (1997) attenuation model. Using the point-source input method rather than a fault surface rupture introduces error into the model used to generate peak ground acceleration. Whilst the point-source method is the simpler method to use, requiring less demanding calculations, it does not reproduce the physical mechanisms which result in earthquake ground motion

realistically. An earthquake (such as the Northridge 1994 event) is caused by two surfaces sliding past each other, and the energy released from the fault surface generates the ground motion. By isolating the origin of the release of energy to a point-source, the patterns of dispersal of energy are altered drastically. The implications of this change in representation of reality is likely to skew the peak ground acceleration data produced from the model, introducing error which can be seen when comparing observed data to simulated data.

The simulated OpenSHA peak ground acceleration data was compared to the recorded peak ground acceleration data observed as a result of the 1994 Northridge event. The aim was to generate a peak ground acceleration map as similar to the original data as possible. However, there was a difference in the OpenSHA peak ground acceleration estimates and those observed during the 1994 Northridge event. The OpenSHA peak ground acceleration simulated lower values than the recorded peak ground acceleration during the 1994 Northridge earthquake. The majority of negative error is located in the San Fernando Valley, which suggests the input parameters used in the OpenSHA tool might not represent the fault process observed during the 1994 Northridge earthquake with sufficient accuracy. Another reason may be that there is a difficulty in the model to simulate ground amplifications in basin soils. In addition, it must be noted that the peak ground acceleration values recorded during the 1994 Northridge earthquake were significantly greater than is typically expected during a $M_w$6.7 earthquake event (Jones et al., 1994). This may be why the OpenSHA model underestimates ground motion in the San Fernando Valley. As the San Fernando Valley is predominantly flat terrain, it was not affected by landsliding and, thus, does not greatly affect the ability of the landslide hazard model to estimate landslide probability.

The positive error between the OpenSHA model-simulated peak ground acceleration and the recorded peak ground acceleration was mostly confined to the northwest of the epicentre, in the rougher terrain. This is where the OpenSHA peak ground acceleration simulated higher values than the recorded peak ground acceleration during the 1994 Northridge earthquake. This may be due to several reasons, such as the model's point-source origin, or a limitation

in determining ground motion in rough terrain. This discrepancy could also be due to error in the peak ground acceleration map in steeply sloped areas produced from the recorded event. Very few recording stations were located in steeply sloping areas where landslides occurred. Field evidence of topographic amplification suggests that ground motion the mountainous areas where landslides occurred was much higher than would have been modelled by interpolating between flat land sites.

As there is substantial error in peak ground acceleration simulated data in the mountainous areas, this has implications on the reliability of landslide probability estimates using the logistic regression hazard model. Since the OpenSHA model overestimates peak ground acceleration in rougher terrain, it follows that the landslide hazard model is likely to over-estimate landslide probability in these susceptible regions. Therefore, when interpreting the earthquake-triggered landslide exposure maps, the likely over-estimation of landslide probability must be taken into consideration based on the error in the OpenSHA model. In addition, when interpreting the exposure to significant earthquake ground motion, it should be acknowledged that it is likely these ground motion estimates are likely to be under-estimated in the San Fernando Valley.

## 2.3 Limitations of an empirical approach

The empirical approach adopted in this project has several limitations, such as the availability, accessibility, and quality of the data used in modelling earthquake-triggered landslides. Expert-driven or holistic methods of modelling probability and losses caused by earthquake-triggered landslides are alternative methods.

The main limitation of adopting an empirical approach to earthquake and landslide modelling is that the quality and accuracy of the model is restricted by data availability. Despite the data revolution that is currently underway, there is not a global method used to record earthquake-triggered landslides, and the impact of the landslides. Landslide inventories are more frequently recorded after an earthquake event, particularly since

satellite imagery has become more widely available. However, the creation of comprehensive earthquake-triggered landslide inventories is not widely available for more historic earthquake events. Loss data attributed to landslides or to cause of death from a multi-hazard event are not widely available. Collection of data in the aftermath of a disaster is typically only conducted for urgent and rapid assessment of the situation, in order to prioritise emergency management and response. Records may be kept of the cause of death or injury as a result of a disaster for isolated events, but these are rarely available for open access online.

Another limitation of the empirical approach is that in some instances, despite the availability of data (i.e. the data has been created), the data may not be accessible or openly available for use. This paradigm is changing as we begin to see more open accessibility of data and data sharing on the internet; geonodes are particularly useful for data sharing. Alternatively, if data is not readily accessible via download on the internet, but it is known that it exists (such as a published paper makes reference to the existence) researchers can contact the creators of data to request access to the data. This successfulness of this method depends on the licencing and ownership of the data, and the individual choices made by the creators of the data.

Even if the data is available and accessible, the quality and reliability of the data and source may not be suitable for use in the research. For example, soil and geology data has recently become available in digital format for the whole globe. However, the spatial resolution of these data may not be on a scale in line with an earthquake-triggered landslide inventory map. In addition, the internet has led to a vast amount of new data to be available worldwide to anyone with a computer and internet connection. Distinguishing between the available resources to determine usefulness, and trustworthiness, will remain the role of the person accessing the data. The source and the methodology that has led to the creation of openly available data must be first critically assessed before use.

Data-driven methods of landslide susceptibility and hazard analysis are also sensitive to the training data used (Wang, 2008). A slight change of the input data can lead to a great change in the regression coefficients (Wang, 2008). In landslide models, the sensitivity is highly influenced by the landslide inventory map. Landslide absence/presence data are used to train the landslide susceptibility model as examples of negative/positive training data. Determining the absence or presence of a landslide body is open to interpretation; the deposition of landslide material could be considered as 'positive', but there is also an argument that only the landslide scar be considered a 'positive'. The inventory map has inherently high uncertainty. This combination of highly uncertain data input and sensitive models makes the landslide susceptibility models unstable, which should be taken into consideration when interpreting the results of the regression (Wang, 2008).

Empirical landslide susceptibility models are also location-specific and not capable of capturing general susceptibility relationships. They cannot be automatically applied to another geographical location. Without consideration of the physical processes and mechanisms involved in landsliding, the models behave like a 'coincidence fit' of the data in the study area and may lead to coarse or misleading regression relationships (Wang, 2008). These relationships are meaningless without consideration of the physical processes behind them, and are even more meaningless when applied to other locations (Wang, 2008).

An alternative approach to the empirical method is to bypass data and instead source from expert opinions in an expert knowledge-based approach. Expert knowledge is "a combination of theoretical understanding of the problem and a collection of heuristic problem-solving rules that has shown through experience to be effective in the domain" (Luger and Chakrabarti, 2005; in Wang, 2008). The expert knowledge-based system is typically comprised of three components: user, knowledge base, and inference engine (Wang, 2008). The user provides information or facts to the expert knowledge-based system and receives expert advice or expertise in response (Figure 63). The knowledge base captures the domain specific knowledge, particularly the relationships between events and

phenomena (Wang, 2008). The inference engine consists of algorithms for manipulating the knowledge in the knowledge base and draws corresponding conclusions based on the information supplied by the user (Wang, 2008).

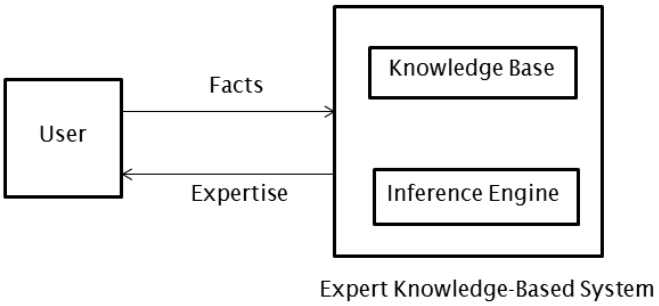


Figure 63. Basic architecture of an expert knowledge-based system (after Giarratano and Riley, 1998).

The main advantage of an expert knowledge-based approach to landslide susceptibility modelling is that is bypasses the need for complete, accurate, and reliable data. The relationships between coefficients and landslide susceptibility are based on knowledge of the physical processes behind landslide occurrence. Experts will have built up this intuitive knowledge from years of experience and research in the local area. A major advantage of qualitative expert knowledge-based methods is that it does not require a landslide inventory. Therefore, a landslide susceptibility assessment can be applied to a region where no landslides have previously occurred (Hong et al., 2007). A limitation of the expert-driven approach is that it can be significantly less accurate than the quantitative approach (Hong et al., 2007).

A compromise between the expert approach and empirical approach is to take a more holistic approach by combining the two. An example of this is the Weights of Evidence (WOE) method. WOE is a quantitative statistical approach, where conditional probability (based on the Bayesian model) is founded on evidence. Positive and negative weights are assigned to parameters to estimate susceptibility. A positive weight indicated that the parameter class is favourable for the occurrence of landslides (such as slope gradient). A negative weight indicates the presence of the class reduces the landslide susceptibility (such as vegetation).

Weights around zero indicate there is no relation between the occurrence of landslides and the parameter. The benefit of this method is that is combines both the positive aspects of the purely quantitative approach and the purely qualitative approach.

## 2.4 Geographical Bias

There is geographical bias in the distribution of studies found in the systematic literature search in Paper 2. Europe (in particular Turkey) has a high representation in the literature review of logistic regression studies. European studies make up 43% of logistic regression studies selected for the literature review analysis, whilst 47% have been conducted in Australasia. This does not reflect the observed pattern of landsliding globally. The number of landslide occurrences (Figure 64) and also the susceptibility to landsliding (Figure 65) shows there are more events and a higher susceptibility to landsliding in areas such as Asia and South and Central America, compared to Europe.

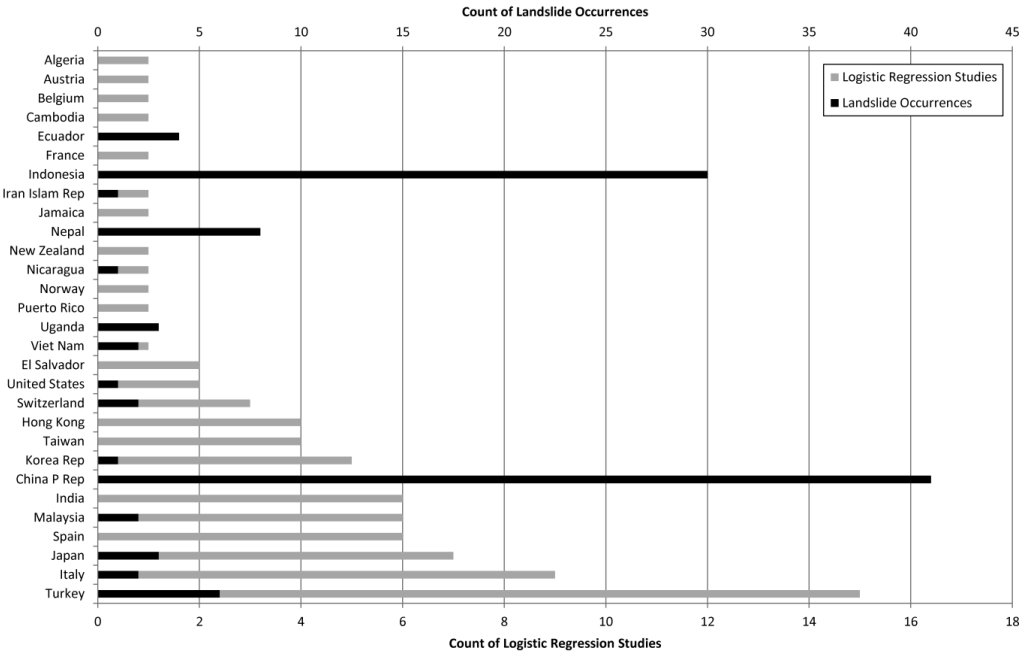


Figure 64. Plot of the country of origin for each logistic regression landslide study, against the number of recorded landslide occurrences during the same timescale (2000-2013). Data on landslide occurrences are sourced from EM-DAT (CRED, 2014). Note the landslide occurrence data only refers to recorded landslide events where at least one of the following criteria are fulfilled: ten or more people reported killed, hundred or more people reported affected, declaration of a state of emergency, call for international assistance. The data therefore may not reflect the true landslide occurrence rates per country, but should give enough information to be able to compare against landslide logistic regression study rates in each country.

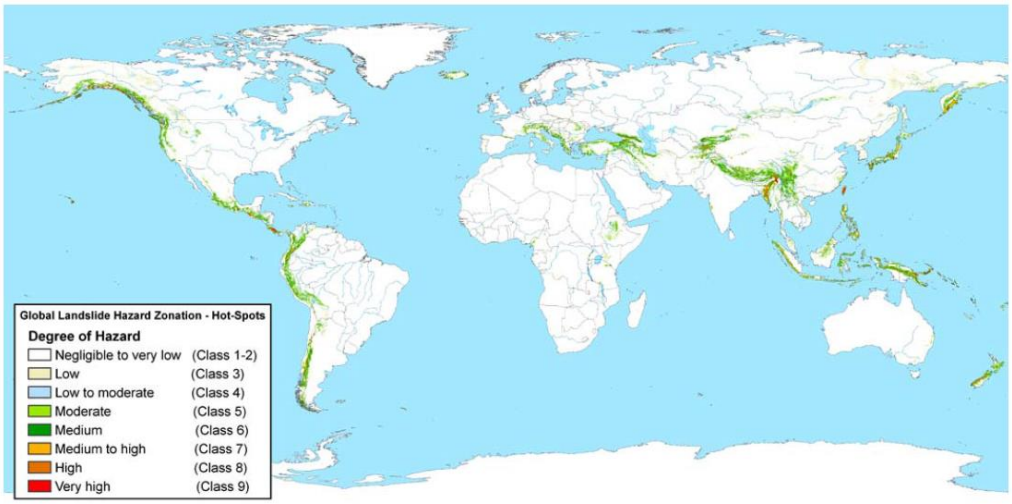


Figure 65. Global hotspot landslide zonation (Nadim et al., 2006, fig 7, p166).

The high proportion of landslide logistic regression studies conducted in Europe could reflect the funding opportunities for landslide-associated research in Europe. For example, Turkey dominates the logistic regression studies with 15 out of the 92 studies conducted in the country. For the 13 papers where the landslide inventories were located in Turkey, at least one of the authors was employed in either a university or institution in Turkey (Table 30). Geographic location of authors of landslide logistic regression papers is likely to be the reason for the proliferation of landslide studies conducted in certain countries, rather than a reflection of the geographic severity or frequency of landslide occurrence.

Table 30. Studies found in the systematic literature search, where the research was conducted in Turkey.

| **Author(s) of paper** | **Year** | **Study site** |
|---|---|---|
| Akgun and Bulut | 2007 | Arsin-Yomra |
| Akgun et al. | 2012 | Izmir |
| Akgun | 2012 | Izmir |
| Can et al. | 2005 | Agustu |
| Can et al. | 2005 | Egerci |
| Can et al. | 2005 | Klemen |
| Duman et al. | 2006 | Cekmece Area, Istanbul |
| Ercanoglu and Timaz | 2011 | Azdavay |
| Kincal et al. | 2009 | Izmir |
| Nefeslioglu et al. | 2008 | Kelkit Valley |

| | | |
|---|---|---|
| Ozdemir and Altura. | 2013 | Sultan Mountains |
| Suzen and Kaya. | 2011 | Asarsuyu |
| Yalcin et al. | 2011 | Trabzon |
| Yesilnacar and Topal. | 2005 | Hendek |
| Yilmaz | 2009 | Kat, Tokat |

Despite aiming for comprehensiveness in literature searching, there are limitations in what can be found. It is likely there are publications in other languages investigating landslide logistic regression analysis; this may be particularly true for Asian countries and South American countries. However, the search terms were conducted in English, thus limiting the geographic and language scope of the results from the search. This could be an additional contributing factor to the geographic bias in the literature search results.

The geographical distribution of landslide logistic regression papers in Paper 2 is a problem as it introduces bias into the literature review analysis. The covariates found to be significant in the analysis in Paper 2 will be partly dominated by the ones found significant in Europe. Europe has a different geological, topographical and climatology compared to other regions with landslides globally, for example South America. Whilst the general principles and physical processes behind landsliding as a natural phenomenon should be found to be significant in each landslide event, the dominating processes behind landsliding are likely to be different given different geological, topographical and climatological conditions. This will impact the significance of relationships with covariates entered into the logistic regression analysis studies.

Therefore, whilst the results provide a list of covariates commonly found to be associated significantly with landslide occurrence, which can be used in future logistic regression studies, the geographical bias of the logistic regression studies used in the systematic literature review should be taken into consideration when interpreting the results; extrapolation of results globally should be treated with caution.

## 2.5 GIS Parameters

Capturing parameters used in developing logistic regression models of landslide hazard in a format suitable for GIS is often problematic. Recording natural phenomena in a computerised system requires assumptions to be made and compromises the accurate representation of reality. There are multiple sources where error can be introduced into the process.

Landslide inventories are typically created from satellite imagery, comparing before and after images to delineate changes in the environment which would suggest a landslide. Whether this method is conducted by human interpretation or by computer calculations, both methods can introduce error into the accuracy of delineating the landslide occurrence. Determining the landslide area, i.e. where the landslide initiated, where the scar appears, and where the material is deposited, is important. When the spatial resolution of the study site is higher, clearly defining the rupture zone is important. In lower spatial resolution studies, the whole movement can be used to analyse the relationship with causal factors with minimal errors in calculations. However, at higher spatial scales, the conditions under which landslides are generated can be very different to the conditions where the landslide debris settles further down the slope. Using the full movement of the landslide can introduce noise to the data and therefore inaccurate susceptibility maps. Care must be taken to accurately delineate the rupture zone, and use this spatial area to establish statistical relationships with causal factors.

Peak ground acceleration data from and earthquake event is initially captured on seismometers in the region, and the peak ground acceleration in between stations is estimated, rather than observed. Therefore the accuracy of peak ground acceleration data from an earthquake event is reliant on the spatial density of seismometers to capture the observed ground motion, and the accuracy of the computational method or model used to infer the peak ground acceleration values between stations. The accuracy of peak ground

acceleration data from earthquake events can be reduced particularly in rough terrain, where recording stations are sparse, and the ability to determine peak ground acceleration in steep topography is highly complex using attenuation models. For example, of the 200+ recording stations used to record the Northridge earthquake shaking, very few were located in steeply sloping areas where landslides occurred (Figure 66). The field evidence of topographic amplification suggests that the shaking in the mountains was much higher than would have been modelled by interpolating between flat land sites. The ShakeMap for the Northridge 1994 event was generated using the recorded ground motions from seismometers in Ventura and Los Angeles Counties and interpolated between stations using the attenuation model and ground amplification factors of Borcherdt (1994).

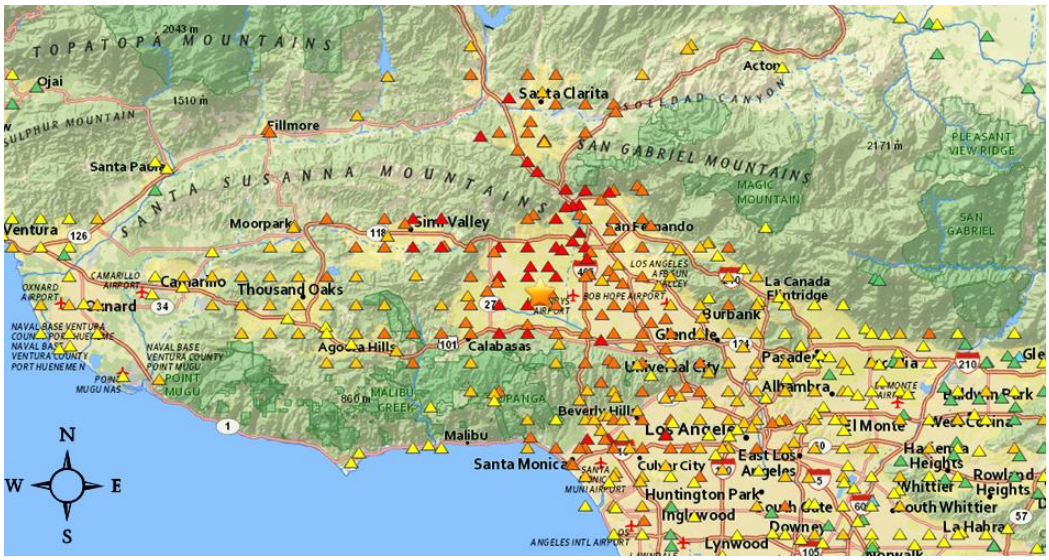


Figure 66. Map showing the location of seismic recording stations in the Northridge area. The triangles represent recording stations; the star represents the epicentre of the 1994 Northridge earthquake. Note the lack of recording stations in the Santa Susana Mountains and San Gabriel Mountains, where the majority of landslides were observed.

Parameters such as geology, soil, land cover, and vegetation are typically at low spatial resolution, unless a detailed study was conducted in the region. Capturing these parameters in a GIS environment means that each grid cell or vector area is assigned a ‘type’. Using geology as an example, this infers that geology type changes abruptly, which is rarely the case in nature. This not only inaccurately represents reality accurately, but also has implications on the output of susceptibility and hazard maps. If one particular type of

geology is significantly associated with landsliding, then when estimating landslide probability, the results will show an abrupt change spatially when one significantly related geology type ends and another less significantly related geology type begins. This can be seen particularly in the results of Paper 4, where the underlying geology influences the patterns of landslide probability quite clearly.

The location of faults is difficult to capture in a GIS environment for two reasons. The first is that the fault lines recorded only show where the faults are estimated to emerge onto ground level. Since faults are below the surface, determining their exact location is inherently uncertain. Once an earthquake has occurred on the fault, and there are sufficient recording stations to capture the movement, there is more certainty as to its location. However, faults rarely occur vertically through the ground, therefore the epicentre and the fault rupture zone may be in a different spatial location than the mapped fault line. The second difficulty is that not all fault lines are known. The fault line that caused the 1994 Northridge earthquake was a previously unmapped fault. For example, the causative fault of the Northridge earthquake is part of a broad system of thrust faults at the Big Bend of the San Andreas fault, resulting from the left step in the Pacific-North American plate boundary (Jones et al., 1994). The hypocentre was 18 km beneath the city of Northridge in the San Fernando Valley on a blind thrust fault striking N58°W and dipping 42°southward (Harp and Jibson, 1996). However, the fault was not mapped before the event and did not extend to the surface (Jones et al., 1994).

## 2.6 Autocorrelation

Landslide occurrence data tend to exhibit clustering, or spatial autocorrelation, i.e. if one cell is classified as a landslide, the neighbouring cells are more likely to be as well (Augustin et al., 1996; Van Den Eeckhaut et al., 2005). Neighbouring cells tend to have similar characteristics, and if the input covariates do not fully reflect the conditions of landslide occurrence, then the residuals from a fitted model will exhibit spatial autocorrelation

(Augustin et al., 1996). Furthermore, the probability of occurrence of a landslide in one cell may not be independent of whether landslides occur in a neighbouring cell (Augustin et al., 1996).

Therefore, when logistic regression analysis using all the cells within the study area is performed, computed test statistics are too often declared significant under the null-hypothesis (Van Den Eeckhaut et al., 2005). Fitted probabilities of presence/absence data obtained from an ordinary logistic model may not reflect the true level of clustering in the distribution of landslides (Augustin et al., 1996).

Besides the autocorrelation resulting from the homogeneity of landslide units, spatial correlation may exit in the set of parameters at a range of difference scales (Atkinson and Massarri, 2011). Spatial data are frequently autocorrelated up to a certain distance called the range of autocorrelation (Brenning, 2005). In developing the landslide susceptibility and hazard models, the existence of relationships between the input parameters should be taken into consideration (Brenning, 2005). For example, there is likely to be a relationship between slope gradient and lithology because lithology types weather at different rates, and are found in different topographical locations e.g. lithology types such as depositional sedimentary varieties are likely to be found on floodplains, and therefore will have a strong correlation with low or flat slope gradients.

A limitation of the logistic regression modelling approach is that it ignores the possibility of spatial autocorrelation in the residuals (Augustin et al., 1996; Erener and Duzgun, 2010). This may increase the explanation power of the susceptibility assessment, which is partly why logistic regression analysis is popular as a landslide susceptibility assessment method (Erener and Duzgun, 2010). The logistic regression model represents the relationship between the landslide occurrence and influencing factors for the entire study region; susceptibility maps may contain large errors for some parts of the study region in which the constructed relationship may not be strong, because of local variations (Erener and Duzgun,

2010). This reduces the reliability of the produced susceptibility maps (Erener and Duzgun, 2010).

When this spatial correlation is not accounted for in the regression model and the residuals of the fitted model map are autocorrelated, it violates the assumption of the logistic regression that residuals are independent and identically distributed (Atkinson and Massarri, 2011). This can lead to incorrect significance estimates for the parameters (Atkinson and Massarri, 2011). In addition, by modelling landslide susceptibility on a cell-by-cell basis, the spatial context is ignored and the resulting map may include abrupt changes in predicted susceptibility between neighbouring cells where actual susceptibility is similar (Atkinson and Massarri, 2011). This can be seen in the results of the landslide susceptibility and hazard models in Paper 3 and Paper 4, where the probability of landsliding abruptly changes, matching the geology coefficient's spatial distribution.

A way of avoiding or reducing this problem is if only one cell (typically the central cell) for each landslide occurrence is used for the creation of the susceptibility map (Van Den Eeckhaut et al., 2005). Another method is to randomly select a subset of the landslide cells for use in the training data (Chang et al., 2007; Atkinson and Massarri, 2011). This second method was used to select training data for Paper 3 and Paper 4. A third method, which attempts to address the correlation between input parameters is to analyse the relationships between them, and use only a selection of parameters in developing the model that are shown to be independent of each other, e.g. if slope gradient and lithology are shown to be significantly correlated, only select one as an input parameter in to train the model. However, there are more sophisticated alternatives which can circumvent or at least reduce the autocorrelation issue further.

Spatial regression is a global spatial modelling technique in with spatial autocorrelation among the regression parameters are taken into account, and thus circumvent the spatial autocorrelation issue in logistic regression (Erener and Duzgun, 2010). Whilst the logistic

regression method assumes a global model of relationships within the entire study site, the spatial regression method takes into account the reality that different influencing parameters may have different degrees of effect at the local scale for the study region (Erener and Duzgun, 2010).

Spatial logistic regression, the so-called autologistic regression model, has been used extensively in ecology to circumvent this problem, but has not been widely adopted for landslide susceptibility modelling (Atkinson and Massarri, 2011). Autologistic models allow for spatial autocorrelation in the presence/absence data (Augustin et al., 1996). The basic objective of autologistic regression is to account for the (potentially informative) spatial correlation between neighbouring cells, in addition to the correlation between the response and explanatory variables (Atkinson and Massarri, 2011). This is done by forming an autocovariate, by estimating the landslide susceptibly of each cell in a grid as a (typically inverse distance) weighted average of its neighbours (Atkinson and Massarri, 2011). The more neighbouring cells included in the calculation, the larger the decrease in deviance (Atkinson and Massarri, 2011).

Results show that the logistic regression model underperforms compared to spatial regression models, and the spatial regression model gives more realistic results (Erener and Duzgun, 2010). However, the spatial regression model is much more computationally demanding and therefore takes longer to perform (Augustin et al., 1996; Erener and Duzgun, 2010).

## 3.0 Further Investigation

### 3.1 Global earthquake-and-landslide fatality model

The main limitation experienced in fitting a global earthquake-and-landslide fatality model was the availability of sufficiently detailed data. The accuracy of the model presented in

Paper 1 can be increased with a more accurate "population exposed" model, utilising more accurate peak ground acceleration models and finer spatial resolution population data.

The circular buffer model used in Paper 1 to estimate population exposed to ≥0.18 g shaking is very simplistic (Figure 67). It ignores differences in the initial earthquake rupture process and geological and geomorphological effects on ground motion (Field et al., 1997; Tibaldi et al., 1995; Brown and Ghilarducci, 2013; Geli et al., 1988; Hovius and Meunier, 2012; Sidle and Ochiai, 2006). The OpenSHA application used in Paper 4 is an improvement on the estimated area affected within the model as the peak ground acceleration data produced with OpenSHA takes into consideration factors such as the depth of the rupture, geology, soil type, and topographic features (Field et al., 2005b; Field et al., 2003). Whilst the OpenSHA model is itself a simplification of the spatial distribution of peak ground acceleration, it provides a more accurate depiction of the area affected by ≥0.18 g for earthquake events (Figure 67). The circular buffer underestimates the area affected by ≥0.18 g shaking by 24.3% compared to the recorded shaking distribution. The OpenSHA model underestimates the area affected by 15.8% compared to the recorded shaking, showing an increased accuracy.

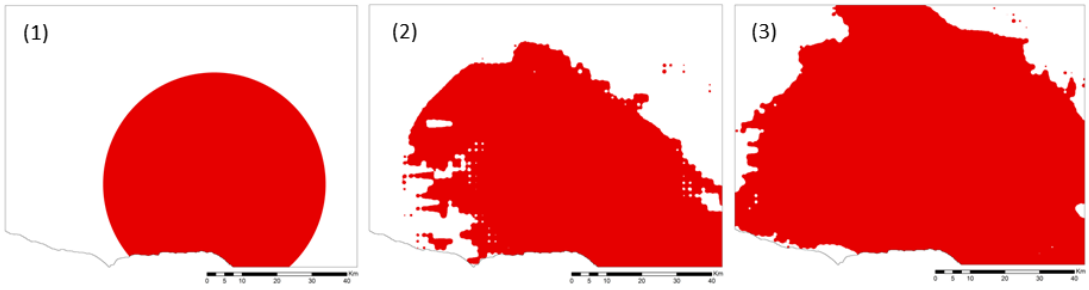


Figure 67. Area affected by ≥0.18 g predicted for the $M_w$6.7 Northridge 1994 earthquake simulation using (1) the area affected circular buffer model used in Paper 1, (2) the OpenSHA generated peak ground acceleration used in Paper 4, and (3) the recorded peak ground acceleration during the 1994 Northridge earthquake.

The estimation of the area affected can also be improved further using a feature of the OpenSHA model not used in the studies in Paper 3 and Paper 4. In the studies presented in this thesis, the OpenSHA peak ground acceleration was modelled using the input parameters

of a point source of each earthquake scenario. The peak ground acceleration was then calculated by the model, dispersing the seismic energy according to the selected attenuation model, taking into account soil and topographical influences on peak ground acceleration dispersal. However, there is a more complex model included in OpenSHA, where the initial rupture area is used as the input, rather than a point source. This represents the physical process of fault rupture more realistically. This method was not used in Paper 3 and Paper 4 due to the unavailability of initial fault rupture data. However, determining the depth, width, length, and dip of the rupture is possible to calculate. Whilst this calculation is beyond the scope of this thesis, further investigation could calculate these input variables and be used to re-calculate the peak ground acceleration variable and therefore a more accurate depiction of exposed areas.

Finer spatial resolution population data would increase the accuracy of population exposed estimates (Figure 68). In Paper 1, Gridded Population of the World (GPWv3) data at 2.5 arc minutes spatial resolution were used to estimate the number of people exposed to >0.18 g for each earthquake (CIESIN, 2005). Paper 4 used gridded population data from census block geography for California (Seirup and Yetman, 2006). Whilst this spatial resolution is not available globally, the difference in population estimates using the world gridded population compared to the census population data is large (Figure 68). For the magnitude 6.7 earthquake scenario presented in Paper 4, the census data estimate 3,871,315 people exposed to ≥0.18 g; using the gridded population of the world data, this estimate of exposed population rises to 4,033,864 people.

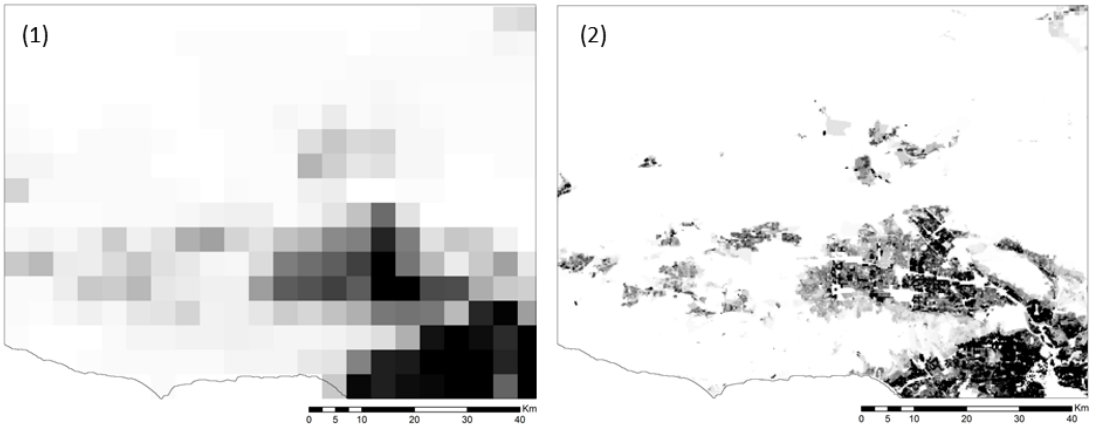


Figure 68. Population density for the Northridge site comparing (1) GPWv3 at 2.5 arc min used in Paper 1; and (2) population data at the census scale for 250 $m^2$ spatial resolution used in Paper 4.

## 3.2 Statistical Method

Logistic regression was chosen as the statistical method for fitting the landslide hazard model for several reasons covered in Papers 2, 3 and 4. However, there are many other multivariate statistical analysis approaches that can also be used to predict landslide probability (Brenning, 2005; Hervas and Bobrowsky, 2009). The advantage of the logistic regression method is that it is fairly easy to implement, with highly accurate prediction results, and is able to produce a probability of landsliding map as a result of peak ground acceleration. It is one of the most popular methods for assessing landslide probability, the other being Discriminant Analysis (DA) (Brenning, 2005; Santacana et al., 2003). Another method gaining popularity and high success rates is artificial neural networks (ANN) (Yesilnacar and Topal, 2005).

Using a different statistical method other than logistic regression to fit a landslide hazard model would be unlikely to change considerably the factors that were significantly associated with landsliding. Each statistical method attempts to find relationships between landslide occurrence (and/or non-occurrence) and environmental or triggering factors. The precise means by which the method determines the significant factors may vary between statistical methods; however, the underlying mechanisms of landsliding should be represented where possible in each method. For example, slope will always have a large

correlation with landsliding because landslides by their nature require a slope from which to fail (Sidle and Ochiai, 2006). For earthquake-triggered landslides, although environmental factors such as geology and topographic features will affect the susceptibility to landsliding, ground shaking is the dominant extrinsic factor in determining failure. Without the earthquake causing ground shaking, it is highly unlikely that the landslides would occur. Peak ground acceleration will always have a large correlation with failure whatever the statistical method because, as the trigger, it is the most dominant factor in earthquake-triggered landslide events.

The recommendations from Paper 2 can also be used to guide other statistical methods of modelling landslide susceptibility and hazard. For example, the choice of covariates to include in any statistical analysis will be dependent on data availability and a range of site-specific factor; however, the choice of parameters to initially include should be selected in an informed and systematic way. A comprehensive list of initial covariates should be included, before systematically eliminating the non-significant covariates through fitting the statistical model. The systematic literature search of landslide logistic regression studies undertaken in Paper 2 provides valuable information in the form of a list of covariates which can be used as a starting point for selecting parameters to be included in any future landslide susceptibility or hazard modelling, whatever statistical method is selected.

Other recommendations which are just as applicable to other statistical methods as logistic regression analysis are:

- Publish all the covariates entered into the logistic regression, whether or not they are found to be significant as a result of the logistic regression fitting.
- Publish the landslide types recorded in the landslide inventory because landslide type can affect which covariates are found to be significant. When multiple types are present, report the proportion of each type of landslide found in the study site.

- Publish the landslide density for the covariates found to be significant; this will provide a more in-depth understanding of the relationship between landsliding and covariates.

### 3.3 Alternative Scenarios in Southern California

The number of scenarios simulated for Northridge in Paper 4 can be increased to assess the earthquake-triggered landslide hazard in other locations in Southern California. For example, the earthquake epicentre could be changed to occur in a different location on fault lines in Southern California. There are many fault lines present in the study site and in the surrounding region (Figure 69).

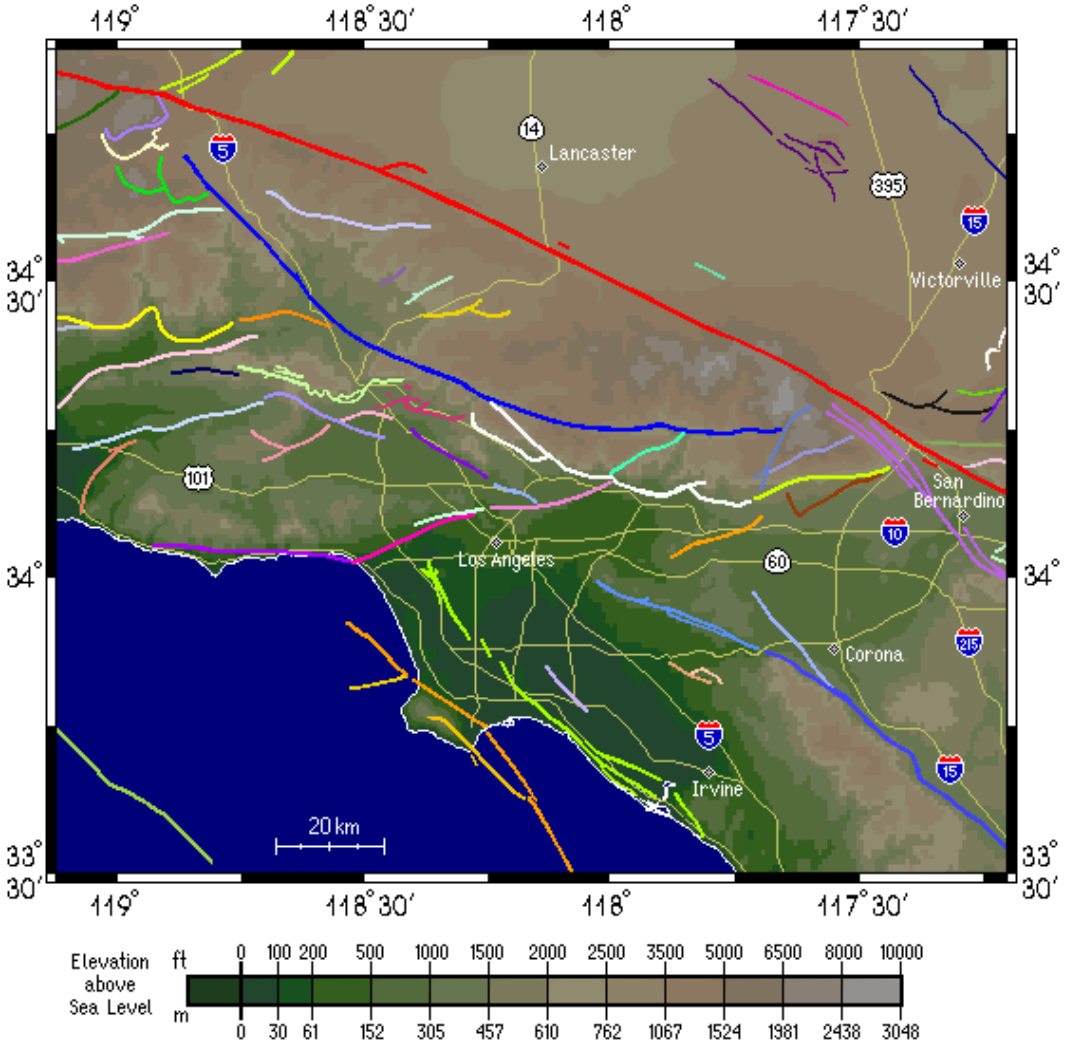


Figure 69. Faults of Southern California. Sourced from Southern California Earthquake Data Center, (http://www.data.scec.org/significant/losangeles.html), accessed 11/06/2014.

The study presented in this thesis is confined to exploring what would happen if the 1994 earthquake occurred tomorrow, albeit with varying magnitude. The likelihood of the earthquake occurring at the same location a second time is not calculated in this study, although the region is seismically active and prone to earthquakes. On 17th March 2014 a $M_w$4.4 earthquake occurred not far from the epicentre of the 1994 Northridge earthquake event (Figure 70). There were no landslides as a result of the 2014 Westwood earthquake; supporting Keefer's (1984) findings that $M_w$4.0 is the lowest threshold earthquake shaking typically triggers landslides. However, the event serves as a reminder of the risk from earthquakes in the region. It would be useful for urban planning and disaster management to simulate alternate earthquake scenarios in the surrounding region.

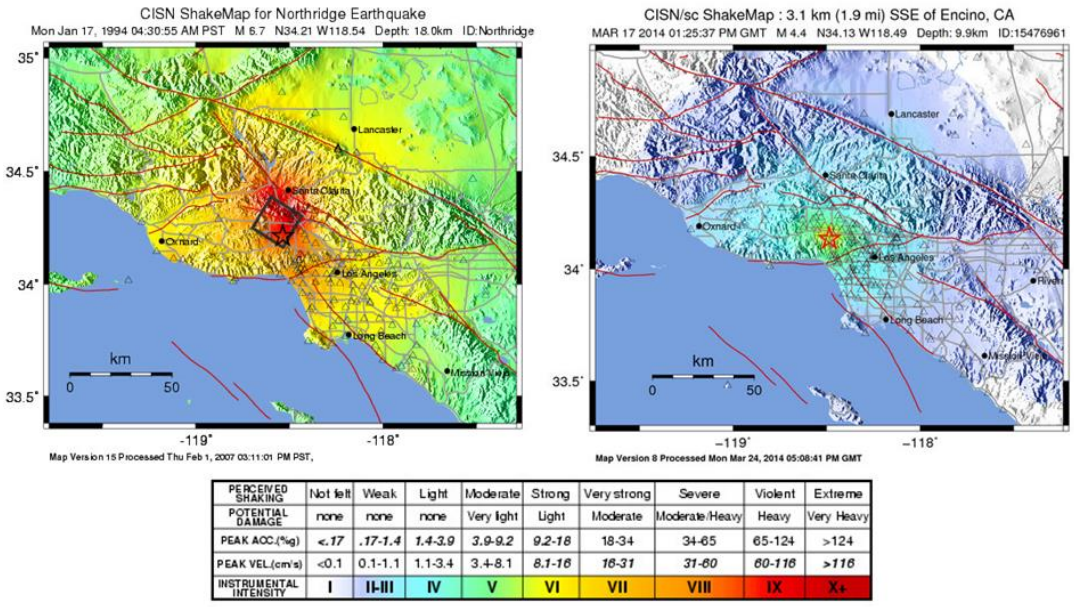


Figure 70. USGS ShakeMaps for (left) the $M_w$6.7, 1994 Northridge earthquake, and (right) the $M_w$4.4, 2014 Westwood earthquake.

It would also be valuable for urban planners to run scenarios using projected future assets and population distributions. Whilst every effort was made to use the most recent, available asset data for the Northridge simulations, the most recent records of population and housing distributions were available only for the year 2000. Models of future estimates of population and housing density for the Northridge site would be useful to determine the exposure of assets to earthquake and landsliding in the future. Los Angeles has a rapidly expanding urban

area. This region's exposure to future earthquakes and triggered landslides, and the associated risk to assets and human life, could increase rapidly as the urban area expands.

### 3.4 Loss Model

Rather than predicting losses, Paper 4 resulted in an exposed assets analysis, due to limitations in the availability of sufficient earthquake and earthquake-triggered landslide loss models. However, there are several datasets which could be used to tentatively link earthquake shaking and earthquake-triggered landslides to a rough estimate of losses from earthquake scenarios. Peek-Asa et al. (2000) conducted a study to map earthquake-related deaths and hospital admissions as a result of the Northridge 1994 earthquake. This data could be used to link deaths and injuries to peak ground acceleration and landslide susceptibility, developing a model of earthquake and earthquake-triggered human losses on a small scale for the Northridge scenario. However, such a model would have a high error and uncertainty rate, and would not be able to be applied to any other location or earthquake magnitude.

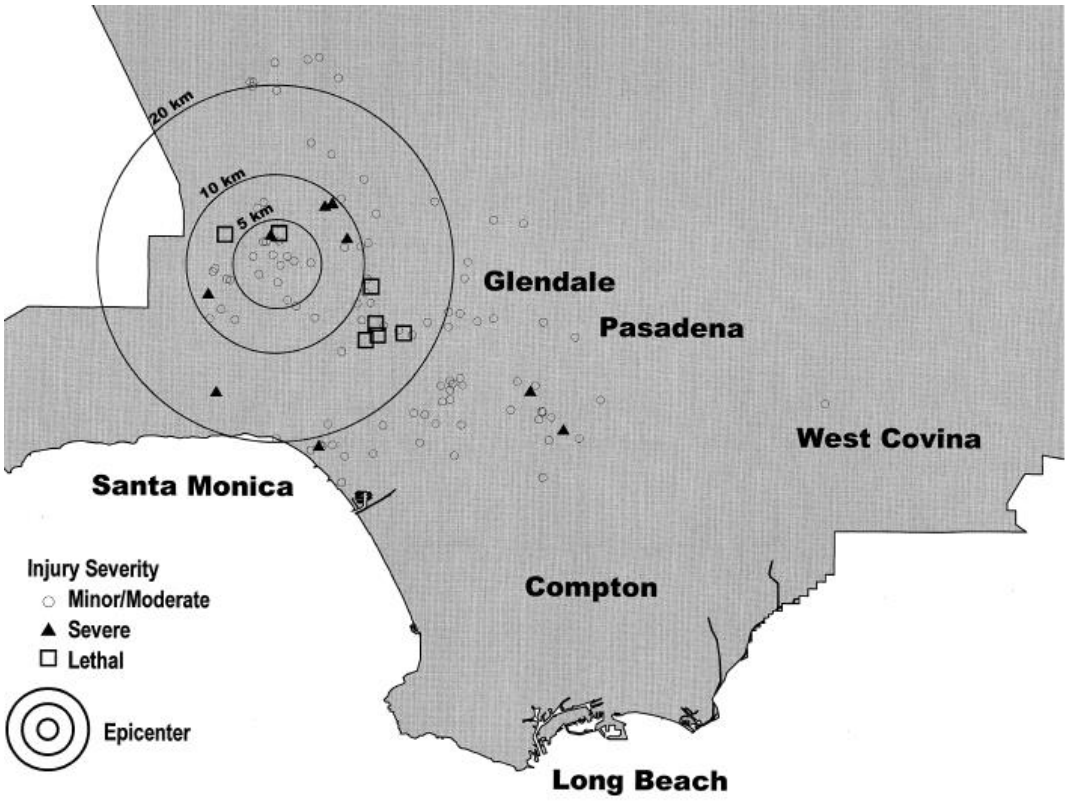


Figure 71. 1994 Northridge earthquake injury locations by injury severity (taken from Peek-Asa et al., 2000, figure 1, p8).

In addition to the injury and death data recorded from the Northridge 1994 earthquake, there exists a dataset of building damage per building footprint as a result of the event. Building footprints for Los Angeles County were produced from the LAR-IAC2 Project (2008) and made publically available as of November 1, 2012. This is a proprietary dataset provided courtesy of the Los Angeles Region Imagery Acquisition Consortium (LAR-IAC), Pictometry International Corporation and The Sanborn Map Company Incorporation. Combining the building damage data with data outlining each building in the Los Angeles County, this could be used to create a model of building damage as a result of earthquake shaking. However, building damage data was not collected systematically outside of the valley basin, and building footprint data is not available in the Ventura County, therefore the model would not be able to estimate building damage as a result of earthquake-triggered landslides due to scarcity of data in the region affected by landslides.

### 3.5 Application to other study sites

As long as suitable data exists, the same methodology presented in Paper 3 and Paper 4 to develop a logistic regression earthquake-triggered landslide hazard model can be repeated anywhere in the world. Some examples of earthquake events where landslides were triggered and known landslide inventory maps were published are outlined here.

Peak ground acceleration data was recorded by the Taiwan Central Weather Bureau for the Taiwan Chi-Chi earthquake in 1999. A landslide inventory map for the Hoshe basin in Central Taiwan is available from the published authors of "Modeling typhoon- and earthquake-induced landslides in a mountainous watershed using logistic regression" (Chang et al., 2007). This landslide inventory map was not used in this thesis as a study site because the landslide inventory is very small in scale in comparison with the scale of the earthquake. However, the Chi-Chi earthquake has a great range of other interesting data, such as detailed peak ground acceleration and GPS-located fatalities (Figure 72) (Pai et al., 2004; Tsai et al., 2001). Building damage data were also recorded in the aftermath of the Chi-Chi earthquake

(Figure 72) (Lee et al., 2003; Tsai et al., 2001). There are also other landslide inventory data that have been published (Figure 72) (Lee, 2013). Whilst a wealth of data exists and has been published on the Chi-Chi earthquake, which combined could be used to develop earthquake and earthquake-triggered human and building loss models, the data is not accessible online. Data availability is dependent on published authors' discretion and legal ownership issues of the data.

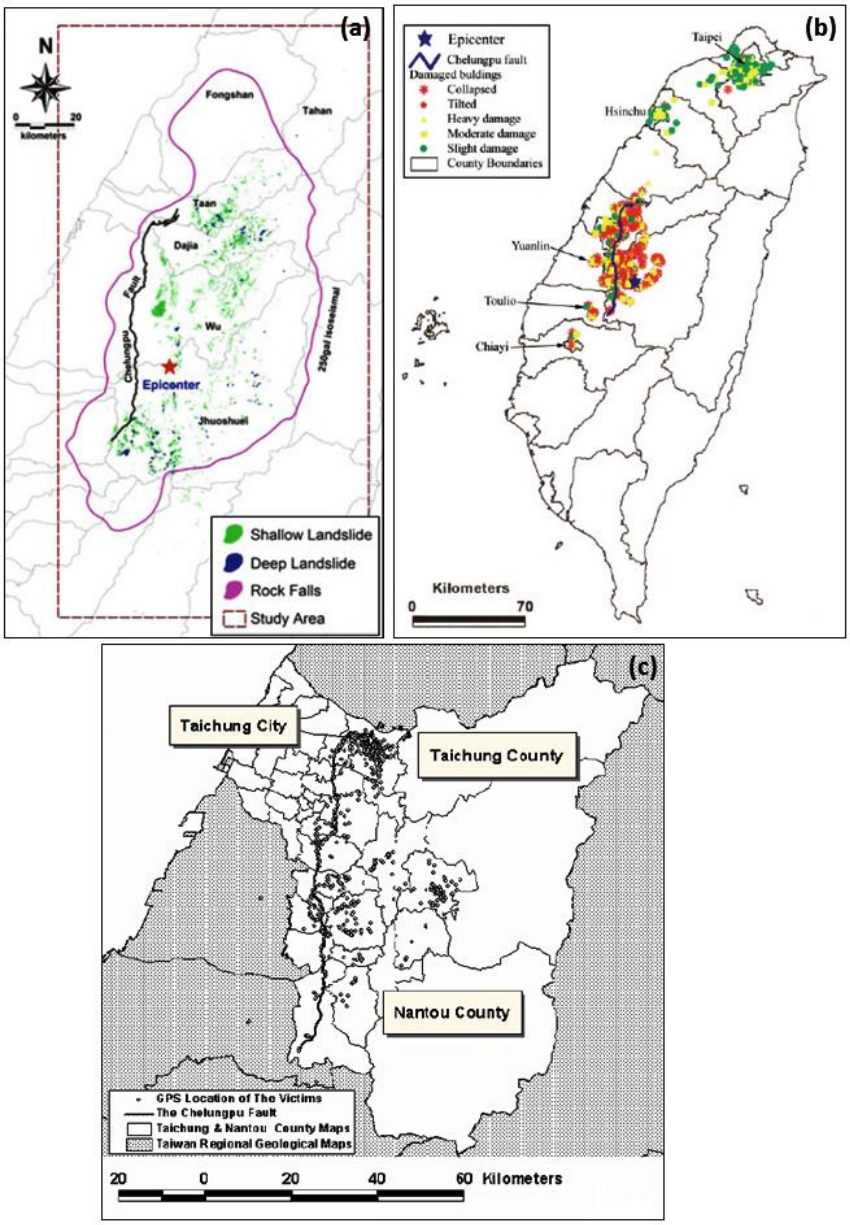


Figure 72. A selection of data available for the Chi-Chi earthquake: (a) landslide inventory map (acquired from Lee, 2013, figure 22.1.a, page 217); (b) distribution of damaged buildings from the Chi-Chi earthquake (acquired from Tsai et al., 2001, figure 2, page 1302); (c) spatial distribution of victims located using GPS (acquired from Pai et al., 2004, figure 2, page 6).

The 1997 Umbria-Marche, Italy earthquake triggered multiple rock falls. The landslide inventory map for this event is available for download online or via published authors, along with soil, geology, and building damage data (Marzorati et al., 2002). However, the peak ground acceleration data is only available at sparse resolution from the Italian Accelerometric Archive (ITACA), which limits the ability to fit an earthquake-triggered landslide hazard model.

The 2008 M7.2 Iwate-Miyagi Nairiku earthquake in Japan triggered landslides in the provinces of Hanokidachi and Kurikoma. The landslide inventory maps are available directly from the authors of "High resolution DEMs in the study of rainfall-and earthquake-induced landslides: Use of a variable window size method in digital terrain analysis" (Iwahashi et al., 2012). However, the landslide events are sparsely distributed in both provinces, and the peak ground acceleration data is at a comparatively low spatial resolution, which will likely reduce the strength of relationships between independent and dependent covariates, and the predictability of models developed from such data.

## 4.0 Thesis in Context

### 4.1 Landslide Susceptibility and Hazard

Landslide susceptibility assessments typically use long-term landslide inventories to assess risk. This method overlooks the increased potential for landsliding as a result of direct earthquake shaking. This method is used because earthquake-triggered landslide events are relatively rare compared to rainfall-triggered events because the return period for earthquakes is longer than for rainfall events, and therefore the majority of landslide susceptibility assessments are based on rainfall-triggered landslides, due to the more readily available data (van Westen et al., 2006; Nadim et al., 2006).

This can be a problem for regions with high seismic risk in rough terrain, which may experience relatively small numbers of rainfall-triggered landslides. Landslide susceptibility

assessments will generally account for the risk of rainfall-triggered landslides because the data for rainfall-triggered landslides can be available on a yearly basis to conduct these assessments. However, the risk from earthquake-triggered landslides will usually be under-represented. As the earthquake magnitude increases between simulations in Paper 4, the area affected by high probability of landsliding increases in size and spreads to areas which did not experience landsliding in the 1994 Northridge earthquake. The relationship between earthquake magnitude and area affected by landsliding is non-linear. Any risk assessment for these areas due to earthquakes and subsequent landsliding could therefore be significantly underestimated as they are based on previous landslide occurrences.

Long-term landslide susceptibility assessments will also underrepresent earthquake-triggered landslide risk because rainfall-induced landslides occur in different locations to earthquake-induced landslides, as seen in Paper 2. Even though landslide susceptibility assessments identify slopes relatively unstable compared to others, in terms of slope gradient, geology, vegetation etc., they will not be able to account for the spatial variability in earthquake shaking. The spatial differences in earthquake ground motion can increase the likelihood of failure on a slope with higher peak ground acceleration, compared with lower peak ground acceleration, even if the inherent properties of the slopes are the same. With large differences in ground motion, areas which previously may have been considered more stable could experience landsliding due to high levels of shaking, whilst areas further from the epicentre with low levels of shaking could remain stable, even if they previously were considered more prone to landsliding. Susceptibility to landsliding as a result of an earthquake trigger is therefore spatially variable, and needs to be treated as such.

The results from the systematic review of the literature in Paper 2 suggest that landslide risk assessments should treat earthquake-induced landslides separately from rainfall-induced landslides. The trigger type determines which covariates are found to be significant in the logistic regression analysis. The trigger type therefore affects the likely location of secondary landsliding. Including the triggering variable in logistic regression analysis has been shown

in Paper 3 to increase the accuracy of prediction of likely landslide locations as a result of earthquake ground motion. Earthquake-triggered landslide hazard models can be used to calculate earthquake-triggered landslide hazard for a variety of earthquake scenarios in a region, to assess the risk posed by earthquake-triggered landslides. To be able to predict the spatial location of potential landslides as a result of a given earthquake scenario, the pattern of ground motion should be taken into consideration. Accounting for cascading effects such as causation and amplification is needed in hazard and risk assessment especially for areas in high seismic risk locations, located near rough terrain.

## 4.2 Earthquake-Induced Landslide Hazard Model

Identifying the potential locations of landslides in the aftermath of an earthquake can be vital in prioritising the distribution of debris clearing efforts, to be able to re-establish access to cut off areas requiring relief (Hovius and Meunier, 2012). Landslides often block roads and access routes, hampering rescue efforts following an earthquake. The 2004 Niigata-Chuetsu earthquake caused landslides to block access roads to smaller villages affected by the earthquake posing a serious challenge to reopening (Kieffer et al., 2006). The landslides from the 2005 Kashmir earthquake damaged many of the roads linking to the rest of Pakistan, disrupting relief efforts in the first few days after the earthquake; indeed, disaster relief efforts relied heavily upon aviation resources (Marui and Nadim, 2009). In April 2014, a Magnitude 8.2 earthquake struck Chile, causing multiple landslides which blocked roads in Northern Chile. These landslides hampered evacuation efforts as residents left the coast to reach higher ground to avoid a potential tsunami. Approximately half the road closures in California due to significant earthquakes are because of landslides rather than shaking damage (Wald et al., unpublished).

Papers 2, 3, and 4 all showed that peak ground acceleration is significantly associated with landsliding. Whilst landslide susceptibility modelling using logistic regression is fairly common, it was shown in Paper 2 that only two studies were found during the systematic

literature search to have included peak ground acceleration in logistic regression analysis[5]. Papers 3 and 4 both contribute to this body of work and show that including peak ground acceleration creates a model that can be used to predict landslide probability in any future earthquake scenario where the peak ground acceleration variable is available. Since 2007, the USGS has produced near-real-time ShakeMaps of ground motion through the PAGER programme following significant global earthquakes, which can be used in such situations.

Secondary hazards are highlighted as potential additional contributions to losses, currently unaccounted for in PAGER's shaking-based estimates (Wald et al., 2012). There is currently no quantitative coseismic landslide hazard model available to estimate the potential location of landslides as a result of earthquake shaking. The USGS is in the process of developing models to address this research gap (Nowicki et al., 2014). The results presented in Paper 2 can provide an inventory of covariates likely to be significantly associated with earthquake-triggered landslides which could increase the predictive accuracy of a global earthquake-triggered landslide model; it also provides a guide to best practice for logistic regression studies to increase the consistency and comparability between global studies. The results from Papers 3 and 4 and the methodology presented validate the suitability of such a method for calculating the probability of landslide occurrence due to a particular earthquake, contributing to the body of work addressing this research gap.

The covariates chosen for inclusion for Nowicki et al.'s (2014) logistic regression landslide hazard study are fairly simple, selected based on globally available, temporally static data. Nowicki et al.'s (2014) model uses slope, wetness (Compound Topographic Index), material

[5] Paper 2 reviews papers published at the time of the search (15th February 2013 and 5th July 2013). Since the systematic search, a notable paper has been published using peak ground acceleration in logistic regression analysis for landslide hazard assessment. The paper by Nowicki et al., (2014) is referred to in the following Discussion section in relation to the results presented in the thesis.

strength (friction coefficient), and peak ground acceleration to fit the logistic regression model. Preliminary tests suggest that finer-resolution geological parameters could improve the regression results found in Nowicki et al.'s (2014) study. The logistic regression models in Papers 3 and 4 include a wider range of variables than the model proposed in Nowicki et al. (2014). These variables were chosen from the inventory provided in Paper 2. Several covariates not used by Nowicki et al. (2014) were found to be significantly associated with landslides in Papers 3 and 4. The covariates found significantly associated with landslides (not included in the Nowicki et al., 2014 paper) were: curvature, drainage density, distance to drainage, elevation, fault density, distance to fault line, plan curvature, profile curvature, distance to ridgeline, roughness, stream power index, aspect, soil type and vegetation.

Whilst some of these variables are currently unavailable at the global scale (such as soil type and vegetation), the remainder were created from global digital elevation models. There are sufficiently detailed digital elevation models for the globe that these variables could be calculated for inclusion in a global landslide hazard model. The results from this thesis demonstrate that the inclusion of geological and geomorphic variables such as those used in Papers 3 and 4 can increase the accuracy of a global earthquake-induced landslide hazard model.

The relationship between peak ground acceleration, environmental factors and landslide failure will vary between sites. The method presented in this thesis would need to be repeated for other sites globally to provide region or type-specific landslide hazard models. The USGS has recently created a database of landslide inventories and associated peak ground acceleration data produced by ShakeMap for global earthquake events (Dr D.Wald, 2013, personal correspondence). Logistic regression modelling can use these newly created databases to develop a global landslide hazard model to predict landslide probability in the immediate aftermath of an earthquake, as shown in Paper 4.

To be able to apply the global earthquake-induced landslide hazard model for rapid response and loss estimates through PAGER, the inputs required are simply the spatial distribution of peak ground acceleration, which is computed through ShakeMap. The results from the research in this thesis demonstrate that logistic regression is a suitable and fast method to predict landslide probability as a result of earthquake ground motion. This information should be useful for emergency responders to prioritise and organise relief efforts, identifying isolated communities in need of aid, and coordinating debris-clearing to re-establish road connections, or clear landslide dams to reduce the risk of subsequent outburst floods.

### 4.3 Cascading Hazards

The four papers presented in this thesis deal mostly with the causation and amplification effects of cascading hazards, rather than association and coincidence (Duncan et al., 2013). The amplification effects of cascading hazards were explored in Paper 1, using fatalities as a way of comparing hazard outcomes and severity. Although there were not enough detailed, separated data to determine whether the amplification effect of a cascading event was greater than the sum of the constituent parts of the single hazards, it was demonstrated that earthquake-and-landslide cascading events resulted in an amplification of fatalities compared to single earthquake-only events.

In Paper 4, although the OpenSHA model predicted high risk to buildings and people in the San Fernando Valley due to earthquake shaking, there was an additional risk to buildings and people in the hills of the surrounding region due to earthquake-triggered landsliding. Earthquake hazard risk assessments would not normally account for the risk from earthquake-induced landslides (Kappes, 2010). They are therefore underrepresenting the risk associated with potential secondary landslides, which are associated with an increase in losses.

In terms of causation, results from Paper 2 show that the type of primary hazard (earthquake shaking or rainfall) can affect the factors significantly associated with the secondary hazard (landsliding) in a cascading hazard chain. In much of the literature assessing landslide risk and hazard, landslides are treated as a single hazard, without accounting for the triggering variable (Nadim et al., 2006; Dilley et al., 2005). Long-term landslide susceptibility assessments overlook the increased potential for landsliding as a result of direct earthquake shaking because they are based on historic long-term landsliding. Earthquake-triggered landslide events are relatively rare compared to rainfall-triggered events. Therefore, the majority of landslide susceptibility assessments are typically based on rainfall-triggered landslides (van Westen et al., 2006; Nadim et al., 2006).

Logistic regression is one of the most commonly used statistical methods for estimating landslide susceptibility and hazard in the literature, as shown in Paper 2. Papers 2, 3 and 4 show that logistic regression modelling is a useful method for earthquake-triggered landslides, where the secondary hazard is very clear-cut (either a landslide occurred or it did not). Logistic regression has potential to be a useful method for modelling cascading hazards when the spatial data are available for each of the hazards in a cascading chain, although the applicability of the logistic regression method would depend on the hazard type. Landslides are particularly disposed to logistic regression because they have a clear physical boundary. However, there are several studies which have used logistic regression analysis to model secondary hazard probabilities, as shown in Figure 73 (Goda et al., 2011; Pradhan, 2009; Jomelli et al., 2007; Dong et al., 2011; De Vasconcelos et al., 2001). Whilst logistic regression analysis is not a common method for predicting hazard probabilities for secondary hazards other than landslides, the studies in the literature show that other hazards could utilise the method of predicting hazard probability presented in Paper 3 and in simulating ‘what-if’ scenarios as in Paper 4.

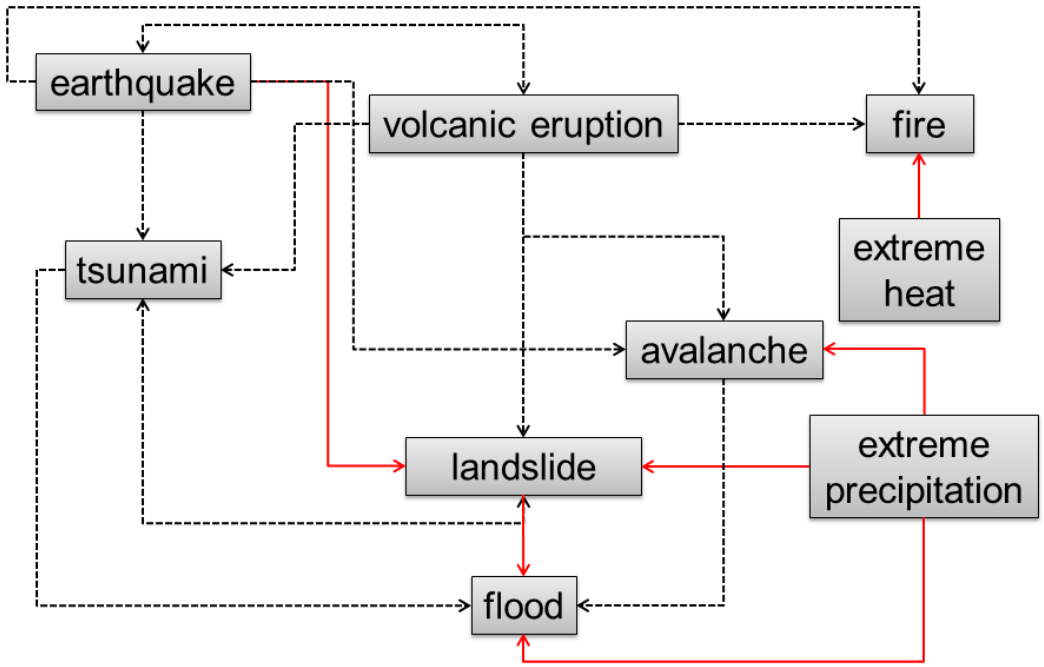


Figure 73. Diagram showing the causative links between a selection of natural hazards. The red, undashed lines represent occasions in the literature where logistic regression analysis has been used to predict the probability of the secondary hazard.

### 4.4 Multi-Hazard Risk Assessment

In multi-hazard risk assessment, risk is typically calculated for each individual hazard using the risk equation (Equation 1). The Risks for individual hazards are then summed to assess the multi-hazard risk. This method ignores the potential amplification effect of interacting hazards (Kappes, 2010). There is agreement among the majority of multi-hazard risk literature that the sum of the individual risks does not adequately account for the total risks from multiple interacting hazards. Whilst the results from Paper 1 show that there is an association with the presence of a secondary hazard with an increase in loss, compared to a single hazard; there is currently not enough sufficiently detailed global fatality data available to establish conclusively whether this increase in fatalities is greater than the sum of its constituent parts. In order to develop a multi-hazard risk model accounting for the amplification and interaction effects, several new sources of data and models are required, in particular to improve the vulnerability component of the risk equation (Equation 1).

A major problem in assessing interacting multi-hazard risk will be acquiring sufficiently detailed and separate data for each of the constituent hazards. Currently, the majority of fatality or loss data are attributed to the primary hazard event in global hazard databases. A new method of collecting data would be required to create an empirical loss model for cascading hazards. The direct cause of death (attributed to a particular hazard type) would need to be ascertained and recorded for each person. In addition to this, the location of the person at the time of the event would need to be established and documented, for example with GPS. With this information, it would be possible to calculate the number of people killed by each hazard type, and with spatial information on landslide locations, shaking intensity, and population density, the proportion of fatalities caused directly by the earthquake and by the subsequent landsliding can be calculated. With these data, an empirical earthquake-induced landslide loss model could be fitted. Presently these data are very seldom collected; in the aftermath of an earthquake, in particular, the precise cause of death (whether due to earthquake shaking or landslide burial) and the location is rarely recorded.

Little work has been conducted on quantifying the physical vulnerability of people and buildings due to earthquake-triggered landslides. Studies creating fragility curves for physical vulnerability of population to landslides are mostly based on limited, isolated landslide events and expert judgement (SafeLand, 2011). The large uncertainties and complexities associated with the physical vulnerability of people to landslides indicate that creating purely empirically-based fragility curves for earthquake-triggered landslides may be too difficult at this time. It is incredibly data-intensive to model all interactions between hazards, and such data may not be possible to collect or record in the aftermath of disasters. Therefore, a combined empirical and expert-driven earthquake-triggered landslide loss model could be a more realistic approach to modelling multi-hazard risk assessment.

# 8. CONCLUSIONS

The aim of this thesis was "To explore probability of landsliding given the earthquake hazard, and the potential impacts of coseismic landslides, within the context of the field of cascading hazards". The following list outlines the conclusions of the research presented in this thesis in relation to the original aim.

- The presence of a triggered landslide is associated with a significant increase in the number of fatalities related to an earthquake event compared with when no landslide is triggered, independent of other factors (including seismic magnitude, building strength and population affected).
- To be able to determine whether cascading events result in greater losses than the sum of the constituent hazards, the fatalities caused by the coseismic landslides alone need to be separated from those caused by the triggering earthquake. Such data currently do not exist.
- The significant covariates associated with landsliding are different for earthquake-induced landslides compared with rainfall-induced landslides, since the triggering mechanism affects susceptibility to landsliding. Earthquake-induced landslide probability should be assessed separately to rainfall-induced landslide probability.
- The use of peak ground acceleration as a covariate in logistic regression analysis increases the predictive accuracy of earthquake-induced landslide hazard models. It can also be used to predict landslides as a result of different peak ground acceleration spatial distributions.
- If the Northridge earthquake occurred tomorrow, exactly as in 1994, the event would likely result in greater losses than the 1994 event because of human development in the region.

- If the Northridge earthquake occurred with a higher magnitude than $M_w$6.7, the areas affected by high levels of shaking and high probability of landsliding would increase in spatial extent. Areas unaffected by landslides in 1994 are more at risk of landslides at higher magnitudes; the relationship between earthquake magnitude and area affected by landslides is non-linear. This short-term susceptibility to earthquake-induced landslides is not accounted for in long-term general landslide susceptibility assessments, which rely on historic landslide occurrence.
- The method used in Paper 4 can be used to develop models to predict landslides as a result of earthquake shaking using OpenSHA-generated peak ground acceleration maps, or future ShakeMaps as a result of potential future earthquake events.

# 9. THESIS REFERENCES


ABE, S., AND SUZUKI, N., 2006. Nonlinear Processes in Geophysics Complex-Network Description of Seismicity. *Nonlinear Processes in Geophysics***,** 145-150.

ABRAHAMSON, N. A. 2000. Effects of rupture directivity on probabilistic seismic hazard analysis. *In:* Proceedings of the 6th International Conference on Seismic Zonation, 2000 Palm Springs, CA. Earthquake Engineering Research Institute (EERI).

ABRAHAMSON, N. A. & SILVA, W. 1997. Empirical response spectral attenuation relations for shallow crustal earthquakes. *Seismological Research Letters,* 68**,** 94-127.

AIR, 2013. Study of impact and the insurance and economic cost of a major earthquake in British Columbia and Ontario/Quebec. *In:* CANADA, I. B. O. (ed.). Boston, USA: AIR Worldwide.

AIR, 2014. *AIR worldwide*. Available: http://www.air-worldwide.com/Models.

AITA, M. 2014. *Email correspondence regarding EQECAT,* 22nd October 2014.

AKGUN, A. 2012. A comparison of landslide susceptibility maps produced by logistic regression, multi-criteria decision, and likelihood ratio methods: a case study at Izmir, Turkey. *Landslides,* 9**,** 93-106.

AKGUN, A. & BULUT, F. 2007. GIS-based landslide susceptibility for Arsin-Yomra (Trabzon, North Turkey) region. *Environmental Geology,* 51**,** 1377-1387.

AKGUN, A., KINCAL, C. & PRADHAN, B. 2012. Application of remote sensing data and GIS for landslide risk assessment as an environmental threat to Izmir city (west Turkey). *Environ Monit Assess,* 184**,** 5453-70.

AKI, K. 1993. Local Site Effects on Weak and Strong Ground Motion. *Tectonophysics,* 218**,** 93-111.

ALEOTTI, P. & CHOWDHURY, R. 1999. Landslide hazard assessment: summary review and new perspectives. *Bull Eng Geol Env,* 58**,** 21-44.

ALEXANDER, D. 2001. Natural hazards. *In:* ALEXANDER, D. & FAIRBRIDGE, R. (eds.) *Encyclopedia of environmental science.* Kluwer, Dordrecht.

ALLEN, T. I., MARANO, K. D., EARLE, P. S. & WALD, D. 2009. PAGER-CAT: A composite earthquake catalog for calibrating global fatality models. *Seismological Research Letters,* 80**,** 57-62.

ALLSTADT, K., VIDALE, J. E. & FRANKEL, A. D. 2013. A Scenario Study of Seismically Induced Landsliding in Seattle Using Broadband Synthetic Seismograms. *Bulletin of the Seismological Society of America,* 103.

ANDERSON, J. R., HARDY, E. E., ROACH, J. T. & WITMER, R. E. 1976. A Land Use And Land Cover Classification System For Use With Remote Sensor Data. *U.S. Geol. Survey Prof. Paper 964* 28.

ANDONE, D., FAGARASAN, I., HOSSU, A. & MEREZEANU, D. 2006. Advanced control system for nonlinear processes. *Wmsci 2006: 10th World Multi-Conference on Systemics, Cybernetics and Informatics, Vol Iii, Proceedings***,** 336-340.

AREFI, M., MONTAZERI, A., POSHTAN, J. & JAHED-MOTLAGH, M. 2006. Nonlinear model predictive control of chemical processes with a Wiener identification approach. *2006 IEEE International Conference on Industrial Technology, Vols 1-6***,** 1686-1691.

ARIAS, A. 1970. A measure of earthquake intensity. *In:* HANSEN, R. (ed.) *Seismic Design for Nuclear Power Plant.* MIT Press Cambridge.

ARMONIA, 2007. Assessing and mapping multiple risks for spatial planning: approaches, methodologies and tools in Europe.

ASHLEY, R. & VERBRUGGE, R. J. 2006. Comments on "A critical investigation on detrending procedures for nonlinear processes". *Journal of Macroeconomics,* 28**,** 192-194.

ATKINSON, G. M. & BOORE, D. M. 1997. Some comparisons between recent ground-motion relations. *Seismological Research Letters,* 68**,** 24-40.
ATKINSON, P. M. & MASSARI, R. 1998. Generalised linear modelling of susceptibility to landsliding in the central Apennines, Italy. *Computers & Geosciences,* 24**,** 373-385.
ATKINSON, P. M. & MASSARI, R. 2011. Autologistic modelling of susceptibility to landsliding in the Central Apennines, Italy. *Geomorphology,* 130**,** 55-64.
AUGUSTIN, N. H., MUGGLESTONE, M. A. & BUCKLAND, S. T. 1996. An autologistic model for the spatial distribution of wildlife. *Journal of Applied Ecology,* 33**,** 339-347.
AURELIUS, E. 1994. The January 17, 1994 Northridge, CA earthquake: An EQE International Summary Report. Houston, TX: EQE International.
AVERILL, M. G., KELLER, G. R., MILLER, K. C., SRODA, P., BOND, T. & VELASCO, A. 2006. Data fusion in geophysics: Seismic tomography and crustal structure in Poland as an example. *Geoinformatics: Data to Knowledge,* 397**,** 153-168.
AYALEW, L. & YAMAGISHI, H. 2005. The application of GIS-based logistic regression for landslide susceptibility mapping in the Kakuda-Yahiko Mountains, Central Japan. *Geomorphology,* 65**,** 15-31.
BAGDOEV, A. G. & SEDRAKIAN, D. M. 2006. Wave processes in nonlinear beams during propagation of waves in pulsar plasmas with different magnetic field orientations. *Astrophysics,* 49**,** 350-357.
BARTANA, A., KOSLOFF, D. & RAVVE, I. 2006. On "Angle-domain common-image gathers by wavefield continuation methods" (Paul C. Sava and Sergey Fomel, 2003, GEOPHYSICS, 68, 1065-1074). *Geophysics,* 71**,** X1-X3.
BASSLER, K. E., GUNARATNE, G. H. & MCCAULEY, J. L. 2006. Markov processes, Hurst exponents, and nonlinear diffusion equations: With application to finance. *Physica a-Statistical Mechanics and Its Applications,* 369**,** 343-353.
BASSOMPIERRE, C., LI, S. & CADET, C. 2006. Activated sludge processes state estimation: A nonlinear moving horizon observer approach. *2006 American Control Conference, Vols 1-12,* 1-12**,** 2904-2909.
BEAVERS, J. E., EATHERTON, M. R., GILSANZ, R. E., RICLES, J. M. & LIN, Y. C. 2012. The August 23, 2011 Magnitude 5.8 Virginia Earthquake in the Eastern United States - An Engineering Perspective. *In:* Proceedings of the 15th World Conference on Earthquake Engineering, 2012 Lisbon, Portugal.
BEDNARIK, M., MAGULOVA, B., MATYS, M. & MARSCHALKO, M. 2010. Landslide susceptibility assessment of the Kralovany-Liptovsky Mikulas railway case study. *Physics and Chemistry of the Earth,* 35**,** 162-171.
BIAGIOLA, S. & SOLSONA, J. 2006. State estimation in batch processes using a nonlinear observer. *Mathematical and Computer Modelling,* 44**,** 1009-1024.
BILHAM, R. 2006. Geophysics - Dangerous tectonics, fragile buildings, and tough decisions. *Science,* 311**,** 1873-1875.
BO, C. M., WANG, Z. Q., BO, C. M., JUN, L. & LIN, J. G. 2006. Fault tolerant PID control based on software redundancy for nonlinear uncertain processes. *IEEE ICMA 2006: Proceeding of the 2006 IEEE International Conference on Mechatronics and Automation, Vols 1-3, Proceedings***,** 2211-2216.
BO, C. M., WANG, Z. Q., LIN, J. G., ZHANG, S. & ZHANG, G. M. 2006. The online models based fault tolerant control for multiple sensor fault of multi-variable nonlinear processes. *2006 IEEE International Joint Conference on Neural Network Proceedings, Vols 1-10***,** 936-943.
BOMMER, J. J. & RODRIGUEZ, C. E. 2002. Earthquake-induced landslides in central America. *Engineering Geology,* 63**,** 189-220.
BOORE, D. M. & ATKINSON, G. M. 2008. Ground-motion prediction equations for the average horizontal component of PGA, PGV, and 5%-Damped PSA at spectral periods between 0.01s and 10.0s. *Earthquake Spectra,* 24**,** 99-138.
BOORE, D. M., JOYNER, W. B. & FUNAL, T. E. 1997. Equations for estimating horizontal response spectra and peak acceleration from western North American

earthquakes: A summary of recent work. *Seismological Research Letters,* 68**,** 128-153.
BORCHERDT, R. D. 1994. Estimates of site-dependent response spectra for design (methodology and justification). *Earthquake Spectra,* 10**,** 617-653.
BORISOV, A. V. 2006. Backward representation of Markov jump processes and related problems. II. Optimal nonlinear estimation. *Automation and Remote Control,* 67**,** 1466-1484.
BOSLAUGH, S. 2012. *Statistics in a Nutshell*, O'Reilly Media.
BRENNING, A. 2005. Spatial prediction models for landslide hazards: review, comparison and evaluation. *Natural Hazards and Earth System Sciences,* 5**,** 853-862.
BROSKY-DORSEY, R., CULL, J. & PATTI, A. F. 2006. Using geophysics to locate elevated soil zinc and natural organic matter to influence metal bioavailability. *Proceedings of the Second IASTED International Conference on Advanced Technology in the Environmental Field***,** 218-221.
BROWN, E. G. J. & GHILARDUCCI, M. S. 2013. 2013 State of California Multi-Hazard Mitigation Plan. *In:* SERVICES, C. G. S. O. O. E. (ed.). Mather, California.
BRYANT, 2005. *Natural Hazards,* New York, Cambridge University Press.
BUCKNAM, R. C., COE, J. A., CHAVARRIA, M. M., GODT, J. W., TARR, A. C., L.A., B., RAFFERTY, S., HANCOCK, D., DART, R. L. & JOSHNSON, M. L. 2001. Landslides triggered by Hurricane Mitch in Guatemala - Inventory and Discussion. USGS Open File Report.
BUDIMIR, M. E. A., ATKINSON, P. M. & LEWIS, H. G. 2014. Earthquake-and-landslide events are associated with more fatalities than earthquakes alone *Natural Hazards*.
BUDIMIR, M.E.A., ATKINSON, P.M., & LEWIS, H.G. 2015. A systematic review of landslide probability mapping using logistic regression. *Landslides Journal*.
BUDIMIR, M. E. A., ATKINSON, P. M. & LEWIS, H. G. 2015b. Coseismic landslide hazard probability modelled as a function of the earthquake trigger for the 1994 Northridge, California event. *Landslides*.
BUI, D. T., LOFMAN, O., REVHAUG, I. & DICK, O. 2011. Landslide susceptibility analysis in the Hoa Binh province of Vietnam using statistical index and logistic regression. *Natural Hazards,* 59**,** 1413-1444.
BURSKII, V. P. 2006. On nonlinear differential equations that describe localized processes. *Journal of Nonlinear Mathematical Physics,* 13**,** 516-522.
BUZNA, L., PETERS, K., AMMOSER, H., KUHNERT, C. & HELBING, D. 2007. Efficient response to cascading disaster spreading. *Physical Review E,* 75.
BUZNA, L., PETERS, K. & HELBING, D. 2006. Modelling the dynamics of disaster spreading in networks. *Physica a-Statistical Mechanics and Its Applications,* 363**,** 132-140.
CAMPBELL, K. W. 1997. Empirical Near-Source Attenuation Relationships for Horizontal and Vertical Components of Peak Ground Acceleration, Peak Ground Velocity, and Pseudo-Absolute Acceleration Response Spectra. *Seismological Research Letters,* 68**,** 154-179.
CAMPBELL, K. W. 2000. Erratum: Empirical Near-source Attenuation Relationships for Horizontal and Vertical Components of Peak Ground Acceleration, Peak Ground Velocity, and Pseudo-absolute Acceleration Response Spectra. *Seismological Research Letters,* 71**,** 352-354.
CAMPBELL, K. W. & BOZORGNIA, Y. 2003. Updated near-source ground motion (attenuation) relations for the horizontal and vertical components of peak ground acceleration and acceleration response spectra. *Bulletin of the Seismological Society of America,* 93**,** 314-331.
CAN, T., NEFESLIOGLU, H. A., GOKCEOGLU, C., SONMEZ, H. & DUMAN, T. Y. 2005. Susceptibility assessments of shallow earthflows triggered by heavy rainfall at three catchments by logistic regression analyses. *Geomorphology,* 72**,** 250-271.
CARDONA, O. D., ORDAZ, M. G., REINOSO, E., YAMIN, L. E. & BARBAT, A. H. 2012. CAPRA - Comprehensive Approach to Probabilistic Risk Assessment:

International Initiative for Risk Management Effectiveness. *15th World Conference on Earthquake Engineering.* Lisboa.
CARPIGNANO, A., GOLIA, E., DI MAURO, C., BOUCHON, S. & NORDVIK, J. P. 2009. A methodological approach for the definition of multi-risk maps at regional level: first application. *Journal of Risk Research,* 12**,** 513-534.
CARRARA, A., CARDINALI, M., DETTI, R., GUZZETTI, F., PASQUI, V. & REICHENBACH, P. 1991. Gis Techniques and Statistical-Models in Evaluating Landslide Hazard. *Earth Surface Processes and Landforms,* 16**,** 427-445.
CARRO, M., DE AMICIS, M., LUZI, L. & MARZORATI, S. 2003. The application of predictive modeling techniques to landslides induced by earthquakes: the case study of the 26 September 1997 Umbria-Marche earthquake (Italy). *Engineering Geology,* 69**,** 139-159.
CHAKRAVARTHI, V. & SUNDARARAJAN, N. 2006. On "The gravitational attraction of a right rectangular prism with density varying with depth following a cubic polynomial" (Juan Garcia-Abdeslem, 2005, GEOPHYSICS, 66, 1793-1804). *Geophysics,* 71**,** X17-X18.
CHANDA, K. C. 2006. Sampling properties of U-statistics for a class of stationary nonlinear processes. *Annals of the Institute of Statistical Mathematics,* 58**,** 635-646.
CHANG, K. T., CHIANG, S. H. & HSU, M. L. 2007. Modeling typhoon- and earthquake-induced landslides in a mountainous watershed using logistic regression. *Geomorphology,* 89**,** 335-347.
CHAUHAN, S., MUKTA, S. & ARORA, M. K. 2010. Landslide susceptibility zonation of the Chamoli region, Garhwal Himalayas, using logistic regression model. *Landslides,* 7**,** 411-423.
CHIOU, B. S. J. & YOUNGS, R. R. 2008. An NGA model for the average horizontal component of peak ground motion and response spectra. *Earthquake Spectra,* 24**,** 173-215.
CHOU, Y. S. & JIH, K. T. 2006. Robust control of a class of time-delay nonlinear processes. *Industrial & Engineering Chemistry Research,* 45**,** 8963-8972.
CIESIN 2005. Gridded Population of the World, Version 3 (GPWv3). Palisades, NY: CIESIN, Columbia University.
COMBINED, U. 2004. *USGS Combined (2014) Attenuation Relationship*. Available: http://www.opensha.org/glossary-attenuationRelation-USGS_COMBO_2004.
COMMISSION, E. 2011. Risk assessment and mapping guidelines for disaster management. *Commission staff working paper.* European Union.
COSENTINO, P. L. 2006. Unconventional micro-geophysics for engineering and cultural heritage artifacts. *Geophysical Solutions for Environment and Engineering, Vol 1 and 2***,** 650-657.
COSTACHE, G. 2006. Distributed data acquisition system for environment monitoring nonlinear processes. *Device Applications of Nonlinear Dynamics***,** 201-210.
CRAMPIN, S. 2006. The New Geophysics: a new understanding of fluid-rock deformation. *Eurock 2006 Multiphysics Coupling and Long Term Behaviour in Rock Mechanics***,** 539-544.
CRED. 2014. *EM-DAT: The International Disaster Database*. Available: www.emdat.be.
CUNNINGHAM, K. J., RENKEN, R. A., WACKER, M. A., ZYGNERSKI, M. R., ROBINSON, E., SHAPIRO, A. M. & WINGARD, G. L. 2006. Application of carbonate cyclostratigraphy and borehole geophysics to delineate porosity and preferential flow in the karst limestone of the Biscayne aquifer, SE Florida. *Perspectives on Karst Geomorphology, Hydrology, and Geochemistry,* 404**,** 191-208.
CYRANOSKI, D. 2006. Geophysics: Magical mantle tour. *Nature,* 440**,** 1108-1110.
DAI, F. C. & LEE, C. F. 2002. Landslide characteristics and, slope instability modeling using GIS, Lantau Island, Hong Kong. *Geomorphology,* 42**,** 213-228.

DAI, F. C. & LEE, C. F. 2003. A spatiotemporal probabilistic modelling of storm-induced shallow landsliding using aerial photographs and logistic regression. *Earth Surface Processes and Landforms,* 28**,** 527-545.

DAI, F. C., LEE, C. F., LI, J. & XU, Z. W. 2001. Assessment of landslide susceptibility on the natural terrain of Lantau Island, Hong Kong. *Environmental Geology,* 40**,** 381-391.

DAI, F. C., XU, C., YAO, X., XU, L., TU, X. B. & GONG, Q. M. 2011. Spatial distribution of landslides triggered by the 2008 Ms 8.0 Wenchuan earthquake, China. *Journal of Asian Earth Sciences,* 40**,** 883-895.

DAS, D. P., MOHAPATRA, S. R., ROUTRAY, A. & BASU, T. K. 2006. Filtered-s LMS algorithm for multichannel active control of nonlinear noise processes. *Ieee Transactions on Audio Speech and Language Processing,* 14**,** 1875-1880.

DAS, I., SAHOO, S., VAN WESTEN, C., STEIN, A. & HACK, R. 2010. Landslide susceptibility assessment using logistic regression and its comparison with a rock mass classification system, along a road section in the northern Himalayas (India). *Geomorphology,* 114**,** 627-637.

DAS, P. K. & GHOSH, A. 2006. Phase changes in nonlinear processes in interacting Fock space. *International Journal of Modern Physics B,* 20**,** 433-443.

DE GRAFF, J. V., CANNON, S. H. & GALLEGOS, A. J. 2007. Reducing post-wildfire debris flow risk through the Burned Area Emergency Response (BAER) process. *In:* SCHAEFER, V. R., SCHUSTER, R. L. & TURNER, A. K., eds. 1st North American Landslide Conference, 2007 Vail, Colorado. AEG Special Publication, 1440-1447.

DE VASCONCELOS, M. J. P., SILVA, S., TOME, M., ALVIM, M. & PEREIRA, J. M. C. 2001. Spatial prediction of fire ignition probabilities: Comparing logistic regression and neural networks. *Photogrammetric Engineering and Remote Sensing,* 67**,** 73-81.

DELMONACO, G., MARGOTTINI, C. & SPIZZICHINO, D. 2006. Report on new methodology for multi-risk assessment and the harmonisation of different natural risk maps.

DELMONACO, G., MARGOTTINI, C. & SPIZZICHINO, D. 2007. ARMONIA methodology for multi-risk assessment and the harmonisation of different natural risk map. *Applied Multi-Risk Mapping of Natural Hazards for Impact Assessment.*

DEN EECKHAUT, M., VANWALLEGHEM, T., POESEN, J., GOVERS, G., VERSTRAETEN, G. & VANDEKERCKHOVE, L. 2006. Prediction of landslide susceptibility using rare events logistic regression: A case-study in the Flemish Ardennes (Belgium). *Geomorphology,* 76**,** 392-410.

DEPIPPO, T., DONADIO, C., PENNETTA, M., PETROSINO, C., TERLIZZI, F. & VALENTE, A. 2008. Coastal hazard assessment and mapping in Northern Campania, Italy. *Geomorphology,* 97**,** 451-466.

DHU, T., ROBINSON, D., CLARK, D., GRAY, D. & ROW, P. 2008. Event-based earthquake risk modelling. *14th World Conference on Earthquake Engineering.* Beijing, China.

DHU, T., ROBINSON, D., SINADINOVSKI, C., JONES, T., CORBY, N., JONES, A. & SCHNEIDER, J. 2002. Earthquake hazard. *In:* DHU, T. & JONES, T. (eds.) *Earthquake risk in Newcastle and Lake Macquarie.*

DI FINIZIO, S., PENA, A., TRIFONOV, T., CARVAJAL, J. J., AGUILO, M., PALLARES, J., RODRIGUEZ, A., ALCUBILLA, R., MARSAL, L. F., DIAZ, F. & MARTORELL, J. 2006. Growth of 2D KTP photonic crystals for efficient second order nonlinear optical processes - art. no. 61820X. *Photonic Crystal Materials and Devices III (i.e. V),* 6182**,** X1820-X1820.

DILLEY, M., CHEN, R. S., DEICHMANN, U., LERNERLAM, A. L. & ARNOLD, M. 2005. Natural Disaster Hotspots: A Global Risk Analysis. *Natural Disaster Hotspots: A Global Risk Analysis***,** 1-134.

DING, Y., ZENG, L. & ZHOU, S. Y. 2006. Phase I analysis for monitoring nonlinear profiles in manufacturing processes. *Journal of Quality Technology,* 38**,** 199-216.

DLUGOLECKI, A. 2009. Climate change and its implications for catastrophe modelling. *Coping with climate change: risks and opportunities for insurers.*
DOMOGATSKY, G. V., KOPEIKIN, V. I., MIKAELYAN, L. A. & SINEV, V. V. 2006. Neutrino geophysics at Baksan: On searches for antineutrinos and radiogenic-heat sources in the interior of the Earth. *Physics of Atomic Nuclei,* 69**,** 43-50.
DONG, J. J., TUNG, Y. H., CHEN, C. C., LIAO, J. J. & PAN, Y. W. 2011. Logistic regression model for predicting the failure probability of a landslide dam. *Engineering Geology,* 117**,** 52-61.
DUMAN, T. Y., CAN, T., GOKCEOGLU, C., NEFESLIOGLU, H. A. & SONMEZ, H. 2006. Application of logistic regression for landslide susceptibility zoning of Cekmece Area, Istanbul, Turkey. *Environmental Geology,* 51**,** 241-256.
DUNCAN, M., EDWARDS, S., KILBURN, C., TWIGG, J. & CROWLEY, K. 2013. From multi-hazard concept to multi-hazard assessment: lessons from the Philippines. *First Dynamics and Impact of Interacting Natural Hazards Workshop.* University College London.
DWORAK, D., DRABINA, A. & WOZNICKA, U. 2006. Numerical estimation of real and apparent integral neutron parameters used in nuclear borehole geophysics. *Applied Radiation and Isotopes,* 64**,** 844-853.
EL-MASRI, S., AND TIPPLE, G., 1997. Urbanization, poverty and natural disasters: vulnerability of settlements in developing countries. *Reconstructing after Disasters,* 12**,** 141-158.
ELSWORTH, D., VOIGHT, B., THOMPSON, G. & SR, Y. 2004. Thermal-hydrologic mechanism for rainfall-triggered collapse of lava domes. *Geology,* 32**,** 969-972.
EQECAT. 2014. *Catastrophe Risk Models and Perils*. Available: http://www.eqecat.com/catastrophe-models/.
ERCANOGLU, M., GOKCEOGLU, C. & VAN ASCH, T. W. J. 2004. Landslide susceptibility zoning north of Yenice (NW Turkey) by multivariate statistical techniques. *Natural Hazards,* 32**,** 1-23.
ERCANOGLU, M. & TEMIZ, F. A. 2011. Application of logistic regression and fuzzy operators to landslide susceptibility assessment in Azdavay (Kastamonu, Turkey). *Environmental Earth Sciences,* 64**,** 949-964.
ERENER, A. & DUZGUN, H. S. B. 2010. Improvement of statistical landslide susceptibility mapping by using spatial and global regression methods in the case of More and Romsdal (Norway). *Landslides,* 7**,** 55-68.
ERLINGSSON, U. 2005. GIS for natural hazard mitigation - experiences from designing the HazMit GIS expert system suggests the need for an international standard. *GIS Planet.* Portugal.
EUROPEAN GEOPHYSICAL SOCIETY., AMERICAN GEOPHYSICAL UNION. & EUROPEAN GEOSCIENCES UNION. 1994. Nonlinear processes in geophysics. Katlenburg-Lindau, Germany: European Geophysical Society.
FARIFTEH, J., FARSHAD, A. & GEORGE, R. J. 2006. Assessing salt-affected soils using remote sensing, solute modelling, and geophysics. *Geoderma,* 130**,** 191-206.
FEDI, M. & QUARTA, T. 2006. On "Wavelet denoising of aeromagnetic data" (George E. Leblanc and William A. Morris, 2001, GEOPHYSICS, 66, 1793-1804). *Geophysics,* 71**,** X21-X22.
FIELD, E. H. 2000. A modified ground-motion attenuation relationship for southern California that accounts for detailed site classification and a basin-depth effect. *Bulletin of Seismological Society of America,* 90**,** 209-221.
FIELD, E. H., DAWSON, T. E., FELZER, K. R., FRANKEL, A. D., GUPTA, V., JORDAN, T. H., PARSONS, T., PETERSON, M. D., STEIN, R. S., WELDON II, R. J. & WILLS, C. J. 2008. The Uniform California Earthquake Rupture Forecast, Version 2 (UCERF 2). *Open-File Report.* USGS.
FIELD, E. H., GUPTA, N., GUPTA, V., BLANPIED, M., MAECHLING, P. & JORDAN, T. H. 2005. Hazard calculations for the WGCEP-2002 earthquake forecast using

OpenSHA and distributed object technologies. *Seismological Research Letters,* 76**,** 161-167.
FIELD, E. H., GUPTA, V., GUPTA, N., MAECHLING, P. & JORDAN, T. H. 2005. Hazard Map Calculations Using Grid Computing. *Seismological Research Letters,* 76**,** 565-573.
FIELD, E. H., JOHNSON, P. A., BERESNEV, I. A. & ZENG, Y. H. 1997. Nonlinear ground-motion amplification by sediments during the 1994 Northridge earthquake. *Nature,* 390**,** 599-602.
FIELD, E. H., JORDAN, T. H. & CORNELL, C. A. 2003. OpenSHA: A Developing Community-Modeling Environment for Seismic Hazard Analysis. *Seismological Research Letters,* 74**,** 406-419.
FIELD, E. H., SELIGSON, H. A., GUPTA, N., GUPTA, V., JORDAN, T. H. & CAMPBELL, K. W. 2005. Loss estimates for a Puente Hills blind-thrust earthquake in Los Angeles, California. *Earthquake Spectra,* 21**,** 329-338.
FLEMING, G. 2002. Learning to live with rivers - the ICE's report to government. *Proceedings of the Institution of Civil Engineers-Civil Engineering,* 150**,** 15-21.
FRITZ, H. M., BLOUNT, C., SOKOLOSKI, R., SINGLETON, J., FUGGLE, A., MCADOO, B. G., MOORE, A., GRASS, C. & TATE, B. 2007. Hurricane Katrina storm surge distribution and field observations on the Mississippi Barrier Islands. *Estuarine Coastal and Shelf Science,* 74**,** 12-20.
FRY, J. A., XIAN, G., JIN, S. M., DEWITZ, J. A., HOMER, C. G., YANG, L. M., BARNES, C. A., HEROLD, N. D. & WICKHAM, J. D. 2011. National Land Cover Databse for the Conterminous United Sates. *Photogrammetric Engineering and Remote Sensing,* 77**,** 859-864.
GARCIA-ABDESLEM, J. 2006. On "The gravitational attraction of a right rectangular prism with density varying with depth following a cubic polynomial" (Juan Garcia-Abdeslem, 2005, GEOPHYSICS, 66, 1793-1804) - Reply to the discussion - V. Chakravarthi and N. Sundararajan. *Geophysics,* 71**,** X18-X19.
GARCIA-RODRIGUEZ, M. J. & MALPICA, J. A. 2010. Assessment of earthquake-triggered landslide susceptibility in El Salvador based on an Artificial Neural Network model. *Natural Hazards and Earth System Sciences,* 10**,** 1307-1315.
GAULL, B. A., MICHAEL-LEIBA, M. O. & RYNN, J. M. W. 1990. Probabilistic earthquake risk maps of Australia. *Australian Journal of Earth Sciences,* 37**,** 169-87.
GELI, L., BARD, P. Y. & JULLIEN, B. 1988. The Effect of Topography on Earthquake Ground Motion - a Review and New Results. *Bulletin of the Seismological Society of America,* 78**,** 42-63.
GIARRATANO, J. C. & RILEY, G. D. 1998. *Expert systems: principles and programming*.
GILL, J. C. & MALAMUD, B. D. 2013. Reviewing and visualising natural hazard interactions to inform hazard mitigation and management priorities. *First Dynamics and Impact of Interacting Natural Hazards Workshop.* University College London, London, UK.
GLASS, R. J., CONRAD, S. H., KAPLAN, P. G., BRODSKY, N. S. & BROWN, T. J. 2008. Complex Science: Implications for Critical Infrastructures. *Physical Review*.
GNEDIN, Y. N., SOLOV'EV, A. A. & AVAKYAN, S. V. 2006. Space Solar Patrol and some fundamental questions of astrophysics, solar physics, and geophysics. *Journal of Optical Technology,* 73**,** 218-221.
GODA, K., ATKINSON, G. M., HUNTER, J. A., CROW, H. & MOTAZEDIAN, D. 2011. Probabilistic Liquefaction Hazard Analysis for Four Canadian Cities. *Bulletin of the Seismological Society of America,* 101**,** 190-201.
GODT, J., SENER, B., VERDIN, K., WALD, D., EARLE, P., HARP, E. & JIBSON, R. 2008. Rapid assessment of earthquake-induced landsliding. *Proceedings of the First World Landslide Forum, United Nations University, Tokyo***,** 4.
GORSEVSKI, P. V., GESSLER, P. E., FOLTZ, R. B. & ELLIOT, W. J. 2006. Spatial Prediction of Landslide Hazard using Logistic Regression and ROC Analysis. *Transactions in GIS,* 10**,** 395-415.

GRANGER, K., JONES, T., LEIBA, M. & SCOTT, G. 1999. *Community risk in Cairns: a multi-hazards risk assessment*. Australian Geological Survey Organisation AGSO. Available: http://www.ga.gov.au/hazards/reports/cairns/ [Accessed 25th February 2013].

GREENBERG, R. 2006. Tides on Europa - Linking Celestial Mechanics, geology, and geophysics. *Chaotic Worlds: From Order to Disorder in Gravitational N-Body Dynamical Systems,* 227**,** 289-305.

GREIVING, S. 2006. *Integrated risk assessment of multi-hazards: a new methodology*, Geological Survey of Finland.

GUO, B. L. & HUANG, D. W. 2006. Existence of weak solutions and trajectory attractors for the moist atmospheric equations in geophysics. *Journal of Mathematical Physics,* 47.

GUZZETTI, F., REICHENBACH, P., CARDINALI, M., GALLI, M. & ARDIZZONE, F. 2005. Probabilistic landslide hazard assessment at the basin scale. *Geomorphology,* 72**,** 272-299.

HADJI, R., BOUMAZBEUR, A., LIMANI, Y., BAGHEM, M., CHOUABI, A. & DEMDOUM, A. 2013. Geologic, topographic and climatic controls in landslide hazard assessment using GIS modeling: A case study of Souk Ahras region, NE Algeria. *Quaternary International,* 302**,** 224-237.

HAMZA, A. M., MEZIANE, K. & MAZELLE, C. 2006. Oblique propagation and nonlinear wave particle processes. *Journal of Geophysical Research-Space Physics,* 111.

HANLEY, J. A. & MCNEIL, B. J. 1983. A Method of Comparing the Areas under Receiver Operating Characteristic Curves Derived from the Same Cases. *Radiology,* 148**,** 839-843.

HARINARAYANA, T. & ZLOTNICKI, J. 2006. Special issue of journal of applied geophysics "electrical and electromagnetic studies in geothermally active regions" - Preface. *Journal of Applied Geophysics,* 58**,** 263-264.

HARP, E. L. & JIBSON, R. 1995. Inventory of landslides triggered by the 1994 Northridge, California earthquake. U.S. Geological Survey Open-File Report 95-213.

HARP, E. L. & JIBSON, R. W. 1996. Landslides triggered by the 1994 Northridge, California, earthquake. *Bulletin of the Seismological Society of America,* 86**,** S319-S332.

HASEGAWA, A. 1974. Instabilities and Nonlinear Processes in Geophysics and Astrophysics. *Reviews of Geophysics,* 12**,** 273-280.

HATCH, D. 2006. Advances in geophysics. *South African Journal of Geology,* 109**,** 431-432.

HAVENITH, H. B., VANINI, M., JONGMANS, D. & FACCIOLI, E. 2003. Initiation of earthquake-induced slope failure: influence of topographical and other site specific amplification effects. *Journal of Seismology,* 7**,** 397-412.

HE, Y. P. & BEIGHLEY, R. E. 2008. GIS-based regional landslide susceptibility mapping: a case study in southern California. *Earth Surface Processes and Landforms,* 33**,** 380-393.

HELBING, D., AMMOSER, H., AND KUHNERT, C., (ed.) 2005. *Disasters as extreme events and the importance of network interactions for disaster response management,* Berlin: Springer.

HELBING, D. & KUHNERT, C. 2003. Assessing interaction networks with applications to catastrophe dynamics and disaster management. *Physica a-Statistical Mechanics and Its Applications,* 328**,** 584-606.

HENGL, T. & REUTER, H. I. 2010. *Worldgrids - a public repository and a WPS for global environmental alyers: Slope Map*. Available: http://worldgrids.org/doku.php?id=wiki:slpsrt3 [Accessed 9th February 2012].

HERVAS, J. & BOBROWSKY, P. 2009. Mapping: Inventories, Susceptibility, Hazard and Risk. *In:* SASSA, K. & CANUTI, P. (eds.) *Landslides: Disaster Risk Reduction.* Berlin: Springer.

HEWITT, K. & BURTON, I. 1971. Hazardousness of a place: a regional ecology of damaging events. *Toronto Press, Toronto*.
HIGGS, S. 23rd October 2014 2014. *RE: Email correspondence regarding AIR worldwide.*
HINZE, W., COAKLEY, B., HILDENBRAND, T., KELLER, G. R., LI, X., PLOUFF, D., RAVAT, D. & WEBRING, M. 2006. On "New standards for reducing gravity data: The North American gravity database" (W. J. Hinze et al., 2005, Geophysics, 70, J25-J32) - Reply to the discussion. *Geophysics,* 71**,** X32-X33.
HIRTH, G. 2006. Geophysics - Protons lead the charge. *Nature,* 443**,** 927-928.
HOLLAND, P. 24th October 2014 2014. *RE: Email correspondence regarding RMS.*
HONG, Y., ADLER, R. & HUFFMAN, G. 2007. Use of satellite remote sensing data in the mapping of global landslide susceptibility. *Natural Hazards,* 43**,** 245-256.
HOVIUS, N. & MEUNIER, P. 2012. Earthquake ground motion and the pattern of seismically induced landslides. *In:* CLEAGUE, J. J. & STEAD, D. (eds.) *Landslides: Types, Mechanisms and Modeling.* 2nd ed.: Cambridge University Press.
HU, J. X. & ZAHLE, M. 2006. Jump processes and nonlinear fractional heat equations on metric measure spaces. *Mathematische Nachrichten,* 279**,** 150-163.
HU, M. L., WANG, C. Y., SONG, Y. J., LI, Y. F., CHAI, L., SEREBRYANNIKOV, E. E. & ZHELTIKOV, A. M. 2006. Mode-selective mapping and control of vectorial nonlinear-optical processes in multimode photonic-crystal fibers. *Optics Express,* 14**,** 1189-1198.
IRVING, E. 2006. Geophysics - Same old magnetism. *Nature,* 444**,** 43-45.
IWAHASHI, J., KAMIYA, I. & YAMAGASHI, H. 2012. High-resolution DEMs in the study of rainfall- and earthquake-induced landslides: Use of a variable window size method in digital terrain analysis. *geomorphology,* 153-154**,** 29-38.
JAISWAL, K. & WALD, D. 2008. *Creating a Global Building Inventory for Earthquake Loss Assessment and Risk Management: Open-File Report 2008-1160: Appendix VII: PAGER_database_v1.4.xls.* Available: http//pubs.usgs.gov/of/2008/1160/downloads/PAGER_database/ [Accessed 4th March 2012].
JAISWAL, K. & WALD, D. 2010. An Empirical Model for Global Earthquake Fatality Estimation. *Earthquake Spectra,* 26**,** 1017-1037.
JIA, L. & CHIU, M. S. 2006. Adaptive feedback-feedforward control for a class of nonlinear chemical processes. *ICICIC 2006: First International Conference on Innovative Computing, Information and Control, Vol 1, Proceedings***,** 93-96.
JIBSON, R. W. 1993. Predicting earthquake-induced landslide displacements using Newmark's sliding block analysis. *Transportation research record,* 4**,** 9-17.
JIBSON, R. W. 2007. Regression models for estimating coseismic landslide displacement. *Engineering Geology,* 91**,** 209-218.
JIBSON, R. W. & HARP, E. L. 2012. Extraordinary Distance Limits of Landslides Triggered by the 2011 Mineral, Virginia, Earthquake. *Bulletin of the Seismological Society of America,* 102**,** 2368-2377.
JIBSON, R. W., HARP, E. L. & MICHAEL, J. A. 2000. A method for producing digital probabilistic seismic landslide hazard maps. *Engineering Geology,* 58**,** 271-289.
JOHNSTON, B. F., DEKKER, P., WITHFORD, M. J., SALTIEL, S. M. & KIVSHAR, Y. S. 2006. Simultaneous phase matching and internal interference of two second-order nonlinear parametric processes. *Optics Express,* 14**,** 11756-11765.
JOHNSTON, M. 2006. The International Commission on the History of Geological Sciences (INHIGEO) Symposium on History of Geophysics - Prague and the Czech Republic, July 2-12, 2005. *Episodes,* 29**,** 56-58.
JOMELLI, V., DELVAL, C., GRANCHER, D., ESCANDE, S., BRUNSTEIN, D., HETU, B., FILION, L. & PECH, P. 2007. Probabilistic analysis of recent snow avalanche activity and weather in the French Alps. *Cold Regions Science and Technology,* 47**,** 180-192.
JONES, D. K. C. 1995. The relevance of landslide hazard to the International decade for Natural Disaster Reduction. *In:* Landslide Hazard Mitigation with Particular

Reference to Developing Countries, 1995 London: Royal Academy of Engineering. 19-33.
JONES, L., AKI, K., BOORE, D., CELEBI, M., DONNELLAN, A., HALL, J., HARRIS, R., HAUKSSON, E., HEATON, T., HOUGH, S., HUDNUT, K., HUTTON, K., JOHNSTON, M., JOYNER, W., KANAMORI, H., MARSHALL, G., MICHAEL, A., MORI, J., MURRAY, M., PONTI, D., REASENBERG, P., SCHWARTZ, D., SEEBER, L., SHAKAL, A., SIMPSON, R., THIO, H., TINSLEY, J., TODOROVSKA, M., TRIFUNAC, M., WALD, D. & ZOBACK, M. L. 1994. The Magnitude-6.7 Northridge, California, Earthquake of 17-January-1994. *Science,* 266**,** 389-397.
JONES, R. 2006. Revealing the buried past: Geophysics for archaeologists. *American Journal of Archaeology,* 110**,** 504-505.
JORDAN, P., TURNER, K., NICOL, D. & BOYER, D. 2006. Developing a Risk Analysis Procedure for Post-Wildfire Mass Movement and Flooding in British Columbia. *1st Speciality Conference on Disaster Mitigation.* Calgary, Alberta, Canada.
JORDAN, T. H. & FIELD, E. H. 2006. Continued development of Open Seismic Hazard Analysis (OpenSHA) in support of a community modeling environment for seismic hazard analysis. *Final Technical Report.* USGS.
JOSHI, A. & XIAO, M. 2006. Controlling nonlinear optical processes in multi-level atomic systems. *Progress in Optics, Vol 49,* 49**,** 97-175.
KAMP, U., GROWLEY, B. J., KHATTAK, G. A. & OWEN, L. A. 2008. GIS-based landslide susceptibility mapping for the 2005 Kashmir earthquake region. *Geomorphology,* 101**,** 631-642.
KAPPES, M. S., KEILER, M., AND GLADE, T., (ed.) 2010. *From single- to multi-hazard risk analyses: a concept addressing emerging challenges*: Proceedings of the 'Mountain Risks' International Conference, Nov 2010.
KAPPES, M. S., KEILER, M., AND GLADE, T., 2010. The relevance of multi-hazard risk analyses for risk reduction in a dynamic world. *Proceedings of the 2010 Summer Institute for Advanced Study of Hazard and Risk*.
KAPPES, M. S., KEILER, M., VON ELVERFELDT, K. & GLADE, T. 2012. Challenges of analyzing multi-hazard risk: a review. *Natural Hazards,* 64**,** 1925-1958.
KATES, R. W. & HAARMANN, V. 1992. Where the Poor Live - Are the Assumptions Correct. *Environment,* 34**,** 4-&.
KAWAJIRI, Y. & BIEGLER, L. T. 2006. Nonlinear programming superstructure for optimal dynamic operations of simulated moving bed processes. *Industrial & Engineering Chemistry Research,* 45**,** 8503-8513.
KEEFER, D. & WILSON, R. 2011. *Effects from Earthquake-Triggered Landslides*. USGS. Available: http://pubs.usgs.gov/of/1995/ofr-95-0213/EFFECTS.HTML [Accessed 10/07/2013].
KEEFER, D. K. 1984. Landslides Caused by Earthquakes. *Geological Society of America Bulletin,* 95**,** 406-421.
KEEFER, D. K. 2000. Statistical analysis of an earthquake-induced landslide distribution - the 1989 Loma Prieta, California event. *Engineering Geology,* 58**,** 231-249.
KEEFER, D. K. 2002. Investigating landslides caused by earthquakes - A historical review. *Surveys in Geophysics,* 23**,** 473-510.
KERR, R. A. 2006. Geophysics - Opening the door to a chilly new climate regime. *Science,* 312**,** 350-350.
KERR, R. A. 2006. Geophysics - Stealth tsunami surprises Indonesian coastal residents. *Science,* 313**,** 742-743.
KHAVROSHKIN, O. B. & TSYPLAKOV, V. V. 2006. Nonlinear seismic processes on impact cratering: Information content. *Meteoritics & Planetary Science,* 41**,** A94-A94.
KIEFFER, D. S., JIBSON, R., RATHJE, E. M. & KELSON, K. 2006. Landslides triggered by the 2004 Niigata Ken Chuetsu, Japan, Earthquake. *Earthquake Spectra,* 22**,** 47-73.

KINCAL, C., AKGUN, A. & KOCA, M. Y. 2009. Landslide susceptibility assessment in the Izmir (West Anatolia, Turkey) city center and its near vicinity by the logistic regression method. *Environmental Earth Sciences,* 59**,** 745-756.
KING, J. 2006. Astronomy and geophysics in the secondary curriculum. *Astronomy & Geophysics,* 47**,** 19-23.
KIRCHER, C. A., WHITMAN, R. V. & HOLMES, W. T. 2006. Hazus-MH earthquake-loss estimation methods. *Natural Hazards Review,* 7**,** 45-59.
KLEMENS, G. & FAINMAN, Y. 2006. Optimization-based calculation of optical nonlinear processes in a micro-resonator. *Optics Express,* 14**,** 9864-9872.
KONO, M. 2006. Geophysics - Ships' logs and archeomagnetism. *Science,* 312**,** 865-866.
KORUP, O. 2010. Earthquake-triggered landslides - spatial patterns and impacts. *COGEAR,* Module 1a - Report.
KORUP, O. 2010. Earthquake-triggered landslides – spatial patterns and impacts. *COGEAR,* Module 1a – Report.
LATCHMAN, S. 22nd October 2014 2014. *RE: Email correspondence regarding AIR worldwide.*
LAY, T., KANAMORI, H., AMMON, C. J., NETTLES, M., WARD, S. N., ASTER, R. C., BECK, S. L., BILEK, S. L., BRUDZINSKI, M. R., BUTLER, R., DESHON, H. R., EKSTROM, G., SATAKE, K. & SIPKIN, S. 2005. The great Sumatra-Andaman earthquake of 26 December 2004. *Science,* 308**,** 1127-1133.
LEARNED, J. G., DYE, S. T. & PAKVASA, S. 2006. Neutrino geophysics conference introduction. *Earth Moon and Planets,* 99**,** 1-15.
LEBLANC, G. E. & MORRIS, W. A. 2006. On "Wavelet denoising of aeromagnetic data" (George E. Leblanc and William A. Morris, 2001, GEOPHYSICS, 66, 1793-1804) - Reply to the discussion - M. Fedi and T. Quarta. *Geophysics,* 71**,** X22-X23.
LEE, B. J., CHOU, T. Y. & LEI, T. C. 2003. Development of hazard damaged buildings model by Chi-Chi earthquake data. *In:* Proceedings of the joint NCREE/JRC conference, 2003.
LEE, C. T. 2013. Re-evaluation of factors controlling landslides triggered by the 1999 Chi-Chi earthquake. *In:* UGAI, K. E. A. (ed.) *Earthquake-Induced Landslides.* Berlin, Heidelberg: Springer-Verlag
LEE, K. H. & ROSOWSKY, D. V. 2006. Fragility analysis of woodframe buildings considering combined snow and earthquake loading. *Structural Safety,* 28**,** 289-303.
LEE, S. & EVANGELISTA, D. G. 2006. Earthquake-induced landslide-susceptibility mapping using an artificial neural network. *Natural Hazards and Earth System Sciences,* 6**,** 687-695.
LEE, S., RYU, J. H., WON, J. S. & PARK, H. J. 2004. Determination and application of the weights for landslide susceptibility mapping using an artificial neural network. *Engineering Geology,* 71**,** 289-302.
LEE, Y. L., YU, B. A., EOM, T. J., SHIN, W., JUNG, C., NOH, Y. C., LEE, J., KO, D. K. & OH, K. 2006. All-optical AND and NAND gates based on cascaded second-order nonlinear processes in a Ti-diffused periodically poled LiNbO3 waveguide. *Optics Express,* 14**,** 2776-2782.
LERNER-LAM, A. 2007. Assessing global exposure to natural hazards: Progress and future trends. *Environmental Hazards,* 7**,** 10-19.
LI, H. X. & DENG, H. 2006. An approximate internal model-based neural control for unknown nonlinear discrete processes. *Ieee Transactions on Neural Networks,* 17**,** 659-670.
LI, X. 2006. On "Theta map: Edge detection in magnetic data" (C. Wijns, C. Perez, and P. Kowalczyk, 2005, GEOPHYSICS, 70, L39-L43) - Discussion. *Geophysics,* 71**,** X11-X11.
LI, Y., CHEN, G., TANG, C., ZHOU, G. & ZHENG, L. 2012. Rainfall and earthquake-induced landslide susceptibility assessment using GIS and Artificial Neural Network. *Natural Hazards and Earth System Sciences,* 12**,** 2719-2729.

LIN, G. W., CHEN, H., HOVIUS, N., HORNG, M. J., DADSON, S., MEUNIER, P. & LINES, M. 2008. Effects of earthquake and cyclone sequencing on landsliding and fluvial sediment transfer in a mountain catchment. *Earth Surface Processes and Landforms,* 33**,** 1354-1373.
LIN, Y. D., HUANG, H. P. & YU, C. C. 2006. Relay feedback tests for highly nonlinear processes: Reactive distillation. *Industrial & Engineering Chemistry Research,* 45**,** 4081-4092.
LISIN, A. A., MOGILENSKIKH, D. V. & PAVLOV, I. V. 2006. Nonlinear color interpretation of physical processes. *Recent Progress in Computational Sciences and Engineering, Vols 7a and 7b,* 7A-B**,** 337-340.
LLOYD'S 2013. Catastrophe Modelling: Guidance for non-catastrophe modelling.
LOSETH, L. O., PEDERSEN, H. M., URSIN, B., AMUNDSEN, L. & ELLINGSRUD, S. 2006. Low-frequency electromagnetic fields in applied geophysics: Waves or diffusion? *Geophysics,* 71**,** W29-W40.
LU, G. Y., CHIU, L. S. & WONG, D. W. 2007. Vulnerability assessment of rainfall-induced debris flows in Taiwan. *Natural Hazards,* 43**,** 223-244.
LUGER, G. F. & CHKRABARTI, C. 2005. Knowledge-based probabilistic reasoning from expert systems to graphical models.
LUINO, F. 2005. Sequence of instability processes triggered by heavy rainfall in northern Italy. *Geomorphology,* 66**,** 13-39.
MACINTYRE, A. G., BARBERA, J. A. & SMITH, E. R. 2006. Surviving collapsed structure entrapment after earthquakes: a "time-to-rescue" analysis. *Prehospital Disaster Medicine,* 21**,** 4-19.
MAKEEV, E. V. & CHIRKIN, A. S. 2006. Parametric amplification and up-conversion of optical image in coupled nonlinear optical processes. *12th Central European Workshop on Quantum Optics,* 36**,** 113-120.
MARANO, K. D., WALD, D. J. & ALLEN, T. I. 2010. Global earthquake casualties due to secondary effects: a quantitative analysis for improving rapid loss analyses. *Natural Hazards,* 52**,** 319-328.
MARUI, H. & NADIM, F. 2009. Landslides and multi-hazards. *In:* SASSA, K. & CANUTI, P. (eds.) *Landslides: Disaster risk reduction.* Berlin: Springer.
MARULANDA, M. C., CARRENO, M. L., CARDONA, O. D., ORDAZ, M. G. & BARBAT, A. H. 2013. Probabilistic earthquake risk assessment using CAPRA: application to the city of Barcelona, Spain. *Natural Hazards,* 69**,** 59-84.
MARZOCCHI, W., MASTELLONE, M.L., AND DI RUOCCO, A., 2009. Principles of multi-risk assessment: Interaction amongst natural and man-induced risks. *European Comission,* EU23615.
MARZORATI, S., LUZI, L. & DE AMICIS, M. 2002. Rock falls induced by earthquakes: a statistical approach. *Soil Dynamics and Earthquake Engineering,* 22**,** 565-577.
MATTHEWS, A. J., BARCLAY, J., CARN, S., THOMPSON, G., ALEXANDER, J., HERD, R. & WILLIAMS, C. 2002. Rainfall-induced volcanic activity on Montserrat. *Geophysical Research Letters,* 29.
MAYNARD, T., BEECROFT, N., GONZALEZ, S. & RESTELL, L. 2014. Catastrophe modelling and climate change. *In:* LLOYD'S (ed.).
METTERNICHT, G., HURNI, L. & GOGU, R. 2005. Remote sensing of landslides: An analysis of the potential contribution to geo-spatial systems for hazard assessment in mountainous environments. *Remote Sensing of Environment,* 98**,** 284-303.
MEUNIER, P., HOVIUS, N. & HAINES, A. J. 2007. Regional patterns of earthquake-triggered landslides and their relation to ground motion. *Geophysical Research Letters,* 34.
MEUNIER, P., HOVIUS, N. & HAINES, J. A. 2008. Topographic site effects and the location of earthquake induced landslides. *Earth and Planetary Science Letters,* 275**,** 221-232.

MHASKAR, P., GANI, A. & CHRISTOFIDES, P. D. 2006. Fault-tolerant control of nonlinear processes: Performance-based reconfiguration and robustness. *International Journal of Robust and Nonlinear Control,* 16**,** 91-111.
MIELKE, A. & ROUBICEK, T. 2006. Rate-independent damage processes in nonlinear elasticity. *Mathematical Models & Methods in Applied Sciences,* 16**,** 177-209.
MOTTER, A. E. 2004. Cascade control and defense in complex networks. *Physical Review Letters,* 93.
MURNANE, R. J. 2005. Developing open-source catastrophe risk models. *In:* RISK PERCEPTION INITIATIVE, B. B. S. F. R. (ed.).
NADIM, F., KJEKSTAD, O., PEDUZZI, P., HEROLD, C. & JAEDICKE, C. 2006. Global landslide and avalanche hotspots. *Landslides,* 3**,** 159-173.
NAIMZADA, A. K. & SBRAGIA, L. 2006. Oligopoly games with nonlinear demand and cost functions: Two boundedly rational adjustment processes. *Chaos Solitons & Fractals,* 29**,** 707-722.
NEFESLIOGLU, H. A., DUMAN, T. Y. & DURMAZ, S. 2008. Landslide susceptibility mapping for a part of tectonic Kelkit Valley (Eastern Black Sea region of Turkey). *Geomorphology,* 94**,** 401-418.
NEIGHBORS, C. J., COCHRAN, E. S., CARAS, Y. & NORIEGA, G. R. 2013. Sensitivity Analysis of FEMA HAZUS Earthquake Model: Case Study from King County, Washington. *Natural Hazards Review,* 14**,** 134-146.
NEISHTADT, N. M., EPPELBAUM, L. V. & LEVITSKI, A. G. 2006. Application of piezoelectric and seismoelectrokinetic phenomena in exploration geophysics: Review of Russian and Israeli experiences. *Geophysics,* 71**,** B41-B53.
NELSON, A. 2008. *Travel time to major cities: A global map of accessibility*. Ispra Italy. Available: http://www-tem.jrc.it/accessibility [Accessed 9th March 2012].
NIKOLAEV, N. N., SCHAFER, W., ZAKHAROV, B. G. & ZOLLER, V. R. 2006. Nonlinear k(perpendicular to)-factorization: A new paradigm for hard processes in a nuclear medium. *Multiparticle Dynamics,* 828**,** 375-380.
NOWICKI, A. M., WALD, D. J., HAMBURGER, M. W., HEARNE, M. & THOMPSON, E. M. 2014. Development of a Globally Applicable Model for Near Real-Time Prediction of Seismically Induced Landslides. *Engineering Geology*.
OECD, 2012. Global Modelling of Natural Hazard Risks: enhancing existing capabilities to address new challenges.
OHLMACHER, G. C. & DAVIS, J. C. 2003. Using multiple logistic regression and GIS technology to predict landslide hazard in northeast Kansas, USA. *Engineering Geology,* 69**,** 331-343.
OPPENHEIMER, C. 2003. Climatic, environmental and human consequences of the largest known historic eruption: Tambora volcano (Indonesia) 1815. *Progress in Physical Geography,* 27**,** 230-259.
OZDEMIR, A. & ALTURAL, T. 2013. A comparative study of frequency ratio, weights of evidence and logistic regression methods for landslide susceptibility mapping: Sultan Mountains, SW Turkey. *Journal of Asian Earth Sciences,* 64**,** 180-197.
PAI, C. H., TIEN, Y. M., JUANG, D. S. & WANG, Y. L. 2004. A study on near-fault mortality from the 1999 Taiwan Chi-Chi earthquake. *13th World Conference on Earthquake Engineering.* Vancouver, B.C., Canada.
PANJAPORNPON, C., SOROUSH, M. & SEIDER, W. D. 2006. Model-based controller design for unstable, non-minimum-phase, nonlinear processes. *Industrial & Engineering Chemistry Research,* 45**,** 2758-2768.
PARDESHI, S. D., AUTADE, S. E. & PARDESHI, S. S. 2013. Landslide hazard assessment: recent trends and techniques. *SpringerPlus,* 2**,** 523.
PARISE, M. & JIBSON, R. W. 2000. A seismic landslide susceptibility rating of geologic units based on analysis of characteristics of landslides triggered by the 17 January, 1994 Northridge, California earthquake. *Engineering Geology,* 58**,** 251-270.

PASHAYAN, R. & MKRTCHYAN, M. 2006. Development and application of information system data in the field of geophysics. *Wmsci 2006: 10th World Multi-Conference on Systemics, Cybernetics and Informatics, Vol Vi, Proceedings*, 123-128.
PASOTTI, J. 2006. Geophysics - Ancient cataclysm marred the Med. *Science,* 314**,** 1527-1527.
PECCERILLO, A., FREZZOTTI, M. L., DE ASTIS, G. & VENTURA, G. 2006. Modeling the magma plumbing system of Vulcano (Aeolian Islands, Italy) by integrated fluid-inclusion geobarometry, petrology, and geophysics. *Geology,* 34**,** 17-20.
PEDERSEN, L. B. 2006. On "Magnetic-anomaly Fourier spectrum of a 3D Gaussian source" (Fabio Caratori Tontini, 2005, GEOPHYSICS, 70, L1-5). *Geophysics,* 71**,** X5-X7.
PEDUZZI, P., DAO, H., HEROLD, C. & MOUTON, F. 2009. Assessing global exposure and vulnerability towards natural hazards: the Disaster Risk Index. *Natural Hazards and Earth System Sciences,* 9**,** 1149-1159.
PEEK-ASA, C., RAMIREZ, M. R., SHOAF, K., SELIGSON, H. A. & KRAUS, J. F. 2000. GIS Mapping of Earthquake-Related Deaths and Hospital Admissions from the 1994 Northridge, California, Earthquake. *Annual Epidemiology,* 10**,** 5-13.
PERLES ROSELLO, M. & CANTARERO PRADOS, F. 2010. Problems and challenges in analyzing multiple territorial risks. Methodological proposals for multi-hazard mapping. *Boletin de la Asociacion de Geografos Espanoles,* 52**,** 399-404.
PETERS, D. P. C. & HAVSTAD, K. M. 2006. Nonlinear dynamics in arid and semi-arid systems: Interactions among drivers and processes across scales. *Journal of Arid Environments,* 65**,** 196-206.
PETERS, K., BUZNA, L. & HELBING, D. 2008. Modelling of cascading effects and efficient response to disaster spreading in complex networks. *International Journal of Critical Infrastructures,* 4**,** 46-62.
PETKOVSKA, M. & MARKOVIC, A. 2006. Fast estimation of quasi-steady states of cyclic nonlinear processes based on higher-order frequency response functions. Case study: Cyclic operation of an adsorption column. *Industrial & Engineering Chemistry Research,* 45**,** 266-291.
PETLEY, D. 2012. Global patterns of loss of life from landslides. *Geology,* 40**,** 927-930.
PINHO, R., CROWLEY, H. & BOMMER, J. J. 2008. Open-source software and treatment of epistemic uncertainties in earthquake loss modelling. *The 14th World Conference on Earthquake Engineering.* Beijing, China.
PLOEGER, S. K., ATKINSON, G. M. & SAMSON, C. 2010. Applying the HAZUS-MH software tool to assess seismic risk in downtown Ottawa, Canada. *Natural Hazards,* 53**,** 1-20.
POLLITZ, F. F. 2006. Geophysics - A new class of earthquake observations. *Science,* 313**,** 619-620.
PORTER, K. & SCAWTHORN, C. 2007. Openrisk: open-source risk software, access for the insurance industry.
PRADHAN, B. 2009. Flood susceptible mapping and risk area delineation using logistic regression, GIS and remote sensing. *Journal of Spatial Hydrology,* 9.
PRADHAN, B., LEE, B. & BUCHROITHNER, M. F. 2010. Remote Sensing and GIS-based Landslide Susceptibility Analysis and its Cross-validation in Three Test Areas Using a Frequency Ratio Model. *Photogrammetrie Fernerkundung Geoinformation***,** 17-32.
PREISLER, H. K., BRILLINGER, D. R., BURGAN, R. E. & BENOIT, J. W. 2004. Probability based models for estimation of wildfire risk. *International Journal of Wildland Fire,* 13**,** 133-142.
PRICE, J. G., HASTING, J. T., GOAR, L. D., ARMENO, L. D., JOHNSON, G., DEPOLO, C. M. & HESS, R. H. 2010. Sensitivity analysis of loss estimation modeling using uncertainties in earthquake parameters. *Environmental Engineering Geoscience,* 16**,** 357-367.
PROKESOVA, M. & BENES, V. 2006. Nonlinear filtering in spatio-temporal doubly stochastic point processes driven by OU processes. *Kybernetika,* 42**,** 539-556.

PROVENZALE, A. 1992. Special Topic - Nonlinear Processes in Geophysics. *Annales Geophysicae-Atmospheres Hydrospheres and Space Sciences,* 10**,** 717-718.
PROVENZALE, A. 1993. Special Section Nonlinear Processes in Geophysics - Introduction to the 2nd Part. *Annales Geophysicae-Atmospheres Hydrospheres and Space Sciences,* 11**,** 89-89.
PTUSKIN, V. S. & ZIRAKASHVILI, V. N. 2006. Nonlinear processes in cosmic-ray precursor of strong supernova shock: Maximum energy and average energy spectrum of accelerated particles. *Astrophysics,* 37**,** 1898-1901.
RAJARAMAN, S., HAHN, J. & MANNAN, M. S. 2006. Sensor fault diagnosis for nonlinear processes with parametric uncertainties. *Journal of Hazardous Materials,* 130**,** 1-8.
RAMASESHA, S. 2006. Computation of linear and nonlinear optical response and real time dynamics of intermolecular electronic processes in correlated molecular electronic systems. *Recent Progress in Computational Sciences and Engineering, Vols 7a and 7b,* 7A-B**,** 1252-1255.
RAO, S. S. 2006. On some nonstationary, nonlinear random processes and their stationary approximations. *Advances in Applied Probability,* 38**,** 1155-1172.
REED, J. C., WHEELER, J. O. & TUCHOLKE, B. E. 2005. *Geologic Map of North America, South Sheet, Geological Society of America Continent-Scale Map 001,,* 1:5000000.
REESE, S., KING, A., BELL, R. & SCHMIDT, J. 2007. Regional RiskScape: A Multi-Hazard Loss Modelling Tool. *Modsim 2007: International Congress on Modelling and Simulation***,** 1681-1687.
REMO, J. W. F. & PINTER, N. 2012. Hazus-MH earthquake modeling in the central USA. *Natural Hazards,* 63**,** 1055-1081.
RISKSCAPE, 2011. *About RiskScape*. Available: www.riskscape.org.nz [Accessed 3rd May 2011].
RMS, 2014. *RMS Catastrophe Models*. Available: http://www.RMS.com.
ROBINSON, D., FULFORD, G. & DHU, T. 2006. EQRM: Geoscience Australia's arthquake Risk Model: Technical Manual: Version 3.0. *Geoscience Australia, Canberra.*
RODRIGUEZ, C. E., BOMMER, J. J. & CHANDLER, R. J. 1999. Earthquake-induced landslides: 1980-1997. *Soil Dynamics and Earthquake Engineering,* 18**,** 325-346.
ROJAS, O. J., BAO, J. & LEE, P. L. 2006. Linear control of nonlinear processes: The regions of steady-state attainability. *Industrial & Engineering Chemistry Research,* 45**,** 7552-7565.
SADIGH, K., CHANG, C. Y., EGAN, J. A., MAKDISI, F. & YOUNGS, R. R. 1997. Attenuation relationships for shallow crustal earthquakes based on California strong motion data. *Seismological Research Letters,* 68**,** 180-189.
SAFELAND, 2011. D2.4 Guidelines for landslide susceptibility, hazard and risk assessment and zoning. *In:* SAFELAND (ed.) *Living with landslide risk in Europe: Assessment, effects of global change, and risk management strategies.* Seventh Framework Programme.
SAFELAND, 2011b. D2.5: Physical vulnerability of elements at risk to landslides: Methodology for evaluation, fragility curves and damage states for buildings and lifelines. *In:* SAFELAND (ed.) *Living with landslide risk in Europe: Assessment, effects of global change, and risk management strategies.* Seventh Framework Programme.
SAKAKURA, Y., NODA, M., NISHITANI, H., YAMASHITA, Y., YOSHIDA, M. & MATSUMOTO, S. 2006. Application of A Hybrid Control Approach to Highly Nonlinear Chemical Processes. *16th European Symposium on Computer Aided Process Engineering and 9th International Symposium on Process Systems Engineering,* 21**,** 1515-1520.
SANTACANA, N., BAEZA, B., COROMINAS, J., DE PAZ, A. & MARTURIA, J. 2003. A GIS-based multivariate statistical analysis for shallow landslide susceptibility

mapping in La Pobla de Lillet area (Eastern Pyrenees, Spain). *Natural Hazards,* 30**,** 281-295.
SARABANDI, P. 23rd October 2014 2014. *RE: Email correspondence regarding RMS.*
SCHERER, N. F. 2006. Nonlinear polarizability response studies of solvent dynamics in chemical processes. *Abstracts of Papers of the American Chemical Society,* 231.
SCHERTZER, D. & LOVEJOY, S. 1994. EGS Richardson AGU Chapman NVAG3 Conference: Nonlinear Variability in Geophysics: scaling and multifractal processes. *Nonlinear Processes in Geophysics,* 1**,** 77-79.
SCHULTE, J., WEIGEL, T. & SCHWEIGER, G. 2006. Nonlinear processes in microdroplets: a geometrical optics approach. *Journal of the Optical Society of America B-Optical Physics,* 23**,** 289-293.
SCHWEICKHARDT, T. & ALLGOWER, F. 2006. An approach to linear control of nonlinear processes. *16th European Symposium on Computer Aided Process Engineering and 9th International Symposium on Process Systems Engineering,* 21**,** 1299-1304.
SEIRUP, L. & YETMAN, G. 2006. U.S. Census Grids (Summary File 1), 2000: Metropolitan Statistical Areas. *In:* (SEDAC), N. S. D. A. A. C. (ed.). Palisades, NY.
SEIRUP, L., YETMAN, G. & RAZAFINDRAZAY, L. 2012. U.S. Census Grids (Summary File 3), 1990: Metropolitan Statistical Areas. *In:* (SEDAC), N. S. D. A. A. C. (ed.). Palisades, NY.
SHAKEMAP, 2003. *ShakeMap (2003) Attenuation Relations*. Available: http://www.opensha.org/glossary-attenuationRelation-SHAKE_MAP_2003.
SHI, P. 2002. Theory on disaster science and disaster dynamics. *Journal of Natural Disasters,* 11**,** 1-9.
SHI, P. 2005. Theory and practice on Disaster System Research. *Ppaer for the Fifth Annual IIASA-DPRI Forum*.
SHI, P., SHUAI, J., CHEN, W. & LU, L. 2010. Study on the Risk Assessment and Risk Transfer Mode of Large Scale Disasters. *Earth Surface Processes*.
SIDLE, R. C. & OCHIAI, H. 2006. *Landslides: Processes, Prediction, and Landuse,* Water Resources Monograph.
SIDORENKO, A. V. & SOLONOVICH, N. A. 2006. Electroencephalographic signals as complex nonlinear oscillations reflecting cerebral processes. *Journal of Communications Technology and Electronics,* 51**,** 446-453.
SINGH, B. P. 2006. Optoelectronic and nonlinear optical processes in low dimensional semiconductors. *Bulletin of Materials Science,* 29**,** 559-565.
SLEEP, N. H. 2006. Strategy for applying neutrino geophysics to the earth sciences including planetary habitability. *Earth Moon and Planets,* 99**,** 343-358.
SMITH, K. & PETLEY, D. N. 2009. *Environmental hazards: assessing risk and reducing disaster,* Routledge.
SOMERVILLE, P., COLLINS, N., ABRAHAMSON, N., GRAVES, R. & SAIKA, C. 2001. Ground motion attenuation relations for the Central and Eastern United States: United States Geological Survey Report. San Francisco.
SONNINO, G. 2006. Transport processes in magnetically confined plasmas in the nonlinear regime. *Chaos,* 16.
SPUDICH, P., JOYNER, W. B., LINDH, A. G., BOORE, D. M., MARGARIS, B. M. & FLETCHER, J. B. 1999. SEA99: A revised ground motion prediction relation for use in extensional tectonic regimes. *Bulletin of the Seismological Society of America,* 89**,** 1156-1170.
STAN, S., BALAN, R. & LAPUSAN, C. 2006. Some applications for nonlinear processes of a model based predictive control algorithm. *2006 IEEE International Conference on Automation, Quality, Testing and Robotics, Vols 1 and 2***,** 54-59.
STEVENSON, I., NICHOLSON, P. & HEYNS, T. 2006. High-resolution 3D geophysics in marine diamond mining - How this role will improve and impact the future of marine mining productivity. *Sea Technology,* 47**,** 10-+.

STIRLING, M. W. 2000. A new probabilistic seismic hazard model for New Zealand. *12th World Conderence on Earthquake Engineering.*
STONE, R. 2006. Geophysics: Facing a tsunami with no place to run. *Science,* 314**,** 408-409.
STONE, R. 2006b. Geophysics: The day the land tipped over. *Science,* 314**,** 406-409.
STORK, C. & KAPOOR, J. 2006. On "Delayed-shot 3D depth migration" (Yu Zhang, James Sun, Carl Notfors, Samuel H. Gray, Leon Chernis, and Jerry Young, 2005, GEOPHYSICS, 70, E21-E28). *Geophysics,* 71**,** X25-X27.
STREET, G. J., ABBOTT, S., LADYMAN, M. & ANDERSON-MAYES, A. M. 2006. Interpretation of geophysics for land management planning, Broomehill, Western Australia. *Exploration Geophysics,* 37**,** 379-388.
SUN, J. Q., HUANG, D. X. & LIU, D. M. 2006. Simultaneous wavelength conversion and pulse compression exploiting cascaded second-order nonlinear processes in LiNbO3 waveguides. *Optics Communications,* 259**,** 321-327.
SUZEN, M. L. & KAYA, B. S. 2011. Evaluation of environmental parameters in logistic regression models for landslide susceptibility mapping. *International Journal of Digital Earth,* 5**,** 338-355.
TABUCCHI, T. H. P. & GROSSI, P. 2012. 2011 Tohoku, Japan Earthquake Catastrophe Modeling Response. *15th World Conference on Earthquake Engineering.* Lisboa.
TAKAHASHI, T., TAKEUCHI, T. & SASSA, K. 2006. International Society for Rock Mechanics - Commission on application of geophysics to rock engineering - Suggested methods for borehole geophysics in rock engineering. *International Journal of Rock Mechanics and Mining Sciences,* 43**,** 337-368.
TARVAINEN, T., JARVA, J. & GEREIVING, S. 2006. Spatial pattern of hazards and hazard interactions in Europe. *In:* SCHMIDT-THOME, P. (ed.) *Natural and Technological Hazards and Risks Affecting the Spatial Development of European Regions.* Geological Survey of Finland.
TIAN, Z. Y., YAO, Y. & GAO, J. H. 2006. Research and application of integrated geophysics in dam crack detection. *Geophysical Solutions for Environment and Engineering, Vol 1 and 2***,** 750-754.
TIBALDI, A., FERRARI, L. & PASQUARE, G. 1995. Landslides Triggered by Earthquakes and Their Relations with Faults and Mountain Slope Geometry - an Example from Ecuador. *Geomorphology,* 11**,** 215-226.
TONTINI, F. C. 2006. On "Magnetic-anomaly Fourier spectrum of a 3D Gaussian source" (Fabio Caratori Tontini, 2005, GEOPHYSICS, 70, L1-5) - Reply to the discussion by Laust B. Pedersen. *Geophysics,* 71**,** X7-X10.
TORO, G. R., ABRAHAMSON, N. A. & SCHNEIDER, J. F. 1997. Model of strong ground motions from earthquakes in Central and Eastern North America: best estimates and uncertainties. *Seismological Research Letters,* 68**,** 41-57.
TRALLI, D. M., BLOM, R. G., FIELDING, E. J., DONNELLAN, A. & EVANS, D. L. 2007. Conceptual case for assimilating interferometric synthetic aperture radar data into the HAZUS-MH earthquake module. *Ieee Transactions on Geoscience and Remote Sensing,* 45**,** 1595-1604.
TSAI, Y. B., YU, T. M., CHAO, H. L. & LEE, C. P. 2001. Spatial distribution and age dependence of human-fatality rates from the Chi-Chi, Taiwan, earthquake of 21 September 1999. *Bulletin of Seismological Society of America,* 91**,** 1298-13099.
UNDP, 2004. Reducing Disaster Risk: A Challenge for Development. *UNDP Bureau for Crisis Prevention and Recovery, New York***,** 146.
UNDP, 2013. *International Human Development Indices: Data*. Available: http://hdrstats.undp.org/en/tables/ [Accessed 1st March 2012].
UNU-EHS, 2011. World Risk Report 2011.
USGS, 2012. *Historic Earthquakes: Northridge California, 1994*. Available: http://earthquake.usgs.gov/earthquakes/states/events/1994_01_17.php [Accessed 03/09/2013].
USGS, 2014. *ShakeMap Background*. Available: http://earthquake.usgs.gov/research/shakemap/.

VAN DEN EECKHAUT, M., MARRE, A. & POESEN, J. 2010. Comparison of two landslide susceptibility assessments in the Champagne-Ardenne region (France). *Geomorphology,* 115**,** 141-155.
VAN DEN EECKHAUT, M., VANWALLEGHEM, T., POESEN, J., GOVERS, G., VERSTRAETEN, G. & VANDEKERCKHOVE, L. 2005. Prediction of landslide susceptibility using rare events logistic regression: A case-study in the Flemish Ardennes (Belgium). *Geomorphology,* 76**,** 392-410.
VAN DEN EECKHAUT, M., VANWALLEGHEM, T., POESEN, J., GOVERS, G., VERSTRAETEN, G. & VANDEKEREKHOVE, L. 2006. Prediction of landslide susceptibility using rare events logistic regression: A case-study in the Flemish Ardennes (Belgium). *Geomorphology,* 76**,** 392-410.
VAN HESSEM, D. & BOSGRA, O. 2006. Stochastic closed-loop model predictive control of continuous nonlinear chemical processes. *Journal of Process Control,* 16**,** 225-241.
VAN WESTEN, C. J., RENGERS, N. & SOETERS, R. 2003. Use of geomorphological information in indirect landslide susceptibility assessment. *Natural Hazards,* 30**,** 399-419.
VAN WESTEN, C. J., VAN ASCH, T. W. J. & SOETERS, R. 2006. Landslide hazard and risk zonation - why is it still so difficult? *Bulletin of Engineering Geology and the Environment,* 65**,** 167-184.
VARNES, D. J. 1978. Slope movement types and processes. *In:* CLARK, M. (ed.) *Landslide Analysis and Control.* Washington, DC.
VASANTHI, A., SHARMA, K. K. & MALLICK, K. 2006. On "New standards for reducing gravity data: The North American gravity database" (W. J. Hinze et al., 2005, Geophysics, 70, J25-J32) - Discussion. *Geophysics,* 71**,** X31-X32.
VISHER, S. S. 1924. Tropical cyclones and earthquakes. *Bulletin of Seismological Society of America,* 14**,** 181-184.
WALD, D., LIN, K. W. & TURNER, L. L. unpublished. Connecting the DOTs: Expanding the capabilities of the USGS ShakeCast Rapid Post-Earthquake Assessment System for Departments of Transportation.
WALD, D. J., HEATON, T. H. & HUDNUT, K. W. 1996. The slip history of the 1994 Northridge, California, earthquake determined from strong-motion, teleseismic, GPS, and leveling data. *Bulletin of the Seismological Society of America,* 86**,** S49-S70.
WALD, D. J., JAISWAL, K. S., MARANO, K. D., GARCIA, D., SO, E. & HEARNE, M. 2012. Impact-based earthquake alerts with the U.S. Geological Survey's PAGER system: what's next? *The 15th World Conference on Earthquake Engineering: September 24-28, 2012, Lisbon, Portugal*.
WANG, L., SAWADA, K. & MORIGUCHI, S. 2011. Landslide Susceptibility Mapping by Using Logistic Regression Model with Neighborhood Analysis: A Case Study in Mizunami City. *International Journal of Geomate,* 1**,** 99-104.
WANG, R. 2008. *An expert knowledge-based approach to landslide susceptibility mapping using GIS and fuzzy logic.* University of Wisconsin.
WANG, X. S., HU, J. & GAO, J. B. 2006. Nonlinear dynamics of regenerative cutting processes - Comparison of two models. *Chaos Solitons & Fractals,* 29**,** 1219-1228.
WIJNS, C., PEREZ, C. & KOWALCZYK, P. 2006. On "Theta map: Edge detection in magnetic data" (C. Wijns, C. Perez, and P. Kowalczyk, 2005, GEOPHYSICS, 70, L39-L43) - Reply. *Geophysics,* 71**,** X12-X12.
XU, C., XU, X. W., YAO, X. & DAI, F. C. 2014. Three (nearly) complete inventories of landslides triggered by the May 12, 2008 Wenchuan Mw 7.9 earthquake of China and their spatial distribution statistical analysis. *Landslides,* 11**,** 441-461.
YALCIN, A., REIS, S., AYDINOGLU, A. C. & YOMRALIOGLU, T. 2011. A GIS-based comparative study of frequency ratio, analytical hierarchy process, bivariate statistics and logistics regression methods for landslide susceptibility mapping in Trabzon, NE Turkey. *Catena,* 85**,** 274-287.

YATES, M. A., TSANGARIS, C. L., KINSLER, P. & NEW, G. H. C. 2006. Modelling of angular effects in nonlinear optical processes. *Optics Communications,* 257**,** 164-175.
YESILNACAR, E. & TOPAL, T. 2005. Landslide susceptibility mapping: A comparison of logistic regression and neural networks methods in a medium scale study, Hendek region (Turkey). *Engineering Geology,* 79**,** 251-266.
YETMAN, G., GAFFIN, S.R., AND XING, X. 2004. *Global 15 x 15 Minute Grids of the Downscaled GDP Based on the SRES B2 Scenario, 1990 and 2025*. Available: http://sedac.ciesin.columbia.edu/data/set/sdp-downscaled-gdp-grid-b2-1990-2025 [Accessed 1st March 2012].
YILMAZ, I. 2009. Landslide susceptibility mapping using frequency ratio, logistic regression, artificial neural networks and their comparison: A case study from Kat landslides (Tokat-Turkey). *Computers & Geosciences,* 35**,** 1125-1138.
YIN, J. H., CHEN, J., XU, X. W., WANG, X. L. & ZHENG, Y. G. 2010. The characteristics of the landslides triggered by the Wenchuan M-s 8.0 earthquake from Anxian to Beichuan. *Journal of Asian Earth Sciences,* 37**,** 452-459.
YIN, Y. P., WANG, F. W. & SUN, P. 2009. Landslide hazards triggered by the 2008 Wenchuan earthquake, Sichuan, China. *Landslides,* 6**,** 139-152.
YOO, C. K. & LEE, I. B. 2006. Integrated framework of nonlinear prediction and process monitoring for complex biological processes. *Bioprocess and Biosystems Engineering,* 29**,** 213-228.
YOO, C. K. & LEE, I. B. 2006. Nonlinear multivariate filtering and bioprocess monitoring for supervising nonlinear biological processes. *Process Biochemistry,* 41**,** 1854-1863.
YUAN, R. M., DENG, Q. H., CUNNINGHAM, D., XU, C., XU, X. W. & CHANG, C. P. 2013. Density Distribution of Landslides Triggered by the 2008 Wenchuan Earthquake and their Relationships to Peak Ground Acceleration. *Bulletin of the Seismological Society of America,* 103**,** 2344-2355.
YUAN, X. P., CHEN, H. B. & ZHENG, Z. G. 2006. Nonlinear dynamics in sliding processes: the single-particle case. *Chinese Physics,* 15**,** 1464-1470.
ZHANG, J., HERNANDEZ, G. & ZHU, Y. F. 2006. Copropagating superluminal and slow light manifested by electromagnetically assisted nonlinear optical processes. *Optics Letters,* 31**,** 2598-2600.
ZHANG, P. S., WU, H. S. & LIU, S. D. 2006. Integrated geophysics detection and application for geological structure and abnormity ahead of the laneway in mine. *Geophysical Solutions for Environment and Engineering, Vol 1 and 2***,** 781-787.
ZHANG, Y., SUN, J., NOTFORS, C., GRAY, S. H., CHERNIS, L. & YOUNG, J. 2006. On "Delayed-shot 3D depth migration" (Yu Zhang, James Sun, Carl Notfors, Samuel H. Gray, Leon Chernis, and Jerry Young, 2005, GEOPHYSICS, 70, E21-E28) - Reply to the discussion - Christof Stork and Jerry Kapoor. *Geophysics,* 71**,** X27-X29.
ZSCHAU, J. 2010. MATRIX - New Multi-Hazard and Multi-Risk Assessment Methods for Europe. *In:* COOPERATION, S. F. P. (ed.).
ZUCCARO, G. & LEONE, M. 2011. Volcanic crisis management and mitigation strategies: a multi-risk framework case study. *Earthzine,* 4.
ZYRYANOV, V. N. 2013. Nonlinear pumping-effect in oscillation processes in geophysics. *Water Resources,* 40**,** 243-253.
ZYRYANOV, V. N. & KHUBLARYAN, M. G. 2006. Pumping effect in the theory of nonlinear processes of the thermal conductivity equation type and its application in geophysics. *Doklady Earth Sciences,* 408**,** 674-677.